A study of ligand exchange processes at early transition metal centres: synthesis, mechanism and applications to polymer synthesis

Jolly, Matthew

A Study of Ligand Exchange Processes at Early Transition Metal Centres:

Synthesis, Mechanism and Applications to Polymer Synthesis

by

Matthew Jolly, B.Sc. (Dunelm)

University of Durham

A thesis submitted in part fulfillment of the requirements for the degree of

Doctor of Philosophy at the University of Durham.

January 1994

1 0 JUN 1994

For Mum with all my love

Acknowledgements

Statement of Copyright

The copyright of this thesis rests with the author. No quotation from it should be published without his prior written consent and information derived from it should be acknowledged.

Declaration

The work described in this thesis was carried out in the Department of Chemistry at the University of Durham between October 1990 and September 1993. All the work is my own, unless stated to the contrary, and it has not been submitted previously for a degree at this or any other University.

Financial support

Abbreviations

NMR	Nuclear magnetic resonance	HETCOR	Heteronuclear correlation
COSY	Correlation spectroscopy		
GPC	Gel permeation chromatography	G.C	Gas chromatography
R.O.M.P	Ring opening metathesis polymerisation	ADMET	Acyclic diene metathesis
Q	Dianionic ligand	X	Mono-anionic ligand
Cp	Cyclopentadienyl ligand	Cp*	Pentamethyl - cyclopentadienyl ligand
Ar	2,6-diisopropyl phenyl	Ar^{Cl}	2,6-dichloro phenyl
Ar^F	pentafluoro phenyl	DIPP	2,6-diisopropyl
THF	Tetrahydrofuran	DHF	Dihydrofuran
dme	Dimethoxyethane	dioxan	1,4 dioxane
Pyr	Pyridine	acac	2,4 Pentane dione
PyrHOTf	Pyridinium triflate		
R_f^3	CMe_2CF_3	R_f^6	$CMe(CF_3)_2$
LUMO	Lowest unocupied Molecular orbital	ppm	Parts per million
$\Delta^{1/2}$	Peak width at half height	μ	Peak width
δ	Chemical shift	PDI	Polydispersity index
M_n	Number average molecular weight	M_w	Weight average molecular weight
σ_t	Trans vinylene content	σ_c	Cis vinylene content
HT	Head-tail	TH	Tail-head
HH	Head-head	TT	Tail-tail
T_g	Glass transition temperature		
E_a	Activation energy	Keq	Equilibrium constant
k	Rate constant		

Abstract

A Study of Ligand Exchange Processes at Early Transition Metal Centres: Synthesis, Mechanism and Applications to Polymer Synthesis

This thesis describes studies into the exchange reactivity of early transition metal species containing mono- and dianionic ligands, examining both the intermetal exchange of such ligands and the exchange to and from external substrates. Studies on the metathesis polymerisation of functionalised monomers using well-defined Schock initiators are described.

Chapter 1 highlights the electronic and structural aspects of the ligands employed in this thesis (including oxo, imido, alkylidene, alkoxide and amide moieties) and briefly reviews intermetal ligand exchange reactions. In addition, applications of the olefin metathesis reaction, namely R.O.M.P and ADMET, are reviewed employing the well-defined Schrock type initiators.

Chapter 2 describes the preparation of $Mo(NBu^t)_2(OBu^t)_2$, and examines the reactivity of its imido ligands towards a series of organic substrates including aryl amines, benzaldehyde, dioxygen and isocyanates. Intermetal imido-imido exchange reactivity is inspected for $Mo(NR)_2X_2$ and $CpMo(NBu^t)_2Cl$ systems. The intermetal oxo-imido exchange reaction between $Mo(NBu^t)_2(OR)_2$ and $Mo(O)_2(OR)_2$ is investigated, in which the role of acid catalysis is examined. The effects of increasing the electron withdrawing properties of the ancillary alkoxide ligands by progressive fluorination are probed. The favourable position of the oxo-imido exchange reaction is exploited in the synthesis of the oxo-imido complexes $Mo(O)(NBu^t)(OBu^t)_2$, $Mo(O)(NBu^t)(OR_f^6)_2$ and $Mo(O)(NBu^t)Cl_2.dme$. The intermetal exchange reactivity of mono-anionic X-type ligands is then explored in systems of the type MoQ_2X_2 ($Q = O$, NBu^t; $Q_2 = (NAr)(CHCMe_2Ph)$; $X = Cl$, OR, NHR).

Chapter 3 presents the attempted synthesis of a half-sandwich niobium bis (imido) complex of general formula $CpNb(NR^1)(NR^2)$, starting with the synthesis of imido-amide complexes $CpNb(NR)(NR^1R^2)Cl$ ($R = Bu^t$, $R^1 = R^2 = Et$; $R = Ar$, $R^1 = Bu^t$, $R^2 = H$) via the reaction of $CpNb(NR)Cl_2$ with lithium amides. Further reaction of these imido-amide species with lithium amides result in the formation of $CpNb(NBu^t)(NHBu^t)_2$ and $CpNb(NBu^t)(NHBu^t)(NEt_2)$. The reactivity of the imido ligand in $CpNb(NBu^t)X_2$ is investigated towards aryl amines, butanol, dioxygen and H_2O. Complexes of the type $CpNb(NBu^t)X_2$ ($X = Br$, OPr^i, OR_f^3, OR_f^6 and NC_4H_4) are isolated and employed in mono-anionic intermetal exchange reactions, the results from which are compared with those from analogous reactions in chapter 2.

Chapter 4 outlines metathesis polymerisation studies on hetero-cyclopentenes using the well-defined molybdenum Schrock initiators. The R.O.M.P of 2,3- and 2,5-dihydrofurans are reported. A metallacycle adduct is isolated in the reaction of $Mo(NAr)(CHCMe_2Ph)(OBu^t)_2$ with vinylene carbonate. The reaction of 1-(amino)-3-borolenes with the Schrock initiators is described and a product characterised as a 1-(amino)-2-borolene by X-ray crystallography. The factors that may effect the polymerisability of hetero-cyclopentenes are briefly considered. In addition, the reactivity of functionalised acyclic diallyl species of the type $Q(CH_2CHCH_2)_2$ ($Q = O$, NH, PPh, O_2CO) are explored with the Schrock initiators in acyclic diene metathesis reactions (ADMET). Diallyl ether is found to undergo catalytic ring closure to 2,5 dihydrofuran, while diallyl phenyl-phosphine gives 1-phenyl-2,5 dihydrophosphole.

Chapter 5 gives experimental details for chapters 2-4.

Matthew Jolly (January 1994)

Contents

Chapter Two -   **The Synthesis and Exchange Reactivity of**
half-sandwich niobium imido complexes of the type -
CpNb(NR)X$_2$

Chapter Three - The Synthesis and Exchange Reactivity of Molybdenum Complexes of the type - MoQ_2X_2

NMR characterising data for:

Appendices

Chapter One

Ligand exchange processess at Early Transition Metal centres -

An Overview of the Structure and Bonding of Mono- and Dianionic

Ligands and their Exchange reactivity.

1.1 Introduction

This thesis is concerned with mono- and dianionic ligand exchange processes at early transition metal centres and their applications in polymerisation catalysis.

The first part of the study addresses the synthesis and exchange reactivity of complexes of the Group 5 and 6 triads containing terminal oxo, imido and alkylidene ligands, bound to the metal through multiple bonds.

Relatively little is kown about the intermetal exchange of such ligands, although the synthetic utility of these processes is being increasingly exploited. The study is then extended to the intermetal exchange of mono-anionic ligands, examples of which include halide, amide and alkoxide moieties.

In the second part of this thesis, an important application of alkylidene exchange reactivity is investigated, namely the exchange of metal-alkylidene and olefin fragments (the olefin metathesis reaction). The Ring Opening Polymerisation (R.O.M.P) of heterocyclopentenes has been investigated using well-defined Schrock initiators and extended to acyclic diene metathesis (ADMET) studies on hetero-atom-containing α, ω-dienes with a view to accessing new materials.

The remainder of this chapter is devoted to a review of topics relevant to the subject matter of this thesis including the general structural and electronic characteristics of the various types of ligand employed, a brief overview of intermetal ligand exchange processes for both mono- and dianionic species and general aspects of Ring Opening Metathesis (R.O.M.P) and Acyclic Diene Metathesis (ADMET) employing well-defined transition metal alkylidene complexes.

1.2 Electronic and structural aspects

This section describes the bonding modes commonly observed for the various ligands, concentrating mainly on the structural and electronic aspects of terminally bonded species, and noting similarities between different ligands. As most of the complexes described in this thesis are of the early transition metals in their highest possible oxidation

state (d^0), the ligands will mostly be described as closed shell anions. In this description, productive π-bonding can be envisaged as arising from lone pair donation from the filled ligand p-orbitals to the vacant d-orbitals of the metal centre.

1.2.1 Oxo complexes

Oxo complexes have been found to exhibit a wide number of bonding modes, encompassing both bridging and terminal species. However, only terminal species will be considered herein. For reasons previously outlined, transition metal centres possessing vacant d-orbitals are required for productive π-bonding to arise, therefore the vast majority of terminal metal-oxo compounds are d^0, d^1 and d^2 complexes, with only a few d^4 and d^5 complexes known[1-5]. In complexes with more than two d electrons, an unfavourable population of π* levels would occur, as shown in the ligand field diagram for an octahedral mono-oxo (imido, alkylidyne) complex (figure 1.1).
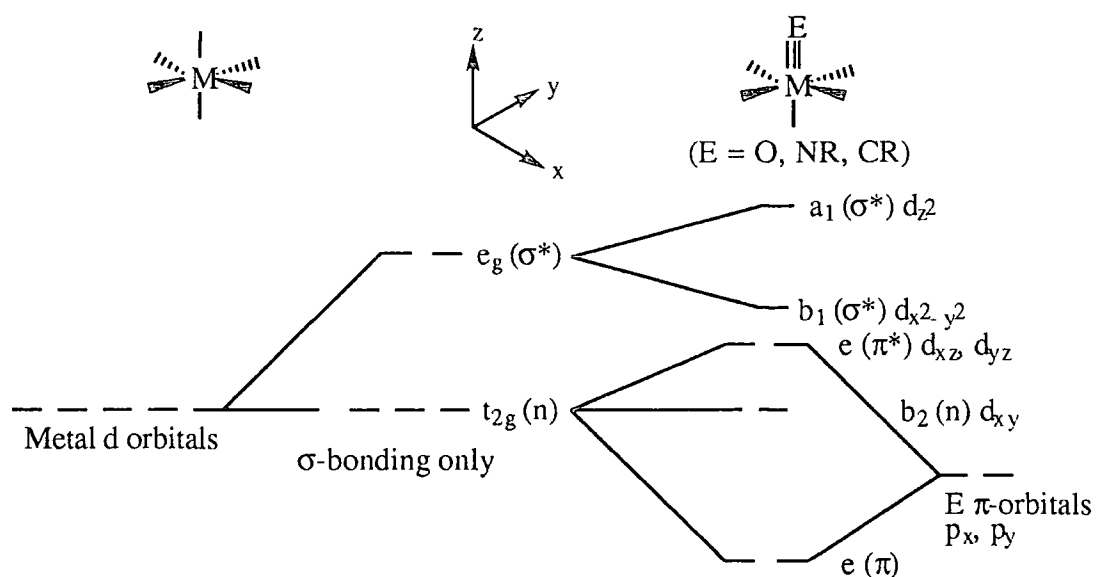
figure 1.1 *The ligand field diagram for a mono-oxo complex*

The d^4 complexes Re(O)X(C$_2$R$_2$)$_2$ get around this by adopting an unusual distorted tetrahedral structure so that the four d-electrons can be accomodated in roughly non-bonding orbitals[6].

2

The terminal oxo ligand can be considered to be a 'two-faced' π–donor, as it possesses two orthogonal degenerate π-symmetry orbitals, which when counted with the low lying σ-bond means it has the potential to form a triple bond. However, the attainment of this bond order depends on whether there is competition for the avaliable d π-orbitals at the metal centre (discussed later in this section). Furthermore, as a consequence of the high electronegativity of oxygen (can tolerate up to three electron pairs), bond orders ranging from three to one can be envisaged. The principal ligand frontier orbitals for the oxo ligand, together with their electronic occupancy are shown schematically in figure 1.2 (considered as a closed shell anion - O^{2-}).
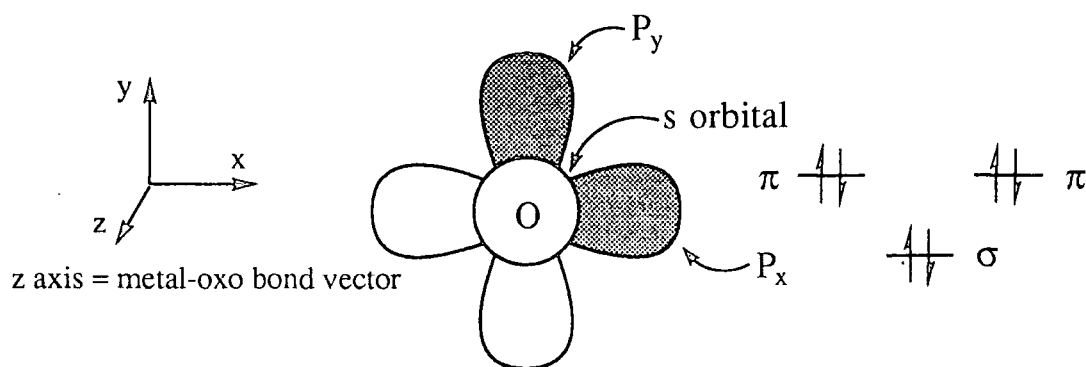
figure 1.2 *The frontier orbitals of the terminal oxo ligand*

1.2.2 Imido complexes

Both terminal and bridging bonding modes have been encountered for the imido ligand, of which the μ_2 - bridging mode is the one most commonly encountered[7-10]. Despite this, there are a large number of monomeric terminal imido complexes which are particularly prevalent in sterically encumbered environments, or when the imido substituent is bulky, some notable examples of which are shown below:

3
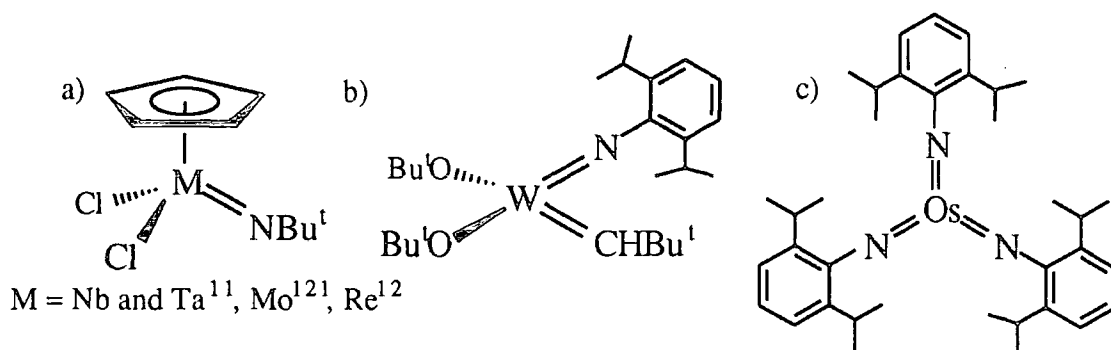
figure 1.3   a) $CpM(NBu^t)Cl_2^{11,121,12}$, b) $W(CHBu^t)(N-2,6-Pr^i_2C_6H_3)(OBu^t)_2^{13}$,

c) $Os(N-2,6-Pr^i_2C_6H_3)_3^{14}$.

The organoimido ligand (NR^{2-}) is isoelectronic with the oxo ligand (O^{2-}), and similarly possesses two filled p orbitals perpendicular to the metal-ligand axis; therefore it can act as a 'two-faced' π-donor. However, the imido ligand is generally construed to be a stronger π-donor, consistent with the reduced electronegativity of nitrogen[15,16]. A linear M-N-R bond angle implies that the nitrogen is sp hybridised, forming two π and one σ bond to the metal centre, whereas a bent arrangement of the imido unit invokes the presence of a lone pair of electrons on the nitrogen, as shown in figure 1.4.

figure 1.4 *Bonding modes of a terminal imido ligand- a) linear, b) bent*

Previously, it has been assumed that a linear or near-linear imido ligand donates it's lone pair of electrons to the metal centre. However, recently this has been drawn into question For example, Bercaw and co-workers have synthesised $Cp*_2Ta(NPh)H$ (figure 1.5), the X-ray structure of which shows a linear imido unit (Ta-N-C (ipso) = $177.8(9)^o)^{17}$. However, this infers that the complex has a 20 electron configuration at tantalum ($Cp*$ ligands are in the η^5- coordination mode). The phenyl ring is in the equatorial plane of the molecule (attributed to steric interactions), and therefore the lone pair of electrons would

be localised on the nitrogen, owing to a lack of an avaliable orbital of the correct symmetry at the metal centre[18]. In this situation, confirmation of the electronic structure would rest on the bond order and not the bond angle. The imido bond length was in fact found to be significantly longer than in comparable terminal tantalum imido compounds, implying that the complex could be an 18 electron species. The molecular structures reported recently by Schrock[19] $Os(N-2,6-Pr^i_2C_6H_3)_3$ and Bergman[20] $Cp_2Zr(NBu^t)(THF)$, similarly show formally 20 electron imido species possessing linear imido ligands. In both these examples, a lone pair of electrons is located in a nitrogen centred non-bonding orbital.
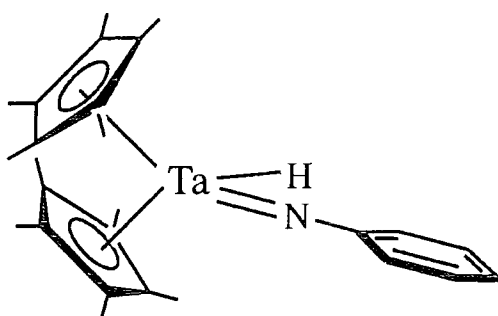
figure 1.5 *Molecular structure of Cp*$_2$Ta(NPh)H*

There has only been one previously reported example of a structurally characterised bent imido ligand - $Mo(NPh)_2(S_2CNEt_2)_2$[21], this complex contains both a bent (Mo-N-C (ipso) = 139.9(4)°) and a near-linear (Mo-N-C (ipso) = 169.4(4)°) imido ligands, and is described as having a double bond (Mo-N = 1.789Å) and a triple bond (Mo-N = 1.754Å) respectively, using the three d-orbitals of π symmetry on the metal centre.

^{13}C NMR of tert-butyl imido complexes

^{13}C NMR shifts have been reported for a number of tert-butyl imido complexes[11,22-24]. It has been shown that the difference in chemical shift between the α- and β-carbons (Δδ), gives an indication of the electron density on the imido nitrogen; a

large $\Delta\delta$ value corresponds to an electron deficient (electrophilic) imido nitrogen, whereas a small value indicates an electron rich (nucleophilic) imido nitrogen[24]. As one proceeds upwards and to the right of the periodic table the $\Delta\delta$ values increase, consistent with the decreasing relative energy of the d-orbitals of the transition metal. This results in a shift of electron density from the imido nitrogen to the metal, and hence rationalises the observed electrophilic character of the imido ligand. Ashcroft and co-workers have shown that imido ligands where $\Delta\delta$ is less than 50, react metathetically with benzaldehyde[25] (behave as a nucleophile), as shown in equation 1.1.

$$M=NBu^t \xrightarrow{\ PhCHO\ } M=O \ + \ PhCH=NBu^t$$

$$(1.1)$$
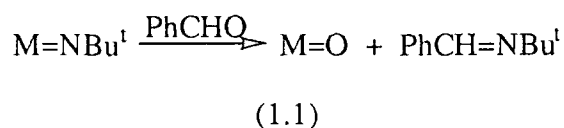
$\Delta\delta$ is also dependent upon the number of multiply bonded groups on the metal centre, as competition for avaliable d π-orbitals will arise. This has the effect of reducing the π bond order of the metal-nitrogen bond and therefore increasing the charge on the imido nitrogen. This trend is clearly illustrated in table 1.1, where successive replacement of the oxo moiety with the better π-donor tert-butyl imido ligand in the osmium (VIII) oxo-imido species, results in a corresponding decrease in $\Delta\delta$. Table 1.1 also shows the decrease in $\Delta\delta$ on moving down the group 6 triad for the homologous series $M(NBu^t)_2(OBu^t)_2$ (M = Cr, Mo and W).

Complex	$\delta C(\alpha)$	$\delta C(\beta)$	$\Delta\delta$	Ref.
$Cr(NBu^t)_2(OBu^t)_2$[a]	76.06	32.61/31.59[b]	44.47/43.45	26
$Mo(NBu^t)_2(OBu^t)_2$[a]	67.94	32.44/32.16[b]	35.50/35.78	27
$W(NBu^t)_2(OBu^t)_2$	65.58	33.79	31.79	28
$OsO_3(NBu^t)$	82.73	27.49	55.24	29
$OsO_2(NBu^t)_2$	75.13	29.64	45.49	30
$OsO(NBu^t)_3$	71.42	30.09	41.33	30

[a] In C_6D_6, all other values in C_7D_8. [b] cannot differentiate between $\delta C(\beta)$ for OBu^t and NBu^t.

table.1.1 *^{13}C chemical shift data (ppm) for some d^0 tert-butyl imido complexes*

1.2.3 Alkylidene complexes

The main difference between the alkylidene ligand and the previously mentioned oxo and imido ligands is that it can only act as a 'single-faced' π-acceptor (when considered as a closed shell dianion), and therefore can only form a double bond ($\sigma + \pi$) to the metal centre. Furthermore, this ligand can only be regarded as a closed shell anion (CR_2^{2-}) when it does not possess any heteroatom substituents and is attached to a high oxidation state metal. In this situation, the complexes are known as 'Schrock type' alkylidenes; the first example, $Ta(CHBu^t)(CH_2Bu^t)_3$[31], was synthesised in 1973 in an attempted preparation of pentakisneopentyl tantalum(V). The other well known class of alkylidene complex are the 'Fischer carbenes', the first of which $(CO)_5W(CH_3)(OCH_3)$[32], was prepared in 1964. Fischer carbenes typically have a low oxidation state metal centre, and possess an α-heteroatom substituent containing lone pairs of electrons (e.g OR, NR_2, SR etc.). They differ mainly from Schrock alkylidenes in that the carbon moiety is electrophilic, whereas the former tend to exhibit nucleophilic behaviour. A series of *ab initio* calculations has laid the foundation to a fuller understanding of the bonding in these complexes, thereby helping to rationalise the

observed reactivities[33-37]. The σ and π bonds of the metal-carbon fragment fall into two distinct types, shown in figure 1.6.
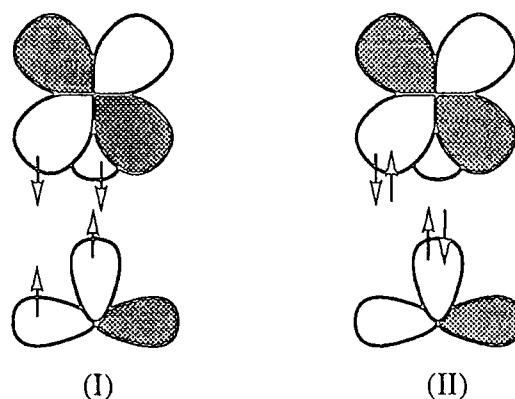
figure 1.6 *Schematic representations of the two types of metal-alkylidene bonding: ethylene - type covalent bonding (I) and donor-acceptor bonding (II).*

Type (I) depicts the bonding in Schrock alkylidenes where an interaction between the triplet carbene and the triplet metal centre result in the formation of a covalent bond (similar to that observed in ethylene). Type (II) shows the bonding in Fischer carbenes with donation of a lone pair from the singlet carbene to an empty metal d-orbital, stabilised by backbonding from a filled metal orbital into a vacant carbene p-orbital. Owing to the presence of this vacant p-orbital, the carbon atom of Fischer carbenes is electrophilic (albeit stabilised by metal back-bonding), whereas the triplet carbene of Schrock alkylidenes is nucleophilic (as in ethylene).

1.2.4 Cis multiply bonded ligands

For both octahedral and tetrahedral d^0 transition metal complexes there are only three orbitals avaliable for π-bonding, therefore it is only possible for one cis multiply bonded ligand to form a triple bond, the other forming a double bond. For octahedral complexes, the previously non-bonding d_{xy} orbital in mono-multiply bonded species can now be utilised (see the ligand field diagram in section 1.2.1). Whereas in tetrahedral

complexes both t_g and e_g orbitals can have the correct symmetry for π-bonding, however, from perturbation theory the total number of π-bonds that can be experienced by the metal centre is calculated to be three[38].

In the majority of complexes containing homoleptic cis multiply bonded ligands, averaging of the π electron density between the two groups arises, reflected by the similar bond lengths and angles observed. Nonetheless, there are exceptions, including $Mo(NPh)_2(S_2CNEt_2)_2$[39] and $MoO_2(acac)_2$[40], in which signficantly different bond parameters are found . Where different cis multiply bonded groups are present, the better π-donor tends to 'win out' forming the triple bond, resulting in a polarisation of electron density on the other multiply bonded group. For example, in the protonation of $MoO(NPh)(S_2CNEt_2)_2$ with HCl (shown in equation 1.2), the better π-donor imido group is left intact with protonation occuring exclusively at the oxo moiety[41].

$$Mo(O)(NPh)(Et_2dtc)_2 \xrightarrow[- H_2O]{2\ HCl} Mo(NPh)Cl_2(Et_2dtc)_2$$

$$\Big\downarrow {\scriptstyle 2\ HCl}$$

$$- PhNH_2 \qquad Mo(O)Cl_2(Et_2dtc)_2$$

(1.2)
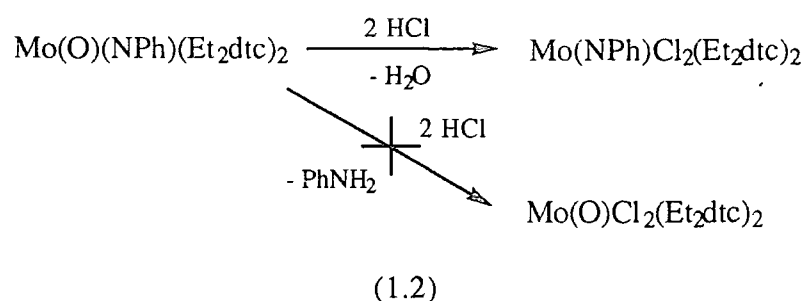
This type of reactivity is substantiated further in the above example by the fact that the imido moiety is protonated off in preference to the oxo ligand, when the more electron withdrawing para-nitrophenyl imido congener is employed.

Spectator effects

A further consequence of a complex possessing cis multiply bonded ligands is the increased reactivity observed for one of the groups. Goddard and Rappé have performed several *ab initio* studies on a range of cis multiply bonded dioxo and and oxo-alkylidene complexes, which show that reaction at the multiply bonded ligand is much more favoured than in examples where only one multiply bonded group is present[35,42]. The

9

main reason for this is the formation of a triple bond or 'super double bond' at the metal centre of the product. This is illustrated by further *ab initio* studies on the proposed molybdate intermediates in the oxidation of propylene to acrylonitrile[43]. It has been shown that in the first step (see figure 1.8), trapping of the proposed allyl radical at the dioxo site is exothermic, whereas this step is endothermic at the mono-oxo site.
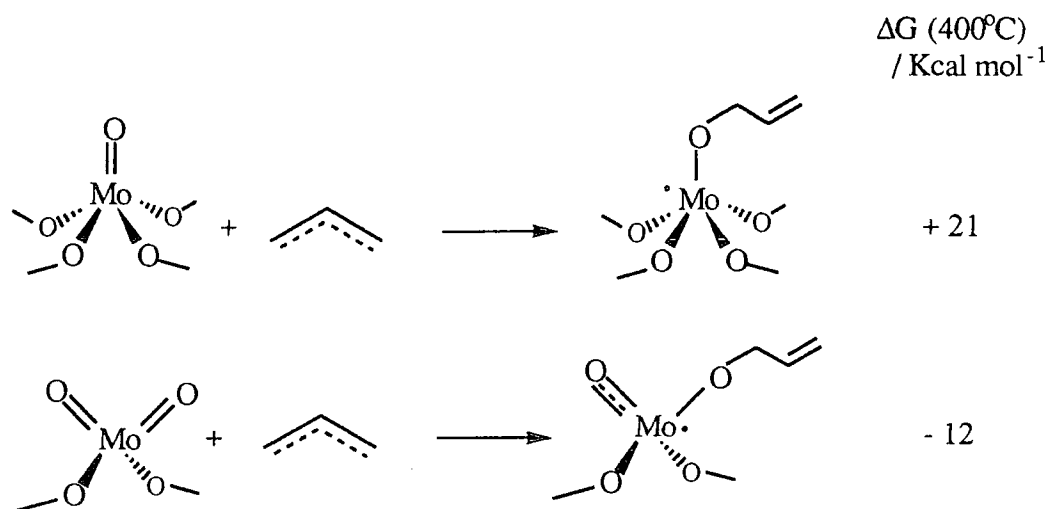
figure 1.8 *Proposed allyl traping at mono- and dioxo molybdenum sites in the oxidation of propylene to acrylonitrile.*

The formation of a 'pseudo' triple metal-oxo bond in the product starting from the dioxo molybdenum reactant favours the reaction at this species. This phenomonon, termed a 'spectator group' effect, is also found for an imido group in the analogous reaction of the ammoxidation of propylene to acrylonitrile[51]. However, the stabilisation of the product by a spectator imido group is about half that calculated for the oxo group. This factor was seized upon in the development of well-defined olefin metathesis catalysts, where stabilisation of the metallacycle intermediate was required only in as much as to make the relative energies of the metallacycle and products proximate. For this purpose, the spectator 2,6-diisopropylphenyl imido ligand has been successfully employed by Schrock in some of the most active metathesis initiators[44,45].

1.2.5 Alkoxide complexes

The mono-anionic alkoxide ligand (OR⁻) is isoelectronic to oxo and imido ligands (O^{2-} and NR^{2-}), and similarly can potentially act as a 'two-faced' π-donor, forming a triple bond to the metal centre. In extremely electron deficient transition metal complexes this situation is realised, for instance, the 'tritox' ligand (Bu^t_3CO) in (tritox)$_2$ZrCl$_2$.LiCl (OEt$_2$)$_2$ displays large M-O-C angles (169°) and short M-O distances (1.895Å), consistent with an sp-hybridised oxygen[46]. Furthermore, the derivative (tritox)$_2$ZrMe$_2$ could be viewed as an analogue of Cp$_2$ZrMe$_2$[47], in that both cyclopentadienyl and alkoxide ligands are 6 electron (mono-anionic) donors. Moreover, the symmetry of the occupied frontier orbitals for both these respective ligands are similar, and in that respect they may be regarded as being pseudo-isolobal (discussed further in section 1.2.7). The other extreme is realised when there are no vacant d-orbitals avaliable on the metal centre for π-bonding, here M-O-C bond angles can approach 120° [48,49]. However, in most cases the observed bond angles lie well inbetween the two extremes.

A notable feature of alkoxide chemistry is the high affinity observed for this ligand to bridge metal centres (in the form of μ_2- and μ_3-OR linkages), which is attributed to the basic nature of the oxygen[50]. The propensity for bridging is mainly dependent upon the steric bulk of the alkoxy substituent, the more branched the substituent, the less likely that bridging will occur.

1.2.6 Amide complexes

For a terminal metal alkyl amido complex there are two bonding possibilities, shown in figure 1.7.

(I)   (II)

$$M-\ddot{N}\text{\tiny////}R \atop \qquad\qquad R$$

$$M-\ddot{N}\text{\tiny\textbackslash////}R \atop \qquad\qquad R$$
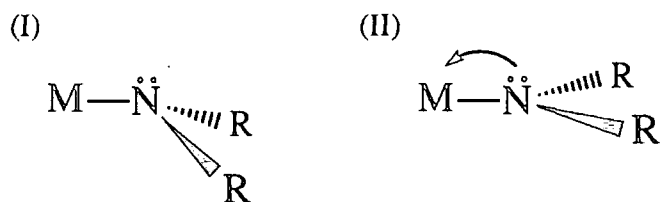
figure 1.7 *Metal-amide bonding possibilities in terminal metal-amides*

Structure (I) shows a metal-nitrogen σ-bond with a pyramidal sp^3 hybridised nitrogen. Structure (II) illustrates possible π-bonding from the p orbital orthogonal to the trigonal planar sp^2 hybridised nitrogen atom, and is predominantly found for high oxidation state early transition metal complexes (vacant d orbitals avaliable for π-donation). In this bonding description the amide is acting as a 'single-faced' π-donor, similar to that of the alkylidene ligand discussed previously. Examples of the amide ligand bridging metal centres are less common than for alkoxide or imido units, presumably reflecting the increased steric congestion around the nitrogen.

The amide ligand (NR_2^-) is isoelectronic with the alkyl ligand (CR_3^-) and shows a number of similarities. For example, the imido-amide complex $Ta(NR)(NHR)_3$[51] (R = alkyl) has it's alkyl counterpart in the Schrock alkylidene complex $Ta(CHR)(CH_2R)_3$[30] (R = Bu^t). Furthermore, early transition metal alkyls and amides undergo many similar types of reactions, eg insertion and metathesis[52].

1.2.7 The isolobal analogy between η^5-cyclopentadienyl and imido ligands

The symmetries of the partly or fully occupied frontier orbitals of the η^5-cyclopentadienyl ligand and those of the imido ligand are similar, both possessing a σ orbital and two degenerate π-orbitals, as shown in figure 1.10 (a) and (b) .
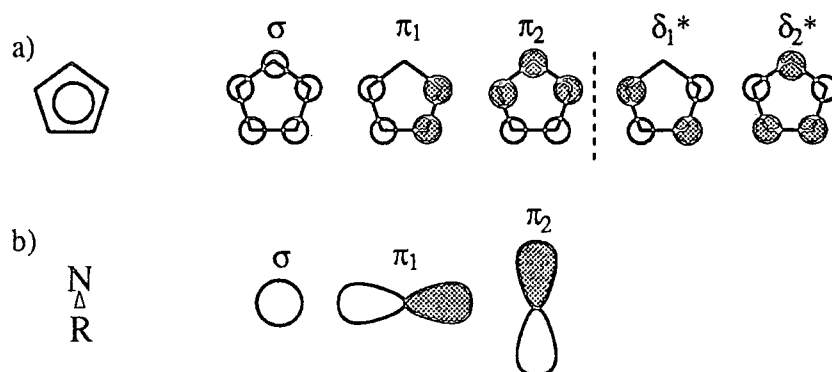
figure 1.10 *The frontier orbitals of the η^5-cyclopentadienyl ligand (a) and the organoimido ligand (b).*

In this respect they may be regarded as being pseudo-isolobal, though not truly isolobal since the η^5-cyclopentadienyl ligand uses five atoms to coordinate to the metal centre whereas the imido ligand only one, and also possesses δ-symmetry orbitals avaliable for π-back donation. When considered as a neutral species the cyclopentadienyl ligand contributes five electrons to the metal centre and therefore one fewer than the imido ligand. Therefore successive progressions along the transition series accompanied by sequential replacement of the cyclopentadienyl unit with an imido ligand would lead to a series of isolobal and valence-isoelectronic species, as illustrated in figure 1.11.
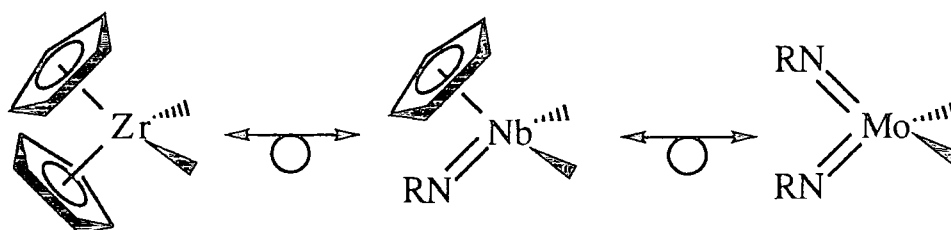
figure 1.11

This concept is particularly useful in that structural and chemical analogies between various established systems can be drawn, and furthermore, predictions of the derivative chemistry of new systems made[53,54]. Recently, this relationship has been pointed out by Schrock in comparing the chemistry of $W(NAr)_2$ and Cp_2M (M = group IV metal)

13

fragments[55]. Furthermore, the advantages of this analogy is that it not only describes common features of imido and cyclopentadienyl complexes, but can be extended to encompass a whole range of ligands with similar frontier orbital characteristics. It is of particular relevance in this thesis, where the reactivity of related $CpNb(NBu^t)X_2$ and $Mo(NBu^t)_2X_2$ species will be examined.

1.3 Intermetal heteroatom exchange reactions

Many heteroatom exchange reactions between transition metal centres have been reported which involve oxidation/reduction at respective metal centres. Such processess can entail one, two and three electron changes[56]. In 1976, the first documented case of the intermetal exchange of an oxygen atom was reported[57] (equation 1.3).

$$Mo^{VI}(O)_2(S_2CNR)_2)_2 + Mo^{II}(CO)_2(S_2CNR_2)_2$$

$$\searrow$$

$$2\,Mo^{IV}(O)(S_2CNR_2)_2 + 2\,CO$$

$$(1.3)$$
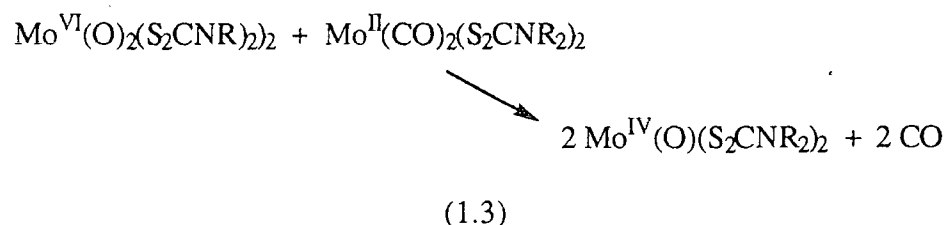
The above example formally represents a two-electron redox process. More recently, Woo and co-workers have examined reactions involving exchange of oxo, nitrido and halide ligands in metalloporphyrin complexes, as shown in figure 1.12[58-60].

(I) $(TTP)Mn^V(N) + (OEP)Mn^{II} \longrightarrow (TTP)Mn^{II} + (OEP)Mn^V(N)$

(II) $(TMP)Ru^{VI}(O)_2 + (TMP)Ru^{II} \longrightarrow 2\,(TMP)Ru^{IV}(O)$

(III) $(OEP)Mn^V(N) + (TTP)Mn^{III}Cl \longrightarrow (OEP)Mn^{III}Cl + (TTP)Mn^V(N)$
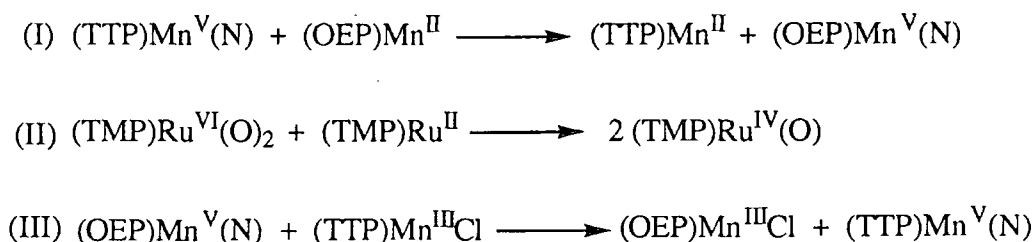
figure 1.12 *Intermetal exchange processes: (I) 3 electron redox process, (II) and (III) are 2 electron processes.(TTP, OEP and TMP = tetradentate dianion porphyrin ligands).*

In these systems, closely related porphyrin ligands are employed so that the reactions can be readily monitored by ^{1}H NMR spectroscopy. For the purpose of this discussion, intermetal exchange reactions which involve a net redox process will not be discussed, owing to the already extensive attention that this area has received.

1.3.1 Mono-anionic ligand exchange

The relatively facile scrambling of mono-anionic ligands between metal centres has been known for some time, commonly being a documented outcome of a variety of synthetic procedures[61,62]. Consequently, there remains a relatively poor understanding of the factors that influence such exchange processes. Yet, these factors are of fundamental importance to our understanding of inorganic reaction chemistry. One of the earliest examples of an intermetal ligand exchange reaction is the well known Schlenk equilibrium[63].

$$2\,RMgX \rightleftharpoons MgX_2 + MgR_2$$
$$\searrow dioxan$$
$$MgX_2.dioxan$$
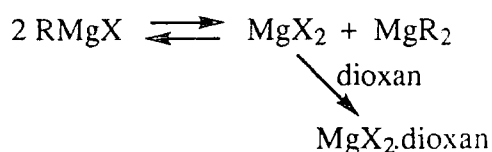
$$(1.4)$$

In equation 1.4, there is an equilibrium between the mono alkyl-halide grignard (RMgX) and the dialkyl grignard (MgR$_2$). In non-coordinating solvents the equilibrium lies well over to the left hand side but if dioxan is introduced, the magnesium halide is complexed thus driving the equilibrium over to the dialkyl Grignard (MgR$_2$). This alkyl-halide exchange equilibrium can occur for early transition metal species and has been observed by A.D.Poole in this laboratory during the attempted synthesis of Cp*Ta(NAr)MeCl *via* reaction of Cp*Ta(NAr)Cl$_2$ with one equivalent of MeMgCl[64]. Attempts to isolate the pure mono alkyl species were unsuccessful since it was contaminated with the dialkyl complex and the dihalide starting material. This was due to an alkyl-halide equilibrium

15

demonstrated from the reverse direction by combining the dihalide/dialkyl complexes and observing the formation of the mono alkyl species:

$$Cp^*Ta(NAr)Me_2 \ + \ Cp^*Ta(NAr)Cl_2 \ \underset{\longleftarrow}{\overset{K_{eq}}{\rightleftharpoons}} \ 2 \ Cp^*Ta(NAr)MeCl$$

$$K_{eq} = 10.8 \ (3)$$

$$(1.5)$$
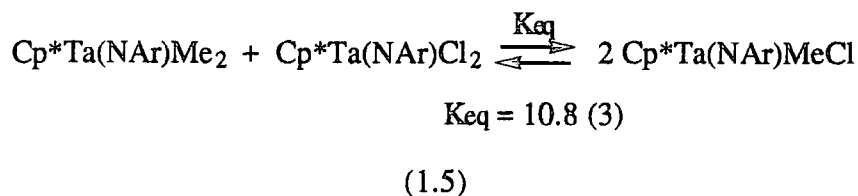
Alkoxide scrambling between metal centres *via* bridging (μ-OR) groups have also been noted previously[65], but no specific mechanistic and thermodynamic details were provided. However, one rare discrete example that has been reported for chloride-aryloxide exchange is shown in equation 1.6[66].

$$(\eta^6\text{-}C_6Me_6)Ta(DIPP)_2Cl \ + \ Ta(DIPP)_2Cl_3.OEt_2$$

$$(\eta^6\text{-}C_6Me_6)Ta(DIPP)Cl_2 \ + \ Ta(DIPP)_3Cl_2.OEt_2$$

$$(1.6)$$
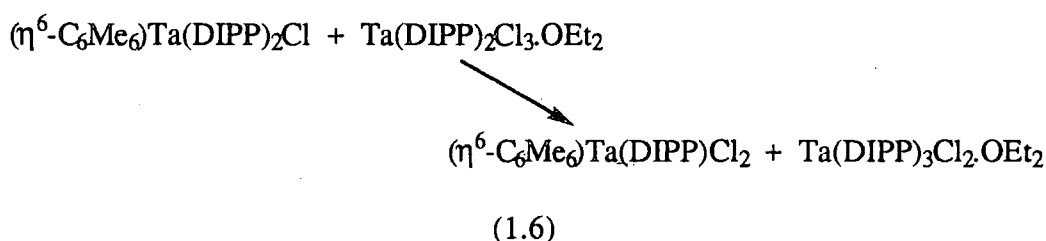
The products are generated quantitatively, due to the formation of the themodynamically stable tris aryloxide complex $Ta(DIPP)_3Cl_2.OEt_2$. The relief of steric congestion around the half-sandwich tantalum complex by substitution of a bulky diisopropyl phenoxide group with a chlorine certainly warrants consideration in this case.

Mono-anionic ligand exchange has been briefly explored in a titanium (IV) system TiX_4 (where X = halide, OR and NR_2), in which reaction with another molecule TiY_4 typically gives rise to a mixture of products of general formula $TiX_{4-n}Y_n$[67,68]. However, analysis of the results obtained was complicated by the presence of the numerous mixed species inherent in this system. In addition, associated species were postulated on the basis of the low field NMR data which further complicated matters.

In general, the position of many of these equilibria often lie almost completely over to the mixed products and therefore such exchange reactions have potential widespread synthetic utility.

1.3.2 Dianionic ligand exchange

The intermetal exchange of dianionic ligands has been briefly exploited by Schrock in the synthesis of new oxo- and imido-alkylidene complexes[69-71], as shown in equation 1.7.

$$W(Q)(OBu^t)_4 \ + \ Ta(CHBu^t)L_2Cl_3$$
$$Q = O, NPh \qquad L = PMe_3, PEt_3$$

$$W(Q)(CHBu^t)L_2Cl_2 \ + \ 0.5[Ta(OBut)_4Cl]_2$$

$$(1.7)$$
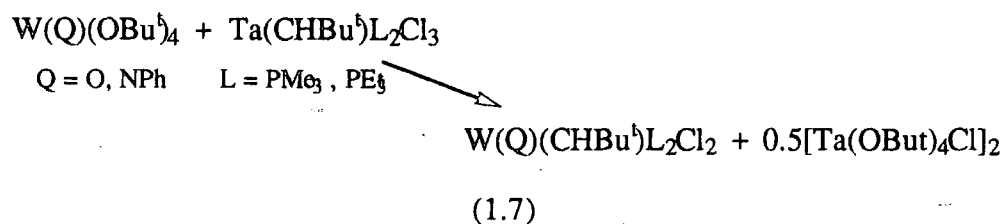
The above reaction involves alkylidene exchange $(CR_2{}^{2-})$, accompanied by the redistribution of the remaining one electron anionic ligands (Cl) and the neutral two electron ligands (PR_3). The reactivity of the early transition metal tantalum neopentylidene complex, in transferring the alkylidene moiety to the tungsten centre, is parallelled to that of a phosphorous ylid[71]. More recently, Schrock has exploited this type of reactivity in synthesising the first alkylidene and alkylidyne complexes of osmium[72], *via* an intermetal oxo-alkylidene exchange reaction, shown in figure 1.13.
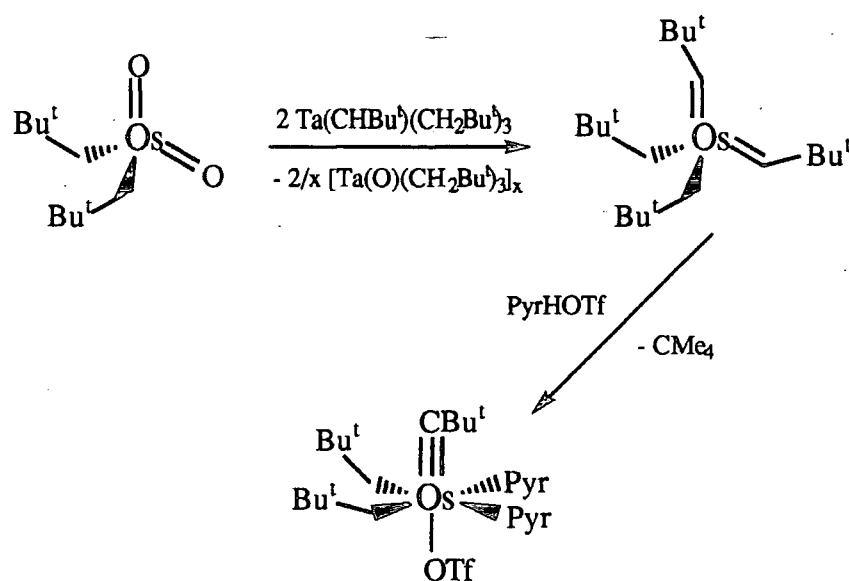
figure 1.13 *alkylidene- and alkylidyne osmium complexes*

Of late, there has been interest in exchanging other dianionic ligands; for instance, Gibson *et al* have shown that the relatively facile intermetal exchange of oxo, imido and alkylidene ligands occur in coordinatively unsaturated Group V (Nb and Ta) and VI (Mo and W) systems[73]. A kinetic study of the oxo-imido exchange reaction between $Mo(NAr)_2(OBu^t)_2$ and $Mo(O)_2(OBu^t)_2$ (equation 1.9) indicates that the exchange reaction proceeds *via* a four centre transition state (shown in figure 1.13), consistent with the negative entropy change calculated for this process. This particular oxo-imido exchange reaction is investigated further for the tert-butyl imido analogue $Mo(NBu^t)_2(OBu^t)_2$ in chapter 2.

$$Mo(NAr)_2(OBu^t)_2 + Mo(O)_2(OBu^t)_2 \underset{\longleftarrow}{\overset{Keq}{\rightleftharpoons}} 2\ Mo(O)(NAr)(OBu^t)_2$$
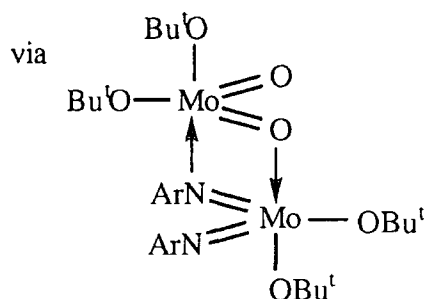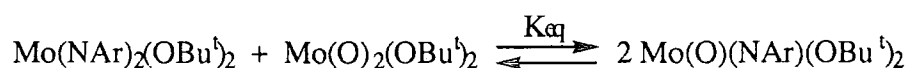
figure 1.13 *Reaction between Mo(NAr)₂(OBuᵗ)₂ and Mo(O)₂(OBuᵗ)₂*

As with mono-anionic exchange, the reactions often proceed to give one set of products, especially in exchange reactions between different metal centres. For example, Schrock has recently synthesised $Os(O)_2(NAr)_2$ quantitatively (equation 1.10) *via* intermetal oxo-imido exchange[74], whereas previously this species was only obtained from a low yield synthesis[19].

$$OsO_4 + Mo(NAr)_2(OBu^t)_2 \xrightarrow{THF} Os(O)_2(NAr)_2 + Mo(O)_2(OBu^t)_2$$

$$(1.10)$$
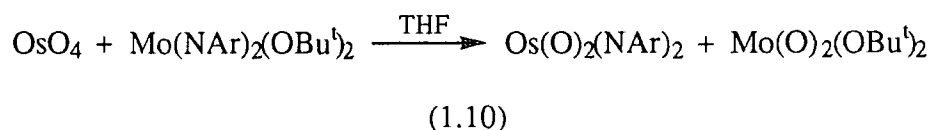
Furthermore, Os(O)(NAr)$_3$ can be isolated in high yield when the stoichiometry is adjusted to 1.5 equivalents of Mo(NAr)$_2$(OBu^t)$_2$. The thermodynamical outcome of both these reactions are rationalised by the preference of the oxo ligand for the early transition metal molybdenum centre.

The synthetic applications of oxo- and imido-imido exchange equilibria are highlighted in chapter 2 of this thesis.

1.4 Olefin metathesis

Metathesis, in chemical terms is the interchange of two units which both individually comprise part of two larger entities. In the case of 'olefin metathesis', it is the exchange of two alkylidene fragments, pairs of which constitute an olefin, as shown in equation 1.11.

$$2 \, RCH = CHR' \; \rightleftharpoons \; RCH = CHR \; + \; R'CH = CHR'$$

(1.11)
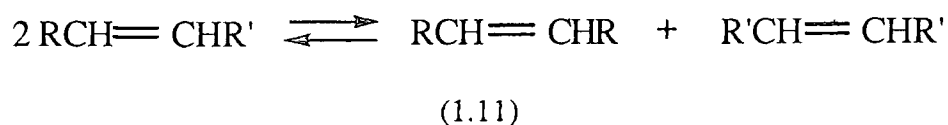
Calderon is credited with introducing the term 'olefin metathesis' in 1967, and also for realising that the ring-opening metathesis polymerisation of cycloalkenes (R.O.M.P), and the olefin exchange of acyclic olefins are, in fact, examples of the same general type of reaction[75].

There are three broad classes of olefin metathesis reactions: (I) exchange or disproportionation of acyclic olefins (as shown in equation 1.11), (II) the ring-opening metathesis polymerisation (R.O.M.P) of cycloalkenes, and (III) intramolecular metathesis reactions, of which (II) and (III) are shown below.

(II) $n \bigcirc \longrightarrow$ (polymer structure)

(III) (diene structure) $\longrightarrow$ (products)
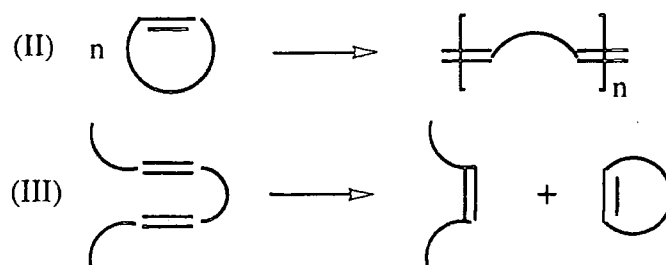
figure 1.14 *(II) R.O.M.P of cycloalkenes and (III) intramolecular metathesis*

These types of reaction are not mutually exclusive, being similar processes, and are often found to occur simultaneously for a given species.

The first example of an olefin metathesis reaction (albeit recognised sometime thereafter) was the R.O.M.P of bicyclo[2.2.1] hept-2-ene (norbornene), using a titanium (IV) catalyst (as shown in equation 1.12), reported in 1955 in a Du Pont patent[76].

$$
n \text{ (norbornene)} \xrightarrow[50^\circ C]{TiCl_4/EtMgBr} \text{ (polymer)}
$$

(1.12)
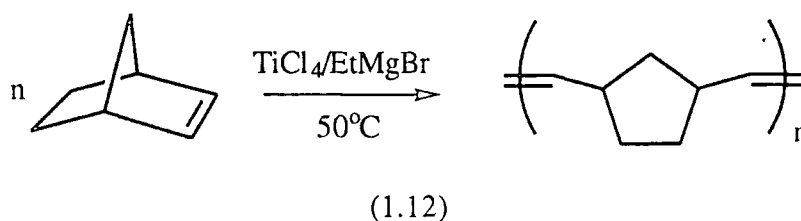
1.4.1 The mechanism of olefin metathesis

The now generally accepted mechanism for olefin metethesis was proposed in 1970 by Herrison and Chauvin, and involves the reversible [2+2] cycloaddition of the olefinic carbon-carbon double bond to a metal carbene species, to afford a metallacyclo-butane intermediate[77]. This intermediate subsequently breaks up either to form a new olefin (productive metathesis), or to regenerate the original olefin (degenerate metathesis), as shown in equation 1.13.

$$
\begin{array}{ccc}
M{=}CHR^1 & & M{=}CHR^2 \\
+ & \rightleftharpoons \quad \text{(metallacyclobutane)} \quad \rightleftharpoons & + \\
R^2CH{=}CHR^3 & & R^1CH{=}CHR^3
\end{array}
$$

(1.13)

20
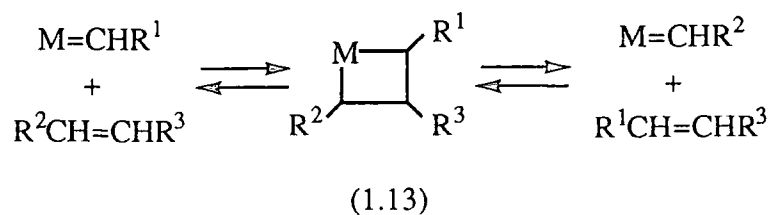
The main evidence for this mechanism at the time came from labelling studies on cross metathesis reactions[78-80], and more recently by the fact that well-defined metal alkylidene conplexes can behave as active R.O.M.P initiators[81-83].

1.4.2 Metathesis initiators

There are three main types of metathesis initiator, the first of which are the early classical ill-defined systems, which typically comprise two or more components. These systems can be divided into heterogenous and homogenous formulations although the distinction is not always clear. The second and third categories encompass well-defined species, namely transition metal carbenes (including Schrock alkylidene and Fischer carbene complexes), and metallacyclobutanes eg.Tebbes reagent.

Classical initiators

Historically, this type of initiating system was the first to be developed and often comprised two or more components, one of which is usually a transition metal species in it's highest oxidation state. Heterogenous formulations include mixed metal oxide species such as Re_2O_7/Al_2O_3[84], $MoO_3/CoO/Al_2O_3$[85] and WO_3/SiO_2[86], whereas homogenous formulations include $WCl_6/EtOH/EtAlCl_2$[87], $WOCl_4/SnMe_4$[88] and $MeReO_3/AlCl_3$[89]. This list is only partially representative of the numerous other initiating systems avaliable, which are reviewed in greater detail in Ivins book[90]. Unfortunately, there are many drawbacks associated with these classical initiating systems, in that for any given formulation, the activity is dependent upon a number of factors. For example, the chemical, thermal and mechanical history, and order and rate of mixing of the catalyst, olefin and co-catalyst. Therefore, quite often results were irreproducible unless particular care and attention to detail was paid. Furthermore, the tolerance of any functionalities present is frequently low, owing to the high Lewis acidity of the metal centre, thereby restricting the number of monomers that could be metathesised. In light of these apparent

disadvantages, the pursuit of Lewis acid free initiators became of paramount importance in this field[91]. A vast research effort by Schrock culminated in the synthesis of highly active four-coodinate molybdenum and tungsten initiators which have many advantages over classical systems[13,92]. The activity of these catalysts can be 'tuned' towards reactivity with acyclic olefins or for the R.O.M.P of cyclic monomers, and therefore they are the choice of initiator employed throughout this thesis, with further discussion concerned solely with their application.

Well-defined four-coordinate molybdenum and tungsten Schrock initiators

The four coordinate 'Schrock' type molybdenum and tungsten initiators $M(CHR)(NAr)(OR')_2$[13,92] (M = Mo, W; R = Bu^t, CMe$_2$Ph; R' = Bu^t, CMe$_2$CF$_3$ and CMe(CF$_3$)$_2$), have only recently become synthetically avaliable. The pseudo tetrahedral geometry of these complexes allows small substrates, such as olefins, to bind to the metal centre, whilst the bulky alkoxide and 'spectator' 2,6-diisopropylphenylimido ligands help to prevent decomposition *via* alkylidene coupling reactions. The molecular structure of $W(CHBu^t)(NAr)(OBu^t)_2$ is shown in figure 1.15, this being typical of the analogous initiators.
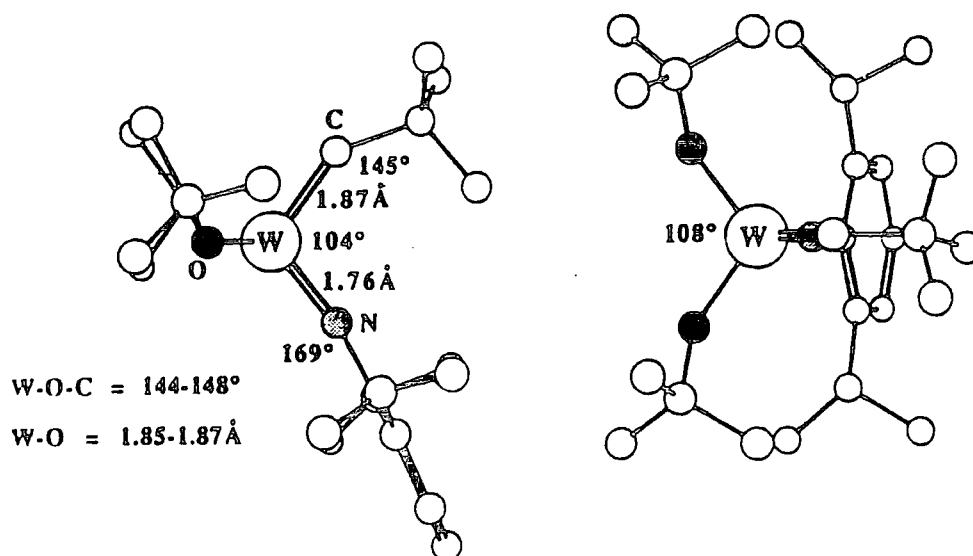
figure 1.15 *Two views of the molecular structure of W(CHBu^t)(NAr)(OBu^t)$_2$*

22

The triply bonded imido group (W-N-C = 169°) forces the β-carbon atom of the alkylidene unit to lie in the same plane as the tungsten, nitrogen and α-carbon atoms. The alkylidene substituent points towards the imido ligand (syn rotamer) in the molecular structure, however, in solution the other isomer in which the alkylidene points away from the imido group (anti rotamer) has been observed[93]. The consequences of these isomers on the polymerisation process are significant, displaying both widely differing reactivities with certain monomers, and affecting the resultant stereochemistry of the polymers generated[94] (discussed further in chapter 4).

The activities of these initiators with acyclic olefins vary dramatically with the nature of the ancillary alkoxide ligands. For example, $W(CHBu^t)(NAr)(OCMe(CF_3)_2)_2$ will metathesise cis-2-pentene at a rate of $\sim 10^3$ turnovers/minute in toluene at room temperature, whereas with $W(CHBu^t)(NAr)(OBu^t)_2$, the corresponding rate of metathesis is only - 2 turnovers/hour[95]. As both these initiators are isostructural, this result is almost certainly related to the different electronic properties of the alkoxides. If the reaction is viewed as the electrophilic attack of the metal on the olefin, then the metal is significantly more electrophilic in $W(CHBu^t)(NAr)(OCMe(CF_3)_2)_2$ than in $W(CHBu^t)(NAr)(OBu^t)_2$, thus rationalising the much increased metathesis rate. The reduced reactivity of the bis tert-butoxide derivative is exploited in the polymerisation of cyclic olefins, in that both the molybdenum and tungsten analogues will react with the strained double bond in norbornene to yield polymers, however, they will not metathesise the double bonds in the growing polymer chain. Therefore polymers can be produced in a controlled 'living' manner.

1.4.3 Living R.O.M.P using well-defined initiators

For a living polymerisation, each monomer unit must add irreversibly, chain transfer and chain termination must be slow on the timescale of the polymerisation reaction itself, and the rate of initiation must be approximately equal to or greater than the rate of propagation[96-98]. Furthermore, the number average molecular weight, M_n, is a

linear function of conversion, thereby implying that M_n can be controlled by the stoichiometry of the reaction. If the above criteria are satisfied, then polymers with the narrowest possible molecular weights can be prepared (polydispersities approaching 1.00). Another advantage of a living polymerisation is that block co-polymers can readily be synthesised[99].

The mechanism of living R.O.M.P

The mechanism for the living R.O.M.P of the highly strained bicyclic norbornene using the initiator $W(CHBu^t)(NAr)(OBu^t)_2$ is shown in figure 1.16[100].
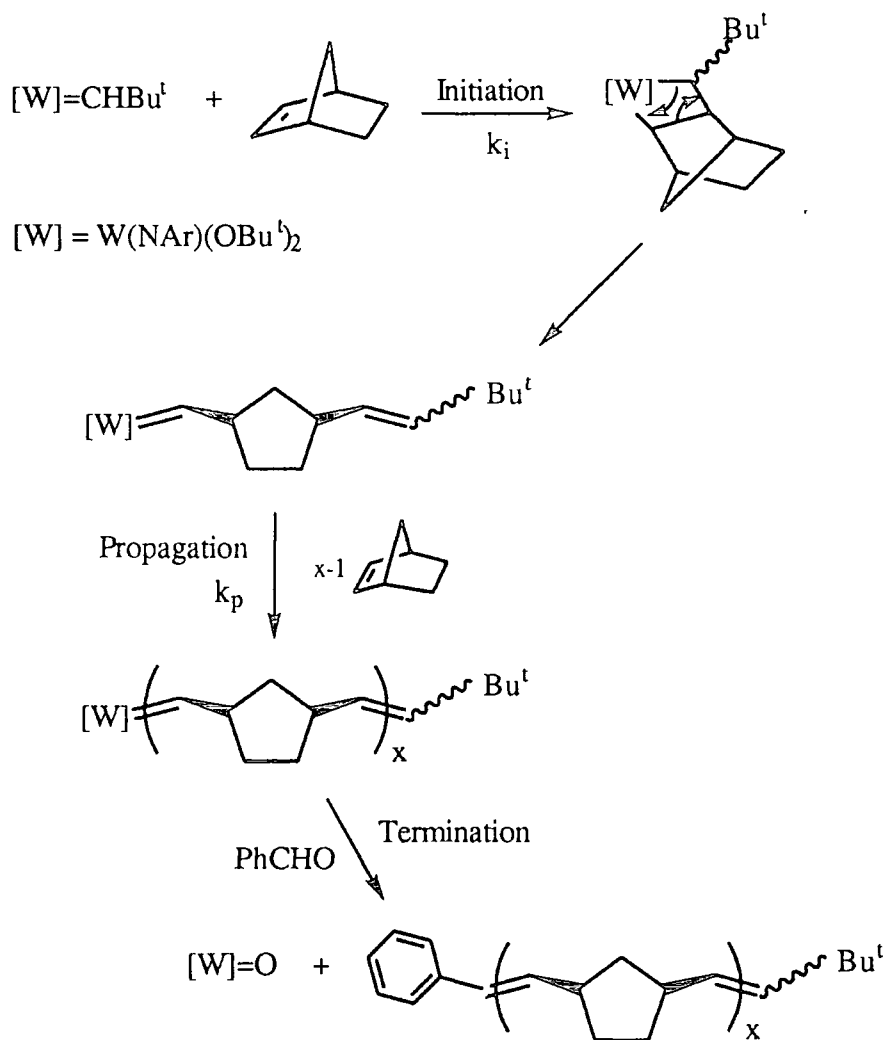
figure 1.16 *The mechanism of the living R.O.M.P of norbornene*

24

In the first step, the initiator reacts with the monomer to form a metallacyclobutane intermediate, which breaks up at a rate k_i to form a propagating alkylidene (first insertion product). This then further reacts with another molecule of monomer at a rate k_p. More monomer can be added and will be continuously consumed at a rate k_p, until termination of the reaction by addition of an aldehyde (typically benzaldehyde), where the polymer is cleaved from the metal centre in a "Wittig like" capping reaction. Throughout the polymerisation, the active site is always attached to the polymer chain and therefore this is an example of a living process. As the identity of the active site on the initiator is known, it's progress can be monitored during the course of initiation and propagation by several techniques.

1.4.4 R.O.M.P of 5-membered rings

Thermodynamic considerations

For highly strained bicyclic olefins, such as norbornenes and norbornadienes, the associated ring strain is large and therefore ring opening is thermodynamically favoured under most conditions. However, for mono-cyclic olefins, the size of the ring is critical in determining whether polymerisation will occur. For 3-,4- and 8-membered rings, R.O.M.P is generally favoured, and will proceed if a suitable mechanism is avaliable[91]. However, in the case of 5-, 6- and 7-membered rings the thermodynamic parameters are finely balanced, due to the small ring strain associated with these species. Physical factors such as temperature, pressure and monomer concentration become more critical in these circumstances, as well as chemical factors, such as the nature of the substituents and their position in the ring. It is notable that cyclohexene does not polymerise as a result of it's small strain energy (ΔH is too small to offset the large positive value of $-T\Delta S$). Generally, favourable conditions for the attempted polymerisation of new species are high monomer concentration (makes ΔS less negative), low temperature (if ΔH is negative) and high pressure (if ΔV is negative).

R.O.M.P of cyclopentene

There are many reports of the polymerisation of cyclopentene with classical initiator systems, owing to the potential importance of poly(1-pentenylene) as an elastomer[90]. However, for the purpose of this review, attention will be focused on it's R.O.M.P with well-defined initiators. Cyclopentene has been examined by Schrock and co-workers using the well-defined initiator $W(CHBu^t)(NAr)(OBu^t)_2$[101]. At -40°C, approximately 95% of the monomer has been converted to polypentamer, but at 25°C, there is only approximately 80% of the original monomer still present. This reversible R.O.M.P of cyclopentene reflects the delicate balance between polymerisation and de-polymerisation in 5-membered ring systems, owing to the small inherent ring strain. In addition, a general feature of the R.O.M.P of this cyclopentene (and certain other cyclic olefins), is that often as well as the formation of high polymer, low molecular weight fractions are also present, consisting of cyclic oligomers. The formation of these species is favoured at low monomer concentrations (i.e in dilute solution) and when the ring strain is lower than that present in the monomer. In this respect, the R.O.M.P of heteroatom containing cyclopentenes is of interest in possibly generating both new cyclic and polymeric materials, which may have technological relevance.

R.O.M.P of functionalised cyclopentenes

To date, there have been very few examples reported of the R.O.M.P of heterocyclopentenes, for both classical and well-defined initiating systems. Classical systems are generally intolerant of functionalities (as previously discussed). However, the well-defined molybdenum Schrock initiators show a high tolerance to varied functionalities[102-104], although interestingly, the same tolerance is not displayed by the tungsten analogues[105]. A possible reason for this may be the increased electrophilicity of tungsten, thereby making it prone to react more readily with a given functionality, or active protons in the polymer chain. Owing to the relatively recent development of the

molybdenum Schrock initiators, there is undoubtedly an early opportunity to explore their activity with hetero-cyclopentenes (in chapter 4).

One rare example of the R.O.M.P of a hetero-cyclopentene, is that of 1,1-disubstituted sila-3-cyclopentenes, which has been successfully polymerised using classical systems[106], and more recently with Mo(CHCMe2Ph)(NAr)(OCMe(CF3)2)2[107]. In the case of the well-defined molybdenum initiator, novel 10-membered ring systems (cyclo-dimers) can also be isolated depending upon the reaction conditions. For instance, in dilute aromatic solvent (d6-benzene), there is an equilibrium mixture of the 10-membered ring (disilacyclodeca-3,8-diene), monomer and a trace of living oligomers. However, in the absence of solvent, the product formed is exclusively polymer. The cyclo-dimer arises by the secondary metathesis or backbiting reactions in which the living alkylidene metathesises a double bond in the living polymer chain. This is consistent with the highly reactive nature of the hexafluoro-t-butoxide initiator, which has been shown to be capable of metathesising ordinary olefins[92]. The overall reactivity is summarised in figure 1.17.

R = R' = Ph

R = Ph, R' = Me

+ [Mo]=CHMe$_2$Ph

[Mo]

[Mo] = (NAr)(OCMe(CF$_3$)$_2$

dilute solution

R'RSi   SiRR'   +
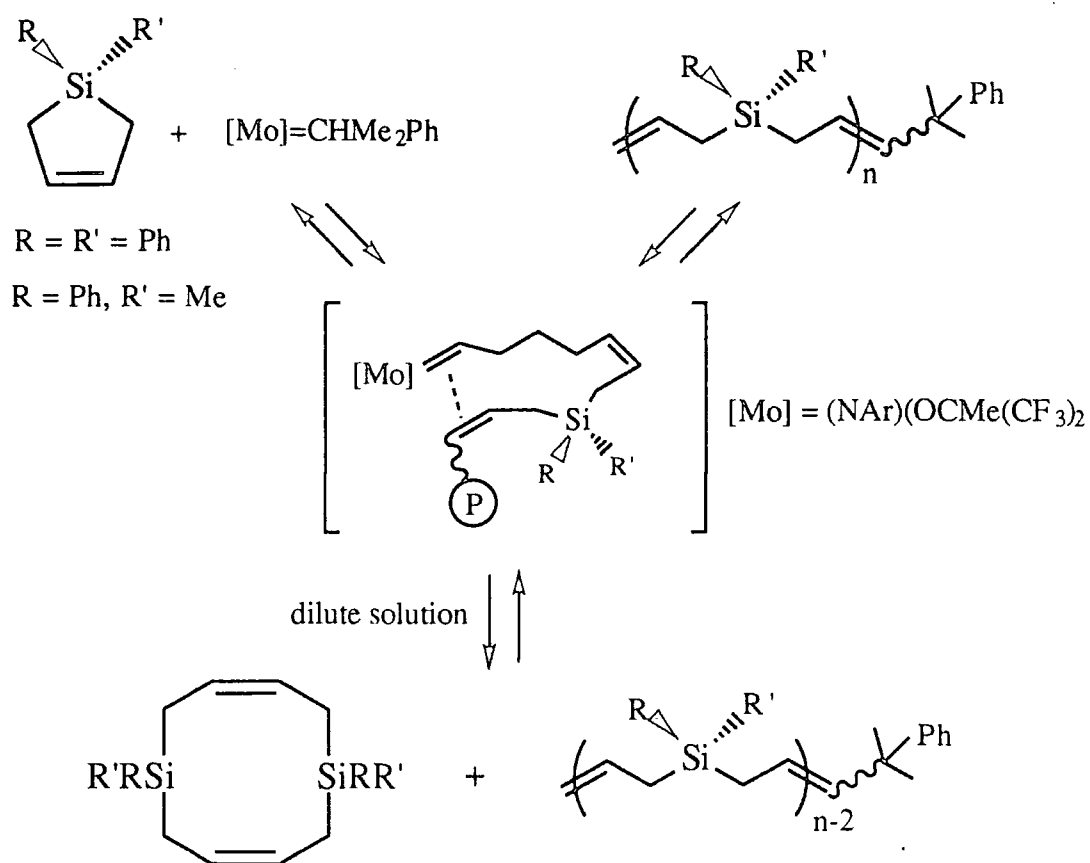
figure 1.17 *The living R.O.M.P of 1,1-disubstituted silacyclopent-3-ene*

A further related example of the living R.O.M.P of a 5-membered heterocycle is that of disilacyclopent-3-ene (figure 1.18), which is found to polymerise irreversibly in high yield and high stereoselectivity (97% trans), using the molybdenum Schrock initiator Mo(CHMe$_2$Ph)(NAr)(OCMe(CF$_3$)$_2$)$_2$[108].

SiMe$_2$
SiMe$_2$
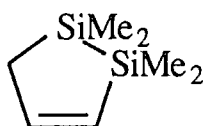
figure 1.18 *1,1,2,2-tetramethyl-1,2-disilacyclopent-3-ene*

On dissolution of a sample of the crude living polymer in d$_6$-benzene, there is no evidence for the formation of any linear or cyclic oligomers. The irreversibility of this

28

reaction is credited to the high torsional strain present in the ring, due to conformationally enforced eclipsing of the methyl groups on the silicons.

1.4.5 Acyclic Diene Metathesis (ADMET)

Acyclic α-,ω-dienes have significant importance in olefin metathesis reactions in that theoretically, given the right conditions, it is possible for polymer to be formed. However, until the advent of well-defined Schrock initiators, the potential of these materials for the synthesis of polymeric materials could not be achieved.

Both inter- and intramolecular metathesis reactions can occur for α-,ω-dienes, resulting in the formation of several possible products. For instance, the intramolecular cyclisation shown below for octa-1-7-diene is particularly favoured, owing to the formation of cyclohexene[109].

91% yield

initiator = $MoCl_2(NO)_2(PPh_3)_2/Me_3Al_2Cl_3$
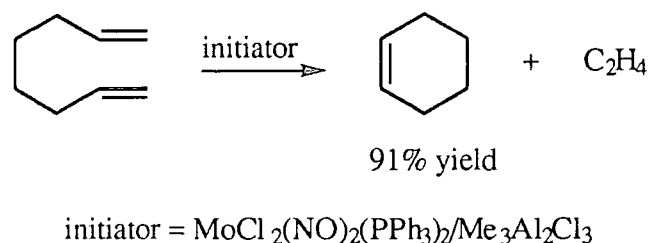
figure 1.19 *Intramolecular cyclisation of octa-1-7-diene*

Intermolecular reactions generally arise when rings with low strain energies (i.e 5- and 6-membered rings) cannot be formed. For example, the double bonds in hexa-1,5-diene are unfavourably situated for intramolecular reaction of either the parent diene (would afford cyclobutene) or the initial metathesis products deca-1,5,9-triene, which would give cycloocta-1,5-diene, as shown in figure 1.20.
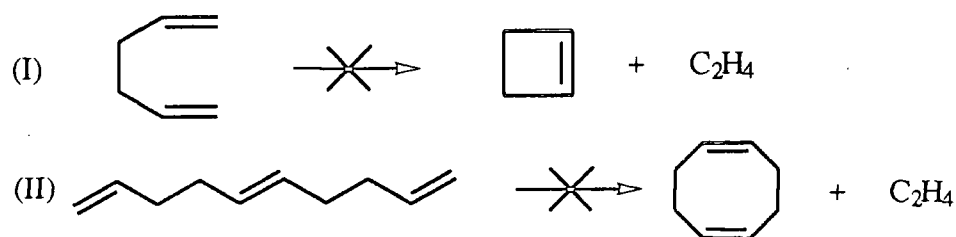
figure 1.20 *Intramolecular cyclisation of (I) hexa-1,5-diene and (II) deca-1,5,9-triene*

In fact, linear products of the type $CH_2=[CHCH_2CH_2CH_2CH]_n=CH_2$ are found when the reaction is catalysed by $WCl_6/EtAl_2Cl_3/MeCCl(OH)CH_2Cl/PPh_3$, with n up to 8 monomer units[110]. Greater molecular weights are achieved when the monomer was treated with $WCl_6/EtAlCl_2$, and a slight vacuum applied to the system[111]. The removal of the ethylene gas evolved (determined by G.C) drives the equilibrium (shown in figure 1.21) over to the product side.

initiator = $WCl_6/EtAlCl_2$
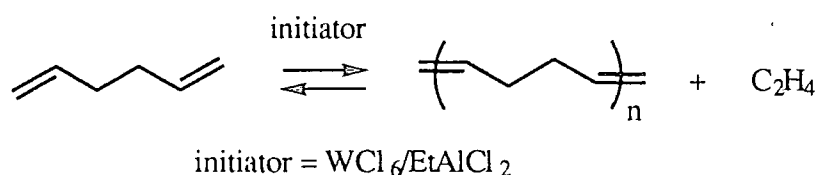
figure 1.21 *ADMET polymerisation of 1,5-hexadiene*

However, the molecular weights achieved were found to be less than 5000, clearly demonstrating that there was some way to go before genuine high polymers could be generated. The low molecular weights were ascribed to competing side reactions, particularly acid catalysed vinyl addition. The evidence for this process was elucidated when styrene was reacted with the aforementioned initiating system. Productive metathesis of this monomer would lead to the formation of stilbene, however, the actual product was polystyrene, formed by vinyl addition reactions, as shown in figure 1.22.
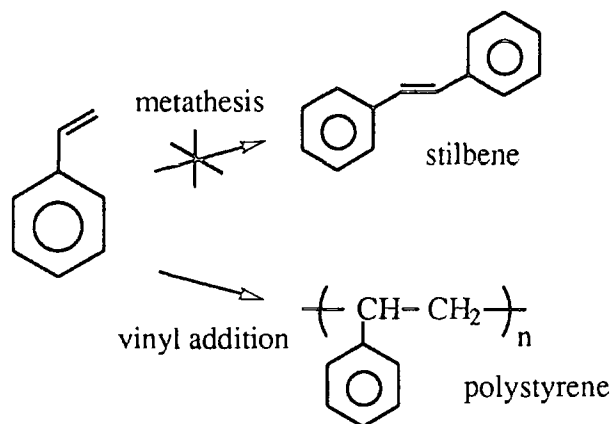
figure 1.22 *Reaction of styrene with WCl$_6$/EtAlCl$_2$*

The lewis acid metal centres are blamed for the above side reaction, therefore a catalyst free of any lewis acid co-catalyst was required if polymers rather than oligomers were to be obtained.

1.4.6 ADMET using the well-defined four coordinate molybdenum and tungsten initiators

The well-defined hexafluoro-tert-butoxide molybdenum and tungsten Schrock initiators are ideal catalysts for ADMET in that they are capable of metathesising ordinary olefins and behave in a uniform manner. Furthermore, they do not contain very strong lewis acid centres and are therefore not likely to propagate vinyl addition reactions[83]. This was indeed shown to be the best choice of initiator; in subsequent reactivity studies with styrene (readily disposed to undergo vinyl addition chemistry), they were found to not only generate the metathesis product (stilbene), but to exhibit more activity than a host of other initiators (see figure 1.22)[112]. When 1,5-hexadiene was treated with W(CHBu^t)(NAr)(OCMe(CF$_3$)$_2$))$_2$[113], the polybutadiene produced was of molecular weight $M_n \sim$ 14,000. Higher molecular weights could be achieved by redissolving the previously prepared polymers and subsequently reacting with a second portion of catalyst. The reaction was performed under high vacuum so that it could be driven towards the product side (by removal of generated ethylene).

31

As a consequence of the tolerance to functionalities displayed by the molybdenum Schrock initiator (discussed in section 1.4.4), ADMET polymerisation has been put to prolific use by Wagener over the past three years for a variety of functionalised α-ω-dienes. Unsaturated polymers containing ether[114], thioether[115], carbonate[116] ester[117], silane[118], siloxane[119] and ketone[120] functionalities have been prepared with this initiator.

Mechanism of ADMET polymerisation

Figure 1.23 displays a typical acyclic diene metathesis polymerisation using for example the molybdenum Schrock initiator $Mo(CHBu^t)(NAr)(OCMe(CF_3)_2)_2$, in which only the simple productive metathesis steps are shown for simplification.
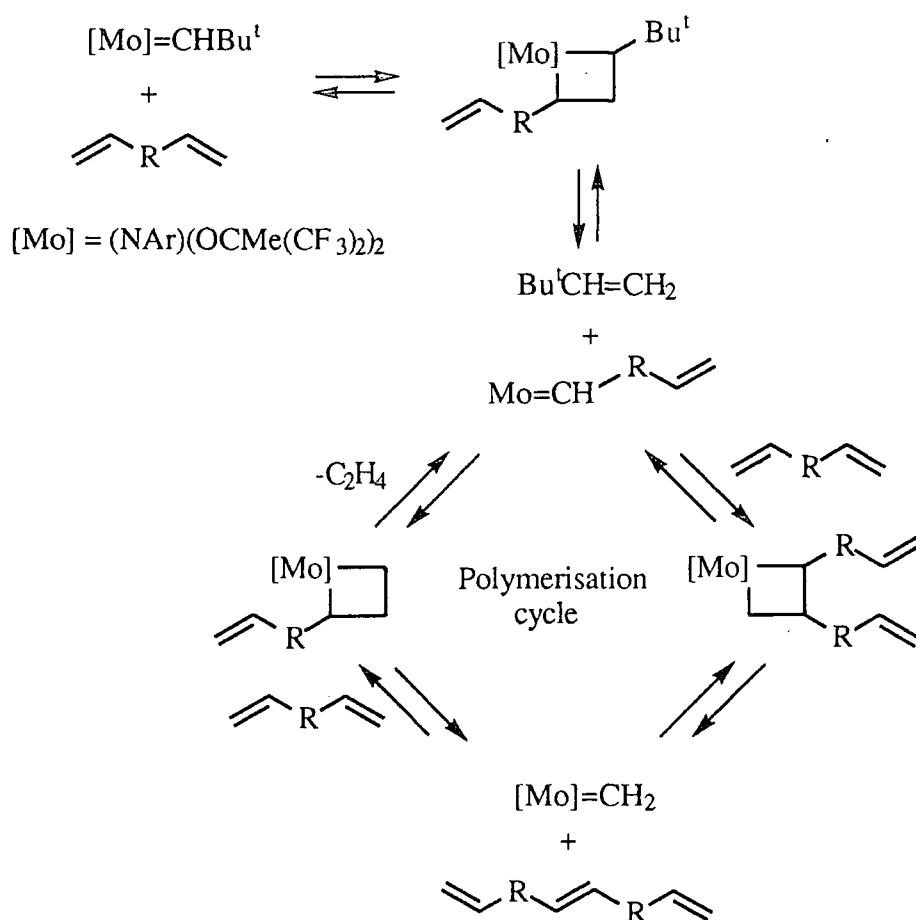
figure 1.23 Mechanism for productive ADMET polymerisation with

The metal alkylidene can attack at either carbon-carbon double bond in the monomer. Ethylene is produced in the polymerisation cycle and therefore, as the process is an equilibrium, the reaction can be driven to completion by the its removal. However, very reactive methylidene complexes are generated which are inherently unstable and therefore could result in the premature end of the cycle, which probably explains why monomer turnovers of greater than 500 equivalents have not been observed[114]. The overall process is therefore a step propagation condensation type polymerisation which should produce a molecular weight distribution of 2.0, whereas in R.O.M.P molecular weight distributions can approach 1.0[97] (consistent with the living chain addition polymerisation for the latter).

1.5 References

1. J.M.Mayer, D.L.Thorn, T.H.Tulip, *J. Am. Chem. Soc.* 1985, **107**, 5454.

2. J.M.Mayer, T.H.Tulip, J.C.Calabrese, E.Valencia, *J. Am. Chem. Soc.* 1987, **109**, 157.

3. M.E.Marmion, K.J.Takeuchi, *J. Am. Chem. Soc.* 1986, **108**, 510.

4. L.Roeker, T.J.Meyer, *J. Am. Chem. Soc.* 1986, **108**, 4066.

5. D.W.Pipes, T.J.Meyer, *Inorg. Chem.* 1986, **25**, 3256.

6. J.M.Mayer, Comments. *Inorg. Chem.* 1988, **8**, 125.

7. C.T.Vroegop, J.H.Teuben, F.Van Bolhuis, J.G.M.Van der Linden, *J. Chem. Soc. Chem. Commun.* 1983, 550.

8. W.A.Nugent, R.L.Harlow, *Inorg. Chem.* 1979, **18**, 2030.

9. F.Preuss, H.Becker, J.Kaus, W.S.Sheldrick, *Z. Naturforsch. part B*, 1988, **43**, 1195.

10. W.A.Nugent, R.L.Harlow, *J. Am. Chem. Soc.* 1980, **102**, 1759.

11. V.C.Gibson, D.N.Williams, U.Siemeling, A.D.Poole, J.P.Mitchell, D.C.R.Hockless, P.A.O'Neil, W.Clegg, *J. Chem. Soc. Dalton trans.* 1992, 739.

12. W.A.Hermann, G.Weichselbaumer, R.A.Paciello, R.A.Fiss, E.Herdtweck, J.Okuda, D.W.Marz, *Organometallics.* 1990, **9**, 489.

13. R.R.Schrock, C.J.Schavarian, J.C.Dewan, *J. Am. Chem. Soc.* 1986, **108**, 2771.

14. I.P.Rothwell, J.L.Kerschner, J.S.Yu, P.E.Fanwick, C.Huffman, *Organometallics.* 1989, **8**, 1414.

15. J.M.Mayer, A.L.Rheingold, C.Cooper, S.J.Geib, *J. Am. Chem. Soc.* 1986, **108**, 3545.

16. J.M.Mayer, A.L.Rheingold, J.C.Bryan, S.J.Geib, *J. Am. Chem. Soc.* 1987, **109**, 2826.

17. J.E.Bercaw, G.Parkin, A.Van Asselt, D.J.Leahy, L.Whinnery, N.G.Hua, R.W.Quay, L.M.Henling, W.P.Schaeffer, B.D.Santarsiero, *Inorg. Chem.* 1992, **31**, 82.

18. R.Hoffmann, J.W.Lauher, *J. Am. Chem. Soc.* 1976, **98**, 1729.

19. R.R.Schrock, J.T.Anhaus, T.P.Kee, M.H.Schofield, *J. Am. Chem. Soc.* 1990, **112**, 1642.

20. R.G.Bergman, F.J.Hollander, P.J.Walsh, *J. Am. Chem. Soc.* 1988, **110**, 8729.

21. E.A.Maata, R.A.D.Wentworth, B.L.Haymore, *J. Am. Chem. Soc.* 1979, **101**, 2063.

22. J.E.Bercaw, J.M.Mayer, C.J.Curtis, *J. Am. Chem. Soc.* 1983, **105**, 2651.

23. R.R.Schrock, S.M.Rocklage, *J. Am. Chem. Soc.* 1982, **104**, 3077.

24. W.A.Nugent, R.J.McKinney, R.V.Kasowski, F.A.Van Gartledge, *Inorg. Chim. Acta.* 1928, **65**, L91.

25. B.R.Ashcroft, G.R.Clark, A.J.Nielson, C.E.F.Rickard, *Polyhedron.* 1985, **5**, 2081.

26. P.W.Dyer, Unpublished results.

27. This thesis, Chapter 2.

28. W.A.Nugent, R.L.Harlow, *Inorg. Chem.* 1980, **19**, 777.

29. A.K.Clifford, C.S.Kobayashi, *Abstracts of, 130th meeting of Am. Chem. Soc,* 1957.

30. K.B.Sharpless, K. Oshima, A.O.Chong, *J. Am. Chem. Soc.* 1977, **99**, 3420.

31. R.R.Schrock, *J. Am. Chem. Soc.* 1974, **96**, 6796.

32. E.O.Fischer, A.Maasböl. *Angew. Chem. Int. Ed. Engl.* 1964, **3**, 580.

33. H.Nakatsuji, J.Ushio, S.Han, T.Yonezawa *J. Am. Chem. Soc,* 1983, **105**, 426.

34. W.A.Goddard III, A.K.Rappé, *J. Am. Chem. Soc,* 1986, **108**, 2180; 4746.

35. W.A.Goddard III, A.K.Rappé, *J. Am. Chem. Soc.* 1982, **104**, 448.

36. M.B.Hall, T.E.Taylor, *J. Am. Chem. Soc.* 1984, **106**, 1576.

37. W.A.Goddard III, A.K.Rappé, *J. Am. Chem. Soc.* 1977, **99**, 3966.

38. C.J.Ballhausen, H.B.Grey, *"Molecular orbital theory"*, W.A.Benjamin, New York.

39. E.A.Maata, R.A.D.Wentworth, *Inorg. Chem.* 1979, **18**, 2409.

40. B.Kamenar, M.Penavic, C. Prout, *Cryst. Struc. Comm.* 1973, **2**, 41.

41. E.A.Maata, R.A.D.Webtworth, *Inorg. Chem.* 1979, **18**, 2409.

42. W.A.Goddard III, A.K.Rappé, *J. Am. Chem. Soc.* 1986, 104, 3287.

43. W.A.Goddard III, J.A.Allison, A.C.S. Symposium series *"solid state chemistry in catalysis"*, 1985, 25, 279.

44. R.R.Schrock, J.C.Dewan, C.J.Schavarian, *J. Am. Chem. Soc.* 1986, 108, 2771.

45. R.R.Schrock, J.S.Murdzek, *Organometallics.* 1987, 6, 1373.

46. T.V.Leuben, P.T.Wolczanski, G.D.Van Duyne, *Organometallics.* 1984, 3, 977.

47. H.Weingold, P.C.Wailes, A.P.Bell, *J. Organomet. Chem.* 1972, 34, 155.

48. M.H.Chisholm, J.C.Huffman, K.Folting, R.J.Tatz, *J. Am. Chem. Soc.* 1984, 106, 1153.

49. M.H.Chisholm, I.P.Rothwell, *"Comprehensive coordination chemistry"*, Volume II, pg 336-364, Pergamon Press, 1987.

50. D.C.Bradley, R.C.Mehotra, D.P.Gauer, *"Metal alkoxides"*, Academic Press, 1978.

51. D.C.Bradley, I.M.Thomas, *Can. J. Chem.* 1962, 40, 1355.

52. M.F.Lappert, P.Power, A.R.Sanger, R.C.Srivastava *"Metal and metalloid amides"*, Wiley, 1980.

53. V.C.Gibson, P.W.Dyer, B.Whittle, J.A.K.Howard, C.Wilson, *J. Chem. Soc. Chem. Commun.* 1992, 1666.

54. V.C.Gibson, J. Chem. Soc. Dalton trans. In press.

55. R.R.Schrock, M.H.Schofield, D.S.Williams, *Organometallics.* 1993, 12, 4560.

56. H.Taube, T.J.Meyer, *"Comprehensive coordination chemistry"*, Volume I, pg 331.

57. G.J-J.Chen, J.W.McDonald, W.E.Newton, *Inorg. Chim. Acta.* 1976, 19, L67.

58. L.K.Woo, J.G.Goll, *J. Am. Chem. Soc.* 1989, 111, 3755.

59. L.K.Woo, D.J.Czapla, J.G.Goll, *Inorg. Chem.* 1990, 29, 3915.

60. J.T.Groves, R.J.Quinn, *J. Am. Chem. Soc.* 1985, 107, 5970.

61. R.D.Gorsich, *J. Am. Chem. Soc.* 1958, 80, 4744.

62. G.E.Coates, D.Ridley, *J. Chem. Soc.* 1965, 870.

63. W.Schlenk, W.Schlenk, *Chem. Ber.* 1929, 62, 920.'

64. A.D.Poole, Ph.D Thesis, University of Durham, 1992.

65. M.H.Chisholm, K. Folting, J.C.Huffman, C.C.Kirkpatrick, *Inorg. Chem.* 1984, **23**, 1021.

66. D.E.Wigley, D.J.Arney, P.A.Wexler, *Organometallics,* 1990, **9**, 1282.

67. H.Weingarten, J.R.Van Wazer, *J. Am. Chem. Soc.* 1965, **87**, 724.

68. H.Weingarten, J.R.Van Wazer, *J. Am. Chem. Soc.* 1966, **88**, 2700.

69. R.R.Schrock, J.H.Wengrovious, *J. Am. Chem. Soc.* 1980, **102**, 4515.

70. R.R.Schrock, J.H.Wengrovious, *Organometallics.* 1982, **1**, 148.

71. R.R.Schrock, S.F.Pederson, *J. Am. Chem. Soc.* 1982, **104**, 7483.

72. R.R.Schrock, A.M.LaPointe, *Organometallics.* 1993, **12**, 3379.

73. V.C.Gibson, M.Jolly, J.P.Mitchell, *J. Chem. Soc. Dalton Trans.* 1992, 1331.

74. R.R.Schrock, G.C.Bazan, J.R.Wolf, *Inorg. Chem.* 1993, **32**, 4155.

75. N.Calderon et al., *Chem. Eng. News.* 1967, **45**, 51.

76. A.W.Anderson, N.G.Merckling, US Pat. 2721189, *Chem. Abstr,* 1955, **50**, 3008.

77. J.L.Herrison, Y.Chauvin, *Makromol. Chem.* 1970, **141**, 161.

78. R.H.Grubbs, D.D.Carr, C. Hoppin, P.L.Burk, *J. Am. Chem. Soc.* 1976, **98**, 3478.

79. T.J.Katz, J.McGinnis, *J. Am. Chem. Soc.* 1977, **99**, 1903.

80. T.J.Katz, R.Rothchild, *J. Am. Chem. Soc.* 1976, **98**, 2519.

81. R.H.Grubbs, L.R.Gilliom, *J. Am. Chem. Soc.* 1986, **108**, 733.

82. R.R.Schrock, *Acc. Chem. Res.* 1990, **23**, 158.

83. J.Kress, J.A.Osborn, R.M.E.Green, K.J.Ivin. J.J.Rooney, *J. Am. Chem. Soc.* 1987, **109**, 899.

84. J.C.Mol, J.A.Moulin, C.Boelhower, *J. Chem. Soc. Chem. Commun.* 1968, 663.

85. J.R.Hardee, *Diss. Abstr. Int. B.* 1979, **40**, 1186.

86. F.R.J.M.Kerhof, R.Thomas, T.A.Molijn, *Recl. Trav. Chim. Pays-bas.* 1977, 96, M21.

87. N.Calderon, E.A.Offstead, J.P.Ward, W.A.Judy, K.W.Scott, *J. Am. Chem. Soc.* 1968, **90**, 4133.

88. J.L.Herrison, Y.Chauvin, N.H.Phung, G.Lefebvre, *C.R. Acad. Sci. Ser. C,* 1969, **269**, 661.

89. W.A.Hermann, J.G.Kuchler, J.K.Felixberger, E.Herdtwick, W.Wagner, *Angew. Chem. Int. Ed. Engl.* 1988, **27**, 394.

90. K.J.Ivin, *"Olefin Metathesis"*, Academic Press, London, 1983.

91. R.R.Schrock, *J. Organomet. Chem.* 1986, **300**, 249.

92. R.R.Schrock, J.S.Murdzek, G.C.Bazan, J.Robbins, M. Dimare, M.O'Regan, *J. Am. Chem. Soc.* 1990, **112**, 3875.

93. R.R.Schrock, G.C.Bazan, W.E.Crowe, M.Dimare, M.B.O'Regan, M.H.Schofield,*Organometallics.* 1991, **10**, 1832.

94. R.R.Schrock, J.Oskam, *J. Am. Chem. Soc.* 1992, **114**, 1589.

95. R.R.Schrock, J.Depue, J.Feldman, C.J.Schavarian, J.C.Dewan, A.H.Liu, *J. Am. Chem. Soc.* 1988, **110**, 1423.

96. L.Gold, *J. Chem. Phys.* 1958, **28**, 91.

97. G.Odian, *"Principles of polymerisation"*, Wiley, New York, 1981.

98. A.H.E.Muller, *"Comprehensive polymer science"*, Pergamon, New York, 1989.

99. A.Noshay, J.E.McGrath, *"Block copolymers"*, Academic Press, New York, 1977.

100. R.R.Schrock, J.Feldman, R.H.Grubbs, L.Cannizo, *Macromolecules.* 1987, **20**, 1169.

101. R.R.Schrock, K.B.Yap, D.C.Yang, H.Sitzman, L.R.Sita, G.C.Bazan, *Macromolecules.* 1989, **22**, 3191.

102. R.R.Schrock, J.S.Murdzek, *Macromolecules.* 1987, **20**, 2640.

103. R.R.Schrock, W.J.Feast, V.C.Gibson, G.Bazan, E.Khosravi, *Polymer. Commun.* 1989, **30**, 258.

104. R.R.Schrock, V.C.Gibson, G.C.Bazan, H.N.Cho, *Macromolecules.* 1991, **24**, 4495.

105. R.R.Schrock, R.T.DePue, J.Feldman, K.B.Yap, D.C.Yang, W.M.Davis, L.Y.Park, M.Dimare, M.H.Schofield, J.T.Anhaus, E.Walborski, E.Evitt, C.Kruger, P.Betz, *Organometallics.* 1990, **9**, 2262.

106. H.Lammens, G.Sartori, J.Siffert, N.Sprecher, *J. Polymer. Sci., Part B*. 1971, **9**, 341.

107. V.C.Gibson, S.P.Collingwood, J.T.Anhaus, W.Clegg, *Organometallics*. 1993, **12**, 1780.

108. L.R.Sita, S.R.Lyon, *J. Am. Chem. Soc.* 1993, **115**, 10374.

109. E.A.Zeuch, W.B.Hughes, D.H.Kubiek, E.T.Kittelman, *J. Am. Chem. Soc.* 1970, **92**, 528.

110. G.Dall'Asta, G.Stigliani, A.Greco, L.Motta, *Chim. Ind. (Milan)*, 1973, **55**, 142.

111. K.B.Wagener, M.L-Hanberg, *Macromolecules*. 1987, **20**, 2949.

112. K.B.Wagener, G.M.Boncella, J.G.Nel, R.P.Duttweiler, M.A.Hillmeyer, *Makromol. Chem.* 1990, **191**, 365.

113. K.B.Wagener, G.M.Boncella, J.G.Nel, *Macromolecules*, 1991, **24**, 2649.

114. K.B.Wagener, K.Brzezinska, *Macromolecules*, 1991, **24**, 5273.

115. K.B.Wagener, J.E.O'Gara, J.D.Portness, *Macromolecules*. 1993, **26**, 2837.

116. K.B.Wagener, J.T.Patton, *Macromolecules*. 1993, **26**, 249.

117. K.B.Wagener, J.T.Patton, *Abs. Am. Chem. Soc.* 1992, **203**, 48.

118. K.B.Wagener, D.W.Smith Jr., *Macromolecules*. 1991, **24**, 6073.

119. K.B.Wagener, D.W.Smith Jr., *Macromolecules*. 1993, **26**, 1633.

120. K.B.Wagener, J.T.Patton, *Abs. Am. Chem. Soc.* 1992, **203**, 49.

121. M.L.H.Green, P.C.Konidaris, P.Mountford, S.J.Simpson, *J. Chem. Soc. Chem. Commun.* 1992, 256.

Chapter Two

The Synthesis and Exchange Reactivity of Molybdenum

Complexes of the type - MoQ_2X_2

2.1 Introduction

This chapter describes the results of investigations into the heteroatom exchange reactivity of four coordinate molybdenum (VI) complexes of the type MoQ_2X_2 ($Q = O$, NR, $(NAr)(CHCMe_2Ph)$; $X = Cl$, NHR, OR). The mechanistic details of the intermetal oxo-imido exchange reaction are probed, and the factors that affect these equilibria are examined. In certain cases a favourable equilibrium may be exploited to synthesise new oxo-imido complexes. The intermetal exchange of mono-anionic (X-type) ligands in several systems of the type MoQ_2X_2 are also investigated and the results discussed in conjunction with one mono-anionic ligand exchange for the $CpNb(NBu^t)X_2$ system later in chapter 3.

Due to the enhanced reactivity of multiply bonded ligands in systems of this type (as discussed in section 1.2.4), the reactivity of the multiply bonded imido ligands in $Mo(NBu^t)_2(OBu^t)_2$ towards a variety of substrates are investigated.

2.2 Imido ligand exchange reactivity of $Mo(NBu^t)_2(OBu^t)_2$

2.2.1 Reaction of $Mo(NBu^t)Cl_2$ with $LiOBu^t$

Preparation of $Mo(NBu^t)_2(OBu^t)_2$ (1)

The reaction of $Mo(NBu^t)_2Cl_2$[1] with two equivalents of $LiOBu^t$ in diethyl ether occured rapidly on warming to room temperature, according to equation 2.1:

$$Mo(NBu^t)_2Cl_2 + 2\,LiOBu^t \longrightarrow Mo(NBu^t)_2(OBu^t)_2 + 2\,LiCl$$
$$(1)$$

$$(2.1)$$

Recrystalisation of (1) from the mother liquor failed to yield a solid product. Nonetheless, (1) was eventually isolated in excellent yield, after removal of the solvent *in vacuo* , as a low melting pale green solid (Mpt = 25-27°C). This low melting point is credited to the

presence of four bulky tert-butyl substituents on the metal centre which would undoubtedly reduce intermolecular forces.

The ^{1}H NMR (400 MHz, C_6D_6) spectrum of (1) revealed two singlet resonances of equal intensity at δ 1.36 and 1.38. An assignment of these methyl resonances to their respective tert-butyl imido and alkoxide ligands could not be made, owing to similar chemical shifts in both the ^{1}H and ^{13}C NMR. The mass spectrum (CI) showed an envelope for the protonated parent (monomeric) molecular ion (Mo^{98}) at 387.

The tunsten and chromium analogues of (1) are known[2,3], the former being a yellow distillable oil at room temperature. Since the molybdenum derivative described here was to feature extensively in the subsequent investigations of imido ligand exchange reactivity, the solid state structure was also of considerable interest to us.

2.2.2 The molecular structure of Mo(NBu^t)$_2$(OBu^t)$_2$ (1)

Chisholm has synthesised the para-tolyl and phenyl imido analogues of (1) via reaction of Mo$_2$(OBu^t)$_6$ with aryl azides as shown in equation 2.2[4]:

$$Mo_2(OBut)_6 + 4\ ArN_3 \longrightarrow [Mo(NAr)_2(OBu^t)_2]_2 + 4\ N_2 + 2\ Bu^tOH$$

$$(2.2)$$
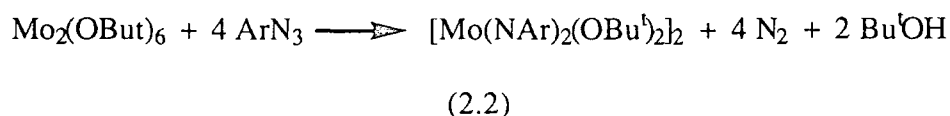
In addition, the 2,6 diisopropylphenyl imido analogue has also been synthesised[5,6].

The molecular structure of the para-tolyl imido derivative is reported as an imido bridged dimer (figure 2.1). However, in solution this complex is monomeric, as determined by cryoscopic molecular weight methods.
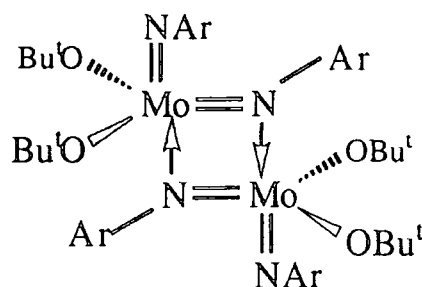
figure 2.1 *Molecular structure of [Mo(NAr)(OBu^t)$_2$(μNAr)]$_2$*

Suitable pale green cubic crystals of (1) were mounted in 0.5 mm Lindemann capillary tubes under an inert atmosphere at ambient temperature. The X-ray data were collected at low temperature (150K) owing to the large thermal vibrations of the complex at room temperature. The structure was solved by Ms.C.Wilson and Professor J.A.K.Howard of Durham University. The molecular structure is illustrated in figures 2.2(a) and 2.2(b) and selected bond distances and angles are given in in table 2.1. Figure 2.2(b) views the molecule in the N(1)-Mo-N(2) plane, from which the two crystallographically distinct imido groups can easily be distinguished (Mo-N(1)-C(9) = 169.6(6)^o, Mo-N(1) = 1.714(5)Å; Mo-N(2)-C(13) = 157.1(5)^o, Mo-N(2) = 1.776(6)Å). The bent imido ligand has a substantially longer metal-nitrogen bond distance than the near linear imido ligand, which may reflect a relative reduction in the π bond order for this imido bond. These differences in imido ligand bond parameters may arise due to competition for the three avaliable π bonding orbitals at the metal centre. Each imido unit can potentially form two π bonds (formally a sp hybridised, 4 electron donor) to the metal centre, but for the tetrahedral geometry there are insufficient π bonding orbitals available. Therefore, there is potentially an electronic compromise in which the bent imido could be considered to form one π bond (formally sp^2 hybridised, 2 electron donor). However this is an extreme description that is not entirely applicable. In reality, these electronic extremes are not realised, instead averaging of the electron density between both imidos at the metal centre (the difference in Mo-N-C bond angles being only 13°) will occur.

Figure 2.1 *The molecular structure of Mo(NBuᵗ)₂(OBuᵗ)₂ (1).*
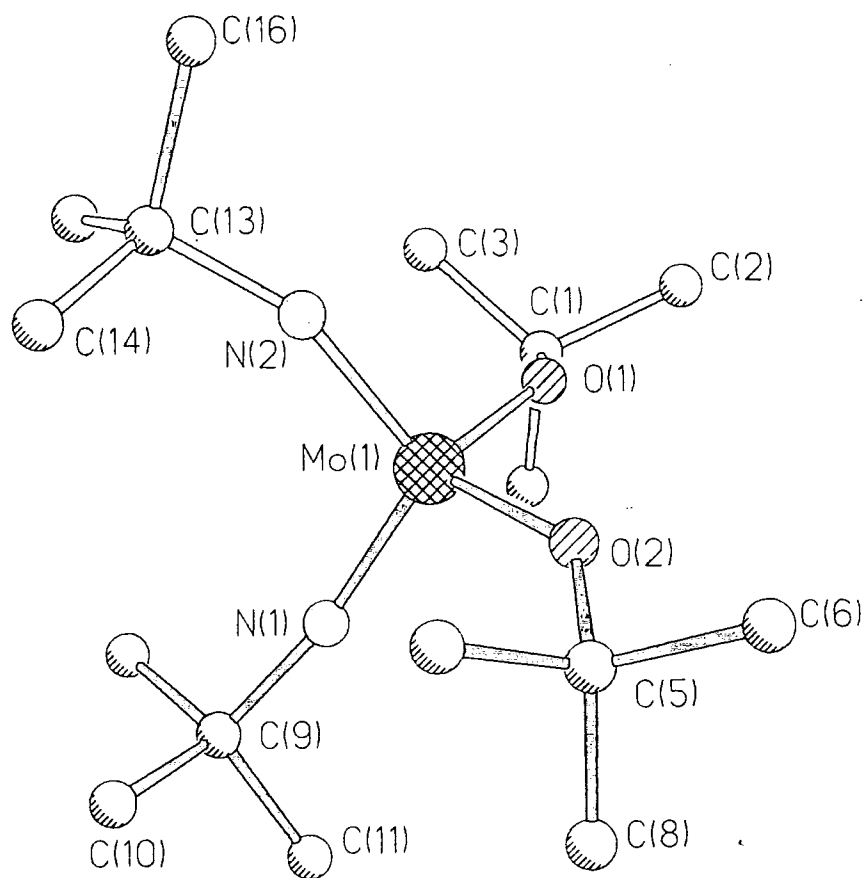
(a) View showing the atom labelling (H atoms omitted for clarity).
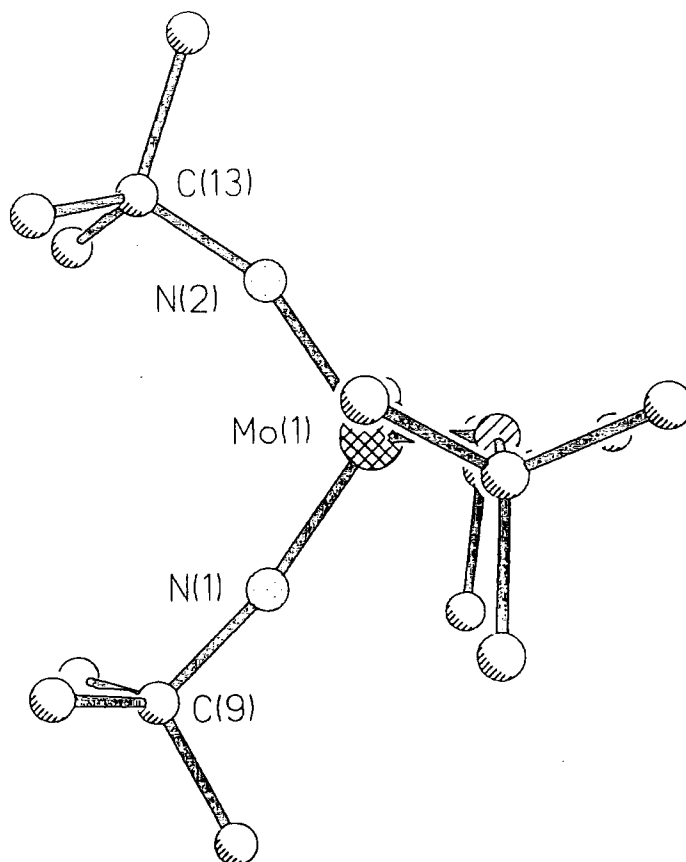
(b) View of the molecule in the N(1)-Mo-N(2) plane.

Mo(1)-O(1)	1.866(5)	Mo(1)-O(2)	1.875(3)
Mo(1)-N(1)	1.714(5)	Mo(1)-N(2)	1.776(6)
O(1)-C(1)	1.424(7)	O(2)-C(5)	1.424(6)
N(1)-C(9)	1.474(7)	N(2)-C(13)	1.444(10)
C(1)-C(2)	1.483(13)	C(1)-C(3)	1.480(10)
C(1)-C(4)	1.482(11)	C(6)-C(5)	1.519(10)
C(7)-C(5)	1.480(13)	C(5)-C(8)	1.519(10)
C(9)-C(10)	1.524(12)	C(9)-C(11)	1.527(13)
C(9)-C(12)	1.525(8)	C(13)-C(14)	1.418(20)
C(13)-C(15)	1.584(14)	C(13)-C(16)	1.542(17)
C(13)-C(14A)	1.615(21)	C(13)-C(15A)	1.510(24)
C(13)-C(16A)	1.389(24)		

O(1)-Mo(1)-O(2)	107.9(2)	O(1)-Mo(1)-N(1)	110.2(3)
O(2)-Mo(1)-N(1)	109.5(2)	O(1)-Mo(1)-N(2)	108.1(2)
O(2)-Mo(1)-N(2)	108.8(2)	N(1)-Mo(1)-N(2)	112.2(3)
Mo(1)-O(1)-C(1)	143.5(4)	Mo(1)-O(2)-C(5)	141.7(4)
Mo(1)-N(1)-C(9)	169.6(6)	Mo(1)-N(2)-C(13)	157.1(5)
O(1)-C(1)-C(2)	106.3(5)	O(1)-C(1)-C(3)	110.1(7)
C(2)-C(1)-C(3)	108.8(6)	O(1)-C(1)-C(4)	111.1(5)
C(2)-C(1)-C(4)	109.3(8)	C(3)-C(1)-C(4)	111.0(6)
O(2)-C(5)-C(6)	105.2(5)	O(2)-C(5)-C(7)	108.9(5)
C(6)-C(5)-C(7)	111.6(7)	O(2)-C(5)-C(8)	109.6(5)
C(6)-C(5)-C(8)	110.7(6)	C(7)-C(5)-C(8)	110.6(6)
N(1)-C(9)-C(10)	108.9(6)	N(1)-C(9)-C(11)	106.8(6)
C(10)-C(9)-C(11)	110.9(6)	N(1)-C(9)-C(12)	109.6(4)
C(10)-C(9)-C(12)	110.6(7)	C(11)-C(9)-C(12)	110.1(6)
N(2)-C(13)-C(14)	110.9(8)	N(2)-C(13)-C(15)	106.3(9)
C(14)-C(13)-C(15)	113.3(10)	N(2)-C(13)-C(16)	107.9(9)
C(14)-C(13)-C(16)	109.4(12)	C(15)-C(13)-C(16)	108.9(8)
N(2)-C(13)-C(14A)	101.3(9)	N(2)-C(13)-C(15A)	114.1(12)
C(14A)-C(13)-C(15A)	97.5(14)	N(2)-C(13)-C(16A)	109.5(15)
C(14A)-C(13)-C(16A)	115.1(16)	C(15A)-C(13)-C(16A)	117.8(14)

table 2.1 *Selected bond distances (Å) and angles (°) for Mo(NBuᵗ)₂(OBuᵗ)₂ (1)*

There are relatively few crystal structures of monomeric four coordinate group VI bis imido complexes for comparison, but a closely related structure W(NBuᵗ)₂(O-2,6-Ph₂C₆H₃)₂ possessing imido bond angles of 159.2(3) and 166.5(3)° has been reported[7]. By contrast, the structures of M(NBuᵗ)₂(2,4,6-Me₃C₆H₂)₂ (M = Cr, Mo) reveal equivalent imido group bond angles (M-N-C ~ 160°)[8]. The six coordinate complex Mo(NPh)₂(Et₂dtc)₂ displays large differences in imido group bond angles (Mo-N-C = 169.4 and 139.4°)[9], but this complex is a coordinatively saturated, formally 20 electron

species and therefore some distortion may be expected, in order to alleviate build up of charge at the electron rich metal centre.

2.2.3 Reaction of $Mo(NBu^t)_2(OBu^t)_2$ (1) with primary aromatic amines - $ArNH_2$ (Ar = 2,6-$Pr^i_2C_6H_3$, 2,6-$Cl_2C_6H_3$, C_6F_5)

a) Reaction of $Mo(NBu^t)_2(OBu^t)_2$ (1) with $ArNH_2$ (Ar = 2,6-$Pr^i_2C_6H_3$)

$Mo(NBu^t)_2(OBu^t)_2$ was mixed with two equivalents of $ArNH_2$ in C_6D_6 at room temperature. A slow reaction ensued with free Bu^tNH_2 and $Mo(NAr)(NBu^t)(OBu^t)_2$ (2) evident in the ^1H NMR spectrum after 2 hours. The mixture was warmed to 60°C whereby equilibrium was attained after 48 hours, with the approximate percentage concentrations of species shown in equation 2.3:

$$
\begin{array}{ccc}
Mo(NBu^t)_2(OBu^t)_2 & & Mo(NAr)_2(OBu^t)_2 \\
(1) & & 35\% \\
0\% & &
\end{array}
$$

ArNH₂   ArNH₂   Bu^tNH₂   Bu^tNH₂

$$Mo(NBu^t)(NAr)(OBu^t)_2$$
$$(2)$$
$$65\%$$

$$(2.3)$$
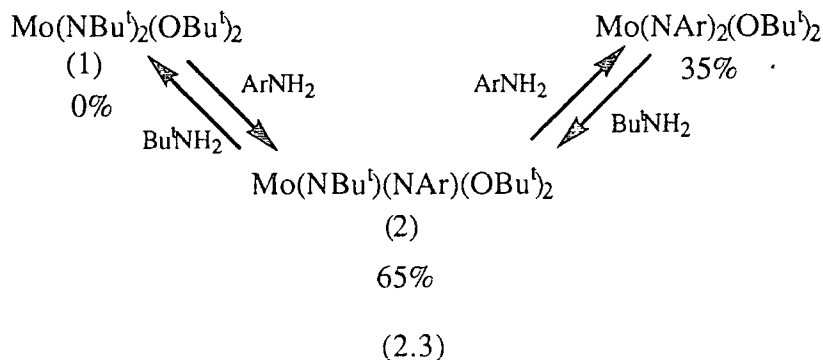
The mixed complex (2) is the most favoured species; however, a substantial amount of $Mo(NAr)_2(OBu^t)_2$ is also present. The same equilibrium concentrations are found when $Mo(NAr)_2(OBu^t)_2$ is treated with two equivalents of Bu^tNH_2[10], although here the attainment of equilibrium is distinctly slower (11 days at 60°C). The reaction is believed to proceed *via* a bis amide intermediate; this will be discussed in more detail in section 3.4.1, where an analogous imido/amine exchange at a four coordinate half-sandwich niobium complex is examined.

The rate of formation of (2) can be dramatically increased by acid catalysis (the effects of which are discussed later in section 2.4).

b) Reaction of Mo(NBu^t)$_2$(OBu^t)$_2$ (1) with Ar^{Cl}NH$_2$ (Ar^{Cl} = 2,6-Cl$_2$C$_6$H$_3$)

The presence of electron withdrawing chlorines on the aryl imido substituent could be foreseen to have a two-fold effect, firstly to increase the relative acidity of the amine and thereby assist in the protonation of the nitrogen of the tert-butyl imido ligand and secondly, to influence the thermodynamic stability of the chloro-arylimido products.

Treatment of Mo(NBu^t)$_2$(OBu^t)$_2$ (1) with two equivalents of Ar^{Cl}NH$_2$ in d$_6$-benzene resulted in the formation of Mo(NAr^{Cl})(NBu^t)(OBu^t)$_2$ (3) within minutes. Equilibrium was reached by 32 hours at room temperature (Keq = 0.08), with approximate percentage concentrations as shown in equation 2.4:

$$
\begin{array}{ccc}
& 2\ \text{Ar}^{Cl}\text{NH}_2 & \\
\text{Mo(NBu}^t)_2(\text{OBu}^t)_2 \xrightleftharpoons[\text{Bu}^t\text{NH}_2]{} & & \text{Mo(NAr}^{Cl})(\text{NBu}^t)(\text{OBu}^t)_2 \\
\text{(1)} & & \text{(3)} \\
70\% & & 30\% \quad \rightleftharpoons\ \text{Ar}^{Cl}\text{NH}_2 \\
& & \\
& & \text{Mo(NAr}^{Cl})_2(\text{OBu}^t)_2
\end{array}
$$

(2.4)
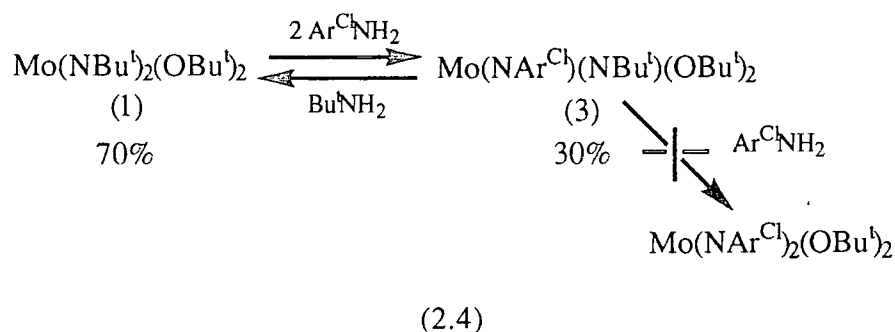
The equilibrium position was heavily in favour of the starting complex (1), indicating the mixed species (3) to be thermodynamically less favourable. There was no evidence for the formation of Mo(NAr^{Cl})$_2$(OBu^t)$_2$. A possible explanation for (3) being disfavoured is the presence of repulsive interactions between lone pairs of electrons on the chlorines of the aryl-imido substituent and the oxygens of the alkoxides.

c) Reaction of Mo(NBu^t)$_2$(OBu^t)$_2$ (1) with Ar^{F}NH$_2$ (Ar^F = C$_6$F$_5$)

The reaction of Mo(NBu^t)$_2$(OBu^t)$_2$ (1) with two equivalents of Ar^{F}NH$_2$ in C$_6$D$_6$ at room temperature resulted in the formation of Mo(NAr^F)(NBu^t)(OBu^t)$_2$ (4), with equilibrium attained in less than 20 hours. Equation 2.5 shows the approximate percentage concentrations at equilibrium:

$$\text{Mo(NBu}^t)_2\text{(OBu}^t)_2 \underset{\text{Bu}^n\text{NH}_2}{\overset{2 \text{ Ar}^F\text{NH}_2}{\rightleftharpoons}} \text{Mo(NAr}^F)\text{(NBu}^t)\text{(OBu}^t)_2$$

(1)   (4)

50%   50% $\rightleftharpoons$ Ar^{F}NH$_2$

$$\text{Mo(NAr}^F)_2\text{(OBu}^t)_2$$
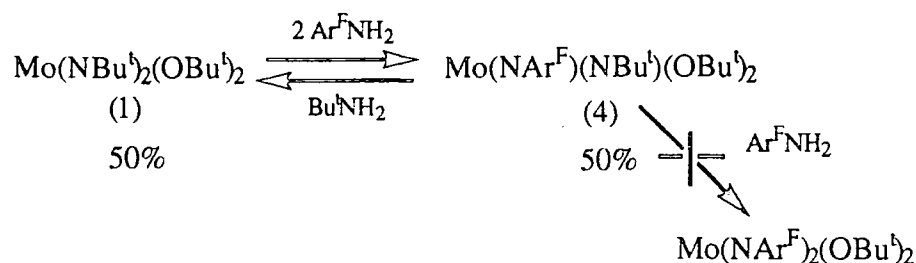
(2.5)

The relatively fast rate of attainment of equilibrium cf.(a), is probably a consequence of reduced steric interactions for this particular amine. As observed for (b), no bis-aryl imido is observed, suggesting that two electron-withdrawing imido groups are not favoured on this electron deficient 14 electron metal centre. It is apparent that the 2,6-$\text{Pr}^i_2\text{C}_6\text{H}_3$ substituted imido is a special case in that the bis-aryl imido is favoured to a significant degree. This could possibly be ascribed to the amphoteric character of the aryl group in that electronic density can be released or removed depending on the requirements of the metal centre.

2.2.4 Reaction of Mo(NBu^t)$_2$(OBu^t)$_2$ (1) with PhCHO

Metal-oxo species have been obseved from the treatment of early transition metal imido complexes with aldehydes and ketones[11-13]. Substituted aldehydes have also been employed in functionalising living alkylidene polymer chains *via* 'Wittig like' capping reactions of the alkylidene moiety[14]. Despite these widespread applications, only one metal-oxo complex has been synthesised directly by addition of an aldehyde[15]:

$$\text{Cr(NBu}^t)_2\text{(OSiMe}_3)_2 + \text{PhCHO} \longrightarrow \text{Cr(O)(NBu}^t)\text{(OSiMe}_3)_2 + \text{PhCHNBu}^t$$

(2.6)

The above reaction stops cleanly after the introduction of one oxo group.

Treatment of Mo(NBu^t)$_2$(OBu^t)$_2$ (1) with two equivalents of PhCHO in C$_6$D$_6$ at room temperature gave rise to slow formation of the oxo-imido complex

46

Mo(O)(NBu^t)(OBu^t)$_2$ (5) and the corresponding Schiff's base PhCHNBu^t, according to equation 2.7:

$$Mo(NBu^t)_2(OBu^t)_2 \underset{\xleftarrow{}}{\xrightarrow{PhCHO}} Mo(O)(NBu^t)(OBu^t)_2 \underset{\xleftarrow{}}{\xrightarrow{PhCHO}} Mo(O)_2(OBu^t)_2$$
$$\text{(1)} \qquad\qquad\qquad \text{(5)}$$

$$(2.7)$$
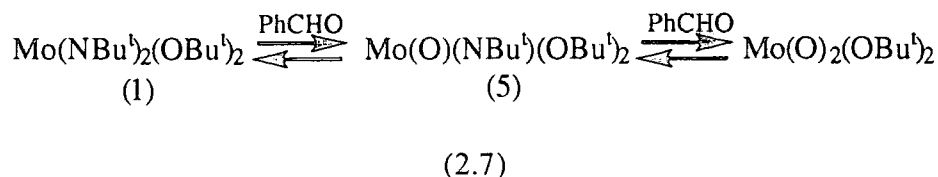
The reaction mixture was warmed to 60°C whereby after 5 days the product was almost exclusively (5), with a trace amount of the dioxo species Mo(O)$_2$(OBu^t)$_2$. No further changes in concentration of these species occured over a prolonged period of time implying that equilibrium had been achieved. However, if the reaction is carried out using an excess of PhCHO (10 equivalents), the reaction proceeds over a period of one week at ca. 60°C, to afford the dioxo complex Mo(O)$_2$(OBu^t)$_2$ exclusively.

Mo(NBu^t)$_2$(OBu^t)$_2$ (1) is far more reactive towards benzaldehyde than the 2,6-Pr$^i_2$C$_6$H$_3$ aryl imido analogue Mo(NAr)$_2$(OBu^t)$_2$[10]. After heating Mo(NAr)$_2$(OBu^t)$_2$ with ten equivalents of PhCHO to 60°C for 7 days in C$_6$D$_6$, there is only 60% conversion to the mono oxo substituted species Mo(O)(NAr)(OBu^t)$_2$ (see section 2.4.5)

2.2.5 Reaction of Mo(NBu^t)$_2$(OBu^t)$_2$ (1) with dioxygen

Molecular oxygen has been found to react with the imido moiety to form a nitrosyl complex in the following example[16,17]:

$$[Re(NAr)Cl_3(PPh_3)_n]_n \xrightarrow[O_2,\Delta]{C_6D_6} ReCl_3(ArNO)(OPPh_3)$$

$$(2.8)$$
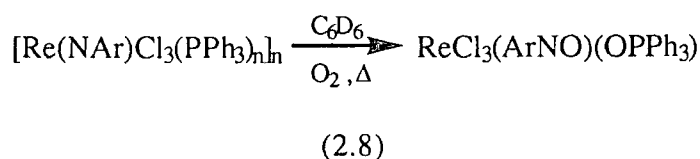
Chisholm has exploited the reactivity of oxygen with molybdenum alkoxide species to synthesise oxo complexes[18]:

$$Mo(OBu^t)_4 + O_2 \longrightarrow [Mo(OBu^t)_4(O_2)]$$

$$Mo(OBu^t)_4 \swarrow \qquad \searrow -2\ But O\cdot$$

$$2\ Mo(O)(OBu^t)_4 \qquad Mo(O)_2(OBu^t)_2$$

(2.9)
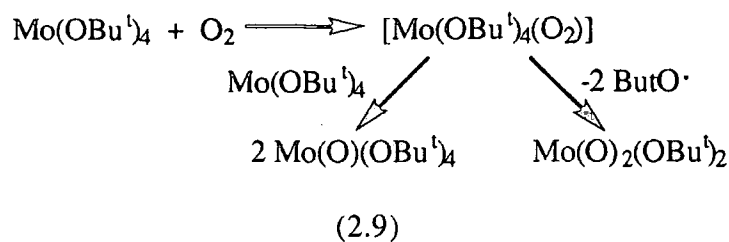
$Mo(NBu^t)_2(OBu^t)_2$ (1) was treated with a large excess of dry oxygen (~1000 equivalents) in d_6-benzene at room temperature. On heating to 60°C for two weeks the product was exclusively $Mo(O)(NBu^t)(OBu^t)_2$ (5). The presence of uncoordinated Bu^tNO was noted in the ^1H NMR spectrum at δ 1.05 (s, 9H, Bu^t), however, several other side products were also present including tert-butanol and 2-methyl propene $Me_2C=CH_2$ {δ 4.74 (s, 2H, CH_2), 1.61 (s, 6H, CMe_2)} . Given the triplet character of oxygen, the reaction is expected to go *via* a radical mechanism and therefore tert-butoxy radicals could be formed, subsequent proton abstraction by these radicals could provide a rationale for the formation of $(CH_3)_2C=CH_2$ (formed from a tert-butyl group). On further heating small quantities of the dioxo complex $Mo(O)_2(OBu^t)_2$ were observed. Equation 2.10 summarises the overall reaction:

$$Mo(NBu^t)_2(OBu^t)_2 + O_2 \xrightarrow{-Bu^tNO} Mo(O)(NBu^t)(OBu^t)_2$$
$$(1) \qquad\qquad\qquad\qquad\qquad (5)$$
$$\Big\downarrow -Bu^tNO$$
$$Mo(O)_2(OBu^t)_2$$

(2.10)
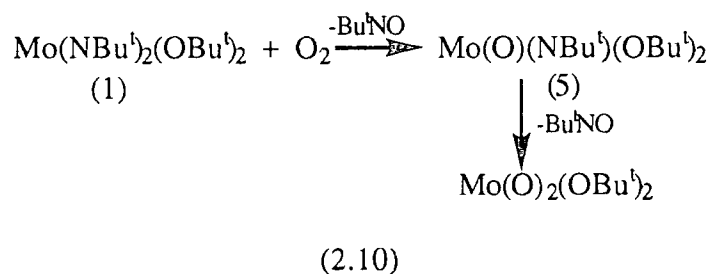
2.2.6 Reaction of $Mo(NBu^t)_2(OBu^t)_2$ (1) with ArNCO (Ar = Ph, 2,6-$Pr^i_2C_6H_3$)

Isocyanates have found wide application in converting an oxo group to an imido moiety[19,20]. Recently, they have been utilised to convert one imido group to another[21]:

$$[(MeC_5H_4)Mo(NPh)(\mu-NPh)]_2 \xrightarrow[\substack{65\% \\ Ar = p\text{-tolyl}}]{ArNCO} [(MeC_5H_4)Mo(NAr)(\mu-NPh)]_2$$

(2.11)
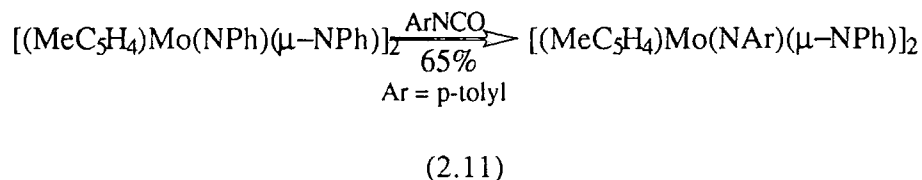
$Mo(NBu^t)_2(OBu^t)_2$ (1) was found to react rapidly with two equivalents of PhNCO at room temperature. The ^1H NMR spectrum after a few minutes showed that all the starting material (1) had been consumed, however, a large number of new resonances prevented identification of any of the new complexes. Isocyanates can undergo formal [2 + 2] coupling reactions *via* both the RNC=O and RN=CO linkages with the metal-imido moiety, as well as forming stable metallacycles; for instance $Mo(NAr)_2(OBu^t)_2$ is believed to form a bis (ureato N, N') complex when treated with PhNCO[5]. Therefore, the reactivity of (1) with PhNCO may lead to a number of possible products. In an attempt to gain a clearer interpretation of the ^1H NMR spectrum, reaction with 2,6-$Pr^i_2C_6H_3NCO$ was attempted, but again several unidentifiable products were obtained.

2.2.7 Other attempted reactions of $Mo(NBu^t)_2(OBu^t)_2$ (1)

The following organic substrates did not effect reaction with $Mo(NBu^t)_2(OBu^t)_2$ (1):

a) Bu^tOH (4 equivalents, 2 weeks at 100°C). The imido group of (1) is stable to Bu^tOH as is that of $Mo(NAr)_2(OBu^t)_2$[10], however late transition metal species have been found to react with alcohols to give bis(alkoxide) species[22].

b) PhN=NPh (1 equivalent, 1 week at 95°C).

c) $(Me_3Si)C=N=C(SiMe_3)$ (1 equivalent, 2 weeks at 100°C)

For both azabenzenes and carbodiimides, low valent early transition metal centres seemed to be required for reaction to afford new imido complexes[23,24].

2.3 Intermetal imido ligand exchange reactivity of Mo(NR)₂XY complexes (R = Buᵗ, Ar, X = Y = OBuᵗ; R = Buᵗ, X = Cp, Y = Cl)

2.3.1 Reaction of Mo(NBuᵗ)₂(OBuᵗ)₂ (1) with Mo(NAr)₂(OBuᵗ)₂

Preparation of Mo(NAr)(NBuᵗ)(OBuᵗ)₂ (6).

The reaction of $Mo(NBu^t)_2(OBu^t)_2$ (1) with one equivalent of $Mo(NAr)_2(OBu^t)_2$ in C_6D_6 results in the formation of the mixed imido complex $Mo(NAr)(NBu^t)(OBu^t)_2$ (6), according to equation 2.12:

$$Mo(NBu^t)_2(OBu^t)_2 \; + \; Mo(NAr)_2(OBu^t)_2$$
$$(1)$$

$$K_{eq}$$

$$2\; Mo(NAr)(NBu^t)(OBu^t)_2$$
$$(6)$$
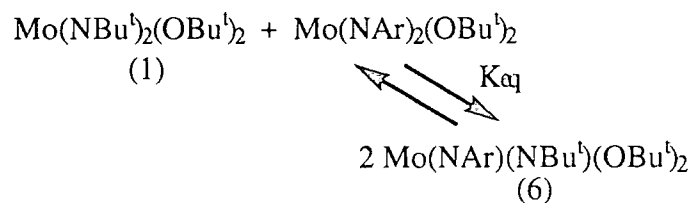
$$(2.12)$$

Equilibrium is attained after 5 days at 60°C (K_{eq} = 25), lying heavily in favour of the mixed imido complex (6). The reaction is believed to go *via* the bridging of aryl and tert-butyl imido groups and is therefore slow compared with oxo-imido exchange, as a result of the steric bulk of these groups. The exchange process of these imido groups is sensitive to the coordination geometry of the metal centre; for example, the closely related 6 coordinate bis imido complexes (shown in equation 2.13) do not undergo exchange in C_6D_6 when heated to 60°C for several weeks[3], implying that coordinative unsaturation at the metal centre is a prerequisite for efficient exchange.

$$Mo(NBu^t)_2Cl_2.dme \ + \ Mo(NAr)_2Cl_2.dme$$

$$\searrow\!\!\!\mid\!\!\!\swarrow \Delta$$

$$2 \ Mo(NAr)(NBu^t)Cl_2.dme$$
$$(A)$$

$$(2.13)$$

In order to illustrate the synthetic utility of such exchange processes, the reaction was repeated on a preparative scale. Equimolar quantities of (1) and $Mo(NAr)_2(OBu^t)_2$ were mixed in heptane and the mixture warmed to 60°C for one week. Analytically pure (6) could be isolated upon crystallisation from pentane at -20°C as a yellow/orange solid in a low yield (15%). When a sample of (6) was dissolved in d_6-benzene at room temperature, low intensity resonances due to (1) and $Mo(NAr)_2(OBu^t)_2$ appeared in the ^1H NMR spectrum over several days, thus demonstrating the equilibrium process from the reverse direction.

2.3.2 Reaction of $Mo(NAr)_2(OBu^t)_2$ with $CpNb(NBu^t)(OBu^t)_2$

$Mo(NAr)_2(OBu^t)_2$ was mixed with one equivalent of $CpNb(NBu^t)(OBu^t)_2$[25] in C_6D_6 at room temperature. Reaction was only observed when the mixture was warmed to 110°C, with signals due to (6) evident in the ^1H NMR spectrum. More forcing conditions were applied by further heating of the mixture to 140°C, whereby equilibrium was reached after 7 days ($K_{eq} = 0.25$).

$$Mo(NAr)_2(OBu^t)_2 \ + \ CpNb(NBu^t)(OBu^t)_2$$

$$\nwarrow\!\!\!\searrow$$

$$Mo(NAr)(NBu^t)(OBu^t)_2 \ + \ CpNb(NAr)(OBu^t)_2$$
$$(6) \qquad\qquad\qquad (7)$$

$$(2.14)$$

The highly elevated temperature required reflects a relatively high energy barrier to product formation. The small equilibrium constant signifies a greater thermodynamic

stability of reactants over products, which is probably due to the unfavourable steric interactions present in $CpNb(NAr)(OBu^t)_2$ (7), discussed later in 3.4.1(a).

Furthermore, intermetal imido exchange in the half-sandwich imido system (equation 2.15) is even slower and requires a temperature of 140^oC for several weeks in order to attain equilibrium[10]:

$$Cp^*Nb(NAr)Cl_2 + CpNb(NBu^t)Cl_2 \rightleftharpoons Cp^*Nb(NBu^t)Cl_2 + CpNb(NAr)Cl_2$$

$$(2.15)$$
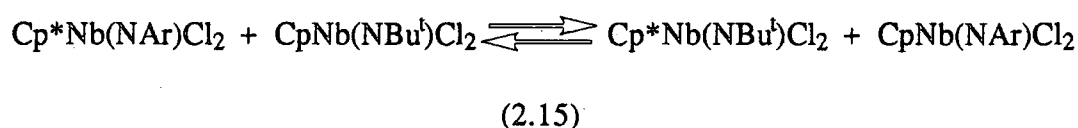
From these investigations it can be concluded that the rate of intermetal imido exchange for the differing coordination environments increases in the order:

$$CpNb - CpNb < CpNb - Mo < Mo - Mo$$

This is consistent with decreasing steric interactions in the four coordinate molybdenum complexes.

2.3.3 Reaction of $CpMo(NBu^t)_2Cl$ with $LiOBu^t$

Attempted preparation of $CpMo(NBu^t)_2(OBu^t)$

In order to assess the effects of increasing the steric demands and the formal electron count at a four coordinate molybdenum bis imido centre, the 18 electron complex $CpMo(NBu^t)_2Cl$ was synthesised, according to the method used by Sundermeyer[26]. Substitution of the chloride for a tert-butoxide ligand was deemed necessary to avoid complication from coincident exchange between different mono-anionic ancillary ligands i.e all the X type ligands would be the same. Mono-anionic ligand exchange is discussed separately in section 2.6.

Chilled diethyl ether was added to a solid equimolar mixture of $CpMo(NBu^t)_2Cl$ and $LiOBu^t$. On allowing the mixture to reach room temperature there was no apparent reaction, however a precipitate was formed over several days. Subsequent filtration and removal of the solvent *in vacuo* produced an oily solid. The ^{1}H NMR spectrum revealed the solid to be a mixture of unreacted $CpMo(NBu^t)_2Cl$ and $Mo(NBu^t)_2(OBu^t)_2$ (1) in a

1:1 ratio, with a small quantity of LiCp present. A reaction scheme was devised in order to rationalise the above observations (see figure 2.3). The formation of a short-lived intermediate is inferred which could either be $Mo(NBu^t)_2(OBu^t)Cl$ or $CpMo(NBu^t)_2(OBu^t)$; the former arising from initial substitution of the cyclopentadienyl ligand, whereas the latter involves replacement of the chloride:

$$CpMo(NBu^t)_2Cl \ + \ 0.5 \ LiOBu^t$$

- LiCp / slow \ - LiCl

$$0.5 \ Mo(NBu^t)_2(OBu^t)Cl \qquad 0.5 \ CpMo(NBu^t)_2(OBu^t)$$

0.5 LiOBu^t \ fast / 0.5 LiOBu^t

$$Mo(NBu^t)_2(OBu^t)_2 \ + \ LiCl$$
$$(1)$$
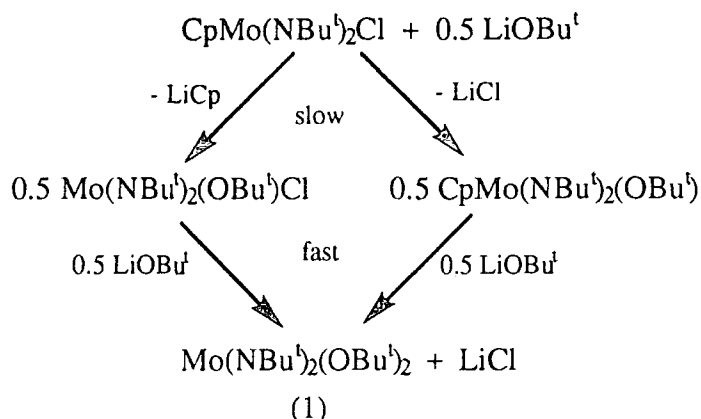
figure 2.3 *Proposed scheme for the reaction of CpMo(NBu^t)$_2$Cl with LiOBu^t*

The reactive intermediate once formed would once formed could react very quickly with LiOBu^t forming (1). This scheme provides a satisfactory explanation for the observed stoichiometry of (1) and $CpMo(NBu^t)_2Cl$. The initial target, $CpMo(NBu^t)_2(OBu^t)$, is probably disfavoured owing to unfavourable steric interactions.

2.3.4 Intermetal exchange reactivity of CpMo(NBu^t)$_2$Cl

a) Reaction of CpMo(NBu^t)$_2$Cl with Mo(NAr)$_2$(OBu^t)$_2$

Equimolar quantities of $CpMo(NBu^t)_2Cl$ and $Mo(NAr)_2(OBu^t)_2$ were mixed in d_6-benzene at room temperature. After heating to 60°C for 48 hours, small amounts of $Mo(NAr)(NBu^t)(OBu^t)_2$ (6) and $CpMo(NAr)(NBu^t)Cl$ (9) were evident in the ^1H NMR spectrum. The reaction was extremely slow at 60°C, so the mixture was heated to 100°C, where shortly thereafter the presence of $Mo(NBu^t)_2(OBu^t)_2$ (1) and $CpMo(NAr)_2Cl$ (10) was noted. Equilibrium was achieved after 6 months; the approximate percentage concentrations of the half-sandwich molybdenum species are shown in equation 2.16:

$$\underset{\substack{\text{Mo(NAr)}_2(\text{OBu}^t)_2 \\ 10\%}}{\text{CpMo(NBu}^t)_2\text{Cl}} \xrightleftharpoons{\text{Mo(NAr)}_2(\text{OBu}^t)_2} \underset{\substack{60\% \\ (9)}}{\text{CpMo(NAr)(NBu}^t)\text{Cl}} \xrightleftharpoons{\text{Mo(NAr)}_2(\text{OBu}^t)_2} \underset{\substack{30\% \\ (10)}}{\text{CpMo(NAr)}_2\text{Cl}}$$

$$(2.16)$$
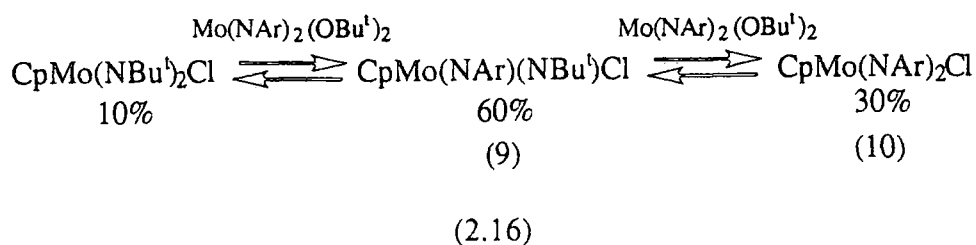
Figure 2.4 depicts the Cp and methine septet (aryl diisopropyl groups) regions of the ^{1}H NMR, clearly showing the three Cp and four aryl proton environments.

Σ CpMo(NBu^t)$_2$Cl
Δ CpMo(NBu^t)(NAr)Cl (9)
† CpMo(NAr)$_2$Cl (10)
Ω Mo(NBu^t)(NAr)(OBu^t)$_2$ (2)
π Mo(NAr)$_2$(OBu^t)$_2$

Cp (C$_5$H$_5$) region

Methine (CHMe$_2$) region
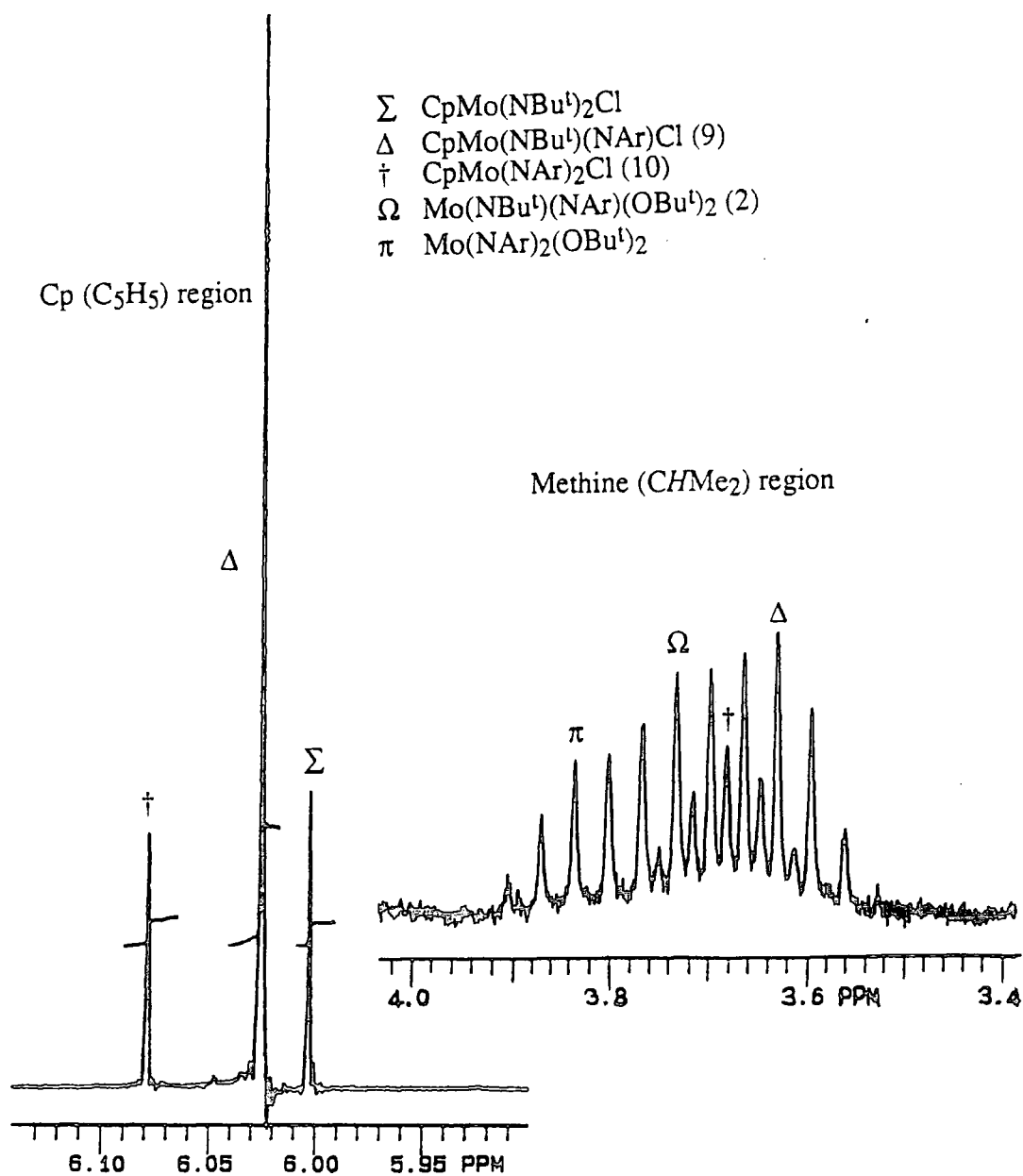
figure 2.4 ^{1}H NMR (200 MHz) spectrum of the reaction of CpMo(NBu^t)$_2$Cl with Mo(NAr)$_2$(OBu^t)$_2$ after 6 months at 100°C.

54

As there are six metal complexes present there are a large number of possible intermetal exchange pathways affecting the overall equilibrium position, however, imido exchange between two "CpMo" species could be discounted as this would be slow compared to "CpMo - Mo" and "Mo - Mo" exchange. Chloride-butoxide exchange can probably also be disregarded; for example when $CpMo(NBu^t)_2Cl$ was mixed with one equivalent of $Mo(NBu^t)_2(OBu^t)_2$ (1) in C_6D_6, no exchange products were observed in the ^1H NMR spectrum even on heating to 100^oC for several months:

$CpMo(NBu^t)_2Cl$ + $Mo(NBu^t)_2(OBu^t)_2$
(1)

$CpMo(NBu^t)_2(OBu^t)$ + $Mo(NBu^t)_2(OBu^t)Cl$
(8)

(2.17)
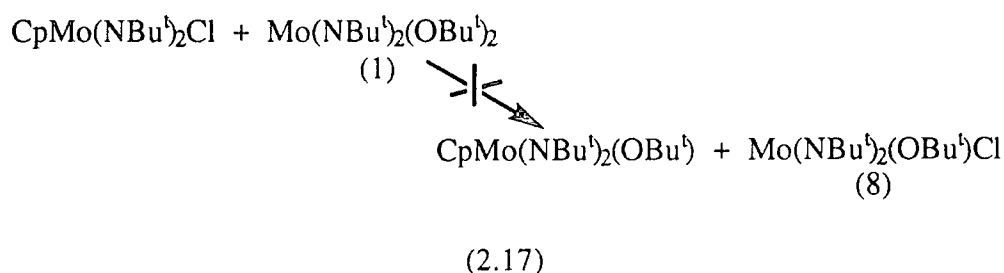
In accordance with the observations from section 2.3.1, the mixed imido species {(6) and (9)} are the most favoured, although in this system the exchange rate is much slower due to unfavourable steric and electronic interactions of the crowded four coordinate half-sandwich molybdenum complex.

b) Reaction of CpMo(NBu^t)_2Cl with CpNb(NAr)Cl_2

Equimolar quantities of $CpMo(NBu^t)_2Cl$ and $CpNb(NAr)Cl_2$[26] wre mixed in d_6-benzene at room temperature. No reaction occured at this temperature or even on heating to 100^oC for 2 weeks. After 1 month at 100^oC there were traces of $CpMo(NAr)(NBu^t)Cl$ (8) and $CpNb(NBu^t)Cl_2$ present in the ^1H NMR, but to date (~ 3 months) the intensity of these signals has not appreciably changed.

$$CpMo(NBu^t)_2Cl + CpNb(NAr)Cl_2$$

$$CpMo(NAr)(NBu^t)Cl + CpNb(NBu^t)Cl_2$$

$$(9)$$
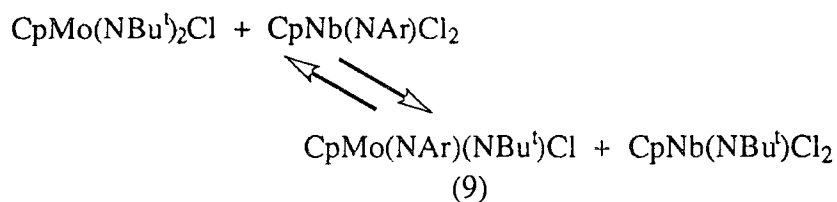
$$(2.18)$$

Increasing the steric bulk of both starting complexes clearly retards the reaction rate.

c) Reaction of CpMo(NBu^t)$_2$Cl with CpNb(NMe)Cl$_2$

CpMo(NBu^t)$_2$Cl was mixed with one equivalent of CpNb(NMe)Cl$_2$[26] in CDCl$_3$ at room temperature. Reaction was found to occur at 100°C and reached completion after one week, according to equation 2.19:

$$CpMo(NBu^t)_2Cl + CpNb(NMe)Cl_2$$

$$CpMo(NMe)(NBu^t)Cl + CpNb(NBu^t)Cl_2$$

$$(11)$$
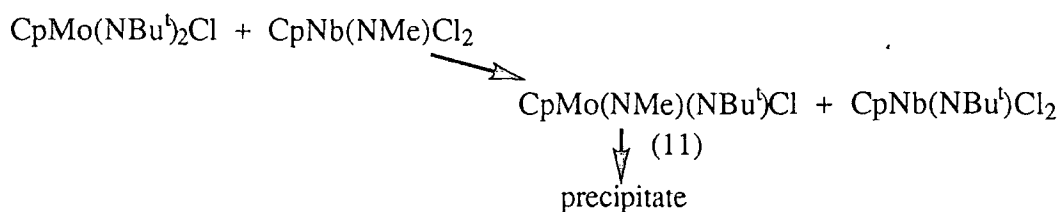
precipitate

$$(2.19)$$

Resonances in the ^{1}H NMR were found only for CpNb(NBu^t)Cl$_2$. However, a dark insoluble precipitate was present and assigned to CpMo(NMe)(NBu^t)Cl (11) (or more likely the subsequent decomposition product thereof). Reaction with CpNb(NMe)Cl$_2$ was much faster than that observed in (b), reflecting the reduced steric bulk of the methyl imido unit.

2.4 A mechanistic study of intermetal oxo-imido exchange

The intermetal oxo-imido exchange reaction has been the subject of a preliminary kinetic study by Dr.J.P.Mitchell for the following system[10]:

$$Mo(NAr)_2(OR)_2 + Mo(O)_2(OR)_2 \underset{K_{eq}}{\overset{}{\rightleftharpoons}} 2\, Mo(O)(NAr)(OR)_2$$

(2.20)
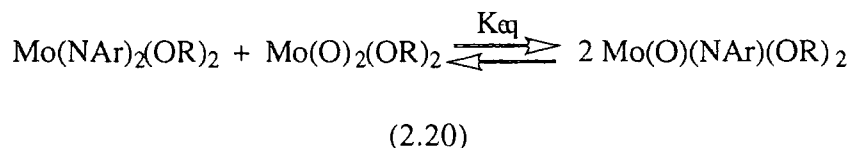
For R = Bu^t, the above reaction was found to proceed slowly over 24 hours at room temperature to reach equilibrium (K_{eq} = 0.08), whereas for the hexafluoro tert-butoxide analogues (R$_f$^{6}) the reaction was much slower, taking several days at 60°C to attain equilibrium. This slower rate may be rationalised due to the stronger oxo and imido-metal multiple bonds, as well as the greater steric interactions for the fluorinated species. The negative entropy determined for the above reaction is consistent with an ordered four-centred transition state containing bridging oxo and imido groups (see section 1.3.2).

For comparative purposes, the tert-butyl imido analogues Mo(NBu^t)$_2$(OR)$_2$ were synthesised as part of this study, as well as the corresponding oxo analogues Mo(O)$_2$(OR)$_2$ (R = Bu^t, R$_f$^{3}, R$_f$^{6}).

2.4.1a) Reaction of Mo(NBu^t)$_2$(OBu^t)$_2$ (1) with Mo(O)$_2$(OBu^t)$_2$

Reaction of equimolar quantities of Mo(NBu^t)$_2$(OBu^t)$_2$ (1) with Mo(O)$_2$(OBu^t)$_2$ in d$_6$-benzene proceeded rapidly at room temperature reaching completion within 40 minutes (equation 2.21). The equilibrium position lies heavily towards the mixed oxo-imido complex (K_{eq} > 2 x 10^2).

$$\text{Mo(NBu}^t)_2\text{(OBu}^t)_2 \ + \ \text{Mo(O)}_2\text{(OBu}^t)_2 \ \underset{}{\overset{K_{eq}}{\rightleftharpoons}} \ 2\,\text{Mo(O)(NBu}^t)\text{(OBu}^t)_2$$
$$\qquad\quad (1) \qquad\qquad\qquad\qquad\qquad\qquad\qquad\qquad (5)$$
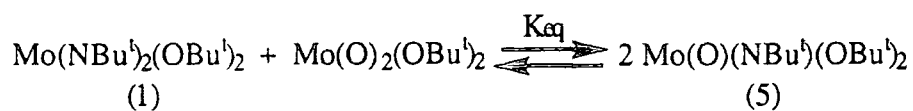
$$(2.21)$$

Resonances in the ^{1}H NMR spectrum for (5) were present at δ 1.38 (NBu^t) and 1.25 (OBu^t), the former resonance being coincident with the NBu^t/OBu^t signal for (1). Figure 2.5 displays the ^{1}H NMR spectrum of the reaction after 5 minutes at room temperature.
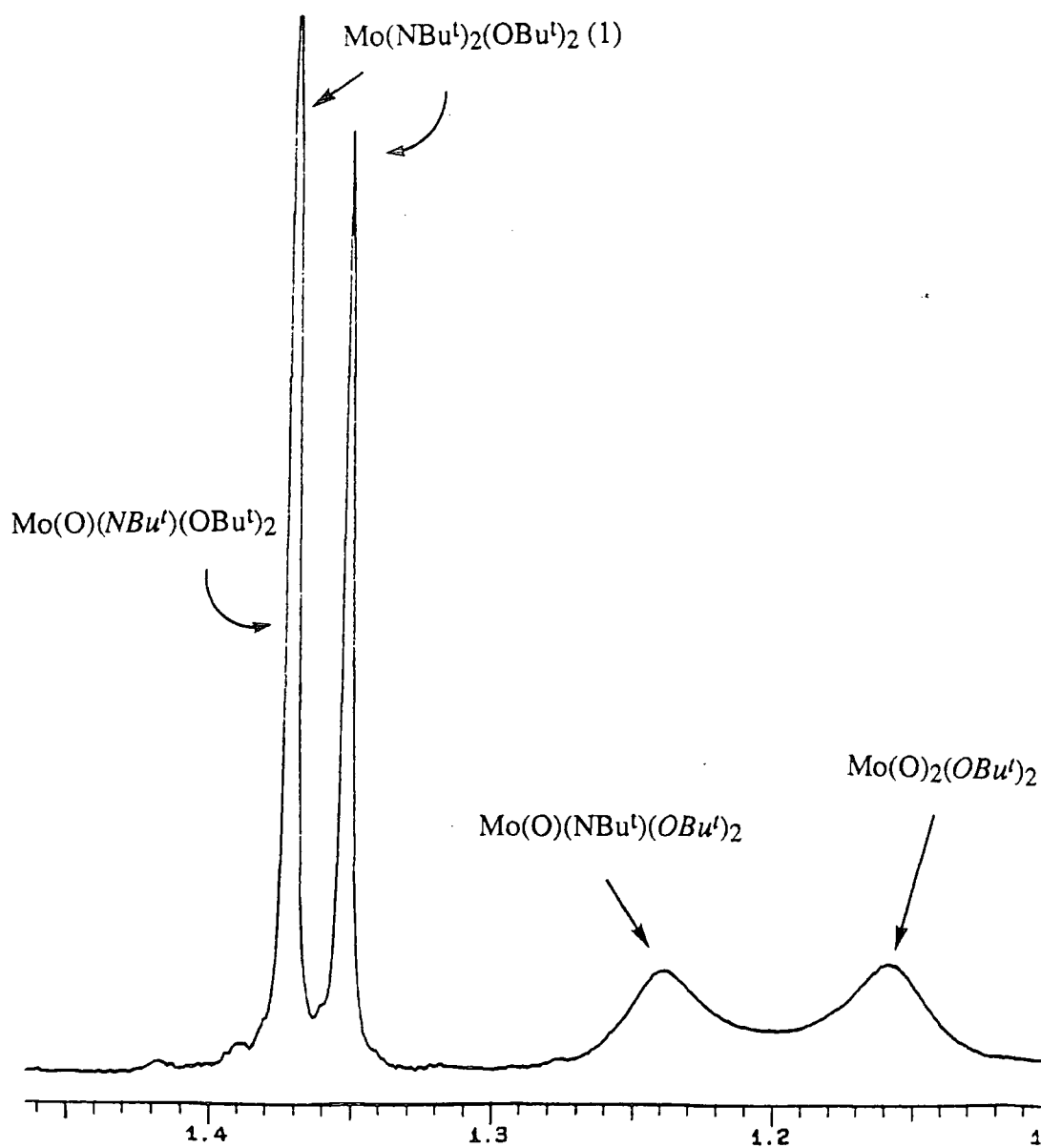
figure 2.5   *^{1}H NMR (200 MHz) spectrum of the reaction of Mo(NBu^t)$_2$(OBu^t)$_2$ (1) with Mo(O)$_2$(OBu^t)$_2$ after 5 minutes.*

The tert-butoxide resonances for $Mo(O)_2(OBu^t)_2$ and $Mo(O)(NBu^t)(OBu^t)_2$ (5) are significantly broadened, a phenomenon attributable to intermetal alkoxide exchange at a rate comparable with the NMR timescale. We have found that this is a general phenomenon, and is also observed for the fluorinated alkoxide species. Intermetal alkoxide exchange will be occuring between all three complexes at different rates (k_1, k_2 and k_3), as labelled in figure 2.6:
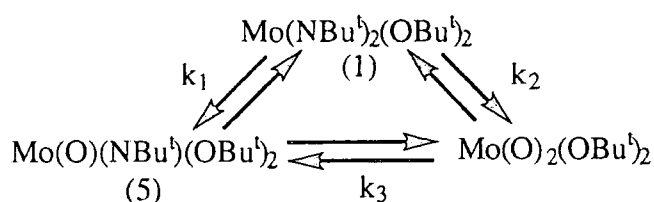
figure 2.6 *Intermetal multi-site alkoxide exchange*

The rate of alkoxide exchange is likely to increase in the order:

$k_1 < k_2 < k_3$, based on decreasing steric congestion by replacement of the oxo group with the large imido unit. It is quite fortuitous that k_3 is comparable with the NMR timescale. Independent determination of this rate constant is difficult, since it is a function of 12 parameters {4 for each species, consisting of relaxation time (T_1), population, chemical shift difference ($\Delta\delta$) and rate constants (k_n)}[27]. However, on cooling a sample of the reaction in d_8-toluene (-10°C), the resonances due to the tert-butoxide protons of $Mo(O)_2(OBu^t)_2$ and (5) are found to sharpen considerably, consistent with a reduced rate of alkoxide exchange (k_3).

Owing to the position of the equilibrium (lying essentially over to the right), the kinetic data could be interpreted by a 2nd order non-reversible approach[28], the rate law for which is given in equation 2.22:

$$\text{Rate} = \frac{d\,[Mo(O)(NBu^t)(OBu^t)_2]}{dt} = k_1\,[Mo(NBu^t)_2(OBu^t)_2][Mo(O)_2(OBu^t)_2]$$

(2.22)

A plot of $1/a-x$ versus time gave a straight line of gradient $k_1 = 3.6(5) \times 10^{-2}$ l mol^{-1}s^{-1}. However, this rate could not always be reproduced and occasionally fluctuated by factors of up to 2-3. Some other external factor was obviously affecting the observed rate of the reaction and it was therefore necessary to investigate this further.

b) Reaction of Mo(NBu^t)$_2$(OBu^t)$_2$ (1) with Mo(O)$_2$(OBu^t)$_2$ in the presence of NEt$_3$

The oxo-imido exchange reaction was performed in the presence of 3, 7 and 20% (% of total moles reactants) and the rate constants determined, as recorded in table 2.2.

reagent	k_1 / x10^{-3} l mols^{-1}	k_1 (relative)
-	36(3)	36
3% NEt$_3$	1.27(9)	1.3
7% NEt$_3$	1.0(13)	1
20% NEt$_3$	1.06(11)	1.1
20% Bu^{t}OH	60(4)	60
3 Bu^{t}OH	1.39(4)	1.4
5% PhCO$_2$H	94(7)	94

table 2.2 *Rate constants for oxo-imido exchange (R = Bu^t)*

Figure 2.7 displays the second order plot for the oxo-imido reaction in the presence of 3% NEt$_3$:
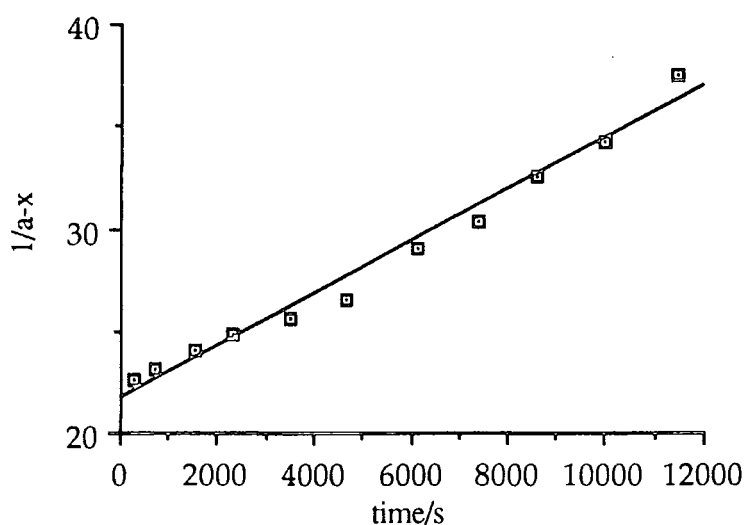
figure 2.7 *2nd order plot for the oxo-imido reaction (R = Bu^t) in the presence of 3% NEt3*

The observed rate constants are (within error) effectively the same ($k_1 \sim 1.0 \times 10^{-3}$ l mol^{-1}s^{-1}). This rate constant is much reduced from that observed in the absence of added base cf.$k_1 = 3.6(5) \times 10^{-1}$ l mol^{-1}s^{-1}. Triethylamine is a good basic σ donor and could be envisaged to coordinate to the metal centres, hence curtailing the bridging of oxo and imido groups. Nevertheless, there is no evidence of NEt3 adducts in the ^{1}H NMR spectrum and even if adduct formation were occuring there would be insufficient base present to reduce the rate by the large factor observed (x 36). It now seemed likely that the reaction could be susceptible to acid catalysis, and that the role of NEt3 could be in removing acidic species.

c) Reaction of Mo(NBu^t)2(OBu^t)2 (1) with Mo(O)2(OBu^t)2 in the presence of PhCO2H

The oxo-imido exchange reaction was performed in the presence of benzoic acid (5%), where the rate was found to be substantially increased (almost 3 times) over that observed in the absence of external reagents (table 2.2), and two orders of magnitude greater than the runs in the presence of NEt3. This undoubtedly established that the reaction is acid catalysed. The acid would be most likely to hydrogen-bond to the basic oxygen of the ancillary butoxide ligands. This would "tie up" one of the oxygen lone pairs and therefore increase the electrophilicity of the metal centre (shown in figure 2.8).

61

The increased lewis acidity of the metal centre would encourage the bridging of multiply bonded ligands between metal centres to occur, inevitably resulting in the relatively rapid formation of the oxo-imido product. This process is a general one, and is therefore likely to be of fundamental importance for the exchange of both dianionic and mono-anionic groups between metal centres.
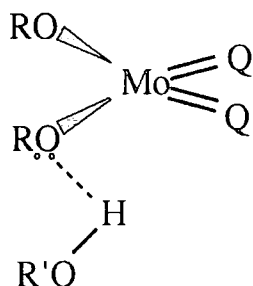
figure 2.8 *The reactive intermediate in the oxo-imido exchange reaction*

A related hydrogen-bonded intermediate has been observed in a late transition metal system and is discussed in section 3.5.11.

d) Reaction of Mo(NBu^t)$_2$(OBu^t)$_2$ (1) with Mo(O)$_2$(OBu^t)$_2$ in the presence of Bu^{t}OH

The most likely source of acid in the oxo-imido exchange reaction in the absence of external reagents would be dissociated Bu^{t}OH itself. The reaction was performed firstly in the presence of a small quantity of Bu^{t}OH (20%), and secondly a large excess (3 equivalents, the second order plot for which is shown in figure 2.9). The resultant rates are shown in table 2.2. A dual role for Bu^{t}OH is clearly apparent: at low concentration, Bu^{t}OH acts as an acid catalyst, increasing the rate of reaction noticeably, whereas at high concentration it slows the rate profoundly. In the former, the rate although substantially increased, is not as large as that observed for a relatively small concentration of benzoic acid. This reflects the greater acidity of benzoic acid, which would lead to stronger hydrogen bonding interactions with the alkoxide ligands, and therefore generate a more electrophilic metal centre. In excess, the catalytic effects of Bu^{t}OH are overridden by it's capacity to bind to the metal centre, hence hindering bridge formation of the multiply bonded groups.
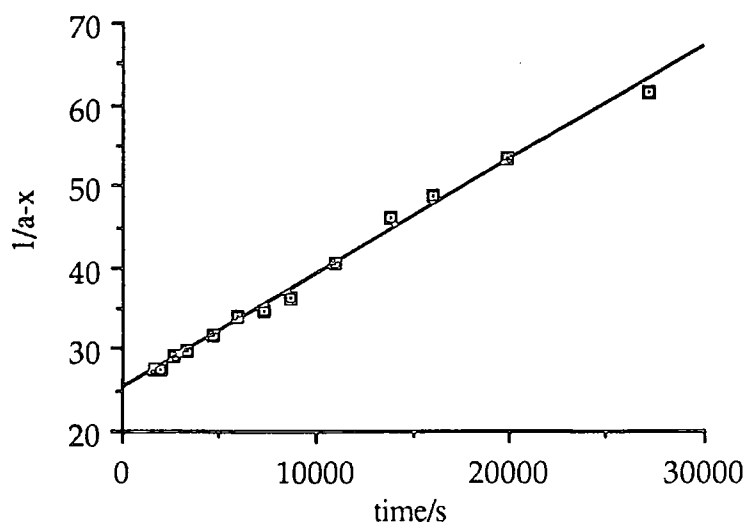
figure 2.9 *2nd order plot for the oxo-imido reaction (R = Bu^t) in the presence of 3 equivalents of Bu^{t}OH*

2.4.2 Reaction of Mo(NBu^t)$_2$(OR$_f^3$)$_2$ (12) with Mo(O)$_2$(OR$_f^3$)$_2$ (13)

Equimolar quantities of Mo(NBu^t)$_2$(OR$_f^3$)$_2$ (12) and Mo(O)$_2$(OR$_f^3$)$_2$ (13) were mixed in d$_6$-benzene at room temperature and the presence of the mixed species Mo(O)(NBu^t)(OR$_f^3$)$_2$ (14) was noted soon thereafter. The reaction proceeded to completion over about 36 hours (K$_{eq}$ > 2 x 10^2).

$$Mo(NBu^t)_2(OR_f^3)_2 \;+\; Mo(O)_2(OR_f^3)_2 \;\underset{}{\overset{k_1}{\rightleftharpoons}}\; 2\,Mo(O)(NBu^t)(OR_f^3)_2$$
$$\text{(12)} \qquad\qquad \text{(13)} \qquad\qquad\qquad \text{(14)}$$

$$(2.23)$$
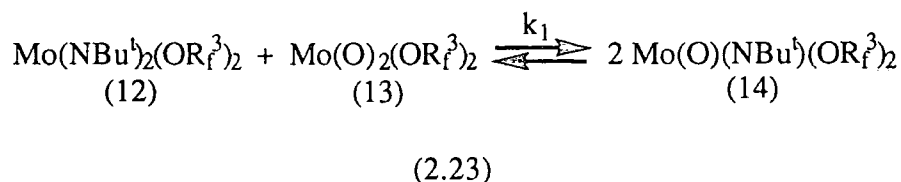
Figure 2.10 shows the ^{1}H NMR spectrum (200 MHz) after 7 hours, in which the methyl resonances of the trifluoro tert-butoxide ligands of (13) and (14) are clearly merged {see section 2.4.1(a)}.

Figure 2.10 ^1H NMR spectrum of the reaction of (12) with (13) after 437 minutes.

Mo(NBu^t)$_2$(OR$_f^3$)$_2$ (12)

Mo(O)(NBu^t)(OR$_f^3$)$_2$ (12)

Mo(O)(NBu^t)(OR$_f^3$)$_2$ (14)

Mo(O)(NBu^t)(OR$_f^3$)$_2$ (14)
+
Mo(O)$_2$(OR$_f^3$)$_2$ (13)
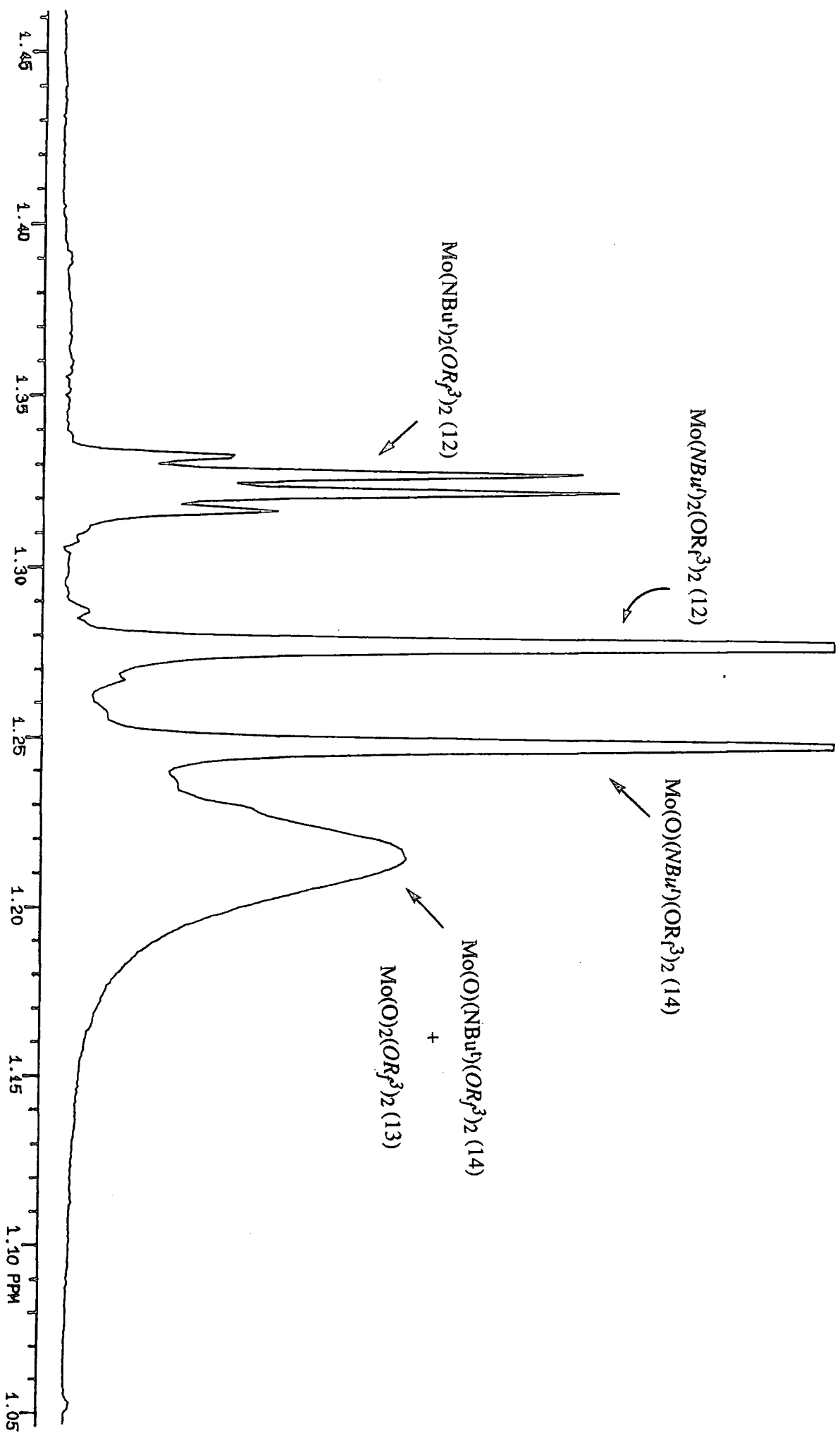
To assess the susceptibility of the reaction to acid catalysis, the reaction was performed separately in the presence of NEt_3 (20%) and benzoic acid (5%). The rate constants are tabulated in table 2.3 {along with those for the hexafluoro tert-butoxide system (R_f^6)}. The reaction rate is not slowed down by the addition of small amounts of NEt_3, but is speeded up in the presence of $PhCO_2H$, demonstrating that the reaction is susceptible to acid catalysis. However, the affects of acid catalysis are small compared to those observed for $R = Bu^t$ (section 2.4.1). A possible explanation for this could be the reduced basicity of the oxygen of the trifluoro tert-butoxide group, therefore rendering it less susceptible to hydrogen bonding.

system	reagent	$k_1 / x10^{-3} \, l \, mols^{-1}$
R_f^3	-	$5.4(4)x10^{-1}$
R_f^3	20% NEt_3	$5.2(3)x10^{-1}$
R_f^3	5% $PhCO_2H$	$1.03(5)$
R_f^6	-	$1.3(1)$
R_f^6	3% NEt_3	$1.25(6)$
R_f^6	5% $PhCO_2H$	$9.6(1)x10^{-1}$

table 2.3 *Rate constants for oxo-imido exchange (R = R_f^3, R_f^6)*

The 2nd order plot for the oxo-imido reaction (R = R_f^3) in the presence of 5% benzoic acid is shown in figure 2.11:
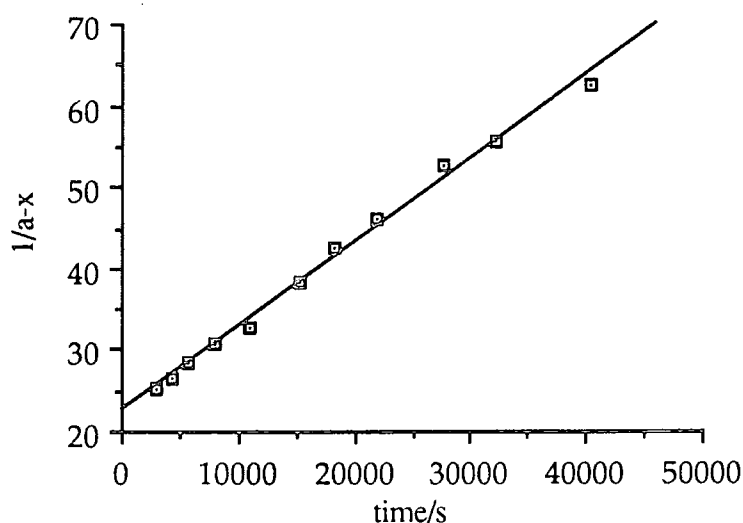
figure 2.11 *2nd order plot for the oxo-imido exchange reaction $(R = Rf^3)$ in the presence of 5% benzoic acid.*

2.4.3 Reaction of $Mo(NBu^t)_2(ORf^6)_2$ (15) with $Mo(O)_2(ORf^6)_2$ (16).

Reaction of $Mo(NBu^t)_2(ORf^6)_2$ (15) with one equivalent of $Mo(O)_2(ORf^6)_2$ (16) in d_6-benzene occured smoothly at room temperature, according to equation 2.24:

$$Mo(NBu^t)_2(ORf^6)_2 + Mo(O)_2(ORf^6)_2 \overset{k_1}{\underset{}{\rightleftharpoons}} 2\, Mo(O)(NBu^t)(ORf^6)_2$$
$$\quad (15) \qquad\qquad (16) \qquad\qquad\qquad (17)$$

$$(2.24)$$
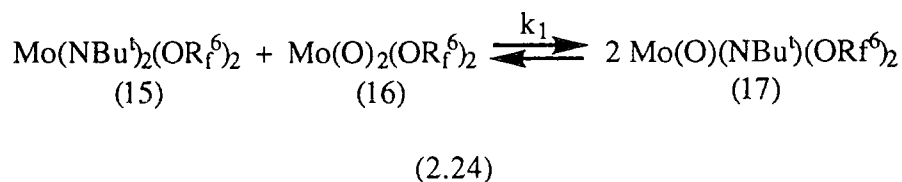
Successive ^1H NMR (400 MHz) spectra at various time intervals are shown in figure 2.12. It is noticeable in figure 2.12, that shifting and coalescing of the methyl resonances (Rf^6) occurs between (16) and the mixed species $Mo(O)(NBu^t)(ORf^6)_2$ (17), in a similar manner to that observed for $R = Bu^t, Rf^3$.

The reaction was performed in the presence of NEt_3 (20%), however complications arose in that an adduct was formed between NEt_3 and $Mo(O)_2(ORf^6)_2$ (16). The adduct was confirmed by the stoichiometric reaction of (16) with one equivalent of NEt_3 in C_6D_6, for which new signals were observed in the ^1H NMR spectrum (see Experimental). The structure of the adduct (shown in figure 2.13) is likely to be closely

Figure 2.12 *Stack plot of the ^1H NMR spectra for the reaction of (15) with (16).*

⊙ $Mo(NBu^t)_2(OR_f^6)_2$ (15)

□ $Mo(O)(NBu^t)(OR_f^6)_2$ (17)
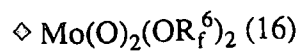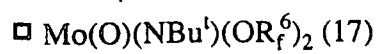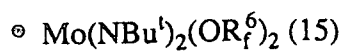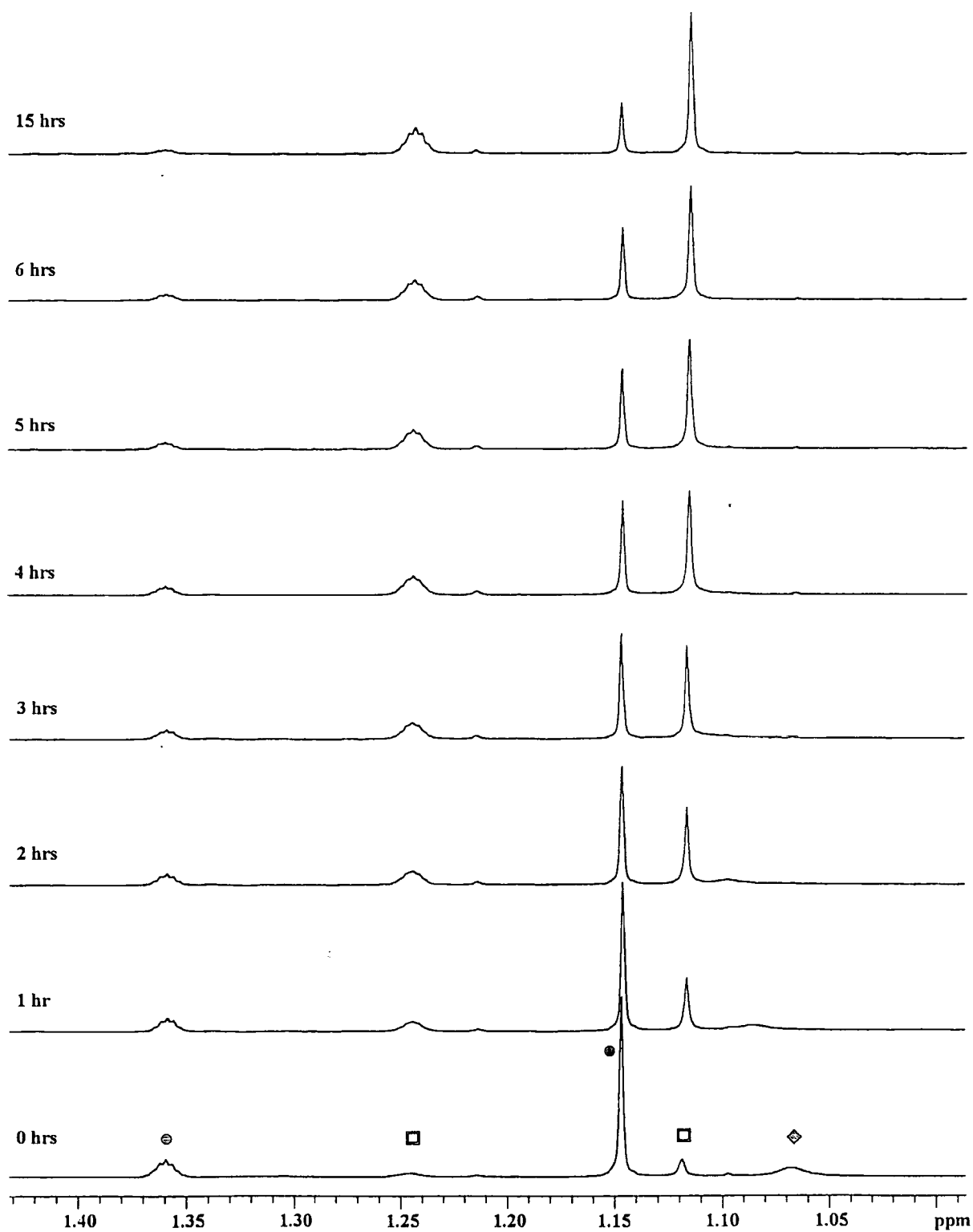
◇ $Mo(O)_2(OR_f^6)_2$ (16)

related to the 5 coordinate trigonal bipyramidal base adducts observed for the hexafluoro tert-butoxide derivative of the Schrock catalyst $Mo(NAr)(CHCMe_2Ph)(OR_f^6)_2.L$, where $L = Bu^tNH_2$[10], PMe_3[29].
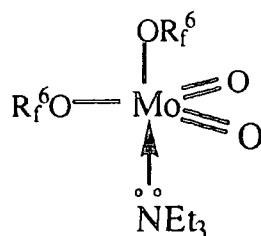
figure 2.13 *NEt_3 base adduct of Mo(O)_2(OR_f^6)_2*

An adduct arises in this example as a consequence of the highly acidic and sterically accessible metal centre of (16). This adduct was found to be inert to oxo-imido exchange, the reaction typically proceeding until all uncomplexed (16) had been consumed. The reaction was performed using a smaller quantity of NEt_3 (3%, the second order plot for which is shown in figure 2.14), where adduct formation would not significantly affect the rate; here the reaction was found to proceed at the same rate as observed in the absence of external reagents (see table 2.3). It is questionable, however, whether an acid source would be removed if all the NEt_3 present is bound to the metal centre of (16). Interestingly, the reaction was found to proceed at the same rate when performed in the presence of $PhCO_2H$ (5%) suggesting that $PhCO_2H$ may not be sufficiently acidic to hydrogen bond to the oxygens of the hexafluoro-tert-butoxide ligands.
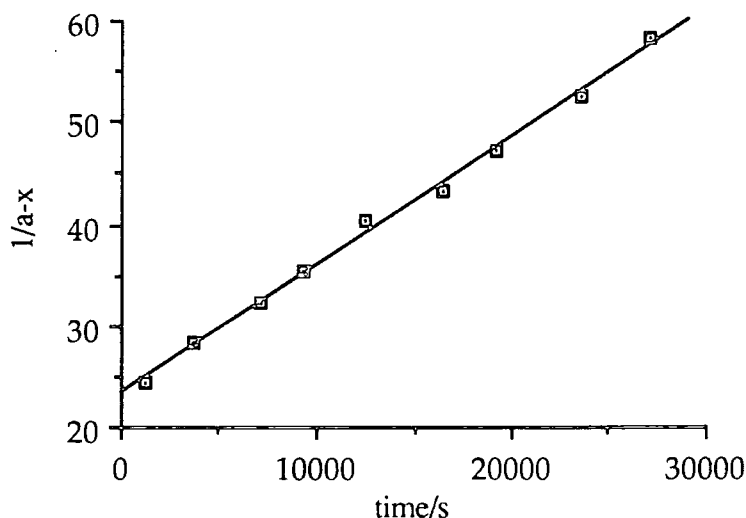
figure 2.14 *2nd order plot for the oxo-imido reaction (R = Rf^6) in the presence of 3% NEt$_3$*

2.4.4 Reaction of Mo(NBu^t)$_2$Cl$_2$.dme with Mo(O)$_2$Cl$_2$.dme

Mo(NBu^t)$_2$Cl$_2$.dme[30,31] was treated with one equivalent of Mo(O)$_2$Cl$_2$.dme in C$_6$D$_6$ at room temperature. After 5 hours, resonances due to Mo(O)(NBu^t)Cl$_2$.dme (18) were observed at δ 1.40(NBu^t), 3.41(dme) and 3.07(dme). The reaction was complete after about 3 days (Keq ~ 200), the rate constant for the forward reaction being 2.3(2)x10^{-4} l mol^{-1}s^{-1}.

$$\text{Mo(NBut)}_2\text{Cl}_2\text{.dme} + \text{Mo(O)}_2\text{Cl}_2\text{.dme} \underset{}{\overset{k_1}{\rightleftharpoons}} 2 \text{ Mo(O)(NBut)Cl}_2\text{.dme}$$
(18)
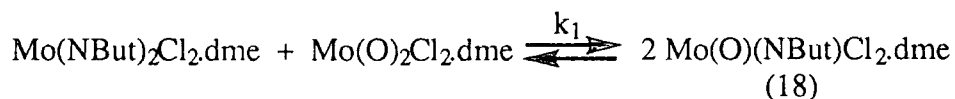
(2.25)

The rate of reaction is much slower than those observed for 4 coordinate oxo-imido exchange (sections 2.4.1-3), consistent with the increased steric congestion for a 6 coordinate system.

2.4.5 Summary

The rate of oxo-tert-butylimido exchange (in the presence of NEt3) is much faster than found for the corresponding oxo-arylimido exchange[10]. The tert-butyl imido nitrogen is more basic than the arylimido nitrogen and therefore will have a greater propensity for bridging, thus lowering the activation energy for formation of the proposed bridged intermediate and thereby assisting the reaction.

Changing the ancillary alkoxide ligands has little effect on the rate of oxo-tert-butylimido exchange, the rate constants (k_1, $l\ mol^{-1}s^{-1}$) for which are:

$$Bu^t (1.0 \times 10^{-3}) \sim R_f^6 (1.3 \times 10^{-3}) > R_f^3 (5.3 \times 10^{-4})$$

This is in direct contrast to the apparently large variation in rates observed on fluorination of the ancillary alkoxide ligands for the oxo-arylimido exchange reaction[10]. However, as the effects of acid catalysis were not clear in the latter system, the rate constants are not directly comparable. Fluorination of the ancillary alkoxides should increase the strength of the respective oxo and imido multiple bonds (decrease rate), nonetheless it would also increase the electrophilicity of the metal centre (increase rate). Presumably a trade-off of effects could possibly be occuring.

The equilibrium constants for all the oxo-tert-butylimido exchange reactions are similar, $K_{eq} > 2 \times 10^2$, showing a strong thermodynamic preference for the oxo-imido species. For oxo-arylimido exchange, the situation is the reverse with the equilibrium position favouring the reactants ($K_{eq} = 0.08$). The origin of this preference may arise as a consequence of competition for the 3 avaliable π orbitals at the metal centre between the two multiply bonded groups. When these groups are electronically disparate, a natural favourable polarisation could occur whereby the stronger π donor would dominate (form 2 π bonds), whereas the weaker π donor would only form one π bond. For the oxo-tert-butylimido complex the difference is large; with the basic tert-butylimido ligand acting as the 2 π donor, whereas for the oxo-arylimido complex this difference would not be as wide, disfavouring this species.

2.5 Synthesis of oxo-imido species

The synthesis of several oxo-imido species were undertaken in an attempt to exploit the favourable position of the oxo-imido exchange equilibria. The reaction conditions employed were as close as possible to those in the NMR experiments.

2.5.1 Reaction of $Mo(NBu^t)_2(OBu^t)_2$ (1) with $Mo(O)_2(OBu^t)_2$

Preparation of $Mo(O)(NBu^t)(OBu^t)_2$ (5)

Equimolar solutions of $Mo(NBu^t)_2(OBu^t)_2$ (1) and $Mo(O)_2(OBu^t)_2$ in toluene were mixed at room temperature. After 1.5 hours the solvent was removed and the pale brown amorphous solid residue was sublimed (298K,$< 10^{-3}$ mm Hg), affording $Mo(O)(NBu^t)(OBu^t)_2$ (5), as a colourless crystalline material in 68% yield.

$$Mo(NBu^t)_2(OBu^t)_2 + Mo(O)_2(OBu^t)_2 \underset{}{\overset{K_{eq}}{\rightleftharpoons}} 2\ Mo(O)(NBu^t)(OBu^t)_2$$
$$(1) \qquad\qquad\qquad\qquad\qquad\qquad\qquad (5)$$
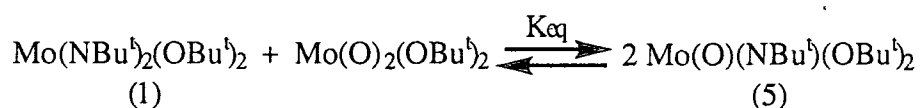
$$(2.26)$$

Complex (5) was extremely unstable, decomposing over several days even under rigorous dry box conditions. The oxo stretch in the infra red spectrum could not be assigned owing to an abundance of bands in the region for a typical mono oxo complex, 900 - 1100 cm^{-1},[32]. Complications arise due to the presence of alkoxide group bands in this region (M-O and O-C fall in the range 900 - 1150 cm^{-1})[33].

C_6D_6 was condensed onto a sample of (5) at liquid nitrogen temperature, the sample warmed quickly to -78°C and a ^1H NMR (400 MHz) spectrum was acquired. The spectrum displayed two singlet resonances at δ 1.38 and 1.25 in the ratio (1:2) attributable to the tert-butyl hydrogens of the imido and alkoxide ligands respectively. On rapid warming to room temperature low intensity resonances due to (1) and $Mo(O)_2(OBu^t)_2$ grew in over several minutes, demonstrating approach to equilibrium in the opposite direction.

69

2.5.2 Reaction of $Mo(NBu^t)_2(ORf^6)_2$ (15) with $Mo(O)_2(ORf^6)_2$ (16)

Preparation of $Mo(O)(NBu^t)(ORf^6)_2$ (17)

An equimolar ethereal solution of $Mo(NBu^t)_2(ORf^6)_2$ (15) and $Mo(O)_2(ORf^6)_2$ (16) was stirred for 4 days at room temperature to give a yellow-green solution. Recrystallisation from the reaction solvent at -78°C afforded yellow crystals of $Mo(O)(NBu^t)(ORf^6)_2$ (17) in a 49% yield, according to equation 2.27:

$$Mo(NBu^t)_2(ORf^6)_2 \;+\; Mo(O)_2(ORf^6)_2 \;\rightleftharpoons\; 2\,Mo(O)(NBu^t)(ORf^6)_2$$
$$\text{(15)} \qquad\qquad \text{(16)} \qquad\qquad\qquad \text{(17)}$$

$$(2.27)$$
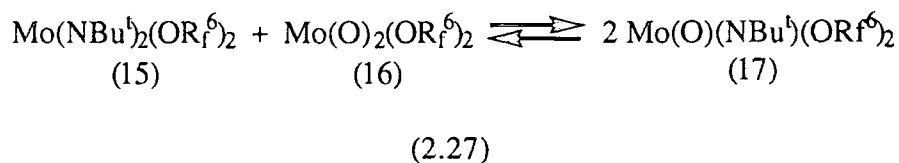
As found for complex (5), these crystals were inherently unstable at room temperature under an inert atmosphere, readily decomposing to afford an orange coloured material. The mass spectrum (EI / m/z) revealed a fragment of mass 531 assignable to $[M - CH_4]^+$, along with a fragment due to CF_3^+ (69). Equilibrium with (15) and (16) occured over several days when a sample of (17) was dissolved in d_6-benzene.

2.5.3 Reaction of $Mo(NBu^t)_2Cl_2.dme$ with $Mo(O)_2Cl_2.dme$

Preparation of $Mo(O)(NBu^t)Cl_2.dme$ (18)

Diethyl ether was added to a solid equimolar mixture of $Mo(NBu^t)_2Cl_2.dme$ and $Mo(O)_2Cl_2.dme$ and the resultant mixture stirred for 5 days at room temperature. $Mo(O)(NBu^t)Cl_2.dme$ (18) was recrystallised from ether at -78°C as a pale green solid in low yield (26%).

$$Mo(NBu^t)_2Cl_2.dme \;+\; Mo(O)_2Cl_2.dme \;\xrightarrow{k_1}\; 2\,Mo(O)(NBu^t)Cl_2.dme$$
$$\text{(18)}$$

$$(2.28)$$

70
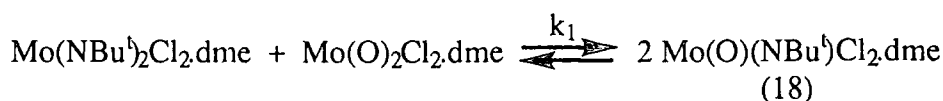
The related oxo-imido complex $Mo(O)(N-1-Adamantyl)Cl_2.dme$ has been synthesised in our laboratory[34], a structural determination for this compound shows cis multiply bonded oxo and imido ligands in a distorted octahedral geometry

When a solution of (18) in C_6D_6 was left for several weeks, resonances due to the starting materials were difficult to detect, suggesting that the equilibrium position may lie further to the right than originally perceived (see section 2.4.4). Fluxional behaviour for the methyls of the dme ligand was observed, the resonance at δ 63.27 in the ^{13}C NMR spectrum being substantially broadened.

2.6 Mono-anionic (X-type) intermetal ligand exchange in $Mo(Q)_2X_2$ system

Relatively little is known about the exchange between metal centres of formal one electron ligands, with only a few examples having been reported in the literature (for a brief review see section 1.3.1). It is the aim of the following sections to examine the exchange equilibria for a given pair of X and Y ligands in several four coordinate molybdenum (VI) systems of the type $Mo(Q)_2X_2$ {$(Q)_2 = (NBu^t)_2$, $(O)_2$ and $(NAr)(CHC(CH_3)_2Ph)$}. For simplicity, these systems were chosen so that reaction with another molecule of the type $Mo(Q)_2Y_2$, could only possibly afford one mixed product:

$$Mo(Q)_2X_2 + Mo(Q)_2Y_2 \xrightleftharpoons{K_{eq}} 2\,Mo(Q)_2XY$$

(2.29)
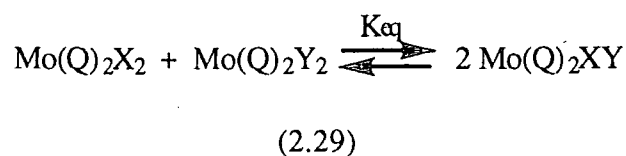
The findings of the subsequent reactions are incorporated in a general discussion in chapter three (section 3.5.11), where a comparison with analogous monovalent exchange reactions for the half-sandwich niobium system $CpNb(NBu^t)X_2$ is made.

71

In order to conduct this study, suitable precursors had first to be synthesised containing a variety of X type ligands spanning halide, amide, and alkoxide moieties. These species were chosen to enable steric and electronic influences to be probed.

2.6.1 Reaction of Mo(NBu^t)$_2$Cl$_2$.dme with LiNHBu^t

Preparation of Mo(NBu^t)$_2$(NHBu^t)$_2$ (19).

The synthesis of Mo(NBu^t)$_2$(NHBu^t)$_2$ (19) has been previously reported from the reaction of Mo(NBu^t)$_2$Cl$_2$[1] with two equivalents of LiNHBu^t by Wilkinson and co-workers[35]. Here, (19) is prepared using the dme precursor Mo(NBu^t)$_2$Cl$_2$.dme. The reaction of Mo(NBu^t)$_2$Cl$_2$.dme with two equivalents of LiNHBu^t proceeds slowly over two days at 60°C in THF, according to equation 2.30.

$$Mo(NBu^t)_2Cl_2.dme \ + \ 2\,LiNHBu^t \ \xrightarrow[60°C]{THF} \ Mo(NBu^t)_2(NHBu^t)_2 \ + \ 2\,LiCl$$
$$(19)$$

$$(2.30)$$
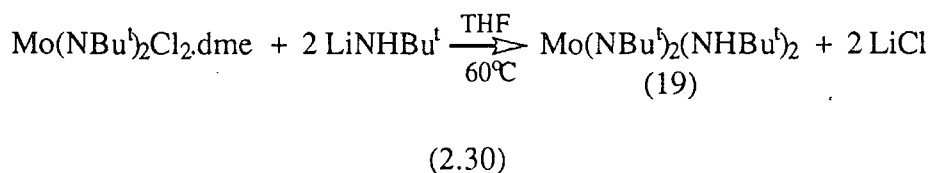
Sublimation afforded pure (19) in 60% yield as a pale yellow solid. The ^{1}H NMR (400 MHz, C$_6$D$_6$) spectrum displayed a resonance arising from the amide proton at δ 5.69, and two equal intensity tert-butyl resonances at δ 1.42 and 1.30. A nuclear Overhauser (nOe) experiment was necessary in order to establish which tert-butyl resonances belonged to the amide/imido ligands. The amide resonance displayed an enhancement when the tert-butyl resonance at δ 1.30 was irradiated, thus allowing the assignment of this signal to that of the tert-butylamide ligand. This contradicts the assignment made for these respective signals in the previously reported synthesis[35]. Subsequently, a ^{1}H - ^{13}C heteronuclear correlation (HETCOR) experiment then enabled the assignment of β-carbon resonances for the tert-butyl amide/imido groups at δ 33.64 (NHBu^t) and 32.84 (NBu^t). A characteristic amide N-H stretch was present in the infrared spectrum at 3350 cm^{-1}.

2.6.2 Reaction of Mo(NBu^t)$_2$Cl$_2$.dme with LiOPr^i

Preparation of Mo(NBu^t)$_2$(OPr^i)$_2$ (20).

The reaction of Mo(NBu^t)$_2$Cl$_2$.dme with two equivalents of LiOPr^i proceeded smoothly at room temperature in diethyl ether to afford Mo(NBu^t)$_2$(OPr^i)$_2$ (20), isolated as a pale yellow oil, according to equation 2.31:

$$Mo(NBu^t)_2Cl_2.dme \ + \ 2 \ LiOPr^i \ \longrightarrow \ 0.5 \ [Mo(NBu^t)_2(OPr^i)_2]_2 \ + \ 2 \ LiCl$$
$$(20)$$

$$(2.31)$$
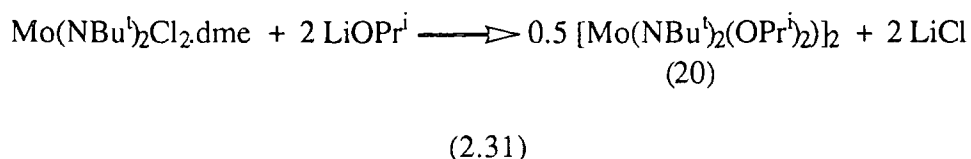
Crystallisation of (20) could be induced on cooling below it's melting point (17 - 20°C). Resonances corresponding to the iso-propoxide groups were located in the ^{1}H NMR spectrum (400 MHz, C$_6$D$_6$) at δ 4.71 (septet) and 1.28 (doublet), for the methine and methyl protons respectively. The mass spectrum (CI, m/z, ^{98}Mo) revealed the protonated parent ion at 359; however the presence of low intensity higher molecular weight fragments was also noted. A crystal structure of (20) was therefore desirable in order to determine the degree of association in the solid state.

2.6.3 The molecular structure of Mo(NBu^t)$_2$(OPr^i)$_2$ (20)

Small cubic crystals of (20) were picked rapidly at ambient temperature (low melting point ca.17 - 20°C) and mounted in 0.5 mm Lindemann capillary tubes under an inert atmosphere. X-ray data were collected at 150K by Ms.C.Wilson and Professor J.A.K.Howard. Preliminary analysis of this data shows the structure to be dimeric and suggests that the bridging units are propoxide ligands (shown schematically in figure 2.15). However, at this stage the structural refinements are incomplete.
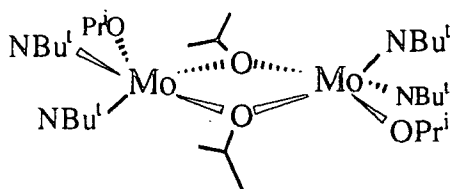
figure 2.15 *Molecular structure of [Mo(NBu^t)$_2$(OPr^i)(μOPr^i)]$_2$*

Iso-propoxide ligands show a greater tendency for bridging than corresponding butoxide groups because of the less crowded steric environment around the oxygen[36]. This is exemplified by the monomeric structure of the tert-butoxide analogue Mo(NBu^t)$_2$(OBu^t)$_2$ (1), shown in section 2.2.1. Of special note in this case is the apparent preference for bridging alkoxides as opposed to bridging imido groups.

2.6.4 ^{13}C NMR - chemical shifts (δ, ppm) of the tert-butyl imido group in Mo(NBu^t)$_2$X$_2$ complexes

Nugent has shown that the difference in chemical shift between the α- and β-carbons of the tert-butyl imido, Δδ, gives an indication of the electronic nature of the imido group[37]. From examination of a series of structurally diverse d^0 tert-butyl imido complexes, decreasing the electron density on the imido nitrogen leads to a downfield shift in the α-carbon resonance and a corresponding upfield shift in the β-carbon resonance. The type of chemical reactivity of the imido group can be predicted on the basis of Δδ values; a large Δδ value is indicative of less charge on the nitrogen and consequently the imido will exhibit electrophilic behaviour, whereas a small Δδ value is characteristic of a nucleophilic imido group. As discussed previously (section 1.2), Δδ varies dramatically on changing the metal or number of imido units on the metal centre. However, changes in Δδ are much more subtle on changing the ancillary ligands for a particular system[26]. The α- and β- carbon resonances, together with the Δδ values for a series of four coordinate molybdenum bis imido complexes of the type Mo(NBu^t)$_2$X$_2$ are recorded in table 2.4:

X	$\delta C(\alpha)$	$\delta C(\beta)$	$\Delta\delta$
NHBu^t	67.22	32.64	33.58
OPr^i	69.09	33.16	35.93
OBu^t	67.94	32.16/44	35.50/35.78
OR$_f^3$	70.02	31.84	38.18
OR$_f^6$	72.23	31.32	40.91
Cl^1	74.13	30.11	44.02

table 2.4 ^{13}C *chemical shift data (ppm) for Mo(NBu^t)$_2$X$_2$*

The magnitude of $\Delta\delta$ lies in the range 33 - 44 ppm and increases in the order:

$$NHBu^t < OBu^t < OPr^i < OR_f^3 < OR_f^6 < Cl$$
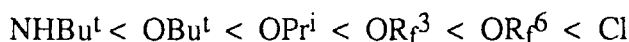
At the lower limit is the tert-butyl amide group, which is consistent with the decreased electronegativity of the nitrogen relative to that of the oxygen in the alkoxide species. The trend in $\Delta\delta$ on fluorination of the tert-butyl alkoxide groups is clear:

$$OBu^t < OR_f^3 < OR_f^6$$

This is consistent with increasing the electronegativity of the alkoxides by the addition of successive CF$_3$ units. At the upper limit, the halide (Cl) shows the largest $\Delta\delta$ values of the series, reflecting the high electronegativity and poor π donor ability compared to the alkoxide species. This series shows clear trends that are useful for comparisons with other systems (see section 3.5.9).

2.6.5 Mono-anionic (X-type) intermetal ligand exchange in the Mo(NBu^t)$_2$X$_2$ system

Typically, equimolar quantities (38 μmols) of Mo(NBu^t)$_2$X$_2$ and Mo(NBu^t)$_2$Y$_2$ were mixed in C$_6$D$_6$ (800μl), and the reactions followed by ^{1}H NMR spectroscopy. The relative intensities of the mixed species Mo(NBu^t)$_2$XY and reactants at equilibrium allowed the determination of equilibrium constants (K$_{eq}$):

$$\text{Mo(NBu}^t)_2\text{X}_2 + \text{Mo(NBu}^t)_2\text{Y}_2 \underset{K_{eq}}{\overset{}{\rightleftharpoons}} 2\,\text{Mo(NBu}^t)_2\text{XY}$$
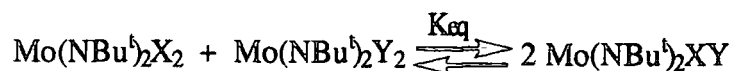
(2.32)

a) Reaction of Mo(NBu^t)$_2$Cl$_2$ with Mo(NBu^t)$_2$(OBu^t)$_2$ (1)

Equimolar quantities of Mo(NBu^t)$_2$Cl$_2$ and Mo(NBu^t)$_2$(OBu^t)$_2$ (1) were mixed at room temperature. A ^{1}H NMR (200 MHz) spectrum was obtained 5 minutes after mixing and the reaction found to have gone to completion (no residual reactants observable). As the reaction was too fast to be followed conveniently by ^{1}H NMR at ambient temperature, a lower limit can be estimated for the second order rate constant $k_1 > 7.7$ l mol^{-1}s^{-1} at 298K (based on the reaction being 99% complete after 5 minutes).

$$\text{Mo(NBu}^t)_2\text{Cl}_2 + \underset{(1)}{\text{Mo(NBu}^t)_2\text{(OBu}^t)_2} \underset{K_{eq}}{\overset{}{\rightleftharpoons}} \underset{(8)}{2\,\text{Mo(NBu}^t)_2\text{(OBu}^t)\text{Cl}}$$
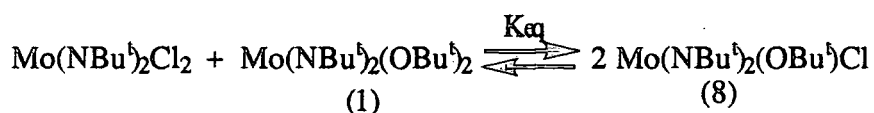
(2.33)

The mixed complex Mo(NBu^t)$_2$(OBu^t)Cl (8) is overwhelmingly favoured ($K_{eq} > 10^4$). The ^{1}H NMR (C$_6$D$_6$) chemical shifts for the mixed species Mo(NBu^t)$_2$(OBu^t)Cl (8) are recorded in table 2.5, along with selected chemical shift values of other mixed species of the general formula Mo(NBu^t)$_2$XY:

| complex | | ^{1}H NMR (C_6D_6, 200 MHz, δ (ppm)) | | |
X	Y	NBu^t	X	Y
Cl	OBu^t	1.29	-	1.26
Cl	NHBu^t	1.32	-	1.14, 8.10(br)
OBu^t	NHBu^t	1.40	1.42	1.26, 6.62(br)
OBu^t	OPr^i	1.37	1.28(d),4.70 (sept)	1.37
OBu^t	OR$_f^3$	1.32	1.30	1.37(m)
OBu^t	OR$_f^6$	1.27	1.26	1.49(sept)
OR$_f^3$	OR$_f^6$	1.23	1.27(m)	1.44(sept)

table 2.5 *^{1}H NMR data for Mo(NBu^t)$_2$XY complexes.*

b) Reaction of Mo(NBu^t)$_2$Cl$_2$ with Mo(NBu^t)$_2$(NHBu^t)$_2$ (19)

The reaction of Mo(NBu^t)$_2$Cl$_2$ with Mo(NBu^t)$_2$(NHBu^t)$_2$ (19) was also found to have reached completion after 5 minutes at room temperature ($K_{eq} > 10^4$), according to equation 2.34:

$$Mo(NBu^t)_2Cl_2 + Mo(NBu^t)_2(NHBu^t)_2 \underset{}{\overset{K_{eq}}{\rightleftarrows}} 2\ Mo(NBu^t)_2(NHBu^t)Cl$$
$$(19) \qquad\qquad\qquad (21)$$

$$(2.34)$$
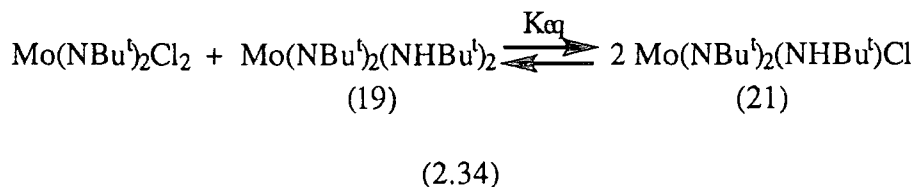
The chemical shifts in the ^{1}H NMR spectrum (C_6D_6) for (21) are given in table 2.5.

c) Reaction of Mo(NBu^t)$_2$(OBu^t)$_2$ (1) with Mo(NBu^t)$_2$(NHBu^t)$_2$ (19)

In contrast to the reactions described in (a) and (b), the reaction between Mo(NBu^t)$_2$(OBu^t)$_2$ (1) and Mo(NBu^t)$_2$(NHBu^t)$_2$ (19) was very slow at room temperature, requiring 15 days for equilibrium to be attained {K_{eq} = 20(2)}.

$$\text{Mo(NBu}^t)_2\text{(NHBu}^t)_2 + \text{Mo(NBu}^t)_2\text{(OBu}^t)_2 \xrightleftharpoons{K_{eq}} 2\ \text{Mo(NBu}^t)_2\text{(NHBu}^t)\text{(OBu}^t)$$

$$\qquad\text{(19)}\qquad\qquad\qquad\text{(1)}\qquad\qquad\qquad\qquad\qquad\text{(22)}$$

$$\text{(2.35)}$$
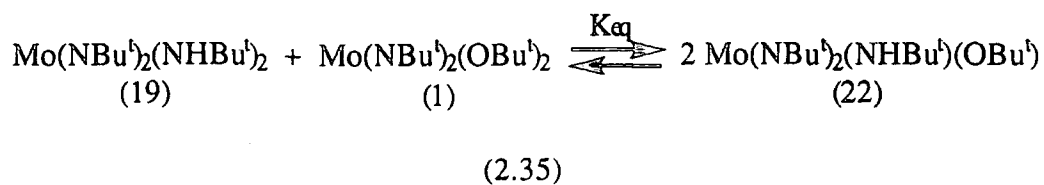
The reaction was closely monitored and the data analysed according to the integrated rate law for a second order reversible reaction[28]:

$$\ln\left[\frac{x\,(a - 2x_e) + ax_e}{a\,(x_e - x)}\right] = \left[\frac{2a\,(a - x_e)}{x_e}\right]k_1 t \qquad \text{(2.34)}$$

where a = starting concentration of (1),

x = concentration of (22) at time t,

x_e = equilibrium concentration of (22).

The plot of $\ln\,[x\,(a - x_e) + ax_e\,/\,a\,(x_e - x)] = \ln\,(f)$, versus time is shown in figure 2.16, the slope of which is $[2a\,(a - x_e)\,/\,x_e]\,k_1$, thus allowing the determination of $k_1 = 5.2(3) \times 10^{-5}$ l mol^{-1}s^{-1}.

figure 2.16 *Plot of ln (f) versus time for OBu^t - NHBu^t exchange*

This reaction is unique for one electron exchange studies of four coordinate molybdenum systems, in that equilibrium is not established almost immediately i.e before 5 minutes (k_1 > 7.7 1 $mol^{-1}s^{-1}$). The rate of reaction is at least 5 orders of magnitude slower than that observed for chloride - butoxide (a) and chloride - amide (b) exchange. This is a consequence of the combination of sterically demanding tert-butoxide and tert-butylamide ligands hindering bridging between the two metal centres. This will be discussed in more detail in section 3.5.11.

d) Reaction of $Mo(NBu^t)_2(OBu^t)_2$ (1) with $Mo(NBu^t)_2(OPr^i)_2$ (20)

A ^1H NMR spectrum arising from an equimolar mixture of $Mo(NBu^t)_2(OBu^t)_2$ (1) and $Mo(NBu^t)_2(OPr^i)_2$ (20), showed the reaction to be complete within 5 minutes at room temperature.

$$Mo(NBu^t)_2(OBu^t)_2 + Mo(NBu^t)_2(OPr^i)_2 \xrightleftharpoons{K_{eq}} 2\ Mo(NBu^t)_2(OBu^t)(OPr^i)$$
$$\text{(1)} \qquad\qquad \text{(20)} \qquad\qquad\qquad \text{(23)}$$

(2.37)

Assignment of the resonances in the ^1H NMR due to $Mo(NBu^t)_2(OBu^t)(OPr^i)$ (23) was difficult owing to the presence of at least 3 signals corresponding to the 5 possible tert-butyl environments, in the range δ 1.36 - 38 ppm. This small range in chemical shift values reflects the similar electronic environments of the products and the reactants. A separate experiment in which (1) and (20) were mixed in a 2:1 ratio was performed and the relative intensities of the 3 signals compared. This enabled the assignment of coincident tert-butyl resonances at δ 1.37 (OBu^t, NBu^t) for (23) to be made. Both experiments were consistent with a final equilibrium position of K_{eq} = 3.0(3). This equilibrium constant shows little thermodynamic preference for either reactants or products, having almost a statistical value for an A + B = 2C equilibrium. Iso-propoxide and tert-butoxide ligands would be expected to exhibit similar electronic and orbital characteristics at the metal centre, consequently there would be expected to be only a slight energetic difference between reactants and products.

e) Reaction of Mo(NBu^t)$_2$(OBu^t)$_2$ (1) with Mo(NBu^t)$_2$(OR$_f^3$)$_2$ (12)

Equilibrium was established between 5 and 10 minutes for the reaction of Mo(NBu^t)$_2$(OBu^t)$_2$ (1) and Mo(NBu^t)$_2$(OR$_f^3$)$_2$ (12) at room temperature.

$$\text{Mo(NBu}^t\text{)}_2\text{(OBu}^t\text{)}_2 + \text{Mo(NBu}^t\text{)}_2\text{(OR}_f^3\text{)}_2 \underset{}{\overset{K_{eq}}{\rightleftharpoons}} 2\ \text{Mo(NBu}^t\text{)}_2\text{(OBu}^t\text{)(OR}_f^3\text{)}$$
$$\text{(1)} \qquad\qquad \text{(12)} \qquad\qquad\qquad \text{(24)}$$

(2.38)

The equilibrium constant {K_{eq} = 7.0(7)} reflects a slight preference for the mixed product Mo(NBu^t)$_2$(OBu^t)(OR$_f^3$) (24).

f) Reaction of Mo(NBu^t)$_2$(OBu^t)$_2$ (1) with Mo(NBu^t)$_2$(OR$_f^6$)$_2$ (15)

Equimolar quantities of Mo(NBu^t)$_2$(OBu^t)$_2$ (1) and Mo(NBu^t)$_2$(OR$_f^6$)$_2$ (15) were mixed at room temperature, whereby equilibrium was reached between 5 and 10 minutes {K_{eq} = 50(3)}.

$$\text{Mo(NBu}^t\text{)}_2\text{(OBu}^t\text{)}_2 + \text{Mo(NBu}^t\text{)}_2\text{(OR}_f^6\text{)}_2 \underset{}{\overset{K_{eq}}{\rightleftharpoons}} 2\ \text{Mo(NBu}^t\text{)}_2\text{(OBu}^t\text{)(OR}_f^6\text{)}$$
$$\text{(1)} \qquad\qquad \text{(15)} \qquad\qquad\qquad \text{(25)}$$

(2.39)
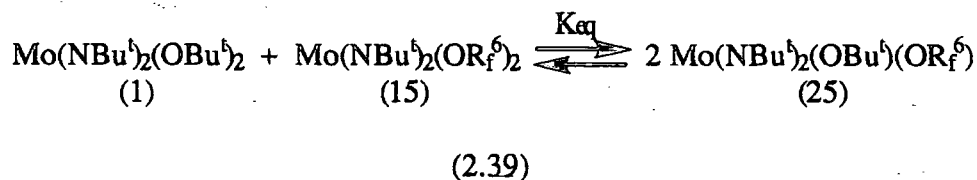
^{1}H NMR resonances for the mixed complex Mo(NBu^t)$_2$(OBu^t)(OR$_f^6$) (25) are collected in table 2.5.

g) Reaction of Mo(NBu^t)$_2$(OR$_f^3$)$_2$ (12) with Mo(NBu^t)$_2$(OR$_f^6$)$_2$ (15)

The reaction of Mo(NBu^t)$_2$(OR$_f^3$)$_2$ (12) with Mo(NBu^t)$_2$(OR$_f^6$)$_2$ (15) reached equilibrium in about 15 minutes at room temperature {K_{eq} = 7.0(2)}. The rate at which equilibrium is reached is qualitatively slower than in both (e) and (f), reflecting increased steric congestion (possibly arising due to fluorine-fluorine interactions) in the transition state {see section 3.5.10(f)-(h)}.

$$\text{Mo(NBu}^t)_2(\text{OR}_f^3)_2 \ + \ \text{Mo(NBu}^t)_2(\text{OR}_f^6)_2 \ \underset{}{\overset{K_{eq}}{\rightleftharpoons}} \ 2\,\text{Mo(NBu}^t)_2(\text{OR}_f^3)(\text{OR}_f^6)$$

$$\text{(12)} \qquad\qquad\qquad \text{(15)} \qquad\qquad\qquad\qquad \text{(26)}$$
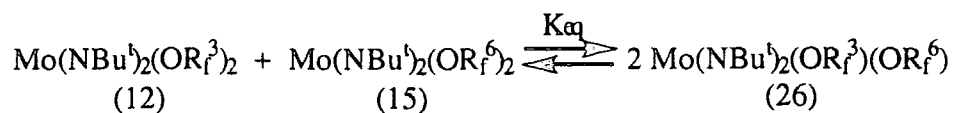
$$\text{(2.40)}$$

Figure 2.17 shows the ^{1}H NMR (200 MHz) at equilibrium. Notably, the equilibrium constant is identical to that achieved in (e). In both cases there is a difference of one CF_3 group between each reactant pair.

The equilibrium constants for reactions (a) - (g) in C_6D_6 at 298K are collected in table 2.6:

X	Y	K_{eq}
Cl	OBu^t	$> 10^4$
Cl	NHBu^t	$> 10^4$
OBu^t	NHBu^t	20(2)
OBu^t	OPr^i	3.0(3)
OBu^t	OR$_f^3$	7.0(7)
OBu^t	OR$_f^6$	50(3)
OR$_f^3$	OR$_f^6$	7.0(2)

table 2.6 *Equilibrium constants (Keq) for X - Y exchange in the Mo(NBu^t)$_2$X$_2$ system*

2.6.6 Intermetal alkoxide exchange in the Mo(NAr)(CHCMe$_2$Ph)(OR)$_2$ (R = Bu^t, R$_f^3$, R$_f^6$) system

The importance of molybdenum alkylidene complexes[38] in olefin metathesis prompted an investigation of alkoxide ligand exchange in this system. The alkoxide exchange equilibrium between the bis tert-butoxide (Bu^t) and bis hexafluoro tert-butoxide

figure 2.17 ^1H NMR spectrum of the reaction of (12) with (15) after 15 minutes.

α Mo(NBu^t)$_2$(OR$_f^6$)$_2$ (15)

β Mo(NBu^t)$_2$(OR$_f^3$)$_2$ (12)

ω Mo(NBu^t)$_2$(OR$_f^3$)(OR$_f^6$) (26)
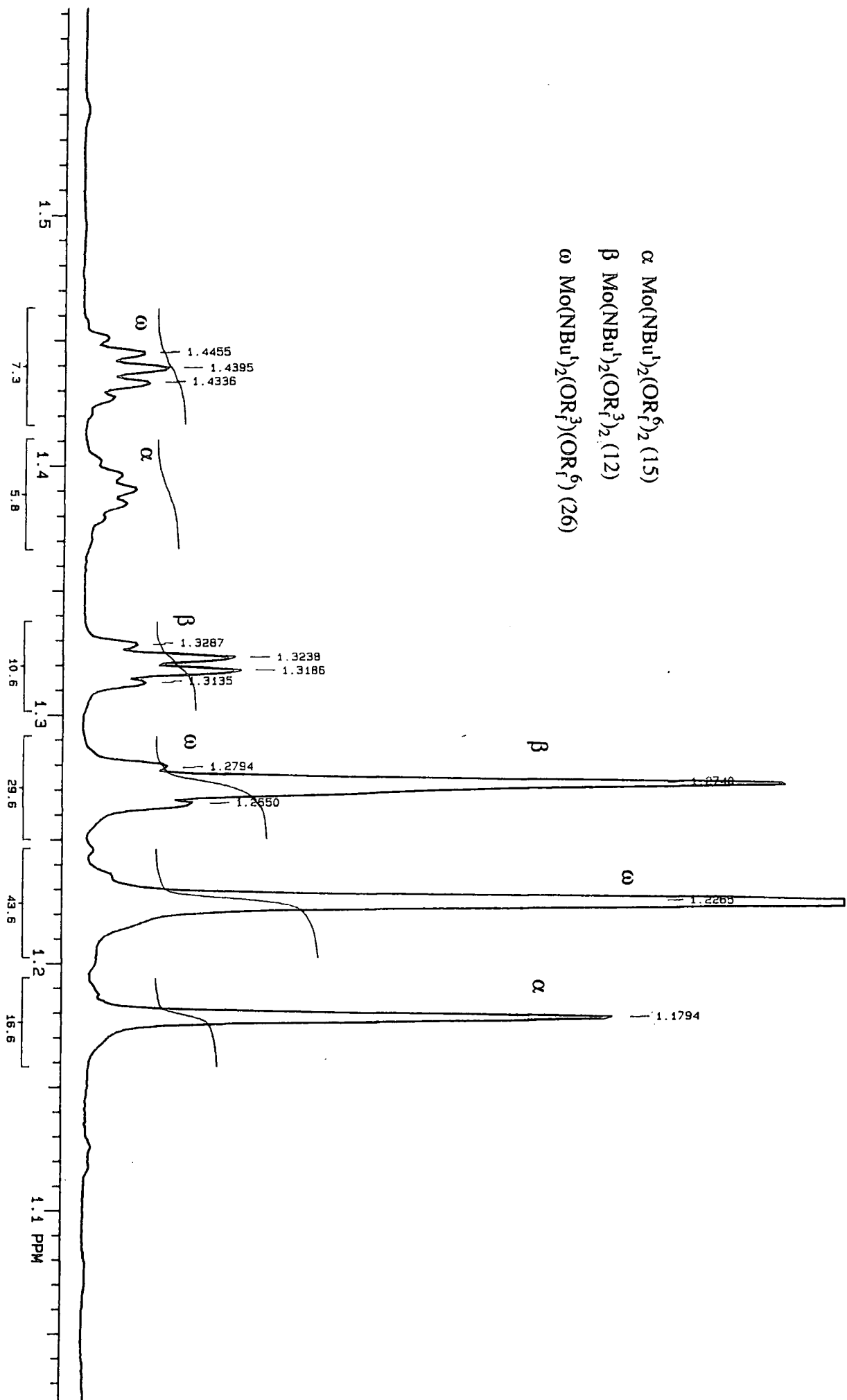
($R_f{}^6$) derivatives has been previously reported[10] ($K_{eq} = 150$). The equilibria of the two other possible permutations i.e (OBu^t - $OR_f{}^3$ and $OR_f{}^3$ - $OR_f{}^6$) are described herein.

a) Reaction of $Mo(NAr)(CHCMe_2Ph)(OBu^t)_2$ with $Mo(NAr)(CHCMe_2Ph)(OR_f{}^3)_2$

Equimolar quantities of the complexes $Mo(NAr)(CHCMe_2Ph)(OBu^t)_2$ and $Mo(NAr)(CHCMe_2Ph)(OR_f{}^3)_2$ were mixed at room temperature. Equilibrium was attained within 5 minutes; equation 2.41 gives the approximate percentages of species at equilibrium:

$$Mo(NAr)(CHCMe_2Ph)(OBu^t)_2 + Mo(NAr)(CHCMe_2Ph)(OR_f{}^3)_2$$

19% K_{eq} 19%

$$2\ Mo(NAr)(CHCMe_2Ph)(OBu^t)(OR_f{}^3)$$
(27)
62%
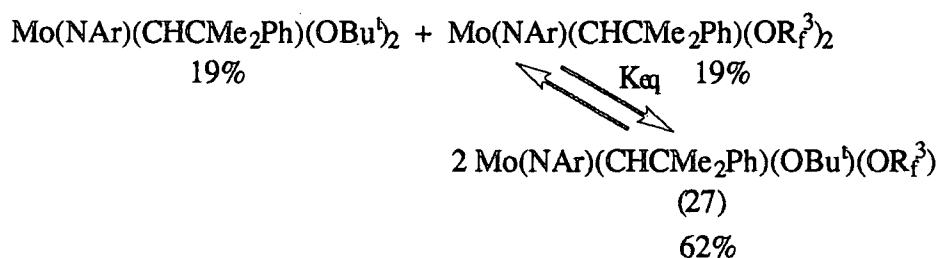
(2.41)

The ^{1}H NMR (400 MHz) spectrum (figure 2.18) shows the resonances due to the mixed species $Mo(NAr)(CHCMe_2Ph)(OBu^t)(OR_f{}^3)$ (27), the characteristic alkylidene proton signal for which is observed at δ 11.50. The alkylidene signal for (27) is almost exactly half way inbetween the alkylidene resonances of the reactant complexes at δ 11.32(Bu^t) and 11.67($R_f{}^3$), and is an indication of an 'averaged' electronic environment in this mixed complex. The equilibrium constant {$K_{eq} = 11.0\ (5)$} was determined by integration of the alkylidene and methine septet (NAr) regions of the spectrum. The data was acquired using a large number of pulses (256) of long relaxation delay time (3 seconds), owing to the long relaxation times (T_1) of alkylidene protons. The equilibrium constant for analogous OBu^t - $OR_f{}^3$ exchange in the $Mo(NBu^t)_2X_2$ system is 7.0(7), corresponding to percentage equilibrium concentrations of 57% (mixed), 21.5% and 21.5%. The difference between these two equilibrium constants does not give a large difference in the equilibrium concentrations of the comparable species.

figure 2.18 *¹H NMR spectrum of the reaction of Mo(NAr)(CHMe₂Ph)(OBuᵗ)₂ with Mo(NAr)(CHMe₂Ph)(ORf³)₂*

α Mo(NAr)(CHMe₂Ph)(OBuᵗ)₂

β Mo(NAr)(CHMe₂Ph)(ORf³)₂

ω Mo(NAr)(CHMe₂Ph)(OBuᵗ)(ORf³)

alkylidene (*CH*Me₂Ph) region

methine (*CH*Me₂) region
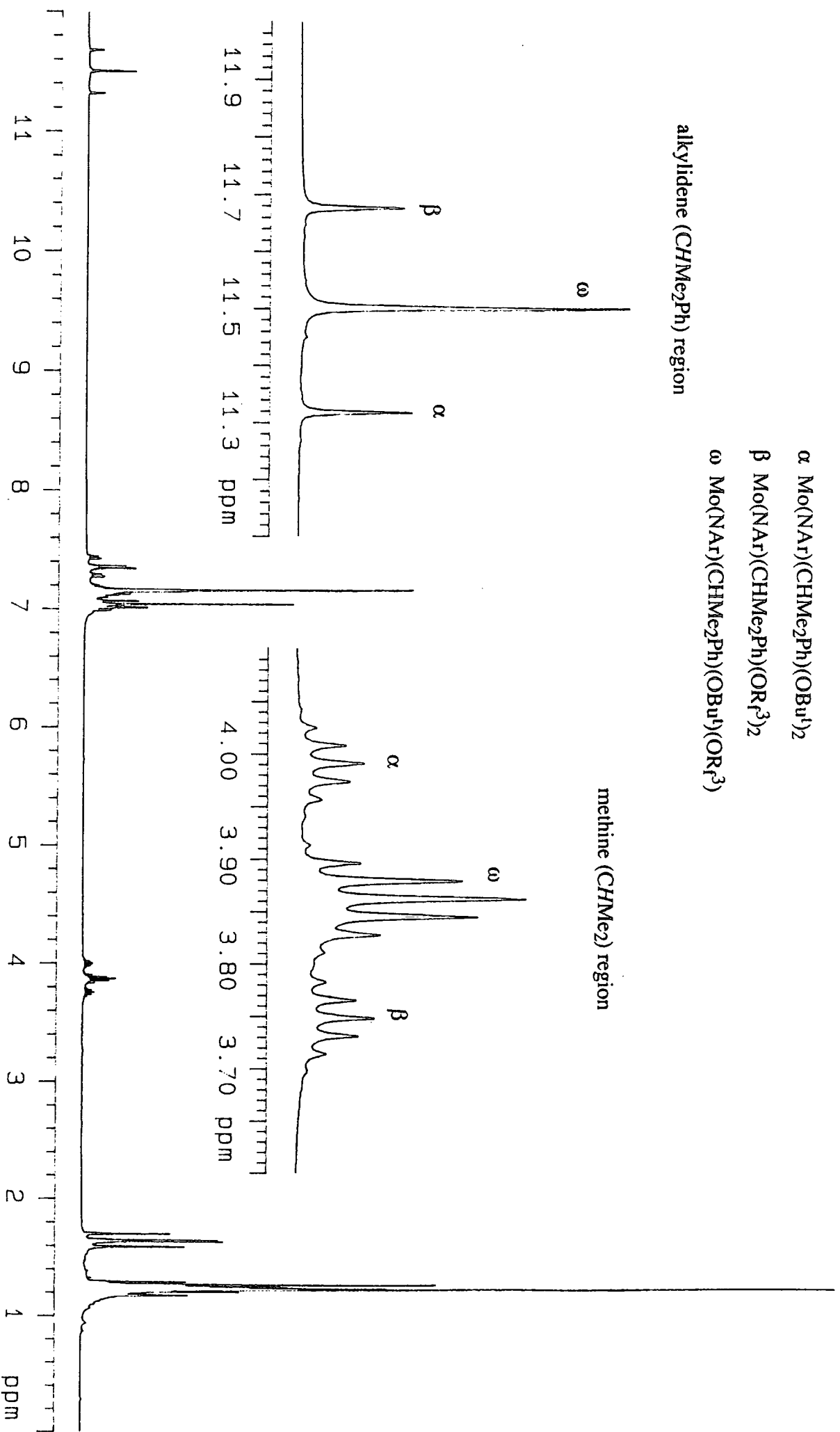
b) Reaction of Mo(NAr)(CHCMe₂Ph)(ORf³)₂ with Mo(NAr)(CHCMe₂Ph)(ORf⁶)₂

The reaction of $Mo(NAr)(CHCMe_2Ph)(OR_f^3)_2$ with one equivalent of $Mo(NAr)(CHCMe_2Ph)(OR_f^6)_2$ at room temperature occured rapidly, the following equilibrium being established{$K_{eq} = 8.0(5)$}:

$$Mo(NAr)(CHCMe_2Ph)(OR_f^3)_2 \; + \; Mo(NAr)(CHCMe_2Ph)(OR_f^6)_2$$

$$K_{eq}$$

$$2 \; Mo(NAr)(CHCMe_2Ph)(OR_f^3)(OR_f^6)$$
$$(28)$$

$$(2.42)$$
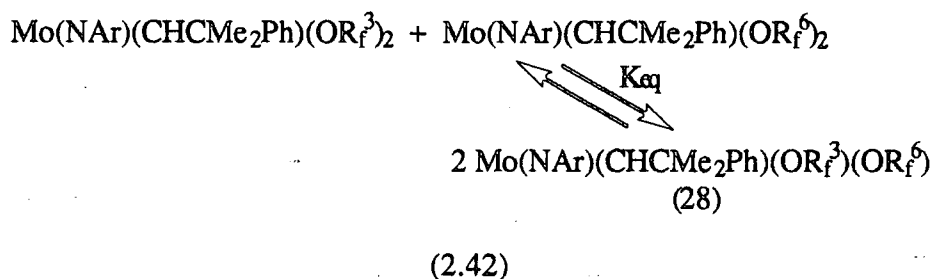
The alkylidene proton resonance for the mixed complex (28) is at δ 11.89 in the ^1H NMR (400 MHz) spectrum, again almost exactly the average of the reactant alkylidene compexes chemical shifts of δ 12.12(R_f^6) and 11.67(R_f^3). The equilibrium constant for the reaction is very similar to that observed previously in the $Mo(NBu^t)_2X_2$ system for OR_f^3 - OR_f^6 exchange {$K_{eq} = 7.0(2)$}. The equilibrium constants for alkoxide exchange in both $Mo(NBu^t)_2X_2$ and $Mo(NAr)(CHCMe_2Ph)X_2$ systems, although not identical are very similar. However, equilibrium is established at a faster rate in the latter system as a consequence of the increased electrophilicity of the metal centre; encouraging alkoxide bridging between the metal centres and subsequent exchange to take place.

2.6.7 Intermetal alkoxide exchange in the $Mo(O)_2(OR)_2$
$(R = Bu^t, R_f^3, R_f^6)$ system

Alkoxide exchange in the four coordinate molybdenum (VI) system $Mo(O)_2(OR)_2$ $(R = Bu^t, R_f^3, R_f^6)$ has been investigated.

a) Reaction of Mo(O)$_2$(OBu^t)$_2$ with Mo(O)$_2$(OR$_f^3$)$_2$ (13)

Equimolar quantities of Mo(O)$_2$(OBu^t)$_2$ and Mo(O)$_2$(OR$_f^3$)$_2$ (13) were mixed at room temperature, where equilibrium was established within 5 minutes.

$$Mo(O)_2(OBu^t)_2 + Mo(O)_2(OR_f^3)_2 \underset{}{\overset{Keq}{\rightleftharpoons}} 2\,Mo(O)_2(OBu^t)(OR_f^3)$$
$$(13) \qquad\qquad\qquad (29)$$
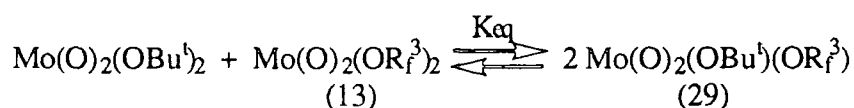
(2.43)

A large broadened signal (peak width ~ 22 Hz) centred at δ 1.11 was present in the ^{1}H NMR (200 MHz) spectrum. This signal incorporated resonances due to all three complexes and was broadened due to alkoxide exchange taking place at rates comparable with the NMR timescale (see section 2.4.1). Unfortunately, the extent of alkoxide exchange broadening was such that an accurate evaluation of the equilibrium constant was not possible, nevertheless, an estimate can be made which places this constant in the range Keq ~ 5 -15.

b) Reaction of Mo(O)$_2$(OBu^t)$_2$ with Mo(O)$_2$(OR$_f^6$)$_2$ (16)

Reaction of Mo(O)$_2$(OBu^t)$_2$ with one equivalent of Mo(O)$_2$(OR$_f^6$)$_2$ (16) resulted in equilibrium in less than 5 minutes at room temperature, according to equation 2.44:

$$Mo(O)_2(OBu^t)_2 + Mo(O)_2(OR_f^6)_2 \underset{}{\overset{Keq}{\rightleftharpoons}} 2\,Mo(O)_2(OBu^t)(OR_f^6)$$
$$(16) \qquad\qquad\qquad (30)$$
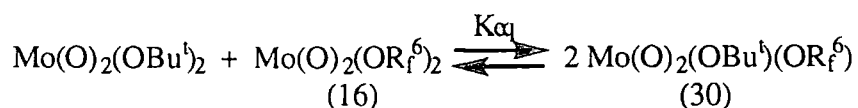
(2.44)

Resonances in the ^{1}H NMR (200 MHz) attributable to the mixed species (30) were present at δ 1.24(sept,OR$_f^6$) and 1.03(OBu^t). The relative intensities of the reactants were difficult to calculate because of alkoxide exchange broadening, however, they were of a lower relative intensity than the reactants in (a) and an estimate of the range of the equilibrium constant Keq = 30 - 80 can be made.

c) Reaction of Mo(O)₂(OR$_f^3$)₂ (13) with Mo(O)₂(OR$_f^6$)₂ (16)

Treatment of $Mo(O)_2(OR_f^3)_2$ (13) with one equivalent of $Mo(O)_2(OR_f^6)_2$ (16) resulted in an equilibrium established within 5 minutes at room temperature.

$$Mo(O)_2(OR_f^3)_2 + Mo(O)_2(OR_f^6)_2 \underset{K_{eq}}{\rightleftharpoons} 2\,Mo(O)_2(OR_f^3)(OR_f^6)$$
$$(13) \qquad\qquad (16) \qquad\qquad\qquad (31)$$
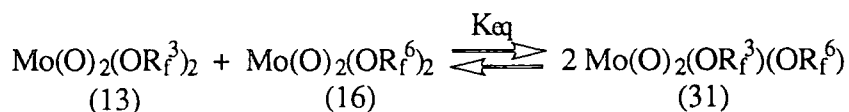
(2.45)

The resonances for the mixed species (31) in the ^{1}H NMR (200 MHz) spectrum could just be discerned from those of the reactants, but were broadened substantially due to a significant proportion of reactants being present. A rough estimate of the equilibrium constant was made ($K_{eq} \sim 5$ - 10).

Overall, the reactions (a) - (c) proved disappointing for the evaluation of accurate equilibrium constants, owing to alkoxide exchange broadening occuring on the NMR timescale. However, qualitative information could still be gathered; the equilibrium position of reactions (a) and (c) appeared to be of similar magnitude, whereas for (b) the position was further over to the side of the products (K_{eq} = 30 - 80). This is consistent with the corresponding alkoxide exchange equilibrium constants for $Mo(NBu^t)_2(OR)_2$ and $Mo(NAr)(CHC(CH_3)_2Ph)(OR)_2$ systems (see sections 2.6.5 and 2.6.6 respectively). It is of interest that the smaller oxo ligand brings the rate of alkoxide ligand exchange within the NMR timescale. Under favourable circumstances, this might have been quite useful for mechanistic investigations. The interchange between 3 species, however, complicates any analysis considerably.

2.6.8 Reaction of $Mo(NBu^t)_2X_2$ with ROH

a) Reaction of $Mo(NBu^t)_2(OBu^t)_2$ (1) with R_f^6OH

Treatment of $Mo(NBu^t)_2(OBu^t)_2$ (1) with two equivalents of R_f^6OH in C_6D_6 resulted in equilibrium within 5 minutes at room temperature, according to equation 2.44, for which the approximate % concentrations of species are given:

$$Mo(NBu^t)_2(OBu^t)_2 \qquad\qquad Mo(NBu^t)_2(OR_f^6)_2$$
$$(1) \qquad\qquad\qquad\qquad\qquad (15)$$
$$12\% \qquad R_f^6OH \qquad R_f^6OH \qquad 12\%$$
$$Bu^tOH \qquad\qquad\qquad\qquad Bu^tOH$$
$$Mo(NBu^t)_2(OBu^t)(OR_f^6)$$
$$(25)$$
$$76\%$$

$$(2.46)$$
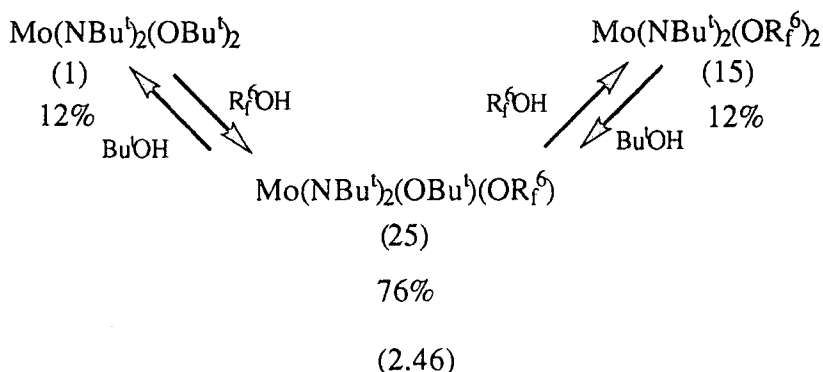
The same equilibrium position is realised from the other side when (15) is treated with two equivalents of Bu^tOH. The greater acidity of R_f^6OH compared to Bu^tOH does not drive the equilibrium over to (15); of more importance is the relative thermodynamic stability of (25) {see section 2.6.5(f)}. The resonances for (15) in the ^1H NMR spectrum were shifted considerably from their normal position, also there was an additional tert-butyl resonance which led to the proposal of the hydrogen bonded adduct $Mo(NBu^t)_2(OR_f^6)_2.Bu^tOH$, probably related to the hydrogen bonded species observed by Bergman and coworkers[39]. In addition, significant hydrogen bonding between the two alcohols was evident in the ^1H NMR spectrum with a broadened signal for the hydroxyl protons at δ 2.2 - 2.4, and the corresponding alkyl proton resonances for Bu^tOH and R_f^6OH were shifted from their normal positions. The proportions of metal species are very similar to those observed for OBu^t - OR_f^6 intermetal exchange {section 2.6.5(f)}. In this system, alkoxide transfer can be viewed as occuring between a proton and a metal centre. Although the mechanism is clearly different from that of intermetal

alkoxide exchange, the two processes can be likened to one another in that both the proton and the high valent early transition metal centre are acidic centres.

b) Reaction of Mo(NBu^t)$_2$(NHBu^t)$_2$ (19) with Bu^{t}OH

Mo(NBu^t)$_2$(NHBu^t)$_2$ (19) was mixed with two equivalents of Bu^{t}OH in d$_6$-benzene at room temperature. The ^{1}H NMR (200 MHz) spectrum after 5 minutes showed that the product was exclusively Mo(NBu^t)$_2$(OBu^t)$_2$ (1)

$$Mo(NBu^t)_2(NHBu^t)_2 + 2\ Bu^tOH \longrightarrow Mo(NBu^t)_2(OBu^t)_2 + Bu^tNH_2$$
$$(19) \qquad\qquad\qquad\qquad\qquad\qquad (1)$$

$$(2.47)$$

The increased acidity of tert-butanol relative to tert-butylamine may assist the above transformation.

The high reactivity of early transition metal amides with alcohols has been exploited in the past to synthesise metal alkoxides[2,40], and has been rationalised in terms of the metal centre having a higher affinity for oxygen[36]. The amphoteric nature of oxygen is an important factor in early transition metal complexes in that oxygen can both accomodate negative charge (due to it's high electronegativity), as well as participate in substantial π back donation (can act as a two faced π donor). In both these aspects the oxygen of the alkoxide is superior to the amide nitrogen (single faced π donor).

2.7   Summary

In this chapter, a variety of ligand exchange reactions have been studied for four coordinate molybdenum systems, including the inter-metal exchange of both mono- and dianionic groups. Further discussion of these findings is deferred until the results for related systems in the following chapter have been considered.

2.8 References

1. J.A.Osborn, J.Kress, G.Schoettel, *J. Chem. Soc. Chem. Commun.* 1989, 1062.

2. W.A.Nugent, R.L.Harlow, *Inorg. Chem.* 1980, **19**, 777.

3. V.C.Gibson, P.W.Dyer. Unpublished Results.

4. M.H.Chisholm, K.Folting, J.C.Huffmann, C.C.Kirkpatrick, *Inorg. Chem.* 1982, **21**, 978.

5. V.C.Gibson, M.Jolly, J.P.Mitchell, *J. Chem. Soc. Dalton Trans.* 1992, 1331.

6. G.C.Bazan. Unpublished Results.

7. I.P.Rothwell, P.E.Fanwick, J.S.Yu, J.L.Kirschner, *Organometallics.* 1989, **8**, 1414.

8. G.Wilkinson, M.B.Hursthouse, A.C.Sullivan, M.Montevalli, *J. Chem. Soc. Dalton Trans.* 1988, 53.

9. E.A.Maata, R.A.D.Wentworth, B.L.Haymore, *J. Am. Chem. Soc.* 1979, **101**, 2063.

10. J.P.Mitchell, Ph.D Thesis, University of Durham, 1992.

11. W.A.Nugent, R.L.Harlow, *J. Chem. Soc. Chem. Commun*, 1978, 579.

12. R.R.Schrock, S.M.Rocklage, *J. Am. Chem. Soc.* 1980, **102**, 7808.

13. F.A.Cotton, W.T.Hall, *J. Am. Chem. Soc.* 1979, **101**, 5094.

14. R.R.Schrock, G.C.Bazan, W.E.Crowe, M.Dimare, M.B.O'Regan, M.H.Schofield, *Organometallics*, 1991, **10**, 1832.

15. W.A.Nugent, *Inorg. Chem.* 1983, **22**, 965.

16. S.Cennini, G. Lamonica, *Inorg. chim. Acta.* 1978, **29**, 187.

17. S.Cennini, G.Lamonica, *J. Chem. Soc. Dalton Trans.* 1980, 1145.

18. M.H.Chisholm, K.Folting, J.C.Huffman, C.C.Kirkpatrick, *Inorg. Chem.* 1984, **23**, 1021.

19. I.S.Kolomnikov, Y.D.Koreshkov, T.S.Lobeeva, M.E.Volpin, *J. Chem. Soc. Chem. commun.* 1970, 1432.

20. W.A.Hermann, E.H.Fischer, D.W.Marz, R.A.Paciello, J.Okuda, G. Weichselbaumer, *Organometallics*. 1990, **9**, 489.

21. M.L.H.Green, K.J.Moynihan, *Polyhedron*. 1986, **5**, 921.

22. R.G.Bergman, R.A.Anderson, R.I.Michelman. *J. Am. Chem. Soc*. 1991, **113**, 5100.

23. F.A.Cotton, S.A.Duraj, W.J.Roth, *J. Am. Chem. Soc*. 1984, **106**, 4749.

24. J.M.Mayer, J.C.Bryan, S.J.Geib, A.L.Rheingold, *J. Am. Chem. Soc*. 1987, **109**, 2826.

25. J.Sundermayer, *Chem. Ber*. 1991, 1977.

26. D.N.Williams, Ph.D Thesis, University of Durham, 1990.

27. J.Sandstrom, "Dynamic NMR spectroscopy", Academic Press, 1982

28. A.A.Frost, R.G.Pearson, *"Kinetics and Mechanism"*, Wiley, New York, 1961.

29. G.C.Bazan, Ph.D Thesis, Massachussetts Institute of Technology, 1990.

30. V.C.Gibson, J.A.K.Howard, P.W.Dyer, B.Whittle, C.Wilson, *J. Chem. Soc. Chem. Commun*. 1992, 1666.

31. R.R.Schrock, H.H.Fox, K.B.Yap, J.Robbins, S.Cai, *Inorg. Chem*, 1992, **31**, 2287.

32. J.Lewis, R.S.Nyholm, C.G.Barraclough, *J. Chem. Soc*. 1959, 3552.

33. J.Lewis, D.C.Bradley, I.M.Thomas, C.G.Barraclough, *J. Chem. Soc*. 1961, 2601.

34. B.Whittle, M.Sc., University of Durham, 1993.

35. G.Wilkinson, A.A.Danopoulos, B.H-Bates, M.B.Hursthouse, *J. Chem. Soc. Dalton Trans*. 1990, 2753.

36. D.C.Bradley, R.H.Mehotra, D.P.Gaur, *"Metal Alkoxides"*, Academic Press, New York, 1978.

37. W.A.Nugent, R.J.McKinney, R.V.Kasowski, F.A.Van-Catledge, *Inorg. Chim. Acta*. 1982, **65**, L91.

38. R.R.Schrock, J.S.Murdzek, G.C.Bazan, J.Robbins, M. Dimare, M.O'Regan, *J. Am. Chem. Soc*. 1990, **112**, 3875.

39. R.G.Bergman, R.D.Simpson, *Organometallics*, 1993, **12**, 781.

40. D.C.Bradley, M.H.Chisholm, M.W.Extine, M.E.Stager, *Inorg. Chem.* 1981, 16, 1794.

Chapter Three

The Synthesis and Reactivity of Half-sandwich Niobium

Imido Complexes of the type - CpNb(NR)X$_2$

3.1 Introduction.

This chapter describes attempts to synthesise a half-sandwich niobium bis-imido complex and intermetal ligand exchange reactions in this half-sandwich system.

A convenient entry into simple half-sandwich niobium imido systems of general fomula $CpNb(NR)Cl_2$ (R = Bu^t, 2,6-$Pr^i_2C_6H_3$) has previously been established in our laboratory by Dr.D.N.Williams[1]. In an attempt to synthesise suitable precursors to the bis imido system, these parent half-sandwich imido dichlorides were reacted with lithium amides to form mono-amide complexes of the type $CpNb(NR)(NR^1R^2)Cl$ ($R^1 = R^2 = Et$, ; R^1 =2,6-$Pr^i_2C_6H_3$, Bu^t and R^2 = H). These compounds were then subsequently reacted with a further equivalent of lithium amide in an attempt to induce an α–elimination reaction, where disproportionation of the proposed bis-amide intermediate was envisaged to occur, forming the bis imido complex and releasing one equivalent of free amine:
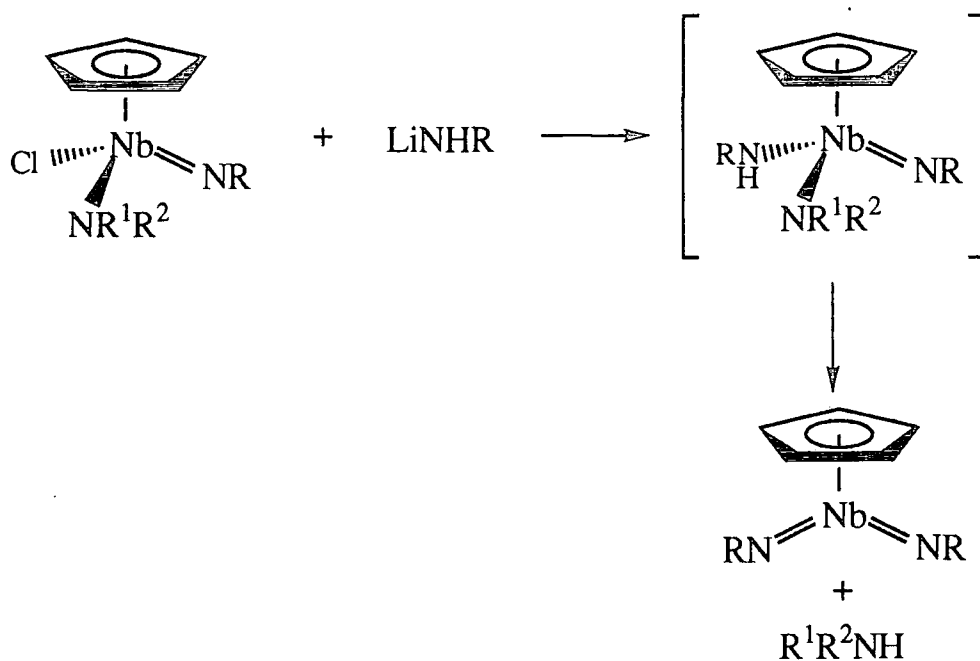
figure 3.1 *Envisaged reaction of CpNb(NR)(NR¹R²)Cl with LiNHR*

Proton transfer in the intermediate would be expected to occur to the most basic metal amide nitrogen; i.e one of the amide groups would be acting in a sacrificial role[2,3].

Intermetal and reagent-induced exchange reactions in the half-sandwich niobium system $CpNb(NBu^t)X_2$ (X = halide, OR, NR^1R^2) are then described, involving both dianionic and monoanionic ligands. A mechanistic study of X-type ligand exchange is carried out for a range of ligands and this together with imido exchange is compared with the observed results from the pseudo-isolobal and valence isoelectronic four coordinate molybdenum system $Mo(NBu^t)_2X_2$.

3.2   Preparation of the imido-amide derivatives

In general, the following reactions were performed by allowing a suspension of the parent imido complex $CpNb(NR)Cl_2$ (R = Bu^t, $2,6-Pr^i_2C_6H_3$) and one equivalent of the appropriate lithium amide to warm to room temperature from -78°C in diethyl ether. Reaction in most cases was complete within a few hours

3.2.1 Reaction of $CpNb(NBu^t)Cl_2$ with $LiNEt_2$

Preparation of $CpNb(NBu^t)(NEt_2)Cl$

Reaction of $CpNb(NBu^t)Cl_2$ with one equivalent of $LiNEt_2$ occurs rapidly on warming to room temperature to afford $CpNb(NBu^t)(NEt_2)Cl$ (1) as a dark red viscous oil in near quantitative yield (equation 3.1).

$$CpNb(NBu^t)Cl_2 \ + \ LiNEt_2 \longrightarrow CpNb(NBu^t)(NEt_2)Cl \ + \ LiCl$$
$$(1)$$

$$(3.1)$$

As found previously for Group 5 and 6 transition metals, the presence of the bulky, highly solubilising diethylamide group can disfavour crystallisation[4,5]. Elemental analysis of complex (1) supports the stoichiometry $NbC_{13}H_{24}N_2Cl$ and a parent molecular ion peak at m/z 336 (^{35}Cl) is observed in the mass spectrum.

The ^1H NMR (400MHz, C_6D_6) spectrum revealed four multiplets at δ 4.15, 3.70, 3.26 and 3.01, each integrating to one proton. These signals were assigned as the four methylene protons on the diethylamide ligand. As a consequence of the chiral niobium metal centre the methylene protons are diastereotopic; furthermore, slow rotation about the niobium - nitrogen bond renders them inequivalent on the NMR time scale as shown in figure 3.2. The coupling of methylene protons to the two inequivalent methyl groups produces two pseudo triplets at δ 1.04 and 0.91. The assignments in figure 3.2 were aided by homonuclear decoupling experiments. Irradiating the methylene protons specifically allowed the signal due to its diastereotopic partner to be identified as well as the resonance arising from the closeby methyl group.

figure 3.2 *The diastereotopic methylene protons in* CpNb(NBu^t)(NEt$_2$)Cl *(1)*
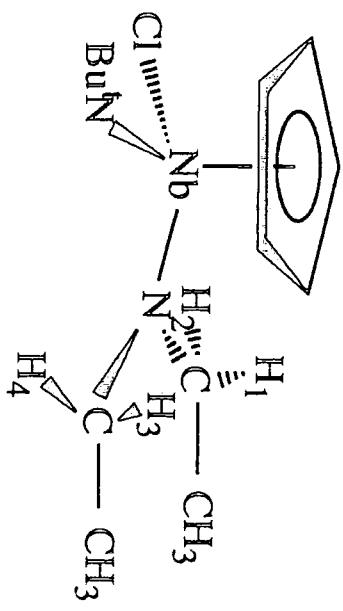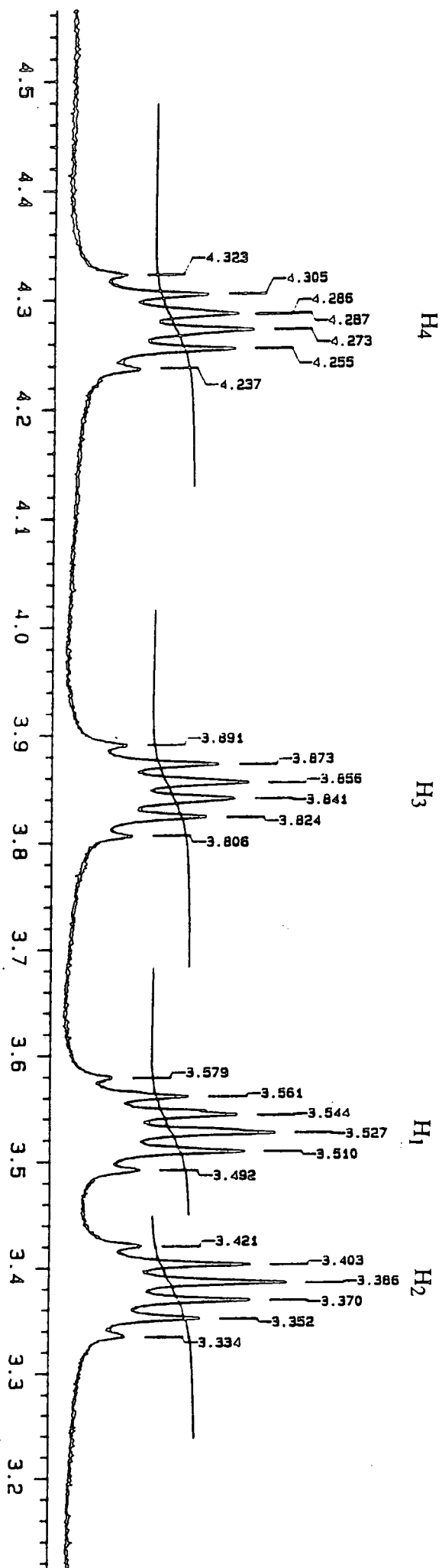
3.2.2 NMR saturation transfer experiments - determination of the energy barrier to rotation about the niobium - nitrogen bond

An anomally observed in each homonuclear decoupling experiment (section 3.2.1) was the disappearance of one of the methylene proton signals on the other carbon. This effect may be explained as arising from saturation transfer. Rotation around the niobium - nitrogen bond by 180° interchanges pairs of diastereotopic methylene protons and therefore spin saturation can occur if the rate of rotation is comparable with the relaxation rate of the protons. Cooling the sample in $CDCl_3$ slows the rotation rate and allows the protons time to relax thus allowing the return of the signal, as shown in figure 3.3. On warming the sample in C_6D_6 to 50°C coalescence was almost achieved between the interchanging pairs of multiplets, but the resolution was poor due to uneven temperature distributions (eddy currents).

When the rate of rotation is similar to the relaxation time of the nuclei, it can be determined according to equation 3.2[6].

$$k = \frac{I_0 R}{I_x} - R \qquad (3.2)$$

k = rotation rate (s^{-1}),

I_x = intensity of the signal at location Y when irradiating at X,

I_0 = intensity of the signal at location Y in the absence of irradiation at X,

R = relaxation rate of the nuclei = $1/T_1$, where T_1 is the relaxation time.

This technique allows for the determination of exchange rates much slower than those determined from line broadening ($k = 10^{-2}$ s^{-1}). The rates of rotation determined at various temperatures are listed in table 3.1

figure 3.3 *Variable temperature homonuclear decoupling of the methylene protons in CpNb(NBu^t)(NEt$_2$)Cl (1)*
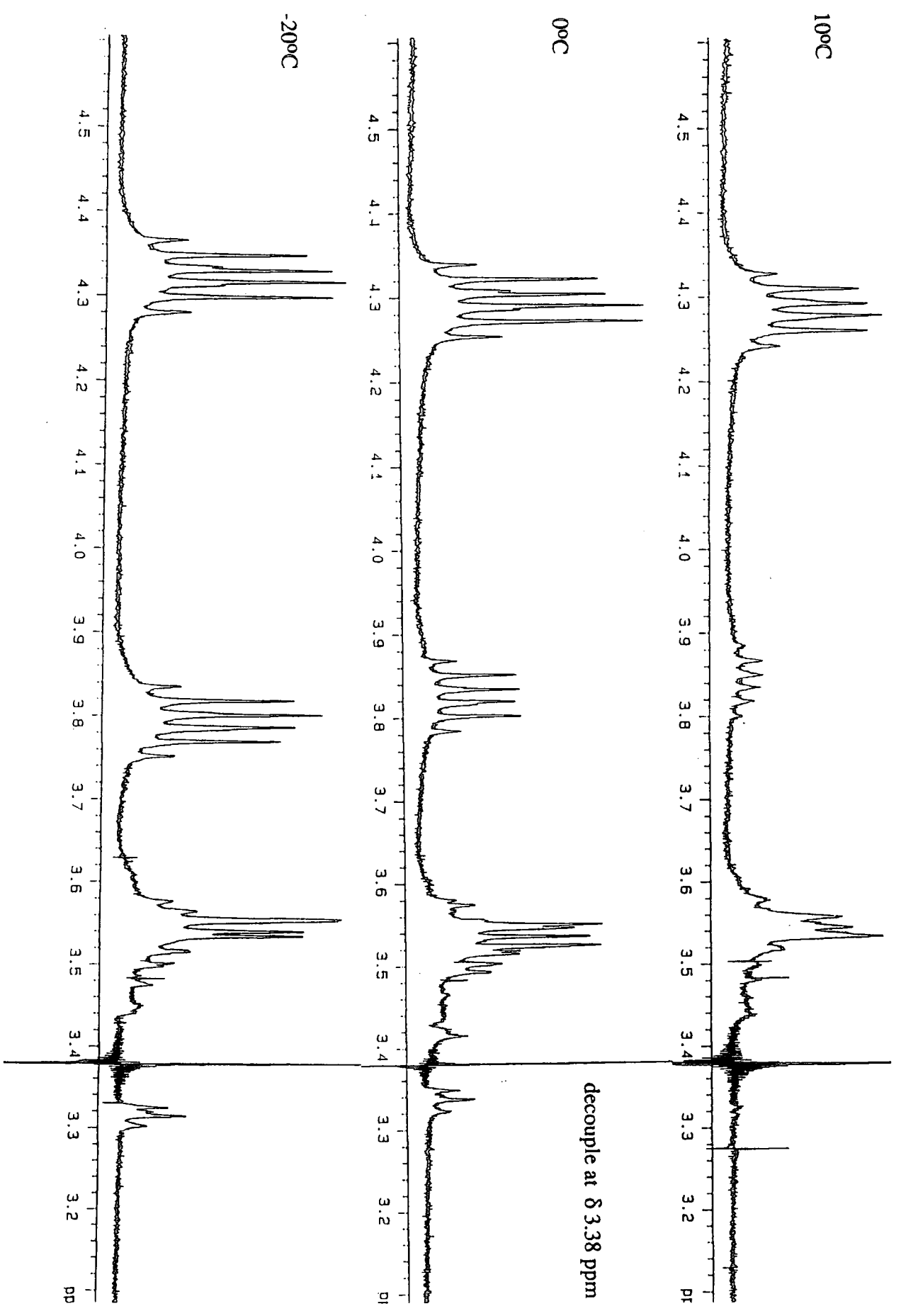
Temperature (K)	k (s^{-1})
263	0.11
268	0.47
273	1.29
278	4.53
283	14.93

table 3.1 *calculated rates of rotation*

The Arrhenius plot for this data is shown in figure 3.4, affording the activation energy barrier $E_a = 151(5.0)$ kJ mol^{-1}.
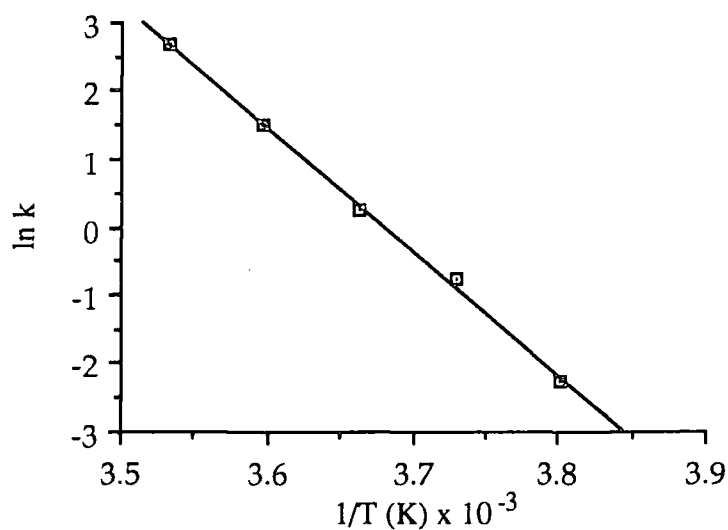
figure 3.4 *Arrhenius plot for rotation around the nitrogen-niobium bond*

The energy barrier to rotation around the nitrogen-niobium bond is three times as large as that determined for rotation around the nitrogen-carbon bond in N, N-dimethylacetamide[7,8], $E_a = 50$ kJ mol^{-1} (figure 3.5).
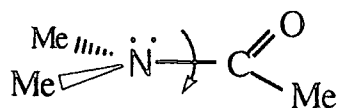
figure 3.5 *N, N-dimethylacetamide*

While rotation is hindered in around the nitrogen-carbon bond in N, N-dimethylacetamide, owing to significant lone pair donation from the nitrogen to the electrophilic carbon, nitrogen lone pair donation is likely to be greater to the electrophilic niobium d^0 metal centre in (1), invoking increased multiple bond character and thereby restricting rotation. In addition, significant steric interactions are present in (1) as a consequence of the bulky diethylamide group in the half-sandwich niobium coordination sphere, which is likely to augment the barrier to rotation.

3.2.3 a) Reaction of CpNb(NBu^t)Cl$_2$ with LiNHAr

b) Reaction of CpNb(NAr)Cl$_2$ with LiNHBu^t

Preparation of CpNb(NAr)(NHBu^t)Cl (2).

a) The reaction of CpNb(NBu^t)Cl$_2$ with one equivalent of LiNHAr in diethyl ether was found to proceed slowly at room temperature (equation 3.3):

$$CpNb(NBu^t)Cl_2 + LiNHAr \longrightarrow CpNb(NAr)(NHBu^t)Cl + LiCl$$
$$(2)$$

$$(3.3)$$

Recrystallisation of the oily product from toluene at -20°C yielded yellow cubes of CpNb(NAr)(NHBu^t)Cl (2) in low yield (30%). The complex was highly moisture sensitive decomposing readily to release tert-butylamine.

The ^{1}H NMR spectrum (C$_6$D$_6$, 400MHz) exhibited a very broad resonance at δ 8.0 due to the amide proton ($\Delta^1/_2$ *ca.* 144 Hz). This broadening may be attributed to the quadrupolar ^{14}N nucleus (I = 1), and in conjunction with the deshielded environment is

characteristic of mono-amide complexes of this type[9,10]. An amide stretch was evident in the infra red spectrum at 3274 cm^{-1} as were strong bands at 1200 cm^{-1} and 812 cm^{-1} assignable to the aryl imido ligand[11].

b) The reacton of CpNb(NAr)Cl$_2$ with one equivalent of LiNHBu^t in diethyl ether proceeded smoothly over 16 hours to afford (2), according to equation 3.4:

$$CpNb(NAr)Cl_2 + LiNHBu^t \longrightarrow CpNb(NAr)(NHBu^t)Cl + LiCl$$

(2)

(3.4)
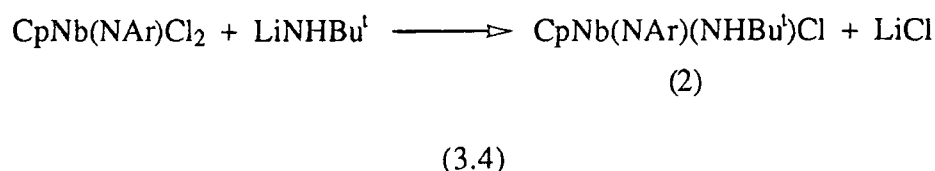
^{1}H and ^{13}C NMR spectroscopy (C$_6$D$_6$) confirmed that this product was identical to that obtained in (a) above. Intramolecular α-proton transfer was therefore occuring in either (a) or (b) and it was postulated that the proton would reside on the more basic tert-butyl nitrogen rather than the aryl nitrogen. A crystal stucture was deemed necessary to estabilish beyond doubt the location of the amide proton and corroborate this assignment.

3.2.4 The molecular structure of CpNb(NAr)(NHBu^t)Cl (2).

Yellow cubic crystals of (2) were grown from diethyl ether at -20°C. A crystal of dimensions 0.39 x 0.35 x 0.29 mm was mounted under an inert atmosphere in a Lindemann capillary tube and the structure was solved by Prof. W. Clegg of the University of Newcastle-upon-Tyne. The molecular structure is illustrated in figures 3.6 (a), (b) and selected bond angles and distances are given in table 3.2.

The molecule possesses a three-legged piano stool geometry, with the amide proton attached to the tert-butyl containing nitrogen (see section 3.2.3). This is also supported by the quasi-linear sp hybridised aryl imido group (Nb-N-C$_{ipso}$ angle = 168.5(3)^o) and the sp^2 hybridised tert-butyl amide group (Nb-N-C angle = 137.7(3)^o). The niobium bond length (1.793(3)Å) falls at the high end of the range expected for niobium imido compounds, typically 1.73-1.79Å[12-14]; this may be a consequence of the

98

molecule posessing a basic tert-butyl amide group thereby increasing the electron density of the niobium centre. The imido substituent is displaced towards the cyclopentadienyl group, explained in terms of the interaction of the nitrogen lone pair with a vacant metal d-orbital trans to the cyclopentadienyl ring[9].

One way of representing this molecule is as a simple triad[15], as shown in figure 3.6 (b). If the molecule is viewed down the N(1) - niobium vector the orientation of the amido substituents is such as to allow the donor p-orbital of the amide ligand to lie in the Nb-N(1)-Cl(1) plane consistent with a 'bent metallocene' orientation. In so doing the amide avoids direct competition for π bonding with the strong π donor imido and Cp groups.

figure 3.6 *The molecular structure of CpNb(NAr)(NHBu^t)Cl (2)*
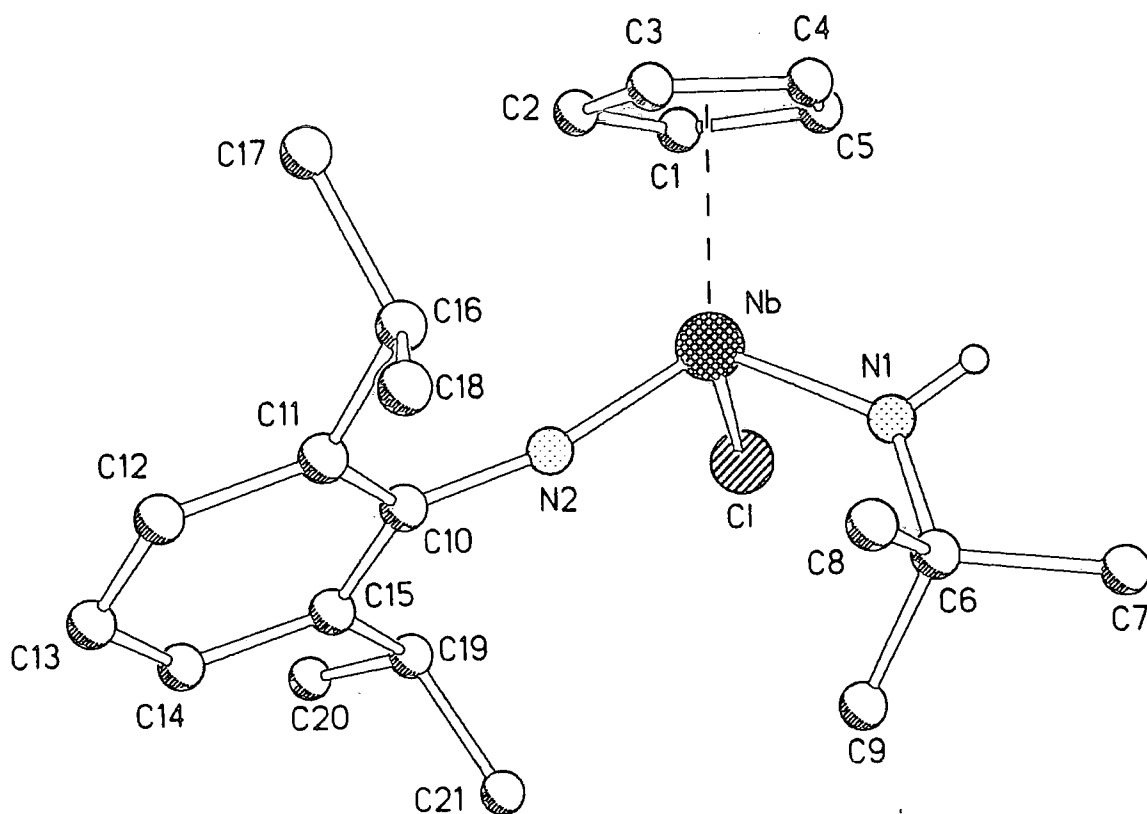
(a) View showing the atom labelling (H atoms omitted for clarity).
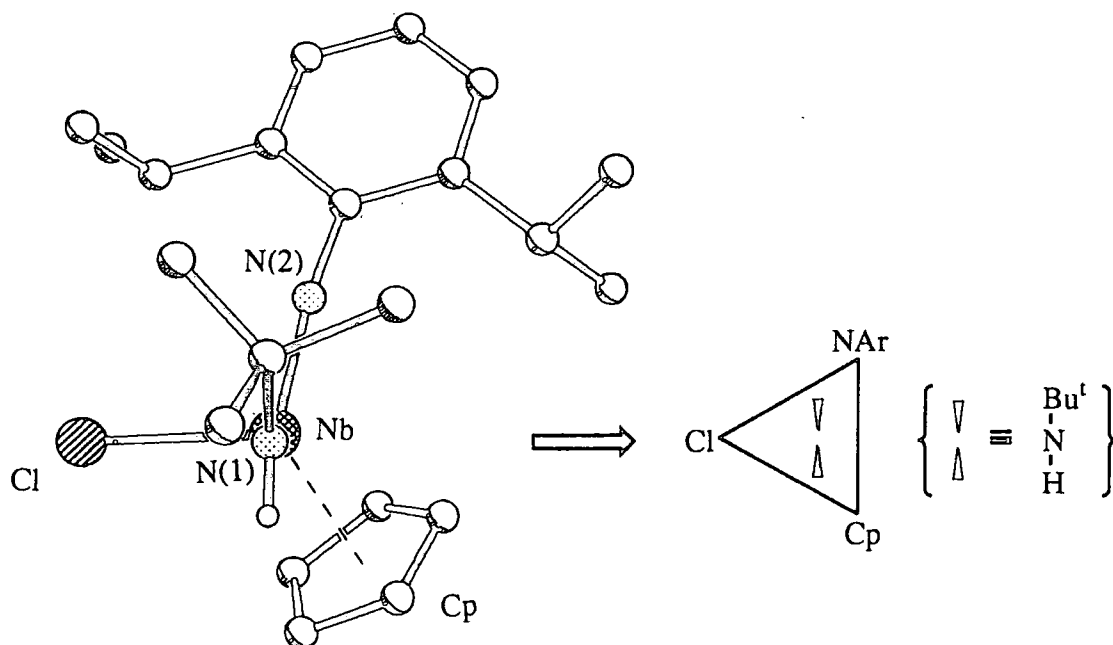
(b) View of the molecule along the N(1) - Nb vector.

Nb - N (1)	1.958 (3)	Nb - N (2)	1.793 (3)
Nb - Cl (1)	2.4004 (11)	Nb - C (3)	2.399 (5)
Nb - C (4)	2.472 (5)	Nb - C (2)	2.436 (4)
Nb - C (5)	2.513 (5)	Nb - C (1)	2.475 (5)
C (1) - C (5)	1.408 (7)	C (1) - C (2)	1.371 (8)
C (3) - C (4)	1.401 (7)	C (2) - C (3)	1.402 (7)
N (1) - C (6)	1.479 (9)	C (4) - C (5)	1.385 (8)
C (6) - C (9)	1.512 (7)	C (6) - C (8)	1.508 (7)
N (2) - C (10)	1.393 (5)	C (6) - C (7)	1.516 (6)
C (10) - C (11)	1.418 (5)	C (10) - C (15)	1.415 (5)
C (11) - C (16)	1.526 (5)	C (11) - C (12)	1.391 (5)
C (13) - C (14)	1.378 (6)	C (12) - C (13)	1.378 (6)
C (15) - C (19)	1.516 (5)	C (14) - C (15)	1.390 (5)
C (16) - C (17)	1.537 (6)	C (16) - C (18)	1.533 (6)
C (19) - C (20)	1.526 (6)	C (19) - C (21)	1.517 (7)

N (1) - Nb - C (3)	106.2 (2)	N (2) - Nb - C (3)	99.5 (2)
N (2) - Nb - Cl (2)	102.37 (10)	N (1) - Nb - Cl (1)	102.87 (11)
C (3) - Nb - Cl (1)	138.03 (12)	N (1) - Nb - C (2)	138.4 (2)
N (2) - Nb - C (2)	96.3 (2)	Cl (1) - Nb - C (2)	108.03 (14)
C (3) - Nb - C (2)	33.7 (2)	N (2) - Nb - C (4)	130.3 (2)
N (1) - Nb - C (4)	84.8 (2)	C (3) - Nb - C (4)	33.4 (2)
Cl (1) - Nb - C (4)	123.67 (14)	C (2) - Nb - C (4)	54.9 (2)
N (1) - Nb - C (1)	130.9 (2)	N (2) - Nb - C (1)	122.8 (2)
Cl (1) - Nb - C (1)	83.33 (13)	C (3) - Nb - C (1)	54.7 (2)
C (4) - Nb - C (1)	54.2 (2)	C (2) - Nb - C (1)	32.4 (2)
N (2) - Nb - C (5)	150.4 (2)	Cl (2) - Nb - C (5)	135.2 (3)
C (3) - Nb - C (5)	54.6 (2)	N (1) - Nb - C (5)	98.1 (2)
C (2) - Nb - C (5)	54.3 (2)	Cl (1) - Nb - C (5)	91.99 (13)
C (1) - Nb - C (5)	32.8 (2)	C (4) - Nb - C (5)	32.3 (2)
C (2) - C (1) - Nb	72.2 (3)	C (2) - C (1) - C (5)	108.8 (5)
C (1) - C (2) - C (3)	107.9 (4)	C (5) - C (1) - Nb	75.1 (3)
C (3) - C (2) - Nb	71.7 (3)	C (1) - C (2) - Nb	75.3 (3)
C (4) - C (3) - Nb	76.1 (3)	C (4) - C (3) - C (2)	107.8 (5)
C (5) - C (4) - C (3)	108.1 (4)	C (2) - C (3) - Nb	74.6 (3)
C (3) - C (4) - Nb	70.5 (3)	C (5) - C (4) - Nb	75.5 (3)
C (4) - C (5) - Nb	72.2 (3)	C (4) - C (5) - C (1)	107.4 (5)
C (6) - N (1) - Nb	137.7 (3)	C (1) - C (5) - Nb	72.1 (3)
N (1) - C (6) - C (9)	109.3 (4)	N (1) - C (6) - C (8)	110.2 (4)
N (1) - C (6) - C (7)	108.1 (3)	C (8) - C (6) - C (9)	110.0 (4)
C (9) - C (6) - C (7)	109.5 (4)	C (8) - C (6) - C (7)	109.6 (4)
N (2) - C (10) - C (15)	119.0 (3)	C (10) - N (2) - Nb	168.5 (3)
C (15) - C (10) - C (11)	120.4 (3)	N (2) - C (10) - C (11)	120.6 (3)
C (12) - C (11) - C (16)	119.5 (3)	C (12) - C (11) - C (10)	118.2 (4)
C (13) - C (12) - C (11)	121.4 (4)	C (10) - C (11) - C (16)	122.2 (3)
C (13) - C (14) - C (15)	121.2 (4)	C (12) - C (13) - C (14)	120.3 (4)
C (14) - C (15) - C (19)	120.6 (4)	C (14) - C (15) - C (10)	118.5 (4)
C (11) - C (16) - C (18)	111.8 (3)	C (10) - C (15) - C (19)	120.9 (3)
C (18) - C (16) - C (17)	110.6 (3)	C (11) - C (16) - C (17)	110.4 (3)
C (15) - C (19) - C (20)	113.7 (4)	C (15) - C (19) - C (21)	111.0 (4)
N (2) - Nb - N (1)	103.65 (14)	C (21) - C (19) - C (20)	109.4 (4)

Table 3.2 *Bond distances (Å) and angles (º) for CpNb(NAr)(NHBuᵗ)Cl (2)*

3.3 Attempted preparation of bis (imido) species, $CpNb(NR^1)(NR^2)$

Half-sandwich imido species of tantalum have been previously prepared by Mayer and Bercaw[16], according to equation 3.5:

$$Cp*TaMe_3Cl + LiNHR \xrightarrow[25°C]{Et_2O} Cp*Ta(NR)Me_2 + LiCl + CH_4$$

(3.5)
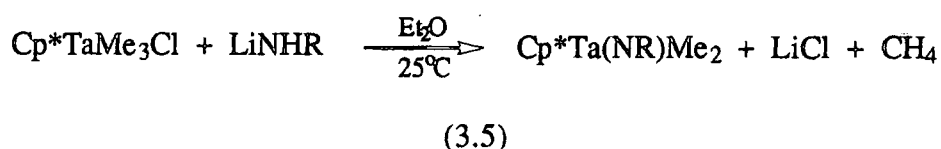
The driving force for the reaction was presumed to be the elimination of methane *via* intramolecular α-proton transfer. This method was adopted by D.N.Williams[9] in attempting to prepare $CpNb(NR^1)(NR^2)$, the driving force for the formation of the second imido group being either elimination of HCl or methane. Instead imido-amide intermediates were isolated (equation 3.6) and elimination of HCl / methane could not be facilitated by heating or adding base (NEt_3, lutidene).

$$CpNb(NBu^t)Cl_{2-n}Me_n + LiNHR \longrightarrow CpNb(NBu^t)(NHR)Me_nCl_{1-n} + LiCl$$
$$(n = 0,1)$$

(A)

$$\Delta / NEt_3 \qquad \nparallel \qquad -HCl / MeH$$

$$CpNb(NBu^t)(NR)$$

(3.6)
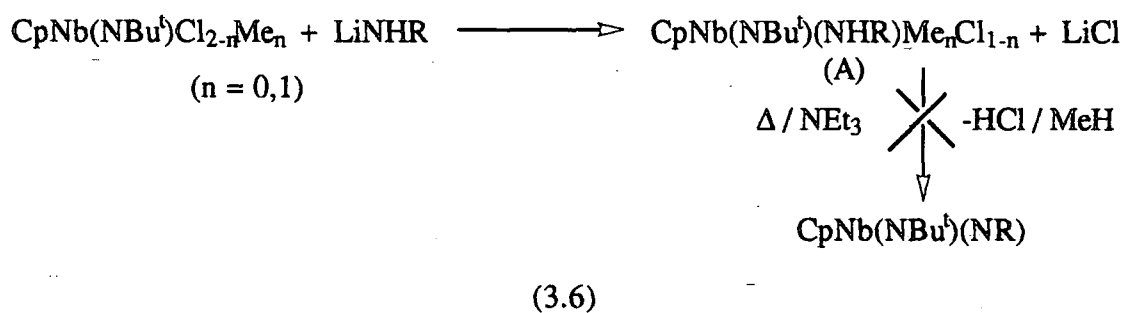
One possibility is that the reaction stopped at the intermediate (A) because of the absence of a suitable empty metal orbital to facilitate proton transfer from the nitrogen to the methyl / chloride substituent. However, in section 3.2.3 proton transfer was observed for the similar complex $CpNb(NAr)(NHBu^t)Cl$ from the amide to the imido nitrogen, in preference to elimination of HCl. With this in mind the adopted strategy was one of envisaging proton transfer from one amide nitrogen to another, eliminating amine and hence forming the bis imido complex. Alternatively, lithium amide could act as an

external dehydrohalogenating agent and form the desired bis imido complex from the imido-amide precursors.

Recently the first group 5 niobium and tantalum bis imido species were synthesised by Wigley et al.[2] (equation 3.7), from which the half-sandwich pyridine stabilised niobium derivative was prepared (equation 3.8).

$$1/2(Nb(NEt_2)_2Cl_3)_2 + 2LiNHAr \xrightarrow{\text{Pyr}} Nb(NAr)_2(Pyr)_2Cl + 2HNEt_3 + 2HCl$$

$$(3.7)$$

$$Nb(NAr)_2(Pyr)_2Cl + NaCp \xrightarrow{\text{Et}_2O} CpNb(NAr)_2(Pyr) + NaCl + Pyr$$

$$(3.8)$$
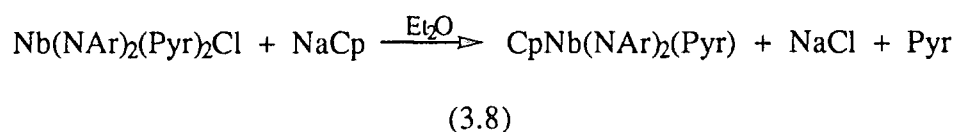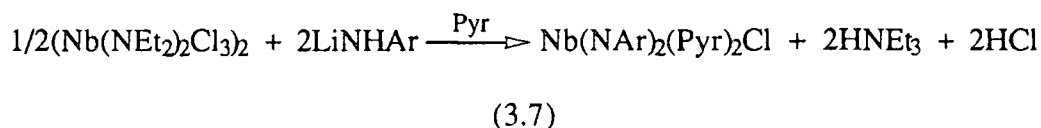
The diethylamide ligands fulfill a sacrificial role. The increased basicity of the diethylamide nitrogen ($pK_B = 3.02$ for $HNEt_2$[17]) relative to that of the arylamide nitrogen ($pK_B = 8$ for H_2NAr) presumably aids proton transfer. It seems that, under the right conditions, intramolecular proton transfer can occur forming free amine and the target molecule.

3.3.1 a) Reaction of CpNb(NBu^t)(NEt$_2$)Cl (1) with LiNHBu^t

b) Reaction of CpNb(NBu^t)(NHBu^t)Cl with LiNEt$_2$

Preparation of 'CpNb(NBu^t)(NHBu^t)(NEt$_2$)' / 'CpNb(NBu^t)$_2$(HNEt$_2$)'

a) Reaction of CpNb(NBu^t)(NEt$_2$)Cl (1) with LiNHBu^t occured on warming to room temperature to afford a pale flocculent precipitate (LiCl) and an orange/red solution according to equation 3.9. The compound was isolated as an orange/brown oil. Attempts to recrystallise the product were unsuccessful as the complex was highly soluble even in pentane at -78°C.

$CpNb(NBu^t)(NEt_2)Cl + LiNHBu^t \longrightarrow {}'CpNb(NBu^t)(NEt_2)(NHBu^t)' + LiCl$

(1)   (3)

or

$'CpNb(NBu^t)_2(HNEt_2)'$

(4)

(3.9)
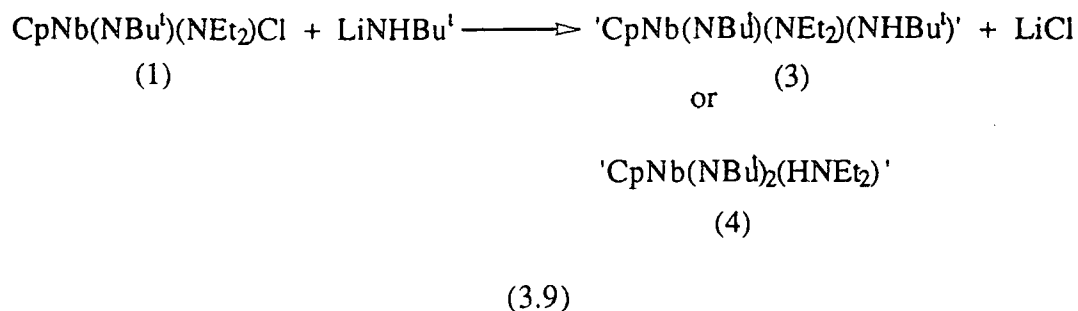
Complexes (3) and (4) are structural isomers or tautomers (as shown in figure 3.7), complex (4) arising from intramolecular proton transfer. It was not possible to obtain an accurate structural assignment of the compound on the basis of ^1H and ^{13}C NMR data (section 3.3.2).

(a) Bis imido structure (4)
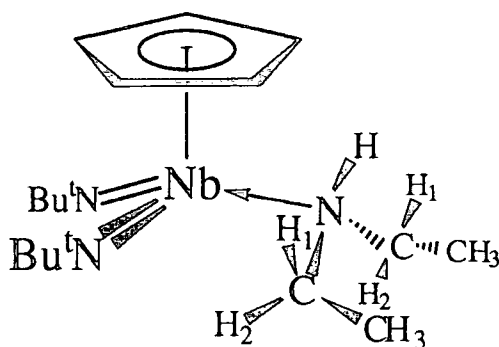
(b) Imido-bis amide structure (3)
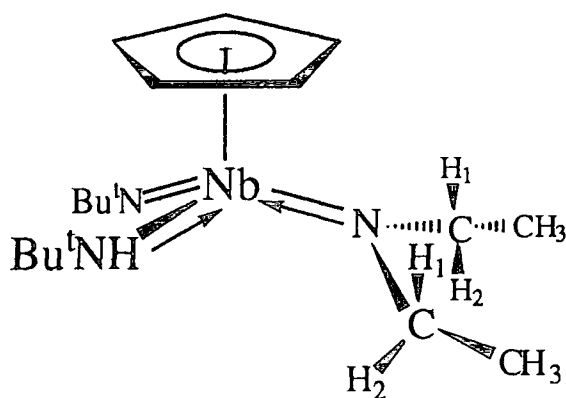
figure 3.7 *The structural isomers of*
'CpNb(NBu^t)(NHBu^t)$_2$' / 'CpNb(NBu^t)$_2$(H$_2$NBu^t)'

The ^{1}H NMR spectrum (C$_6$D$_6$, 400 MHz) of the complex showed inequivalent tert-butyl resonances at δ 1.37 and 1.26. The methylene protons of the diethylamide/amine group appeared as two multiplets at δ 3.50 and 3.27, while the methyl groups of this ligand appear as a pseudo triplet at δ 1.08. The amine/amide resonance was a broad singlet centred at δ 4.55. Only one quaternary carbon C(α) at δ 65.7 could be discerned for the tert-butyl group although two resonances for the methyl carbons C(β) at δ 34.7 and 32.8 were present.

The infra red spectrum showed an absorption at 3345 cm^{-1} for the NH stretch and the parent molecular ion at m/z 373 was present in the mass spectrum.

b) Similarly, the reaction of CpNb(NBu^t)(NHBu^t)Cl[9] with one equivalent of LiNEt$_2$ in diethyl ether produced the aforementioned product after appropriate work up.

$$CpNb(NBu^t)(NHBu^t)Cl + LiNEt_2 \longrightarrow \text{'}CpNb(NBu^t)(NEt_2)(NHBu^t)\text{'} + LiCl$$

(1)   (3)

or

'CpNb(NBu^t)$_2$(HNEt$_2$)'

(4)
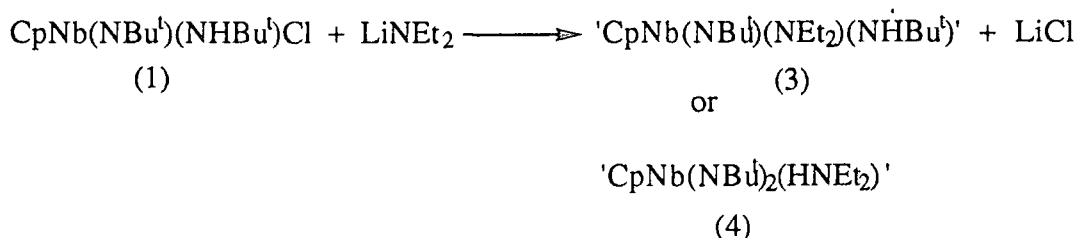
(3.10)

3.3.2 Where does the proton reside?

The two different tert-butyl signals observed in the ^{1}H NMR spectrum could be explained on electronic grounds. If the imido ligand is considered to be a 4 electron (neutral) donor, then complex (4) is a 20 electron species. It is possible that one of the imido groups may be acting as a two electron donor i.e bent not linear[18], rendering the two imido groups inequivalent. However, this process is likely to be highly fluxional at room temperature, reinforced by the observation of equivalent aryl proton signals for the analogous 20 electron complex CpNb(NAr)$_2$(Pyr)[2]. The difference in chemical shift of

the two resonances ($\Delta(\delta)$ 0.11 ppm) is more indicative of chemically differing environments.

Only one quaternary carbon {C(α)} for the tert-butyl groups was found in the ^{13}C NMR δ 65.66 and this chemical shift is typical of an imido rather than an amido tert-butyl environment as shown in table 3.3.

Complex	δC_α(imido)	δC_α(amido)
CpNb(NBu^t)Cl$_2$[9]	70.0	-
CpNb(NBu^t)(NHBu^t)Cl[9]	67.4	57.0
CpNb(NAr)(NHBu^t)Cl	-	59.4
CpNb(NBu^t)(NEt$_2$)Cl	67.8	-
CpNb(NBu^t)(OPr^i)$_2$	65.5	-
CpNb(NBu^t)(OBu^t)$_2$[9]	64.5	-

table 3.3 *^{13}C (C$_6$D$_6$, 100 MHz, ppm) chemical shift data {C(α)} for selected half-sandwich niobium imido complexes containing tert-butyl imido/amido groups*

However, it is possible that an amide resonance due to (3) could be obscured by the methylene carbon signal of the diethylamide ligand at δ 54.0, as this falls in the expected range for a tert-butyl **amide** quaternary carbon (table 3.3).

The diethylamide/amine methylene splitting patterns in the ^{1}H NMR are consistent with either structure shown in figure 3.7; these arise as a consequence of the prochiral methylene protons (assigned as H$_1$ and H$_2$). It is notable that the energy barrier (E$_a$) to rotation around the niobium-nitrogen bond for the diethyamide/amine group is significantly reduced compared to that observed for CpNb(NBu^t)(NEt$_2$)Cl (1) (section 3.2.2), where four inequivalent methylene proton environments are resolved.

The chemical shift of the N$\underline{H}$ signal in the ^{1}H NMR at δ 4.55 cannot be used to differentiate between the two isomers. Although this value is very different from that observed in the monoamide complex CpNb(NAr)(NHBu^t)Cl δ 8.0, it is similar to those

observed in bis amido complexes of the type $M(NBu^t)_2(NHBu^t)_2$, δ 5.0 - 5.7 for M = Mo[19] and M = W[20].

If the complex was the bis imido species (4), it would possess a coordinated diethylamine ligand which could possibly be displaced. However, treatment with PMe_3 in C_6D_6 at elevated temperature (60°C) for several days, did not result in dispacement, the coordinated ligands remaining intact according to the ^1H NMR spectrum.

3.3.3 Reaction of $CpNb(NBu^t)(NHBu^t)Cl$ with $LiNHBu^t$

Preparation of 'CpNb(NBu^t)(NHBu^t)_2' / 'CpNb(NBu^t)_2(H_2NBu^t)'

The reaction of $CpNb(NBu^t)(NHBu^t)Cl$[9] with one equivalent of $LiNHBu^t$ in diethyl ether at ambient temperature generated a highly soluble pale brown oil which was characterised by ^1H and ^{13}C NMR as either of the isomers (5) and (6):

$$CpNb(NBu^t)(NHBu^t)Cl + LiNHBu^t \longrightarrow \text{'}CpNb(NBu^t)(NHBu^t)_2\text{'} + LiCl$$

$$(5) \downarrow$$

$$\text{'}CpNb(NBu^t)_2(H_2NBu^t)\text{'}$$

$$(6)$$
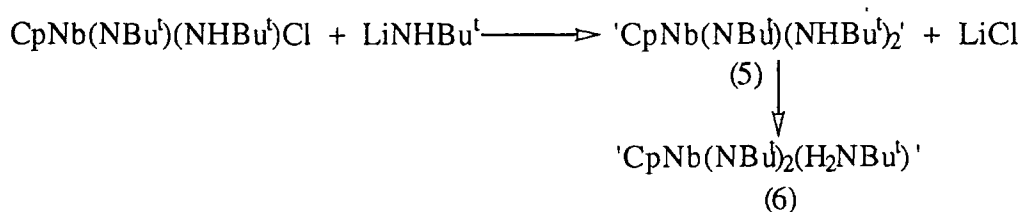
$$(3.11)$$

The ^1H NMR spectrum (C_6D_6, 400MHz) of the complex shows two tert-butyl environments at δ 1.30 and 1.26 of relative intensity 2:1 respectively, a broad NH resonance is present at δ 4.80. The quaternary carbon resonances for the tert-butyl groups were observed at δ 65.7 and 53.8. The parent molecular ion was present in the mass spectrum at m/z 373, and the absorbance due to the NH stretch occurs in the infrared at 3355 cm^{-1}.

As expected this complex is very similar spectroscopically to the diethylamide/amine complex described in sections 3.3.1 - 3. Common features for both species are the different tert-butyl methyl proton environments, similar NH proton resonances (^1H NMR) and NH stretches (infrared). One significant difference here is that

proton transfer between chemically equivalent tert-butylamide groups is not aided by a difference in basicity. The following system highlighting intramolecular α–proton transfer between two tert-butylamide groups demonstrates that the basicity argument is not always an overriding factor in determining whether proton transfer will occur[21]:

$$2[WCl_2(NR^1)(NHBu^t)_2] \xrightarrow{\Delta} [WCl_2(NR^1)(NBu^t)(H_2NBu^t)]_2$$

$$R^1 = Ph, C_6H_4Me\text{-}p$$

$$(3.12)$$
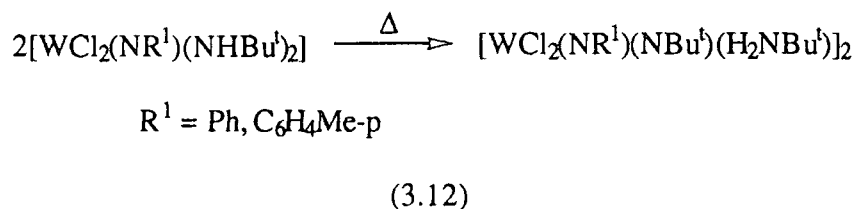
The complex $(WCl_2(NR^1)(NHBu^t)_2)$ is an intermediate observed by NMR in the overall conversion of $[WCl_4(NR^1)]$ to the above product (equation 3.12),*via* reaction with tert-butyl trimethyl silylated amine. This type of transformation can in fact be an equilibrium process, where the final position of the equilibrium depends upon the electron withdrawing capacity of the ancillary ligands[22]. More electron withdrawing groups, for example chloride in the above case (equation 3.12), decrease the π electron-donation and favour formation of the bis imido species. An additional factor of importance is increasing the steric bulk of groups to facilitate intramolecular α-proton transfer. This is a general feature in other transition metal systems, for instance producing alkylidene complexes from bulky neopentyl groups[23].

3.3.4 Further experiments

As in section 3.3.3, the failure to displace a coordinated amine type ligand is also found here, where both thermolysis at 110°C in C_6D_6 and carrying out the reaction, according to equation 3.11, in the presence of pyridine failed to remove the amine. However, a breakthrough was made when an nuclear Overhauser experiment (nOe) was performed. Irradiation of the tert-butyl signal at δ 1.30 gave a significant enhancement of the amide/amine resonance at δ 4.80. This signal at δ 1.30 was due to the methyl protons

of *two* equivalent tert-butyl groups which would support the formulation of the complex CpNb(NBu^t)(NHBu^t)$_2$ (6).

Secondly, when equimolar quantities of the complex (6) and CpNb(NBu^t)Cl$_2$ were mixed in C$_6$D$_6$, the complex CpNb(NBu^t)(NHBu^t)Cl[9] was formed almost quantitavely over several hours at room temperature, presumably *via* a mono-anionic amide-chloride ligand exchange mechanism (see section 3.5).

$$CpNb(NBu^t)Cl_2 + CpNb(NBu^t)(NHBu^t)_2 \longrightarrow 2CpNb(NBu^t)(NHBu^t)Cl$$
$$(5)$$
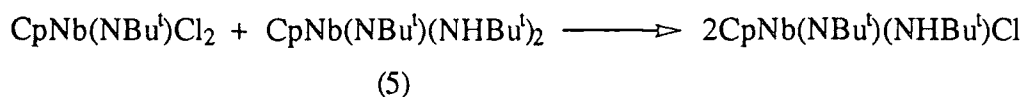
$$(3.13)$$

This process could possibly occur for the bis imido species were there an equilibrium between complexes (5) and (6) but this seems unlikely.

3.3.5 Reaction of CpNb(NBu^t)(NHBu^t)Cl with LiNHAr

Preparation of CpNb(NBu^t)(NHBu^t)(NHAr) (7).

Reaction of CpNb(NBu^t)(NHBu^t)Cl with one equivalent of LiNHAr in diethyl ether afforded the product CpNb(NBu^t)(NHBu^t)(NHAr) (7), isolated as a viscous brown oil.

$$CpNb(NBu^t)(NHBu^t)Cl + LiNHAr \longrightarrow CpNb(NBu^t)(NHBu^t)(NHAr) + LiCl$$
$$(7)$$

$$(3.14)$$

The presence of small quantities of ArNH$_2$ in the product (due to partial hydrolysis) was noted in the ^{1}H NMR spectrum and therefore full analysis of the complex has not been obtained. The arylamine proved difficult to remove from the product due to it's low volatility (Bpt 257°C / 760 mm).

The ^{1}H NMR (C$_6$D$_6$, 250 MHz) spectrum is consistent with a formulation for (7) as shown in equation 3.14, the most striking feature being inequivalent amide proton resonances at δ 6.94 and 5.47. These signals are indicative of two chemically different amide environments and together with the evidence from section 3.3.4, support the formulation of this complex as having an imido-bis amide type structure. Two well separated tert-butyl methyl proton resonances were observed at δ 1.43 and 1.24, assignable to the amido and imido groups respectively, on the basis of characteristic chemical shift values for these species.

3.3.6 Summary

Formation of a half-sandwich bis imido species from monoamide precursors appears to be disfavoured. It may be that coincident formation of both imidos is neccessary, rather than starting from a system where one imido is already present[2,50]. Further evidence for this comes from the observed failure of Cp*Ta(NPh)(NHPh)$_2$, upon thermolysis in the presence of σ-donor ligands, to form a bis imido complex *via* *intramolecular* proton transfer (eliminating aniline)[51]. Another important factor may be that electrophilicity of the niobium metal centre in these systems may not be large enough to favour bis imido formation[21,22]. Although earlier in section 3.2.3 (a), proton transfer did occur to the most basic nitrogen, it suprisingly does not occur between the same groups in section 3.3.5. This reinforces the notion that although the difference in nitrogen basicity can help proton transfer in some systems, it is not always an overriding factor in product formation.

3.4   Imido exchange reactivity of CpNb(NBu^t)X$_2$ (X = Cl, OBu^t)

There has been much derivative chemistry developed on the half-sandwich niobium system CpNb(NR)X$_2$, where work has focused on further functionalisation *via* replacement of the chloride ligands, for example with alkyl, amide, alkoxide and tertiary phosphine units[1,24]. However, relatively little chemistry exploring the reactivity of the

imido unit in this system has been explored. This is not suprising when the relative chemical stability of this multiply bonded group is taken into account. One type of reaction that has been examined is the exchange *between metal centres* of different imido groups[25], as shown in equation 3.15.

$$Cp*Nb(NR)Cl_2 + CpNb(NR^1)Cl_2$$

$$Cp*Nb(NR^1)Cl_2 + CpNb(NR)Cl_2$$

$$(3.15)$$
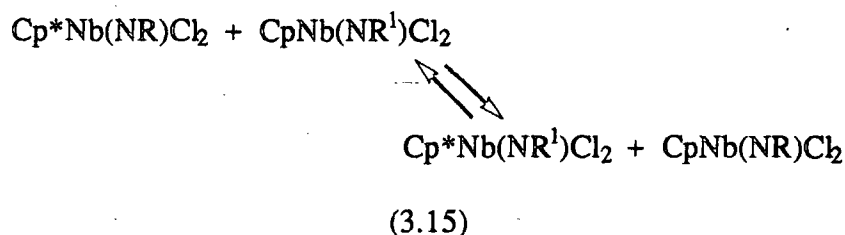
The aim of this section is to investigate the reactivity of the imido group in this system *via* reaction with a series of organic substrates.

3.4.1 Reaction of $CpNb(NBu^t)(OBu^t)_2$ with primary aromatic amines - $ArNH_2$ (Ar = $2,6$-$Pr^i_2C_6H_3$, $2,6$-$Cl_2C_6H_3$, C_6F_5)

Exchange of imido groups using amines has been confined to the late transition metal systems, $Cp^*Ir(NR)$[26] and (η^6-arene)Os(NR)[27] until our recent report on the Group 6 molybdenum system, $Mo(NR)_2(OBu^t)_2$[28]. This series is now extended to the Group 5 system - $CpNb(NBu^t)(OBu^t)_2$, where the tertiary butoxide group is chosen for the ancillary X-type ligand as it appears to be inert to protonation from amines {section 3.5.12 (b)}

(a) Reaction of $CpNb(NBu^t)(OBu^t)_2$ with $ArNH_2$ (Ar = $2,6$-$Pr^i_2C_6H_3$)

$CpNb(NBu^t)(OBu^t)_2$ was mixed with one equivalent of $ArNH_2$ in C_6D_6 at room temperature. No reaction was observed at this temperature or even on heating to 100°C for several weeks. The most probable reason for this lack of reactivity is a steric one. This is consistent with the observation by Bergman that $H_2N(2,6$-$Me_2C_6H_3)$ will react with (η^6-arene)Os(NBu^t) (figure 3.8) while $H_2N(2,6$-$Pr^i_2C_6H_3)$ will not[27]. Electronically both $2,6$-$Me_2C_6H_3$ and $2,6$-$Pr^i_2C_6H_3$ fragments are very similar so the

lack of reactivity in the latter case must be due to the larger steric requirement of this group. Furthermore, the failure to synthesise $CpNb(NAr)(OBu^t)_2$ *via* reaction of $CpNb(NAr)Cl_2$ with $LiOBu^t$ lends support to this steric argument[29].
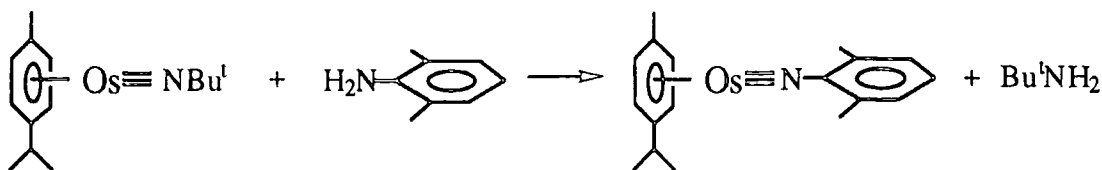
figure 3.8 *The reaction of (η^6-arene)Os(NBu^t) with H$_2$N(2,6-Me$_2$C$_6$H$_3$))*

The above reaction is not reversible, as demonstrated by the failure to detect any (η^6-arene)Os(NBu^t) when (η^6-arene)Os(N(2,6-Me$_2$C$_6$H$_3$) was mixed with 6 equivalents of Bu^{t}NH$_2$. Entropically there is little preference between both sides so the aryl substituted imido must be favoured by enthalpy.

(b) Reaction of CpNb(NBu^t)(OBu^t)$_2$ with Ar^{Cl}NH$_2$ (Ar^{Cl} = 2,6-Cl$_2$C$_6$H$_3$)

The presence of electron withdrawing chlorides on the aryl imido substituent would increase the relative acidity of the amine hydrogens compared to those of 2,6-Pr$^i_2$C$_6$H$_3$NH$_2$, and therefore could assist in the protonation of the tert-butyl imido ligand.

Equimolar quantities of CpNb(NBu^t)(OBu^t)$_2$ and Ar^{Cl}NH$_2$ were mixed in d$_6$ -benzene at room temperature. Maintaining the mixture at 100°C was necessary for reaction to proceed whereby signals corresponding to CpNb(NAr^{Cl})(OBu^t)$_2$ (8) were evident in the ^{1}H NMR (200 MHz) spectrum. Equilibrium was reached after 14 days at this temperature {K_{eq}(100°C) = 0.16(2)}.

$$CpNb(NBu^t)(OBu^t)_2 + Ar^{Cl}NH_2 \rightleftharpoons CpNb(NAr^{Cl})(OBu^t)_2 + Bu^tNH_2$$

(8)

(3.16)
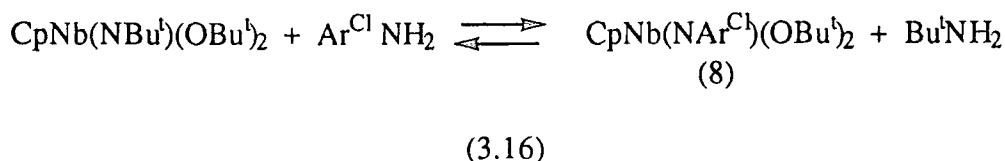
The equilibrium lies strongly in favour of the tert-butyl imido substituent suggesting that this species is preferred thermodynamically. An important factor disfavouring $CpNb(NAr^{Cl})(OBu^t)_2$ in this case may be the presence of lone pair repulsions between the chlorides of the imido substituent and the oxygens of the butoxides.

(c) Reaction of $CpNb(NBu^t)(OBu^t)_2$ with $Ar^F NH_2$ ($Ar^F = C_6F_5$)

Reaction of $CpNb(NBu^t)(OBu^t)_2$ with one equivalent of pentafluoroaniline in C_6D_6 proceeds very slowly at 60°C. At 100°C, equilibrium was attained after 7 days.

$$CpNb(NBu^t)(OBu^t)_2 + Ar^F NH_2 \rightleftharpoons CpNb(NAr^F)(OBu^t)_2 + Bu^t NH_2$$
$$(9)$$
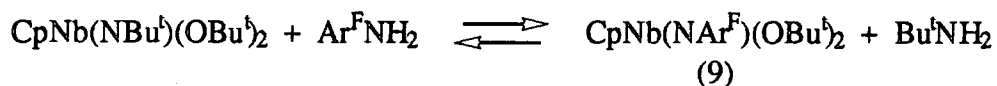
$$(3.17)$$

The equilibrium constant for the reaction at this temperature was $K_{eq} = 15(1)$, lying in favour of (9) (80% of total concentrations). $CpNb(NAr^F)(OBu^t)_2$ (9) is favoured on enthalpy grounds to $CpNb(NBu^t)(OBu^t)_2$, possibly as a consequence of a more electrophilic niobium metal centre being prefered. In this case lone pair repulsions do not appear to be the dominant effect as suggested in (b).

Equilibrium is attained slightly faster than observed in (b) which could be a consequence of the less hindered NH_2 group of this amine.

Overall, the rates of reaction are much slower than those observed for the 4 - coordinate molybdenum system (see section 2.2.3). The increased acidity of the 14e $Mo(NR)_2(OBu^t)_2$ complexes (c.f 16e for $CpNb(NBu^t)(OBu^t)_2$) and decreased steric constraints, owing primarily to the absence of a bulky 'face capping' cyclopentadienyl ligand contribute to it's enhanced reactivity. Also the presence of an ancillary cis multiply bonded ligand has been shown in other systems to increase reactivity[30].

The mechanism of this type of reaction (figure 3.9) is believed to proceed *via* a four legged piano stool base adduct (A), closely related in structure to the PMe$_3$ adduct $CpNb(NR)Cl_2.PMe_3$[1,31]. This species would then undergo intramolecular proton

transfer to give a five coordinate bis amide intermediate (B). The bis amide is not observed in the ^{1}H NMR spectrum and therefore must undergo further rapid proton transfer releasing free amine and the imido complex, which would be favoured entropically. Nevertheless, the stable bis amide intermediate Cp₂Zr(NHBuᵗ)₂[32] has been isolated *via* this type of reaction thus providing a model for the formation of (B).
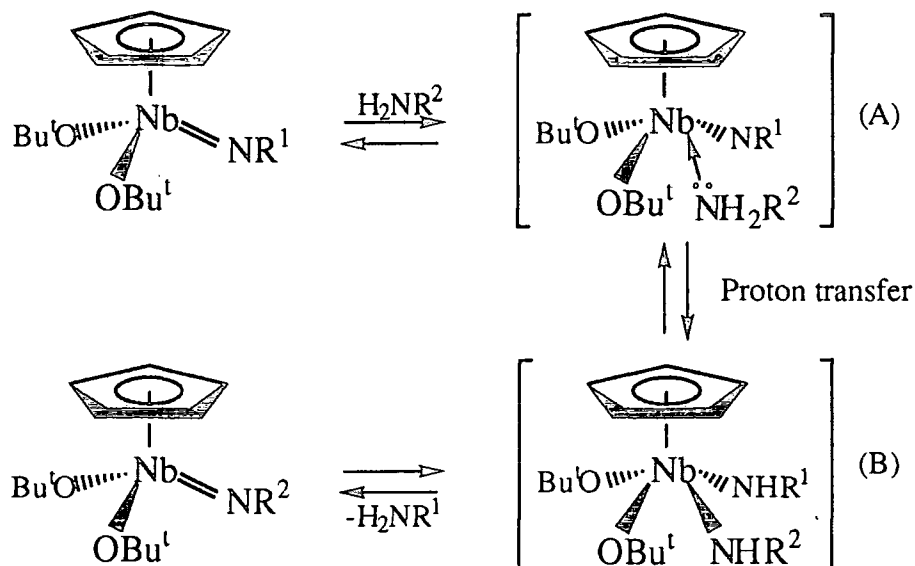
figure 3.9 *Postulated reaction mechanism for imido/amine exchange*

3.4.2 Reaction of CpNb(NBuᵗ)X₂ (X = Cl, OBuᵗ) with BuᵗO H

Displacement of an imido group *via* reaction with alcohols was demonstrated recently by Bradley[33] in the following reaction (equation 3.18):

$$W(NBu^t)_2(NHBu^t)_2 + 4\,ROH \longrightarrow W(NBu^t)(OR)_4 + 3\,Bu^tNH_2$$
$$(R = Pr^i, Bu^t)$$
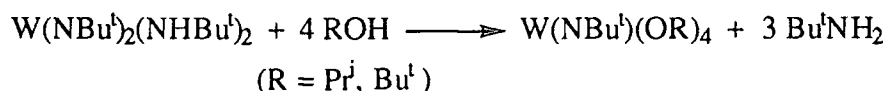
(3.18)

The subsequent displacement of the second imido group could not be achieved by adding excess alcohol. This example of imido substitution induced by alcoholysis is unique.

(a) Reaction of CpNb(NBu^t)(OBu^t)$_2$ with Bu^{t}OH

The following was proposed for the reaction of CpNb(NBu^t)(OBu^t)$_2$ with two equivalents of tert-butyl alcohol:

$$CpNb(NBu^t)(OBu^t)_2 + 2\,Bu^tOH \longrightarrow CpNb(OBu^t)_4 + Bu^tNH_2$$

$$(3.19)$$
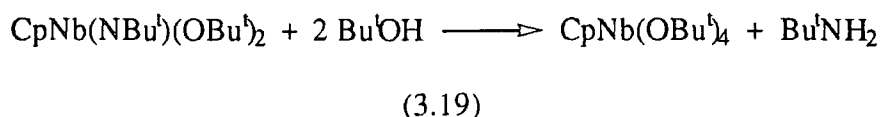
The reaction mixture was heated in C$_6$D$_6$ to 100°C for several weeks but the above reaction could not be facilitated. Reaction of the imido moiety in this system is not favoured, even the more acidic hexafluoro-t-butyl alcohol {pK$_a$(CF$_3$)$_2$CH$_3$COH) = 9.6^{34}, c.f pK$_a$(Bu^{t}OH) = 19.2^{35}} could not protonate off the imido group, although alkoxide exchange is observed in this case {section 3.5.12(a)}.

b) Reaction of CpNb(NBu^t)Cl$_2$ with Bu^{t}OH

Similarly as in (a), the following reaction was postulated:

$$CpNb(NBu^t)Cl_2 + 4\,Bu^tOH \longrightarrow CpNb(OBu^t)_4 + Bu^tNH_2 + 2\,HCl$$

$$(3.20)$$
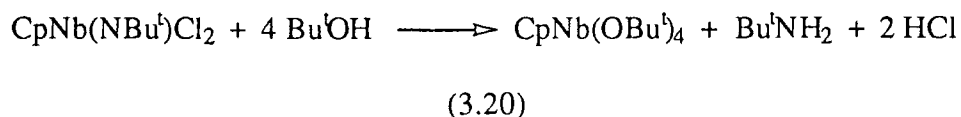
The main difference here is that chloride ligands may also be involved in the exchange processes. The ^{1}H NMR (C$_6$D$_6$, 250 MHz) spectrum of the reaction mixture after 20 minutes at room temperature showed the presence of CpNb(NBu^t)(OBu^t)Cl {see section 3.5.10(b)} and resonances assignable to the new species CpNb(OBu^t)$_2$Cl$_2$ (10) at δ 6.23(Cp) and 1.35 (OBu^t), arising from imido substitution. One suprising feature is that CpNb(NBu^t)(OBu^t)$_2$ is not observed. After 30 minutes there was virtually no CpNb(NBu^t)Cl$_2$ left and the concentration of (10) was increasing relative to that of CpNb(NBu^t)(OBu^t)Cl. This continued until after 1 hour when decomposition of the cyclopentadienyl ligands became apparent

A reaction scheme has been devised (see figure 3.10) outlining some of the possible reaction pathways in order to help rationalise these observations. Protonation from the alcohol can occur at the nitrogen or the chlorine and both these possibilities are explored.

$CpNb(NBu^t)Cl_2$ + Bu^tOH ⟶ $[CpNb(NBu^t)(Bu^tOH)Cl_2]$

(i) -HCl

$CpNb(NBu^t)(OBu^t)Cl$ $[CpNb(NHBu^t)(OBu^t)Cl_2]$

(ii) Bu^tOH -HCl Bu^tOH Bu^tOH -HCl

$[CpNb(NBu^t)(OBu^t)_2]$ $[CpNb(NHBu^t)(OBu^t)_2Cl]$

2HCl -H_2NBu^t   HCl -H_2NBu^t Bu^tOH -H_2NBu^t

$CpNb(OBu^t)_2Cl_2$
(10)
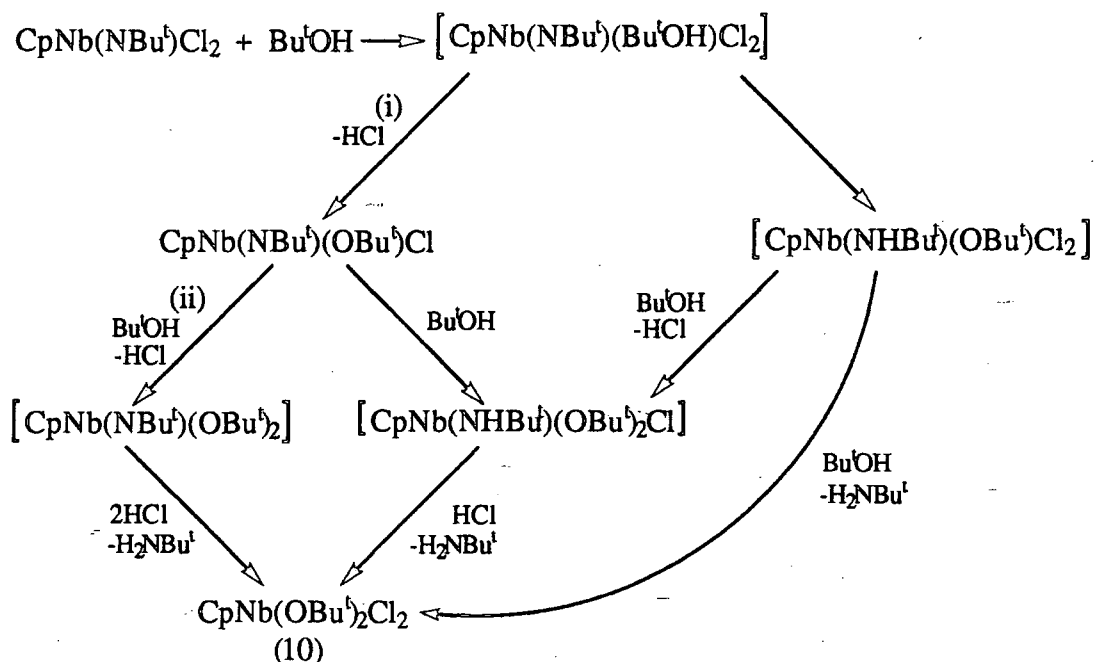
figure 3.10 *Reaction scheme for CpNb(NBu^t)Cl$_2$ with Bu^{t}OH*

The first protonation step (i) at the chlorine must occur in order for $CpNb(NBu^t)(OBu^t)Cl$ to be formed and it seems probable that further protonation at the chlorine (ii) yielding $CpNb(NBu^t)(OBu^t)_2$ could occur. It can be concluded that if $CpNb(NBu^t)(OBu^t)_2$ is formed, it is a short lived transient species. As this complex is chemically inert to Bu^tOH {section 3.4.2 (a)}, reaction with the eliminated HCl could be inferred affording $CpNb(OBu^t)_2Cl_2$ (10) and releasing Bu^tNH_2 (present as $Bu^tNH_3^+Cl^-$). The presence of the strong mineral acid HCl in this system almost certainly explains the protonation of the imido group, although ironically, it also leads to the iminent decomposition of the usually robust half-sandwich cyclopentadienyl ligand (protonated off as cyclopentadiene). Mineral acids have been used directly in this role previously to protonate off imido ligands and halogenate early transition metal centres[36]. Interestingly,

115

further alcoholysis of (10) to produce $CpNb(OBu^t)_4$ does not occur, although this could be attributable to the high steric requirement of four bulky butoxide ligands in a half-sandwich environment.

3.4.3 Reaction of $CpNb(NBu^t)(OBu^t)_2$ with H_2O

The hydrolysis of $CpNb(NBu^t)(OBu^t)_2$ was envisaged to take one of two courses {(i) and (ii), shown in equation 3.21}, with protonation either occuring at the imido or the alkoxide moiety.

$$CpNb(NBu^t)(OBu^t)_2 + H_2O \begin{array}{l} \xrightarrow{(i)} \text{'}CpNb(O)(NBu^t)\text{'} + Bu^tNH_2 \\ \xrightarrow{(ii)} \text{'}CpNb(O)(OBu^t)_2\text{'} + 2 Bu^tOH \end{array}$$

$$(3.21)$$
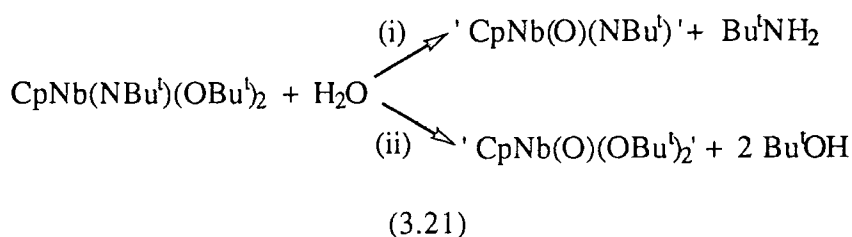
Attempts so far to synthesise mononuclear half-sandwich oxo complexes of group 5 have failed[37], often with polynuclear complexes being formed. By replacing the chlorides with bulky butoxide groups it may be possible to stabilise such a half-sandwich oxo species.

Equimolar quantities of $CpNb(NBu^t)(OBu^t)_2$ and H_2O were mixed in d_6-benzene at room temperature, whereby a pale brown insoluble precipitate was formed. ^1H NMR (250 MHz) showed *both* Bu^tOH and Bu^tNH_2 present in a 2:1 ratio. Since both processes (i) and (ii) are occuring it is likely that the precipitate is an ill-defined polynuclear oxo species.

3.4.4 Reaction of $CpNb(NBu^t)(OBu^t)_2$ with O_2

A sample of $CpNb(NBu^t)(OBu^t)_2$ in C_6D_6 was sealed under an atmosphere of oxygen (> 1000 equivalents) in an NMR tube and warmed to 60°C. After 3 days at 60°C all the starting material had beeen consumed, and an insoluble precipitate formed,

probably related in composition to that observed in the previous section. A number of new signals in the ^{1}H NMR had coincidentally grown in with the consumption of CpNb(NBu^t)(OBu^t)$_2$ and were assigned to tert-butanol, tert-butyl nitroxide and 2-methyl propene (formed by proton abstraction from a tert-butyl group).

3.4.5 Other attempted reactions of CpNb(NBu^t)(OBu^t)$_2$

No observable imido group metathesis was found between CpNb(NBu^t)(OBu^t)$_2$ and the following:

a) Azobenzene (1 equivalent, 100°C for 2 weeks)

b) (Me$_3$Si)N=C=N(SiMe$_3$) (1 equivalent, 100°C for 2 weeks)

c) ArNCO (1 equivalent, 100°C for 2 weeks)

3.5 Mono-anionic (X-type) ligand exchange in the $CpNb(NBu^t)X_2$ system

3.5.1 Introduction

A Mono-anionic ligand exchange study was undertaken for the four coordinate, pseudo-tetrahedral half-sandwich niobium system $CpNb(NBu^t)X_2$. This would enable a direct comparison with the four coordinate $Mo(Q)_2X_2$ system to be made. In keeping with the previous study (see section 2.6), X-type analogues were employed in bimolecular reactions of the following type:
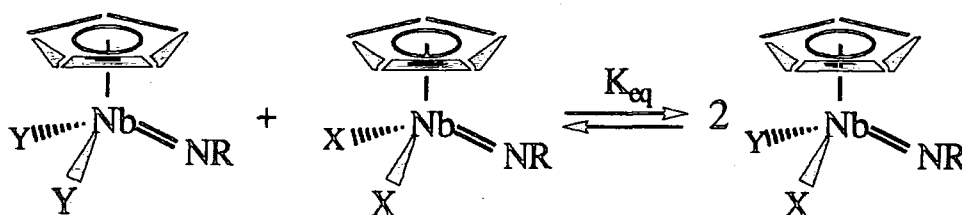
figure 3.11 *CpNb(NBu^t)X$_2$ / Y$_2$ exchange equilibria*

In addition, several other precursors were synthesised ($X = Br$, NC_4H_4) for study.

3.5.2 Reaction of $CpNbBr_4$ with $(Me_3Si)NHBu^t$

Preparation of CpNb(NBu^t)Br$_2$ (11).

The synthesis of $CpNb(NBu^t)Br_2$ (11) was performed utilising the method previously developed in our laboratory for the preparation of $CpNb(NBu^t)Cl_2$[9]; $CpNbBr_4$ was mixed with two equivalents of $Bu^tNH(SiMe_3)$ in dichloromethane solvent, whereby a slow reaction ensued over a period of 24 hours (equation 3.22). The desired product was isolated in low yield (23%) as an orange crystalline solid.

$$\text{CpNbBr}_4 + 2(\text{Me}_3\text{Si})\text{NHBu}^t \xrightarrow{\text{CH}_2\text{Cl}_2} \text{CpNb(NBu}^t)\text{Br}_2 + \text{H}_2\text{NBu}^t + 2\text{Me}_3\text{SiBr}$$
$$(11)$$

$$(3.22)$$

The infra red spectrum revealed weak absorptions attributable to Nb-Br stretches in the range 240-270 cm^{-1}, as well as characteristic stretches for the imido group at 1200 and 800 cm^{-1}.

3.5.3 Reaction of CpNb(NBu^t)Cl$_2$ with LiOPr^i

Preparation of CpNb(NBu^t)(OPr^i)$_2$ (12).

Reaction of CpNb(NBu^t)Cl$_2$ with two equivalents of LiOPr^i in diethyl ether proceeded rapidly on warming to room temperature, according to equation 3.23:

$$\text{CpNb(NBu}^t)\text{Cl}_2 + 2\text{ LiOPr}^i \longrightarrow \text{CpNb(NBu}^t)(\text{OPr}^i)_2 + 2\text{ LiCl}$$
$$(12)$$

$$(3.23)$$

After filtration and subsequent removal of the solvent *in vacuo* , a pale orange non-viscous oil was afforded in excellent yield. Analysis showed this oil to be CpNb(NBu^t)(OPr^i)$_2$ (12).

The low melting point of this complex could be ascribed to the weak intermolecular forces associated with branched propoxide groups[38]. The ^{1}H NMR spectrum (250 MHz, C$_6$D$_6$) showed two doublets due to diastereotopic iso-propoxide methyl groups at δ 1.25 and 1.29, with associated ^{13}C (100MHz, C$_6$D$_6$) signals at δ 26.58 and 26.67. Only one signal for the CH moiety of this propoxide group was present in both the ^{1}H (septet) and ^{13}C (doublet) NMR spectra. The protonated molecular ion was present in the mass spectrum at 348 as were low intensity high molecular weight peaks, possibly due to association *via* bridging propoxide groups.

3.5.4 Reaction of CpNb(NBu^t)Cl$_2$ with LiOBu^t

Preparation of CpNb(NBu^t)(OBu^t)$_2$

This synthesis was previously reported by D.N.Williams[9], according to equation 3.24:

$$CpNb(NBu^t)Cl_2 + 2\,LiOBu^t \longrightarrow CpNb(NBu^t)(OBu^t)_2 + 2\,LiCl$$

$$(3.24)$$
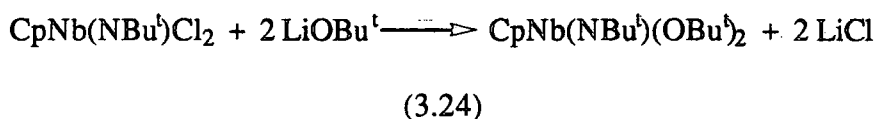
A notable exception to the original preparation was that here the product was isolated as a colourless crystalline solid by sublimation ($< 10^{-3}$ mmHg, 298K).

3.5.5 Reaction of CpNb(NBu^t)Cl$_2$ with LiOR$_f^3$

Preparation of CpNb(NBu^t)(OR$_f^3$)$_2$ (13).

Mixing CpNb(NBu^t)Cl$_2$ with two equivalents of LiOR$_f^3$ in diethyl ether produced CpNb(NBu^t)(OR$_f^3$)$_2$ (13) as shown in equation 3.25:

$$CpNb(NBu^t)Cl_2 + 2\,LiOR_f^3 \longrightarrow CpNb(NBu^t)(OR_f^3)_2 + 2\,LiCl$$

$$(13)$$

$$(3.25)$$
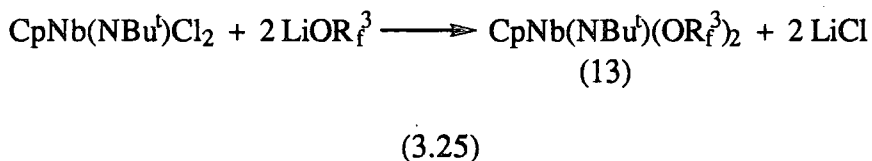
This compound was isolated from solution (Et$_2$O, -78°C) as colourless crystals. Similarly, as for the iso-propoxide derivative (see section 3.5.3), the prochiral metal environment gives rise to inequivalent methyls which were observed for the trifluoro tert-butoxide groups in the ^{1}H and ^{13}C NMR spectra, while a singlet resonance for the equivalent trifluoromethyl groups was present in the ^{19}F NMR spectrum at (376.3 MHz, C$_6$D$_6$) δ -82.53. Complex (13) readily sublimes with a relatively poor vacuum (10^{-2} mmHg, 298K), c.f CpNb(NBu^t)(OBu^t)$_2$ ($< 10^{-3}$mmHg, 298K), owing to the increased volatility afforded by the fluorocarbon groups compared to their hydrocarbon

counterparts[39,40]. Since only the halide derivatives had been structurally characterised previously[9], it was decided to obtain a structure determination of this dialkoxide derivative.

3.5.6 Molecular structure of $CpNb(NBu^t)(OR_f^3)_2$ (13)

Colourless cubic crystals of (13) were obtained by sublimation (10^{-2} mmHg, 298K) onto a water cooled-probe. A crystal of dimensions 0.40 x 0.40 x 0.40 mm was mounted under an inert atmosphere in a Lindemann capillary tube and X-ray data were collected at 150K The structure was solved by Ms.C.Wilson and Professor J.A.K.Howard of Durham University. The molecular structure is illustrated in figure 3.12 and selected bond and interatomic distances and angles are given in table 3.4. The molecule possesses a three-legged piano stool geometry and has a near-linear tert-butyl imido group (Nb-N-C = 165.6(7)°, Nb-N = 1.773(7)Å). Disorder was present in the structure for the cyclopentadienyl and alkoxide ligands and constraints were employed. The cyclopentadienyl ligand was constrained to be a planar regular pentagon and was modelled for two partially occupied sites (in the ratio 55:45). Similarly, the trifluoro-tert-butoxide ligands were modelled for two partially occupied sites.
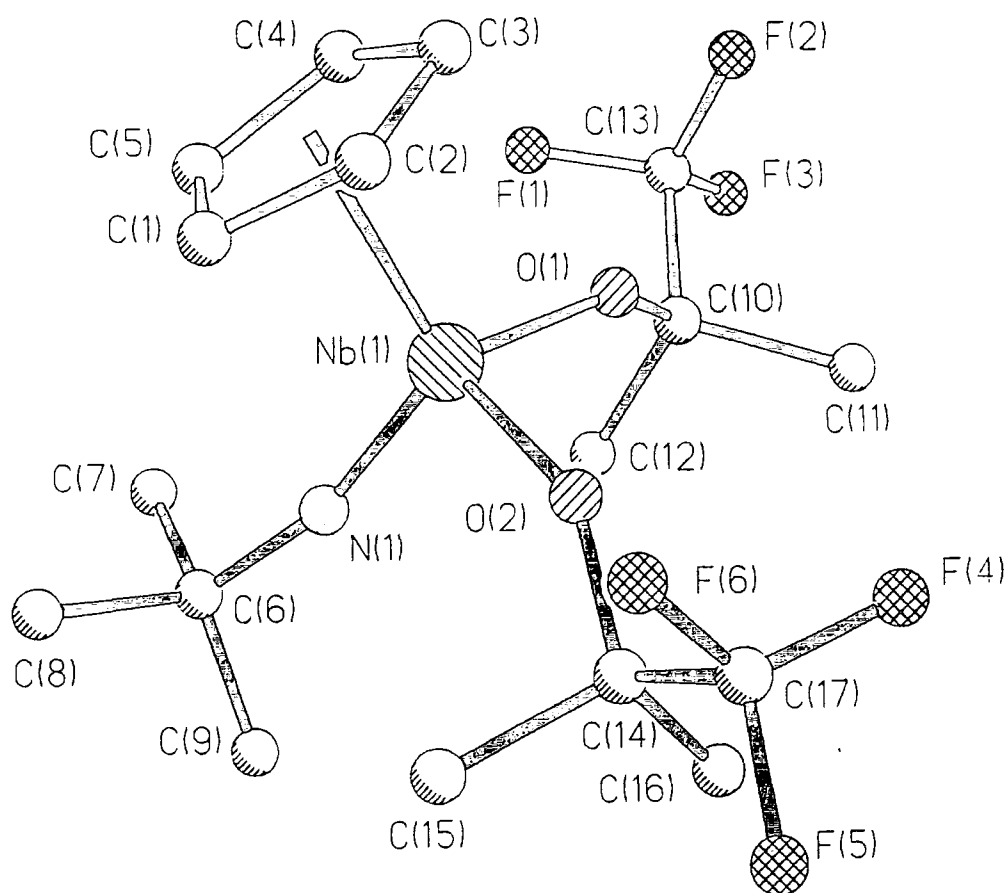
figure 3.12 *Molecular structure of CpNb(NBuᵗ)(ORf³)₂ (13)*

Nb(1)-O(1)	1.930(6)	Nb(1)-O(2)	1.936(6)
Nb(1)-N(1)	1.773(7)	Nb(1)-C(1)	2.440(15)
Nb(1)-C(2)	2.495(15)	Nb(1)-C(3)	2.532(15)
Nb(1)-C(4)	2.501(15)	Nb(1)-C(5)	2.443(16)
Nb(1)-C(1A)	2.477(18)	Nb(1)-C(2A)	2.531(18)
Nb(1)-C(3A)	2.525(17)	Nb(1)-C(4A)	2.467(19)
Nb(1)-C(5A)	2.436(18)	O(1)-C(10)	1.401(10)
O(2)-C(14)	1.398(10)	N(1)-C(6)	1.447(12)
C(1)-C(2)	1.420	C(1)-C(5)	1.420
C(2)-C(3)	1.420	C(3)-C(4)	1.420
C(4)-C(5)	1.420	C(1A)-C(2A)	1.420
C(1A)-C(5A)	1.420	C(2A)-C(3A)	1.420
C(3A)-C(4A)	1.420	C(4A)-C(5A)	1.420
C(6)-C(7)	1.489(19)	C(6)-C(8)	1.544(20)
C(6)-C(9)	1.480(18)	C(10)-C(11)	1.542(12)
C(10)-C(12)	1.542(15)	C(10)-C(13)	1.542(13)
C(10)-C(12A)	1.542(27)	C(10)-C(13A)	1.541(19)
C(13)-F(1)	1.307(14)	C(13)-F(2)	1.307(15)
C(13)-F(3)	1.308(16)	C(13A)-F(1A)	1.307(34)
C(13A)-F(2A)	1.307(33)	C(13A)-F(3A)	1.307(32)
C(14)-C(15)	1.542(17)	C(14)-C(15A)	1.542(16)
C(14)-C(16)	1.541(17)	C(14)-C(16A)	1.542(18)
C(14)-C(17)	1.541(15)	C(14)-C(17A)	1.542(16)

C(17)-F(4)	1.308(22)	C(17)-F(5)	1.308(24)
C(17)-F(6)	1.308(26)	C(17A)-F(4A)	1.308(23)
C(17A)-F(5A)	1.308(24)	C(17A)-F(6A)	1.308(25)

N(1)-Nb(1)-C(5A)	89.5(4)	C(1A)-Nb(1)-C(5A)	33.6(2)
C(2A)-Nb(1)-C(5A)	55.1(4)	C(3A)-Nb(1)-C(5A)	55.1(4)
C(4A)-Nb(1)-C(5A)	33.7(3)	Nb(1)-O(1)-C(10)	145.7(5)
Nb(1)-O(2)-C(14)	145.1(5)	Nb(1)-N(1)-C(6)	165.6(7)
Nb(1)-C(1)-C(2)	75.4(3)	Nb(1)-C(1)-C(5)	73.2(3)
C(2)-C(1)-C(5)	108.0	Nb(1)-C(2)-C(1)	71.1(3)
Nb(1)-C(2)-C(3)	75.0(2)	C(1)-C(2)-C(3)	108.0
Nb(1)-C(3)-C(2)	72.2(2)	Nb(1)-C(3)-C(4)	72.4(3)
C(2)-C(3)-C(4)	108.0	Nb(1)-C(4)-C(3)	74.8(3)
Nb(1)-C(4)-C(5)	71.1(3)	C(3)-C(4)-C(5)	108.0
Nb(1)-C(5)-C(1)	73.0(3)	Nb(1)-C(5)-C(4)	75.5(2)
C(1)-C(5)-C(4)	108.0	Nb(1)-C(1A)-C(2A)	75.6(3)
Nb(1)-C(1A)-C(5A)	71.6(4)	C(2A)-C(1A)-C(5A)	108.0
Nb(1)-C(2A)-C(1A)	71.5(3)	Nb(1)-C(2A)-C(3A)	73.4(4)
C(1A)-C(2A)-C(3A)	108.0	Nb(1)-C(3A)-C(2A)	73.9(4)
Nb(1)-C(3A)-C(4A)	71.2(4)	C(2A)-C(3A)-C(4A)	108.0
Nb(1)-C(4A)-C(3A)	75.7(4)	Nb(1)-C(4A)-C(5A)	72.0(3)
C(3A)-C(4A)-C(5A)	108.0	Nb(1)-C(5A)-C(1A)	74.8(4)
Nb(1)-C(5A)-C(4A)	74.3(3)	C(1A)-C(5A)-C(4A)	108.0
N(1)-C(6)-C(7)	109.4(11)	N(1)-C(6)-C(8)	108.9(9)
C(7)-C(6)-C(8)	104.9(12)	N(1)-C(6)-C(9)	110.8(9)
C(7)-C(6)-C(9)	112.0(11)	C(8)-C(6)-C(9)	110.5(11)
O(1)-C(10)-C(11)	107.6(7)	O(1)-C(10)-C(12)	111.9(7)
C(11)-C(10)-C(12)	109.1(8)	O(1)-C(10)-C(13)	109.8(7)
C(11)-C(10)-C(13)	109.1(7)	C(12)-C(10)-C(13)	109.2(8)
O(1)-C(10)-C(12A)	126.9(13)	O(1)-C(10)-C(13A)	112.0(10)
C(12A)-C(10)-C(13A)	109.2(17)	C(10)-C(13)-F(1)	104.7(9)
C(10)-C(13)-F(2)	108.9(9)	F(1)-C(13)-F(2)	109.8(11)
C(10)-C(13)-F(3)	112.7(9)	F(1)-C(13)-F(3)	110.3(10)
F(2)-C(13)-F(3)	110.3(10)	C(10)-C(13A)-F(1A)	113.9(20)
C(10)-C(13A)-F(2A)	106.8(16)	F(1A)-C(13A)-F(2A)	93.5(22)
C(10)-C(13A)-F(3A)	109.3(18)	F(1A)-C(13A)-F(3A)	112.5(20)
F(2A)-C(13A)-F(3A)	120.3(25)	O(2)-C(14)-C(15)	106.3(9)
O(2)-C(14)-C(15A)	115.0(9)	O(2)-C(14)-C(16)	112.1(9)
C(15)-C(14)-C(16)	109.2(11)	O(2)-C(14)-C(16A)	104.5(9)
C(15A)-C(14)-C(16A)	109.1(11)	O(2)-C(14)-C(17)	110.8(8)
C(15)-C(14)-C(17)	109.2(10)	C(16)-C(14)-C(17)	109.2(9)
O(2)-C(14)-C(17A)	109.7(8)	C(15A)-C(14)-C(17A)	109.2(9)
C(16A)-C(14)-C(17A)	109.1(10)	C(14)-C(17)-F(4)	99.9(12)
C(14)-C(17)-F(5)	110.9(12)	F(4)-C(17)-F(5)	111.5(15)
C(14)-C(17)-F(6)	106.0(14)	F(4)-C(17)-F(6)	119.3(17)
F(5)-C(17)-F(6)	108.6(18)	C(14)-C(17A)-F(5A)	111.3(13)
F(4A)-C(17A)-F(5A)	109.9(15)	C(14)-C(17A)-F(6A)	103.3(13)
F(4A)-C(17A)-F(6A)	120.6(18)	F(5A)-C(17A)-F(6A)	108.4(17)

Table 3.4 *Selected bond and interatomic distances (Å) and angles (°) for*

CpNb(NBu^t)(OCMe₂CF₃)₂

3.5.7 Reaction of $CpNb(NBu^t)Cl_2$ with $LiOR_f^6$

Preparation of $CpNb(NBu^t)(OR_f^6)_2$ (14).

Impure $CpNb(NBu^t)(OR_f^6)_2$ (14) was produced *via* the reaction of $CpNb(NBu^t)Cl_2$ with two equivalents of $LiOR_f^6$ in diethyl ether, according to equation 3.26:

$$CpNb(NBu^t)Cl_2 + 2\,LiOR_f^6 \longrightarrow CpNb(NBu^t)(OR_f^6)_2 + 2\,LiCl$$
$$(14)$$
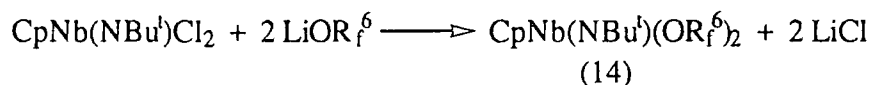
$$(3.26)$$

Pure (14) was obtained as a colourless crystalline compound by sublimation ($< 10^{-3}$ mmHg, 298K). The peak for the protonated parent ion was present in the mass spectrum (CI, m/z) at 592 as was a characteristic peak for the $C_5H_5^+$ ion (65).

The ^{19}F NMR spectrum (C_6D_6) displayed two inequivalent environments at δ -77.93 and -78.57 {analogous to the inequivalent methyl groups of (13)}. Both signals are quartets due to fluorine-fluorine coupling of the inequivalent CF_3 groups, $^4J_{FF} = 9.0$ Hz. These signals were useful in helping to model the lineshape of the observed multiplet in the ^{19}F NMR for the symmetry related hexafluoro tert-butoxide derivative of the Schrock catalyst $Mo(CHC(CH_3)_2Ph)(NAr)(OR_f^6)_2$[41]. Both are $A_3B_3X_3$ spin systems, where A and B are the two different fluorine environments and X is the proton environment. Using the $^4J_{FF}$ and $^4J_{HF}$ parameters for (14), a simple computer program can simulate the lineshape for different values of δ_{AB} (difference in chemical shift between the two fluorine environments). Figure 3.13 shows the simulated and actual ^{19}F NMR resonances of three systems -$CpNb(NBu^t)(OR_f^6)_2$(14), $Mo(O)(NBu^t)(OR_f^6)_2$(17) and $Mo(CHCMe_2Ph)(NAr)(OR_f^6)_2$ (all of which possess prochiral metal centres). On reducing δ_{AB}, roofing of the quartets occurs, until these resonances merge for the Schrock catalyst ($\delta_{AB} \sim 35Hz$). To a good approximation, the modelled systems closely resemble those observed. However, it should be noted that modelling the lineshape becomes more difficult at low δ values as long range couplings become more significant.

figure 3.13 *19F NMR spectra (simulated and actual) of (a) CpNb(NBuᵗ)(ORf⁶)₂ (14), (b) Mo(O)(NBuᵗ)(ORf⁶)₂(17) and (c) Mo(CHCMe₂Ph)(NAr)(ORf⁶)₂.*
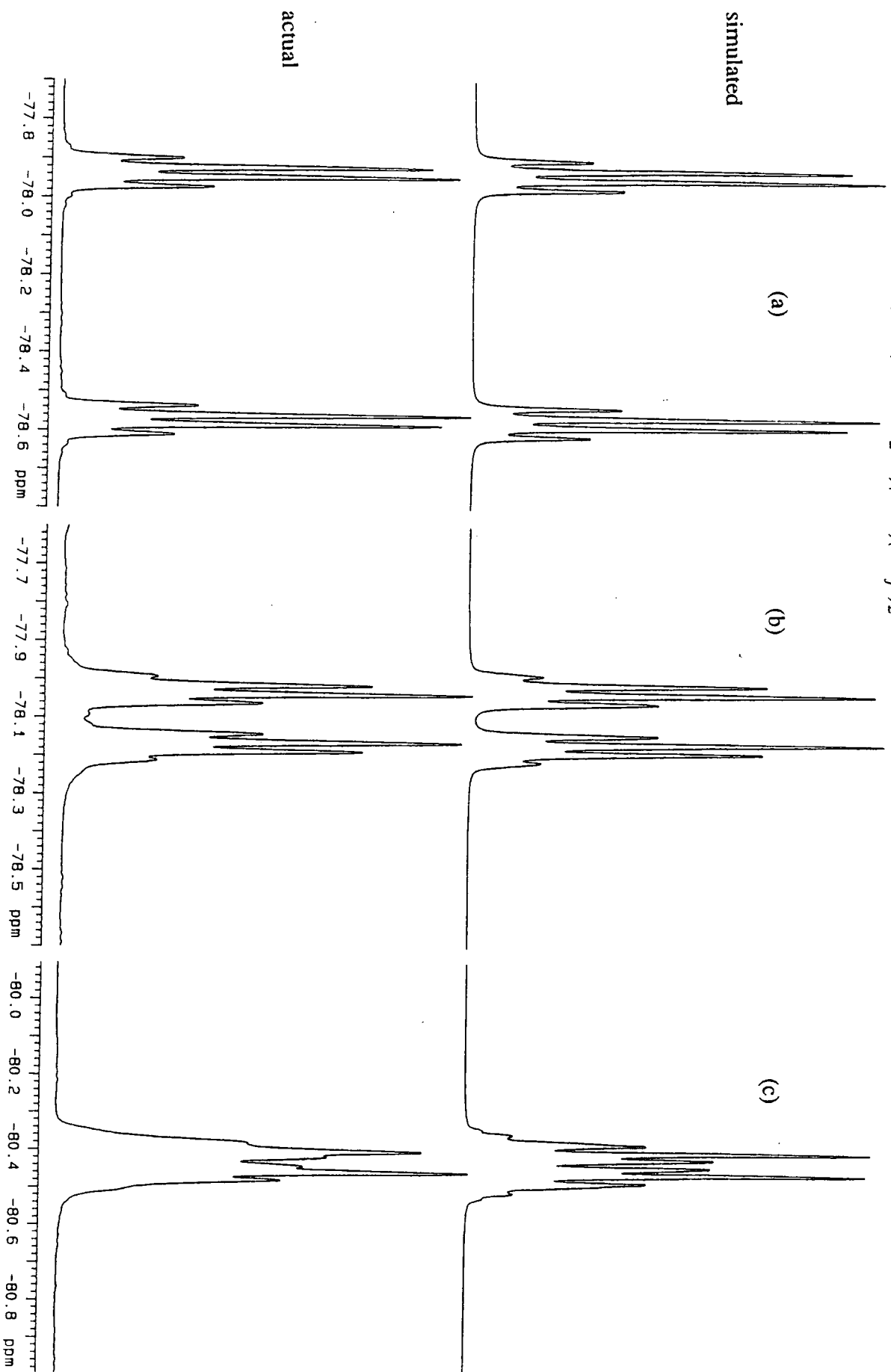
3.5.8 Reaction of CpNb(NBu^t)Cl$_2$ with LiNC$_4$H$_4$

Preparation of CpNb(NBu^t)(NC$_4$H$_4$)$_2$ (15).

Reaction of CpNb(NBu^t)Cl$_2$ with two equivalents of LiNC$_4$H$_4$ occurred rapidly at room temperature. The product was recrystallised from diethyl ether at -40°C as a pale yellow solid (equation 3.27).

$$CpNb(NBu^t)Cl_2 + 2\,LiNC_4H_4 \longrightarrow CpNb(NBu^t)(NC_4H_4)_2 + 2\,LiCl$$
$$(15)$$

$$(3.27)$$

Pyrrolyl ligands can coordinate to transition metal centres *via* η^1 and η^5 bonding modes; η^5-NC$_4$R$_4$ (R = H, Me) complexes are well known[42-44], but this coordination mode is only usually prevalent if the complex is electron defficient or methyl groups are present at the 2 and 5 ring positions (blocking the basic nitrogen from coordination to the metal). Complex (15) might be expected to contain both η^1 and η^5-C$_4$H$_4$N groups, analogous to the isolobal and isoelectronic complex (η^5-C$_5$H$_5$)$_2$(η^1-C$_5$H$_5$)Nb(NBu^t)[45], however this is not the case at room temperature as demonstrated by the equivalent pyrrolyl environments in the ^{1}H and ^{13}C NMR spectra. In η^5 coordination mode, the pyrrolyl group is a poor π donor compared to a cyclopentadienyl group[44,46] and therefore it is not suprising that both pyrrolyl groups coordinate in an η^1 fashion.

3.5.9 ^{13}C NMR - chemical shifts (δ, ppm) of the tert-butyl imido group in CpNb(NBu^t)X$_2$ complexes

The α- and β- carbon resonances, together with the Δδ values for a series of half-sandwich niobium tert-butyl imido complexes of the type CpNb(NBu^t)X$_2$ are recorded in table 3.5:

X	$\delta C(\alpha)$	$\delta C(\beta)$	$\Delta\delta$
NHBu^t	65.65	34.24	31.41
OPr^i	65.47	32.90	32.57
OBu^t [9]	65.41	32.62	32.79
OR$_f$[3]	66.55	32.03	34.52
OR$_f$[6]	68.04	31.43	36.61
NC$_4$H$_4$	68.96	31.75	37.21
Cl[9]	69.98	30.40	39.58
Br	69.92	30.18	39.74

table 3.5 ^{13}C *chemical shift data (ppm) for CpNb(NBu^t)X$_2$*

The magnitude of $\Delta\delta$ lies in the range 30 - 40 ppm and increases in the order:

NHBu^t < OPr^i < OBu^t < OR$_f$[3] < OR$_f$[6] < NC$_4$H$_4$ < Cl < Br
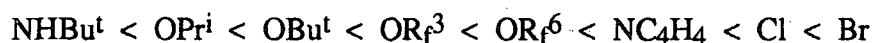
At the lower limit of $\Delta\delta$ is the tert-butyl amide group, which is consistent with the decreased electronegativity of the nitrogen relative to that of the oxygen in the alkoxide species. At the upper limit, the halides (Cl, Br) show the largest $\Delta\delta$ values of the series, reflecting their high electronegativity and poor-π donor ability compared to the alkoxide species. The relatively large $\Delta\delta$ value of the pyrrolyl ligand is of note, which may be attributable to electron density of the nitrogen being involved in the aromatic character of the ring, thereby reducing π donation to the metal.

This series shows a clear trend in $\Delta\delta$ values for each X ligand that are directly comparable with the previously examined Mo(NBu^t)$_2$X$_2$ system (see section 2.6.4)

3.5.10 A mechanistic study of mono-anionic (X-type) intermetal ligand exchange in the $CpNb(NBu^t)X_2$ system

Standard conditions were employed for mono-anionic ligand exchange reactions of the type:

$$CpNb(NBu^t)X_2 + CpNb(NBu^t)Y_2 \underset{k_{-1}}{\overset{k_1}{\rightleftharpoons}} 2\ CpNb(NBu^t)XY$$
$$\ \ \ \ \ \ \ (A) \ \ \ \ \ \ \ \ \ \ \ \ \ (B)$$

$$K_{eq} = k_1 / k_{-1}$$

(3.28)
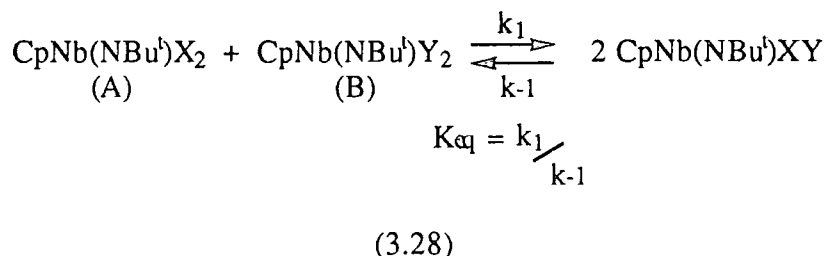
Equimolar quantities (38 μmols) of each compound {(A) and (B)} were mixed in C_6D_6 (800 μl) and the reactions were followed exclusively by ^1H NMR (200 MHz, 298K). Monitoring the variation in peak height and integral intensities of the tert-butyl and cyclopentadienyl resonances allowed 2nd order (reversible / non-reversible) rate constants (k_1 / l mol^{-1}s^{-1}) for the forward reaction process to be calculated.

These rate constants in conjunction with associated equilibrium constants are tabulated in table 3.8. Chemical shift data (δ, ppm) of the mixed $CpNb(NBu^t)XY$ and reactant $CpNb(NBu^t)X_2$ complexes are collected in tables 3.6 and 3.7 respectively.

a) Reaction of CpNb(NBu^t)Cl$_2$ with CpNb(NBu^t)Br$_2$ (11)

CpNb(NBu^t)Cl$_2$ and CpNb(NBu^t)Br$_2$ (11) were mixed at room temperature. A ^1H NMR spectrum of the mixture was obtained 5 minutes after mixing whereupon the reaction was found to have gone to completion; no residual reactants were observable.

$$CpNb(NBu^t)Cl_2 + CpNb(NBu^t)Br_2 \xrightarrow{k_1} 2\ CpNb(NBu^t)ClBr$$
$$\ \ \ \ \ \ \ (11) \ \ \ \ \ \ \ \ \ \ \ \ \ \ \ \ \ (16)$$

(3.29)
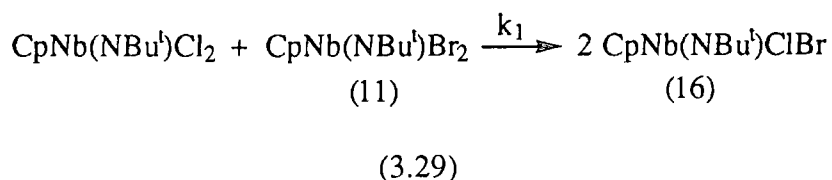
The chemical shifts attributed to (16), shown in table 3.5, are equidistant between the original starting complex signals (table 3.6). This is a general feature of these mixed species and could be viewed as a compromise between two differing electronic environments. As the reaction was too fast to be monitored by NMR at room temperature, a lower limit for the second order rate constant (k_1) can be estimated to be greater than 7.7 l mol^{-1}s^{-1}.

^{1}H NMR (200MHz, C_6D_6) data are tabulated for the mixed species CpNb(NBu^t)XY and the reactants CpNb(NBu^t)X$_2$ in tables 3.6 and 3.7 respectively:

complex		^{1}H NMR (C_6D_6) chemical shift values (δ, ppm)			
X	Y	Cp	NBu^t	X	Y
Cl	Br	5.88	1.04	-	-
Cl	OBu^t	6.06	1.11	-	1.27
Cl	NHBu^t	5.87	1.18	-	1.25, 7.6 (br)
Cl	NC$_4$H$_4$	5.86	1.06	-	6.39 (m), 7.18 (m)
OBu^t	NHBu^t	6.02	1.24	1.35	1.28, 5.6 (br)
OBu^t	OPr^i	6.17	1.17	1.34	1.25 (d), 4.72 (sept)
OBu^t	OR$_f^3$	6.13	1.11	1.26	1.36 (m), 1.38 (m)
OBu^t	OR$_f^6$	6.10	1.04	1.23	1.51 (sept)
OR$_f^3$	OR$_f^6$	6.07	0.96	1.29 (m)	1.45 (sept)

table 3.6 *^{1}H NMR data for CpNb(NBu^t)XY*

complex	^{1}H NMR (C_6D_6) chemical shift values (δ, ppm)		
X	Cp	NBu^t	X
Cl	5.89	1.02	-
Br	5.87	1.06	-
OBu^t	6.18	1.20	1.33
NHBu^t	5.87	1.26	1.30, 4.80 (s, br)
OPr^i	6.17	1.17	1.29 (d), 4.74 (sept)
OR$_f$^{3}	6.10	1.02	1.30 (m), 1.32 (m)
OR$_f$^{6}	6.05	0.92	1.44 (sept)
NC$_4$H$_4$	5.83	1.09	6.38 (m), 7.14 (m)

table 3.7 *^{1}H NMR data for CpNb(NBu^t)X$_2$*

In all cases it can be seen that the Cp and NBu^t chemical shifts of the mixed species CpNb(NBu^t)XY are an average of those found in the reactants CpNb(NBu^t)X$_2$. The β–protons of the NBu^t group move upfield with decreasing electron density at the imido nitrogen consistent with the behaviour observed for the β-carbon resonances (see section 3.5.9).

b) Reaction of CpNb(NBu^t)Cl$_2$ with CpNb(NBu^t)(OBu^t)$_2$

The reaction of CpNb(NBu^t)Cl$_2$ with CpNb(NBu^t)(OBu^t)$_2$ proceeded to completion over a period of two hours at room temperature with no residual reactants remaining (equation 3.30).

$$CpNb(NBu^t)Cl_2 + CpNb(NBu^t)(OBu^t)_2 \xrightarrow{k_1} 2\ CpNb(NBu^t)(OBu^t)Cl$$

(17)
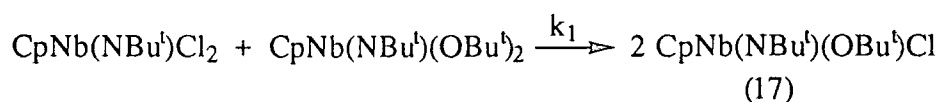
(3.30)

A 2nd order plot (figure 3.14) of 1 / a - x versus time afforded the rate constant k_1 = 1.27(4)x10^{-2} l mol^{-1}s^{-1}.
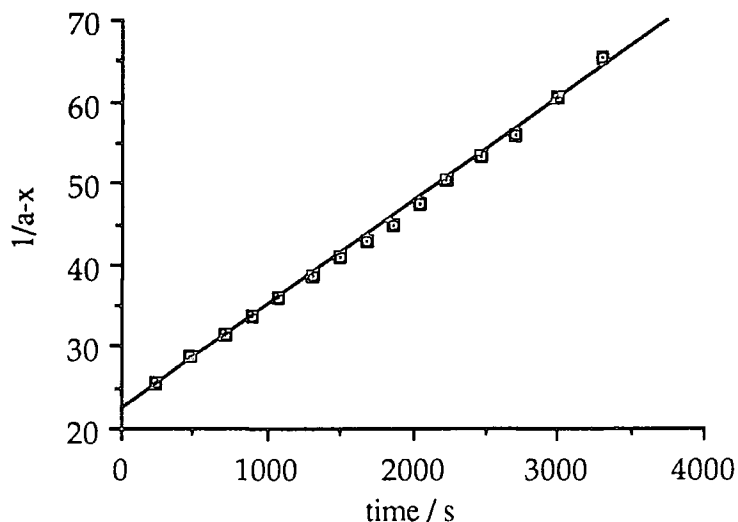
figure 3.14 *2nd order plot for chloride-butoxide exchange between CpNb(NBu^t)Cl$_2$ and CpNb(NBu^t)(OBu^t)$_2$*

The rate of chloride-butoxide exchange is significantly slower than that observed for chloride-bromide exchange, which is anticipated to be largely due to steric reasons.

c) Reaction of CpNb(NBu^t)Cl$_2$ with CpNb(NBu^t)(NHBu^t)$_2$ (5)

On mixing CpNb(NBu^t)Cl$_2$ with (5) at room temperature, a slow reaction ensued whereby no residual reactants could be detected after 24 hours.

$$CpNb(NBu^t)Cl_2 + CpNb(NBu^t)(NHBu^t)_2 \xrightarrow{k_1} 2\ CpNb(NBu^t)(NHBu^t)Cl$$
$$(5)$$
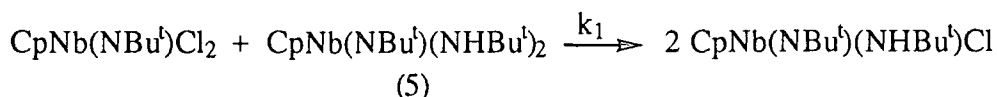
$$(3.31)$$

The resonances in the ^{1}H NMR spectrum attributable to the mixed complex CpNb(NBu^t)(NHBu^t)Cl[9] are collected in table 3.6. The 2nd order plot for the reaction afforded the rate constant k_1 = 9.7 (1)x10^{-4} l mol^{-1}s^{-1} (table 3.8). This rate constant is an

order of magnitude smaller than that observed for chloride-butoxide exchange in the previous example. This is in keeping with the increased steric bulk of an amide relative to an alkoxide group; the two substituents attached to an amide nitrogen lead to smaller Nb-N-C angles {137° for CpNb(NAr)(NHBu^t)Cl (2)}, whereas the singly substituted oxygen of an alkoxide ligand may approach linearity. This feature would hinder the bridging of ligands between metal centres and therefore increase the energy of the proposed four centred transition state (see figure 3.19, section 3.5.11).

d) Reaction of CpNb(NBu^t)(OBu^t)$_2$ with CpNb(NBu^t)(NHBu^t)$_2$ (5)

At room temperature there was no apparent reaction between CpNb(NBu^t)(OBu^t)$_2$ and (5), and therefore the reaction mixture was heated at 60°C. After two weeks, the appearance of the mixed complex (18) could just be detected (equation 3.32).

$$CpNb(NBu^t)(OBu^t)_2 + CpNb(NBu^t)(NHBu^t)_2 \overset{k_1^-}{\underset{}{\rightleftharpoons}} 2\ CpNb(NBu^t)(OBu^t)(NHBu^t)$$
$$(5) \qquad\qquad\qquad\qquad\qquad (18)$$

$$(3.32)$$
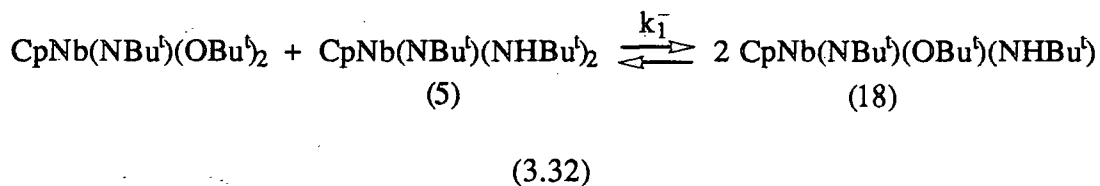
The formation of (18) was very slow at this temperature so the mixture was heated to 100°C. After 60 days at 100°C, (18) comprised only 20% of the total concentration of the reactants/products. An estimate of the 2nd order rate constant ($k_1 = 8 \times 10^{-7}$ l mol^{-1}s^{-1}) was made on the basis of an assumed final equilibrium position {$K_{eq} = 20(3)$, section 2.6.5(c)}.

This reaction is the slowest of the one electron ligand exchange processes studied and arises as a consequence of combining the sterically demanding amide and alkoxide ligands in the cluttered half-sandwich environment.

e) Reaction of CpNb(NBu^t)(OBu^t)$_2$ with CpNb(NBu^t)(OPr^i)$_2$ (12)

Resonances due to CpNb(NBu^t)(OBu^t)(OPr^i) (19) were apparent in the ^{1}H NMR spectrum after 2 hours at room temperature (equation 3.33).

131

$$\text{CpNb(NBu}^t\text{)(OBu}^t\text{)}_2 \; + \; \text{CpNb(NBu}^t\text{)(OPr}^i\text{)}_2 \; \underset{}{\overset{k_1}{\rightleftharpoons}} \; 2 \, \text{CpNb(NBu}^t\text{)(OBu}^t\text{)(OPr}^i\text{)}$$

$$(12) \qquad\qquad\qquad\qquad (19)$$

$$(3.33)$$
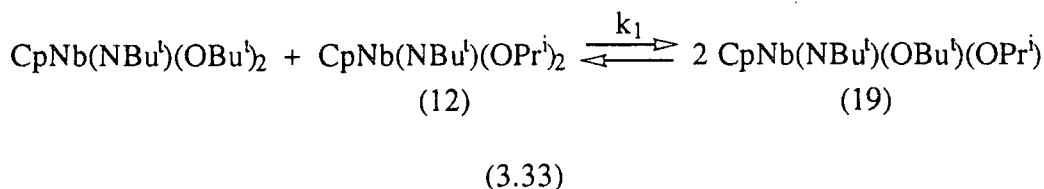
Some difficulty in distinguishing the mixed complex signals from the reactants was encountered as the chemical shifts were almost identical; in fact the Cp resonance for (19) is coincident with that of (12) (tables 3.6 and 3.7). Equilibrium was reached within 48 hours $\{Keq = 4.0(5)\}$. The 2nd order plot of $\ln [x \, (a - x_c) + ax_e \, / \, a \, (x_e - x)] = \ln (f)$, versus time is shown in figure 3.15, the slope of which is $[2a \, (a - x_e) \, / \, x_e] \, k_1$, allowing the determination of k_1 $\{2.8(2)\times10^{-4} \, 1 \, \text{mol}^{-1}\text{s}^{-1}\}$
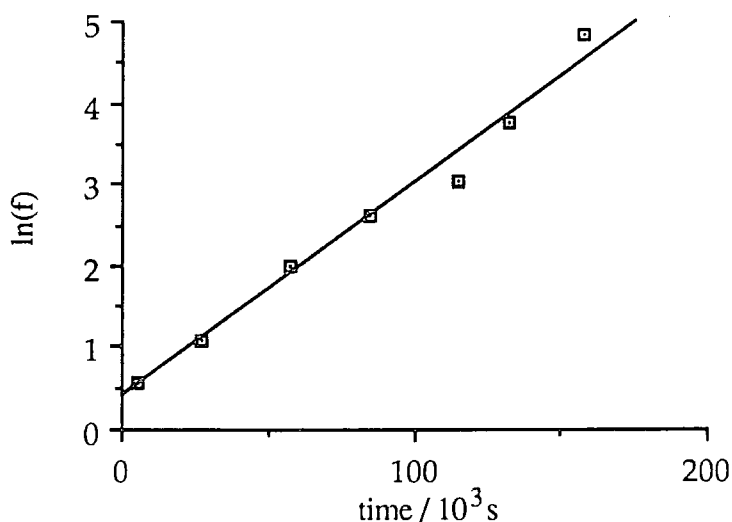
figure 3.15 *Plot of ln (f) versus time for propoxide-butoxide exchange between*

CpNb(NBu^t)(OPr^i)$_2$ and CpNb(NBu^t)(OBu^t)$_2$

The equilibrium constant $\{Keq = 4.0(5)\}$ demonstrates little thermodynamic preference for reactants or products and is very similar to that observed for propoxide-butoxide exchange in the $\text{Mo(NBu}^t\text{)}_2\text{X}_2$ system $\{Keq = 3.0(3)$, see section 2.6.5(d)$\}$.

f) Reaction of CpNb(NBu^t)(OBu^t)$_2$ with CpNb(NBu^t)(OR$_f^3$)$_2$ (13)

A very slow reaction occurred between CpNb(NBu^t)(OBu^t)$_2$ and (13) at room temperature over a period of two weeks (equation 3.34). Therefore, the reaction mixture was heated at 60°C whereby equilibrium was attained after 10 days {Keq(60°C) = 6.7(3), k_1 = 4.1(1)x10^{-5} 1 mol^{-1}s^{-1}}.

$$CpNb(NBu^t)(OBu^t)_2 + CpNb(NBu^t)(OR_f^3)_2 \xrightleftharpoons{k_1} 2\ CpNb(NBu^t)(OBu^t)(OR_f^3)$$

$$\text{(13)} \qquad\qquad\qquad\qquad \text{(20)}$$

(3.34)
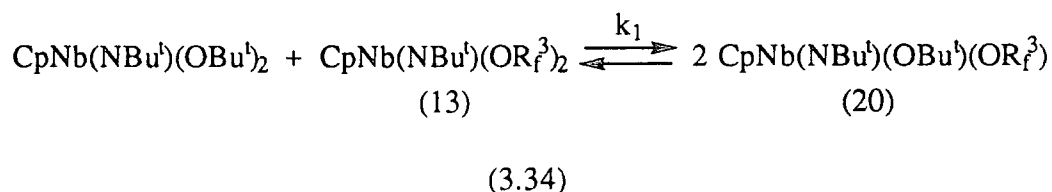
The ^{1}H NMR spectra at various time intervals for the reaction at 70°C are shown in figure 3.16. The equilibrium constant is small, slightly favouring the mixed product (20). The smaller rate constant for the forward reaction compared to that observed in (e) (propoxide-butoxide exchange) reflects the larger size of tert-butoxide ligands.

g) Reaction of CpNb(NBu^t)(OBu^t)$_2$ with CpNb(NBu^t)(OR$_f^6$)$_2$ (14)

The reaction mixture of CpNb(NBu^t)(OBu^t)$_2$ and CpNb(NBu^t)(OR$_f^6$)$_2$ (14) was maintained at 60°C, and the rate constant (k_1) for the formation of the mixed product (21) evaluated as 1.85(9)x10^{-5} 1 mol^{-1}s^{-1}.

$$CpNb(NBu^t)(OBu^t)_2 + CpNb(NBu^t)(OR_f^6)_2 \xrightleftharpoons{k_1} 2\ CpNb(NBu^t)(OBu^t)(OR_f^6)$$

$$\text{(14)} \qquad\qquad\qquad\qquad \text{(21)}$$

(3.35)
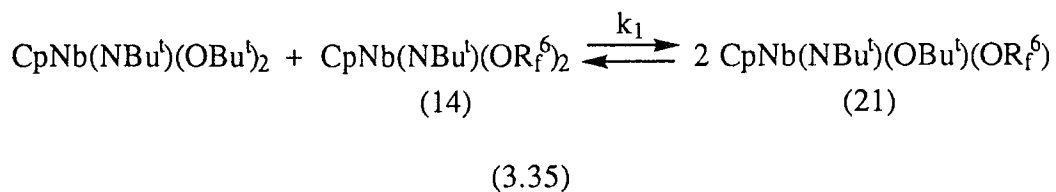
Equilibrium was attained after 70 days at this temperature {Keq(60°C) = 43(5)}, lying heavily in favour of (21). This equilibrium constant is significantly larger than that observed for OBu^t - OR$_f^3$ exchange {Keq(60°C) = 6.7(3)}, which may be a consequence of the greater electronic disparity between the OBu^t and OR$_f^6$ ligands, or a consequence of steric factors (see section 3.5.11)

133

figure 3.16   *Stack plot of the ^1H NMR spectra of the reaction of $CpNb(NBu^t)(OBu^t)_2$ with $CpNb(NBu^t)(OR_f^3)_2$ (13) at 70°C.*

Cp region

alkyl region

96 hrs

72 hrs

48 hrs

24 hrs

12 hrs

0 hrs

6.22   6.18   6.14   6.10   ppm   1.30   1.20   1.10   ppm
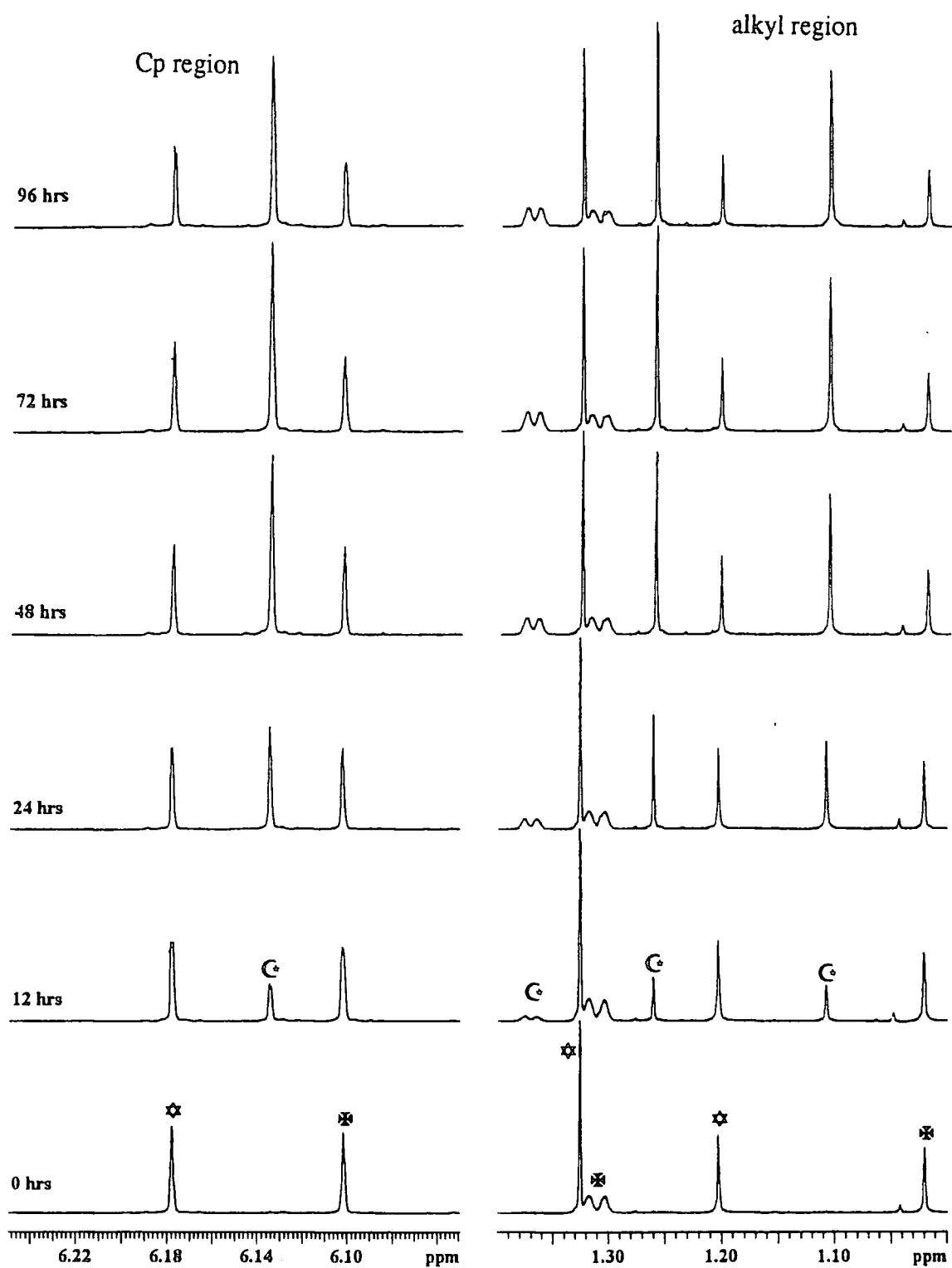
✿ $CpNb(NBu^t)(OBu^t)_2$

✹ $CpNb(NBu^t)(OR_f^3)_2$ (13)

☾ $CpNb(NBu^t)(OBu^t)(OR_f^3)$ (20)

A plot showing the relative rates for OBu^t - OR_f^3 (f) and OBu^t - OR_f^6 (g) exchange processes is shown in figure 3.17, emphasising the slower rate of butoxide exchange on progressively fluorinating these ligands {for (g)}. The steric bulk difference between a fluorinated tert-butyl group compared to a hydrocarbon analogue is relatively small, but of substantial significance are fluorine - fluorine lone pair repulsions in the proposed 5 coordinate bridged dimer transition state (see section 3.5.11).

figure 3.17 *Plots of OBu^t - OR_f^3 (f) and OBu^t - OR_f^6 (g) exchange in the CpNb(NBu^t)X$_2$ system*

h) Reaction of CpNb(NBu^t)(OR$_f^3$)$_2$ (13) with CpNb(NBu^t)(OR$_f^6$)$_2$ (14)

The reaction between (13) and (14) proceeded very slowly (even at 60°C). Therefore, the mixture was maintained at 100°C, whereby equilibrium was reached after about 100 days {Keq(100°C) = 7.0(4)}.

$$CpNb(NBu^t)(OR_f^3)_2 \ + \ CpNb(NBu^t)(OR_f^6)_2 \ \underset{}{\overset{k_1}{\rightleftharpoons}} \ 2 \ CpNb(NBu^t)(OR_f^3)(OR_f^6)$$
$$(13) \qquad\qquad (14) \qquad\qquad\qquad (22)$$

(3.36)

Figure 3.18 displays the ^{1}H NMR spectrum at equilibrium, clearly demonstrating the stability of these complexes to prolonged exposure at high temperatures. The proton

figure 3.18 ^1H NMR spectrum of the reaction of (13) with (14) after 100 days at 100°C.

C₆D₆

Cp region

6.1017
6.0427

△ CpNb(NBuᵗ)(OR$_f^3$)₂ (13)
Ω CpNb(NBuᵗ)(OR$_f^6$)₂ (14)
† CpNb(NBuᵗ)(OR$_f^3$)(OR$_f^6$) (22)

Ω 1.4440
△ 1.3084
  1.3057
△ 1.0213
0.9152

alkyl region

environments for the trifluoro and hexafluoro tert-butoxide ligands are similar in both the mixed species and the reactants {present as coincident quartets (OR_f^3) and septets (OR_f^6)}, fortunately the tert-butyl and cyclopentadienyl resonances are easily distinguishable, allowing the reaction to be readily monitored.

The 2nd order reversible reaction plot for tert-butoxide exchange afforded the forward rate constant $k_1 = 5.8(3) \times 10^{-6}$ l mol^{-1}s^{-1}.

Overall, the rate of alkoxide exchange increases in the order:

$$OR_f^3 - OR_f^6 < OBu^t - OR_f^6 < OBu^t - OR_f^3$$
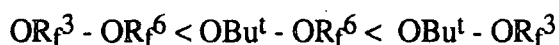
This correlates well with the decreasing number of fluorine - fluorine repulsions.

Of particular note are the similar equilibrium constants for $OBu^t - OR_f^3$ {$K_{eq}(60^oC) = 6.7(3)$} and $OR_f^3 - OR_f^6$ {$K_{eq}(100^oC) = 7.0(4)$} exchange (although not strictly comparable due to the temperature dependence of equilibrium, discussed later in 3.5.11). In each case there is a difference of one trifluoromethyl group (CF_3) between each reactant pair. When this difference is two CF_3 groups, as in (g), the equilibrium constant is much greater {$K_{eq}(60^oC) = 43(5)$}.

i) Reaction of CpNb(NBu^t)Cl$_2$ with CpNb(NBu^t)(NC$_4$H$_4$)$_2$ (15)

The reaction between CpNb(NBu^t)Cl$_2$ and (15) was rapid at room temperature with equilibrium established in approximately 20 minutes {$K_{eq} = 15(5)$}.

$$CpNb(NBu^t)Cl_2 + \underset{(15)}{CpNb(NBu^t)(NC_4H_4)_2} \underset{k_{-1}}{\overset{k_1}{\rightleftharpoons}} \underset{(23)}{2\ CpNb(NBu^t)(NC_4H_4)Cl}$$

(3.37)
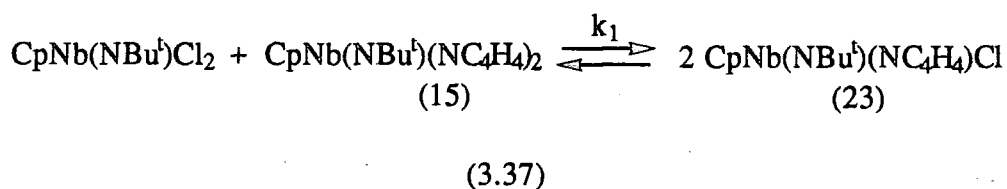
The fast rate of exchange ($k_1 \sim 2.5 \times 10^{-1}$ l mol^{-1}s^{-1}) can be rationalised in both steric and electronic terms. Sterically, the spatial anisotropy of the pyrrolyl ligand means that a rotating η^1 pyrrolyl ligand is less bulky than say a tert-butyl amide ligand and hence able to interact more readily with another metal centre. However, the nitrogen lone pair will be tied up in the aromatic ring and therefore less readily avaliable for bridging. By the same argument this will increase the electrophilicity of the metal centre (reflected by the large

135

$\Delta\delta$ value for this complex, discussed in section 3.5.9) and promote inter-molecular adduct formation.

j) Reaction of CpNb(NBu^t)(OR$_f^3$)$_2$ (13) with Mo(NBu^t)$_2$(OBu^t)$_2$ (1)

Intermetal alkoxide exchange between **different** metal centres was briefly explored *via* the reaction of CpNb(NBu^t)(OR$_f^3$)$_2$ (13) with one equivalent of Mo(NBu^t)$_2$(OBu^t)$_2$ (1). The reaction mixture was maintained at 60°C, whereby equilibrium was attained after 10 days. Interestingly, the ^{1}H NMR spectrum showed the presence of a previously unidentified species containing the CpNb(NBu^t)(OBu^t)$_2$ fragment, which was proposed to be of the form CpNb(NBu^t)(OBu^t)$_2$.Mo(NBu^t)$_2$(OR)$_2$, the structure thereof presumably involving either bridging imido or alkoxide ligands. The resonances for CpNb(NBu^t)(OR)$_2$ were clearly separated in the cyclopentadienyl region of the ^{1}H NMR spectrum, the percentage equilibrium concentrations for which are; CpNb(NBu^t)(OBu^t)$_2$ (10%), CpNb(NBu^t)(OBu^t)(OR$_f^3$) (47%), CpNb(NBu^t)(OR$_f^3$)$_2$ (31%) and CpNb(NBu^t)(OBu^t)$_2$. Mo(NBu^t)$_2$(OR)$_2$ (12%). Unfortunately, owing to an abundance of new resonances in the methyl region of the spectrum, the approximate percentage equilibrium concentrations for species of the type Mo(NBu^t)$_2$(OR)$_2$ could not be evaluated. The rate limiting factor for this slow exchange process is attributed to the sterically innacessible niobium centre. The same equilibrium position was realised starting from CpNb(NBu^t)(OBu^t)$_2$ and Mo(NBu^t)$_2$(OR$_f^3$)$_2$, where equilibrium was attained at a slightly faster rate (6 days at 60°C).

3.5.11 Discussion of intermetal exchange in $CpNb(NBu^t)X_2$ and $Mo(Q)_2X_2$ systems

(i) Kinetic aspects

The main difference between the $CpNb(NBu^t)X_2$ and $Mo(Q)_2X_2$ systems is the rate at which equilibrium is attained. For the $CpNb(NBu^t)X_2$ system, the rates were sufficiently slow in most cases to enable the progress of the reaction to be followed conveniently by ^1H NMR spectroscopy. In contrast, equilibrium was attained generally within 5 minutes at room temperature for the $Mo(Q)_2X_2$ system. This marked variation in reactivity is due to the differing steric and electronic characteristics of the two respective systems. For the half-sandwich niobium system, the sterically bulky 'face-capping' cyclopentadienyl ligand would hinder the bridging of ligands between metal centres (discussed below). In addition, although both systems are formally 16 electron species, competition would exist for the π-bonding orbitals between the two multiply bonded groups in $Mo(Q)_2X_2$ (see section 1.2.4). This would result in a decrease in electron density at the metal centre (increase in Lewis acidity) and hence rationalise the increased reactivity observed for this species.

Since mono-anionic (X-type) intermetal exchange reactions fit 2nd order reversible and non-reversible treatments, a concerted mechanism was proposed involving X and Y ligands bridging between metal centres; the transition state envisaged for the $CpNb(NBu^t)X_2$ sytem is shown below:
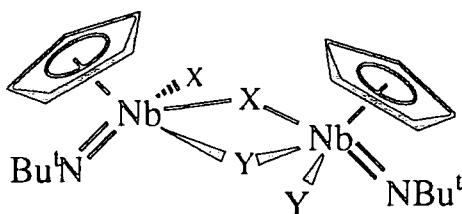
figure 3.19 *The transition state for intermetal mono-anionic ligand exchange in the CpNb(NBu^t)X$_2$ system*

The LUMO for the niobium metal centre is in the NbX_2 ligand plane, pointing out towards the side, and therefore electron pair donation from an external bridging ligand is expected to occur initially at this site[1,47]. This 5 coordinate bimolecular transition state could presumably rearrange to form an edge-shared trigonal bipyramid closely resembling the proposed transition state for intermetal oxo-imido exchange (see section 1.3.2).

For the $CpNb(NBu^t)X_2$ study, the rates of the intermetal exchange reactions (shown in table 3.8) correlate well with the relative sizes of the two exchanging X and Y groups, spanning 7 orders of magnitude. The rates increase in the order:

$$Cl - Br < Cl - OBu^t < Cl - NHBu^t < OBu^t - OPr^i < OBu^t - OR_f^3$$

$$OBu^t - OR_f^3 < OBu^t - OR_f^6 < OR_f^3 - OR_f^6 < OBu^t - NHBu^t$$
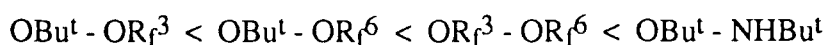
In addition, fluorine - fluorine lone pair repulsions must also be considered for the fluorinated alkoxide exchange reactions.

138

X	Y	Temp(K)	k_1 $(l\,mol^{-1}\,s^{-1})$	k_1 (relative)	K_{eq}
Cl	Br	298	> 7.7	2.8×10^4	$> 10^4$
Cl	OBu^t	298	$1.27(4) \times 10^{-2}$	45.7	$> 10^4$
Cl	$NHBu^t$	298	$9.68(9) \times 10^{-4}$	3.5	$> 10^4$
Cl	NC_4H_4	298	$\sim 2.5 \times 10^{-1}$	9×10^3	15(5)
OBu^t	$NHBu^t$	373	$\sim 8 \times 10^{-7}$	2.9×10^{-3}	*
OBu^t	OPr^i	298	$2.8(2) \times 10^{-4}$	1	4.0(5)
OBu^t	OR_f^3	333	$4.1(1) \times 10^{-5}$	1.5×10^{-1}	6.7(3)
OBu^t	OR_f^6	333	$1.85(9) \times 10^{-5}$	6.7×10^{-2}	43(5)
OR_f^3	OR_f^6	373	$5.8(3) \times 10^{-6}$	2.1×10^{-2}	7.0(4)

table 3.8   *Selected rate (k_1) and equilibrium constants (Keq) for X / Y exchange in the $CpNb(NBu^t)X_2$ system*

By increasing the relative size of the X and Y groups, bridging between metal centres is hindered and therefore the reaction is drastically retarded. The slow limit is realised in this study for exchange of large tertiary butyl amide and alkoxide ligands (OBu^t - $NHBu^t$). It is notable that exchange of this respective pair of ligands is also slow enough in the $Mo(NBu^t)_2X_2$ system for the reaction to be monitored by ^{1}H NMR spectroscopy.

With the recent discovery of the **acid catalysed** exchange of multiply bonded oxo and imido groups (outlined in section 2.4.1), attention was subsequently focused on assessing the influence of acid on the exchange of mono-anionic ligands. In the oxo-imido system it is proposed that hydrogen bonding occurs between the acid and the ancillary alkoxide ligands, resulting in the formation of a highly acidic metal centre. Exchange of the multiply bonded groups at this activated metal centre would then be expected to take place. A closely related mechanism may reasonably account for the

observations of acid catalysed mono-anionic ligand exchange in the niobium system. Its effects are dramatic, speeding up the reaction by several orders of magnitude; for instance, the alkoxide exchange reactions {3.5.10 (b), (e)-(h)}, when performed in the presence of benzoic acid (5%) reach equilibrium in a few minutes at room temperature. This enabled the evaluation of equilibrium constants at room temperature for these slow alkoxide exchange processes, thus allowing their direct comparison with those observed in the $Mo(Q)_2X_2$ system at the same temperature (see table 3.9). This phenomenon is also echoed for exchanging non-alkoxide species, although the rate is not speeded up to the same degree as for the former. Interestingly, the rate of tert-butoxide-amide exchange {3.2.10 (d)} is only increased slightly ($\sim$ x 2), but as the precise role of benzoic acid is not known, conclusions cannot as yet be drawn for this system.

Recently, Bergman has reported that intermetal alkoxide exchange in a coordinatively saturated Rhenium system could be facilitated by a catalytic amount of an alcohol[48] (equation 3.38).

(3.38)
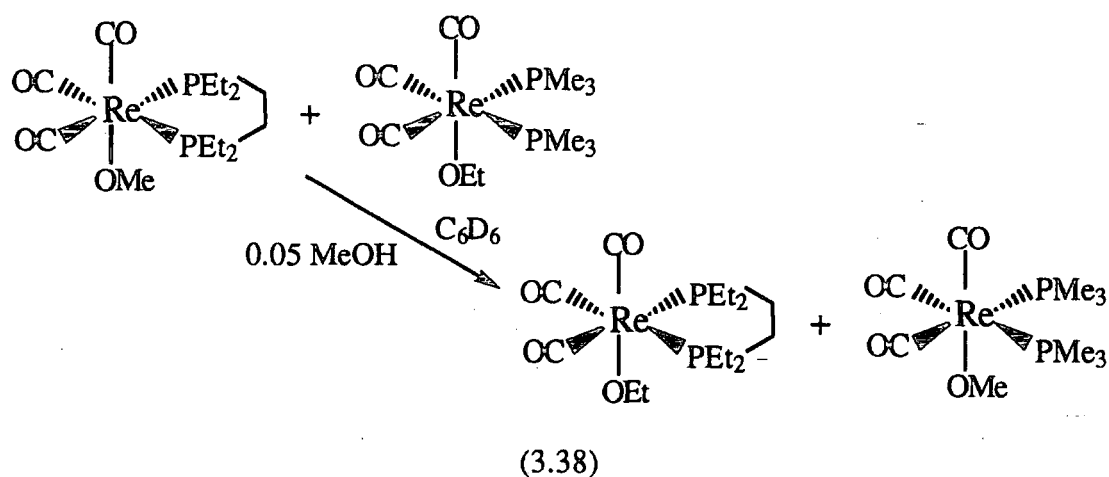
This reaction however does not proceed in the absence of methanol, presumably because a vacant coordination site at the metal centre is not avaliable. The mechanism suggested for the above process was said to be identical to that described for alcohol exchange i.e via the formation of a hydrogen bond between the alcohol and the alkoxide, followed by their respective interchange at the metal centre. In this system these hydrogen-bonded complexes are observable as intermediates in the ^1H NMR spectrum and in certain cases

140

can be directly isolated. In the $Mo(NBu^t)_2X_2$ system, there is also spectroscopic evidence for a hydrogen bonded intermediate {section 2.6 (a)}, however no such species are observed in the $CpNb(NBu^t)X_2$ system. It is doubtful that the acid catalysed intermetal alkoxide exchange process for the latter system is occurring *via* protonation followed by dissociation since the observed rates of exchange are much greater than those typically found in alcoholysis reactions {section 3.5.12 (a)}.

(ii)   Thermochemistry

The equilibrium constants for a given pair of X and Y ligands in each system are strikingly similar (shown in table 3.9).

complex		system (Keq, 298K)			
X	Y	$CpNb(NBu^t)$	$Mo(NBu^t)_2$	$Mo(O)_2$	$Mo(NAr)(CHCMe_2Ph)$
Cl	OBu^t	$> 10^4$	$> 10^4$	-	-
Cl	$NHBu^t$	$> 10^4$	$> 10^4$	-	-
OBu^t	$NHBu^t$	-	20(2)	-	-
OBu^t	OPr^i	4.0(5)	3.0(3)	-	-
OBu^t	OR_f^3	8.8(4)	7.0(7)	5 -15	11.0(5)
OBu^t	OR_f^6	55(4)	50(3)	30 - 80	150(10)
OR_f^3	OR_f^6	9.1(4)	7.0(2)	5 - 10	8.0(5)

table 3.9   *The equilibrium constants for mono-anionic ligand exchange in*

$CpNb(NBu^t)X_2$ and $Mo(Q)_2X_2$ systems

For electronically and sterically disparate pairs of ligands eg OBu^t - Cl and $NHBu^t$ - Cl, the equilibria lie almost completely over to the product side. An electronic compromise could be a favourable enthalpic situation, with the complex possessing both electron

withdrawing and donating groups on the metal centre as opposed to two electronically similar groups (see section 2.4.5). This is exemplified further by fluorinated alkoxide exchange. When there is a difference of one CF_3 group between each reactant pair ie.OBu^t - ORf^3 and ORf^3 - ORf^6 exchange, the equilibrium constants are virtually the same, whereas a difference of two CF_3 groups results in a larger equilibrium constant (OBu^t - ORf^6). Alternatively, relief of steric congestion for the more crowded reactant species could be the driving force for product formation, the equilibrium position moving further toward the products for a larger difference in relative size of the exchanging ligands.

The overall free energy changes for the intermetal exchange reactions fall in the range $\Delta G^o(298K) = - (3 - 23)$ KJmol^{-1}, the associated equilibrium constants ranging from Keq = 3.0 - 10^4 .The magnitude of the ΔG^o values are relatively small compared to typical organic bond forming/breaking reactions (typically, $\Delta G^o \sim 10^2 - 10^3$ KJmol^{-1}). In all cases these ΔG^o values are negative on progressing from reactants to products indicating a preference for the mixed (XY) species. As the free energy changes were only slightly negative for reactions with small associated equilibrium constants, it is possible that in these situations **entropy** could play an important part in favouring the mixed species. Changes in symmetry are an important entropic consideration when considering the rotational energy of molecules in the gas phase, for which Benson's additivity rules were devised[49]. A loss of symmetry on going from reactants to products leads to an increase in entropy. In the $CpNb(NBu^t)X_2$ and $Mo(Q)_2X_2$ systems, a destruction of symmetry occurs on going from the reactants to the products which would result in a favourable increase in entropy ca. $\Delta S^o = - 1.7$ KJmol^{-1} for $CpNb(NBu^t)X_2$ and $Mo(NAr)(CHMe_2Ph)X_2$; $- 3.4$ KJmol^{-1} for $Mo(NBu^t)_2X_2$ and $Mo(O)_2X_2$, which may account in part for the equilibrium constants observed for electronically similar ligands eg. propoxide-butoxide exchange (Keq = 4.0(5), $\Delta G^o = - 3.4$ KJmol^{-1}). It should be noted, however, that this assumes *gas phase* species; the effect in solution is uknown and therefore difficult to quantify.

3.5.12 Reaction of $CpNb(NBu^t)X_2$ with ROH

a) Reaction of $CpNb(NBu^t)(OBu^t)_2$ with R_f^6OH

$CpNb(NBu^t)(OBu^t)_2$ was mixed with two equivalents of R_f^6OH in C_6D_6 at room temperature. Reaction occured immediately with (21) present as the major species after only 20 minutes. Equilibrium was reached after 6 hours, with the approximate equilibrium concentrations given in equation 3.39:

$$CpNb(NBu^t)(OBu^t)_2 \qquad\qquad CpNb(NBu^t)(OR_f^6)_2$$

(3%) R_f^6OH R_f^6OH (14)
                                                       (14%)

$$CpNb(NBu^t)(OBu^t)(OR_f^6)$$
(21)
(83%)

(3.39)
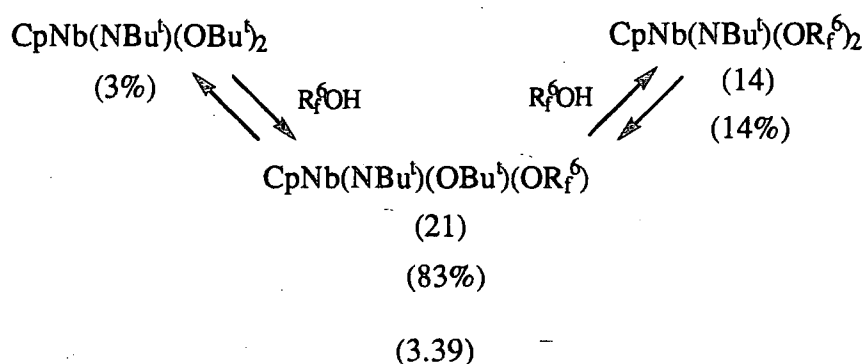
Notably, the mixed product (21) is the most themodynamically favoured species as observed earlier for intermetal exchange {3.5.10 (g)}. The equilibrium shows slight biasing towards (14), with vitually no $CpNb(NBu^t)(OBu^t)_2$ left. The much increased acidity of R_f^6OH ($pK_a = 9.6^{34}$) compared to Bu^tOH ($pK_a = 19.2^{35}$) could possibly account for this. However, the thermodynamic stability of the mixed species (21) appears to be the overiding factor. This is further demonstrated by the observation of the the same equilibrium ratio of products obtained from reaction of $CpNb(NBu^t)(OR_f^6)_2$ with two equivalents of tert-butanol. The attainment of equilibrium in the latter case is much slower (36 hours), possibly reflecting the decreased acidity of tert-butanol although this has no bearing on the thermodynamic outcome.

The rate of alkoxide exchange is much faster between an alcohol and the metal centre than between two metal centres {3.5.10 (g)} as a consequence of significantly reduced steric interactions.

b) Reaction of CpNb(NBu^t)(NHBu^t)$_2$ (5) with Bu^{t}OH

Treatment of CpNb(NBu^t)(NHBu^t)$_2$ (5) with two equivalents of tert-butanol in d$_6$-benzene at room temperature afforded CpNb(NBu^t)(OBu^t)$_2$, quantitatively over 30 minutes, according to equation 3.40:

$$CpNb(NBu^t)(NHBu^t)_2 + 2 \ Bu^tOH \longrightarrow CpNb(NBu^t)(OBu^t)_2 + 2 \ Bu^tNH_2$$
$$(5)$$

$$(3.40)$$
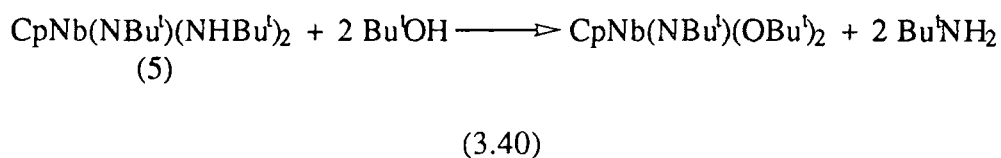
Interestingly, the mixed species CpNb(NBu^t)(NHBu^t)(OBu^t) (18) although formed initially, does not persist with the bis alkoxide being the most favoured species. The increased acidity of tert-butanol relative to tert-butylamine may assist the above transformation. This type of reactivity of bis amide species with alcohols is mirrored in the Mo(NBu^t)$_2$(NHBu^t)$_2$ system {discussed in section 2.6.8(b)}.

3.6 Summary

The results presented in this and the previous chapter provide the first detailed study of ligand exchange reactions between metal centres. A key observation has been the role of acid catalysis, which may have important application in inorganic synthetic methodologies.

3.7 References

1. V.C.Gibson, D.N.Williams, A.D.Poole, J.P.Mitchell, U.Siemeling, W.Clegg, D.C.R.Hockless, P.A.O'Neil, *J. Chem. Soc. Dalton Trans.* 1992, 739.

2. D.E.Wigley, P.A.Wegler, Y-W. Chao, *Inorg. Chem.* 1990, **29**, 4592.

3. D.E.Wigley, D.P.Smith, K.D.Allen, M.D.Carducci, *Inorg. Chem.* 1992, **31**, 1319.

4. D.C.Bradley, I.M.Thomas, *Can. J. Chem.* 1960, **40**, 1355.

5. D.C.Bradley, M.H.Chisholm, M.W.Extine, *Inorg. Chem.* 1977, **16**, 1791.

6. J.K.M.Saunders, B.K.Hunter, *"Modern NMR Spectroscopy"*, Oxford University press, 1987.

7. W.E.Stewart, T.H.Siddall, *III. Chem. Rev.* 1970, **70**, 517.

8. H.Kessler, *Angew. Chem. Int. Ed. Engl..* 1970, **9**, 219.

9. D.N.Williams, Ph.D Thesis, Durham University. 1990.

10. D.E.Wigley, P.A.Wexler, Y-W. Chao, *Inorg. Chem*, 1989, **28**, 3860.

11. W.A.Nugent, J.M.Mayer, *"Metal Ligand Multiple Bonds"*. Wiley, New York, 1988.

12. F.A.Cotton, S.A.Duraj, W.J.Roth, *J. Am. Chem. Soc.* 1984, **106**, 4749.

13. P.A.Finn, M.S.King, P.A.Kitty, R.A.McCarley, *J. Am. Chem. Soc.* 1975, **97**, 220.

14. L.S.Tann, G.V.Goeden, B.L.Haymore, *Inorg. Chem,* 1983, **22**, 1744.

15. V.C.Gibson, *J. Chem. Soc. Dalton Trans.* in press.

16. J.E.Bercaw, J.M.Mayer, C.J.Curtis, *J. Am .Chem. Soc.* 1983, **105**, 2651.

17. J.McMurray, *"Organic Chemistry"*, Monteray, 1984.

18. E.A.Maata, R.A.D.Wentworth, B.L.Haymore, *J. Chem. Soc.* 1979, **101**, 2063.

19. G.Wilkinson, A.A.Danopoulos, B.Hussain-Bates, M.B.Hursthouse, *J. Chem. Soc. Dalton Trans.* 1990, 2753.

20. W.A.Nugent, R.L.Harlow, *Inorg. Chem.* 1980, **19**, 777.

21. D.C.Bradley, R.J.Errington, M.B.Hursthouse, R.L.Short, B.R.Ashcroft, A.J.Nielson, *J. Chem. Soc. Dalton Trans.* 1987, 2059.

22. W.A.Nugent, D.C.Roe, D.M-T.Chan, W.C.Fultz, T.H.Tulip, *J. Am. Chem. Soc.* 1985, 107, 251.

23. R.R.Schrock, J.D.Feldman, *J. Am. Chem. Soc.* 1978, 100, 3359.

24. A.D.Poole, Ph.D Thesis. University of Durham. 1992.

25. V.C.Gibson, J.P.Mitchell, M.Jolly, *J. Chem. Soc. Dalton Trans.* 1992, 1331.

26. R.G.Bergman, D.S.Glueck, J.Wu, F.J.Hollander, *J. Am. Chem. Soc.* 1991, 113, 2041.

27. R.G.Bergman, R.A.Anderson, R.L.Michelman, *Organometallics.* 1993, 12, 274.

28. V.C.Gibson, J.P.Mitchell, M.Jolly, *J. Chem. Soc. Dalton Trans.* 1992, 1329.

29. V.C.Gibson, M. Jolly, Unpublished Results.

30. A.K.Rappe, W.A.Goddard III, *J. Am. Chem. Soc.* 1982, 104, 448.

31. V.C.Gibson, D.N.Williams, *Polyhedron.* 1989, 8, 1819.

32. R.G.Bergman, D.S.Glueck, F.J.Hollander, *J. Am. Chem. Soc.* 1988, 110, 8729.

33. D.C.Bradley, A.J.Howes, M.B.Hursthouse, J.D.Runnacles, *Polyhedron.* 1991, 10, 477.

34. B.L.Dyatkin, E.P.Mochalina, I.L.Knunyants, *Tetrahedron.* 1965, 21, 2991.

35. J.Murto, *Acta. Chem. Scand.* 1964, 18, 1043.

36. E.A.Maata, B.L.Haymore, R.A.D.Wenrworth, *Inorg. Chem.* 1980, 19, 1055.

37. V.C.Gibson, T.P.Kee, *J. Chem. Soc. Chem. Commun.* 1989, 656.

38. D.C.Bradley, M.H.Mehotra, D.P.Gaur, *"Metal Alkoxides"*, Academic Press, New York, 1978.

39. D.C.Bradley, H.Chudzynska, M.B.Hursthouse, M.Montevalli, *Polyhedron.* 1993, 12, 1907.

40. D.C.Bradley, H.Chudzynska, M.B.Hursthouse, M.Montevalli, M.E.Hammond, W.Ruowen, *Polyhedron.* 1992, 11, 375.

41. R.R.Schrock, J.S.Murdzek, G.C.Bazan, J.Robbins, M.Dimare, M.O'Regan, *J. Am. Chem. Soc.* 1990, 112, 3875.

42. R.B.King, M.B.Bisnette, *J. Organomet. Chem.* 1964, 1, 471.

43. N.Kuhn, A.Kuhn, E.M.Lampe, *Chem. Ber.* 1991, 124, 997.

44. W.J.Kelly, W.E.Partham, *Organometallics.* 1992, 11, 438.

45. M.L.H.Green, D.M.Michaelidou, P.Mountford, A.G.Suarez, L-L.Wong. *J. Chem. Soc. Dalton Trans.* 1993, 1593.

46. A.Efraty, N.Jubram, *Inorg. Chem. Acta.* 1980, 44, L191.

47. R.Hoffmann, J.W.Lauher, *J. Am. Chem. Soc.* 1976, 98, 1729.

48. R.G.Bergman, R.D.Simpson, *Organometallics.* 1993, 12, 781.

49. S.W.Benson, *"Themochemical Kinetics"*, Wiley, 1976.

50. D.E.Wigley, T.C.Baldwin, S.R.Huber, M.A.Bruck, *Inorg. Chem.* 1993, 32, 5638.

51. J.E.Bercaw, R.W.Quan, Unpublished results.

Chapter Four

Studies on the Metathesis Polymerisation of some

Functionalised Monomers

4.1 Introduction

This chapter is concerned with an important aspect of metathetical ligand exchange processes, namely the exchange of alkylidene groups of alkenes *via* metal-alkylidene intermediates, the so-called olefin metathesis reaction. We shall primarily be concerned with the metathesis of cyclic olefins giving rise to polymeric materials *via* ring-opening. A particular focus will be the polymerisation and attempted polymerisations of various 5-membered heterocycles using well-defined molybdenum metathesis initiators of the general formula - $Mo(NAr)(CHR)(OR')_2$[1] (R = Bu^t, CMe_2Ph and R' = Bu^t, R_f[3], R_f[6]. The advantages of employing these initiators are numerous; for instance, the molybdenum Schrock initiators are known to be tolerant to a wide range of functionalities[2,3]. The fluorinated alkoxide derivatives (R = R_f[3] and R_f[6]) have been shown to be sufficiently active to metathesise acyclic olefins[4], and owing to the high solubility and single component nature of the initiators, NMR techniques can readily be employed for the observation and characterisation of any propagating species generated, thus enabling a fuller understanding of the polymerisation processes.

It was desirable to explore the reactivity of a number of heterocyclic cyclopentene derivatives of the type shown in figure 4.1 { (a) 3-cyclopentene and (b) 2-cyclopentene} since there have been few examples reported thereof for both classical and well-defined systems[5,6,7], and the resultant polymers are of interest since they will carry a functional group within the polymer backbone.
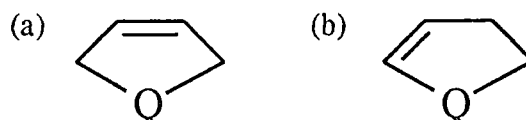
figure 4.1 *Hetero-cyclopentenes*

In order to complement the ring opening metathesis (R.O.M.P) studies of heterocyclic 5-membered rings, a study was undertaken on functionalised acyclic

dienes of the type shown in figure 4.2, since these can give rise to closely related polymers *via* Acyclic Diene Metathesis (ADMET).
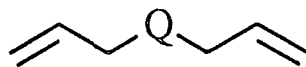
figure 4.2 *Hetero-diallyl species*

4.2 The R.O.M.P of 2,3 and 2,5-dihydrofurans with well-defined molybdenum initiators

4.2.1 Reaction of 2,5 dihydrofuran with Mo(NAr)(CHCMe₂Ph)(OR)₂

Preparation of poly(oxy-2-butenylene) (1)

The polymerisation of 1000 equivalents of neat 2,5 dihydrofuran (DHF) with Mo(NAr)(CHCMe2Ph)(OR)₂ {R = Bu^t (I), R$_f^3$ (II) and R$_f^6$ (III)} was found to occur very slowly with all three initiators, generating poly (oxy-2-butenylene) (1) according to equation 4.1:
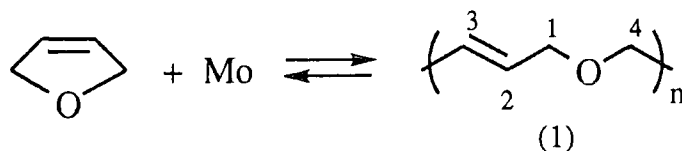
$$(4.1)$$

The viscosity of the mixture was found to increase over a period of 16 hours, after which time no further change was noted. The polymer was cleaved from the initiator by addition of benzaldehyde after subsequent precipitation from a toluene solution of (1) added to methanol (an oily polymer residue was isolated in low yield (10%) in each case). The oily nature of this polymer is ascribed to a low glass transition temperature (T_g) which is below room temperature. This is consistent with the observation that at least four methylene spacers are required between the oxygen and the vinylene in polyunsaturated ethers for the T_g value to approach or exceed room temperature[8].

149

Polymer (1) was found to be moderately air stable, although degradation did occur over long periods in air, probably owing to the acidic methylenic protons. The number average molecular weights (M_n), polydispersities (PDI) and cis / trans content of (1) arising from initiators I, II and III are shown in table 4.1:

Initiator	Cis / Trans*	M_n	PDI
I	93% trans	6800	1.36
II	93% trans	14200	1.55
III	94% trans	4300	2.34

* as determined by ^{1}H and ^{13}C NMR

table 4.1 *Selected data for poly (oxy-2-butenylene)*

The PDI value observed for (I) is relatively low. However, the polymers generated from the fluorinated alkoxide initiators (II and III) show greater molecular weight distributions. As these initiators are sufficiently active enough to metathesise acyclic olefins[1], it is likely that substantial secondary metathesis of the living alkylidene with vinylenes in the existing polymer chain could occur. In this situation the PDI values would tend towards the most probable value of 2[9].

4.2.2 ^{1}H and ^{13}C NMR characterisation of poly(oxy-2-butenylene) - Assignment of polymer microstructure

Poly(oxy-2-butenylene) (1) was found to be readily soluble in $CDCl_3$; the ^{1}H NMR spectrum (400 MHz) is shown in figure 4.3. The β−olefinic cis and trans resonances (H_2) are present at δ 5.65 and 5.74 respectively, the trans resonance characteristically downfield of the cis. The α-methylene resonances (H_1) are observed at δ 3.92(trans) and 3.98(cis). The relative intensities of the cis and trans resonances for both H_1 and H_2 showed the polymer to contain approximately 93% trans olefinic bonds (σ_t = 0.93) for (I), (II) and (III).
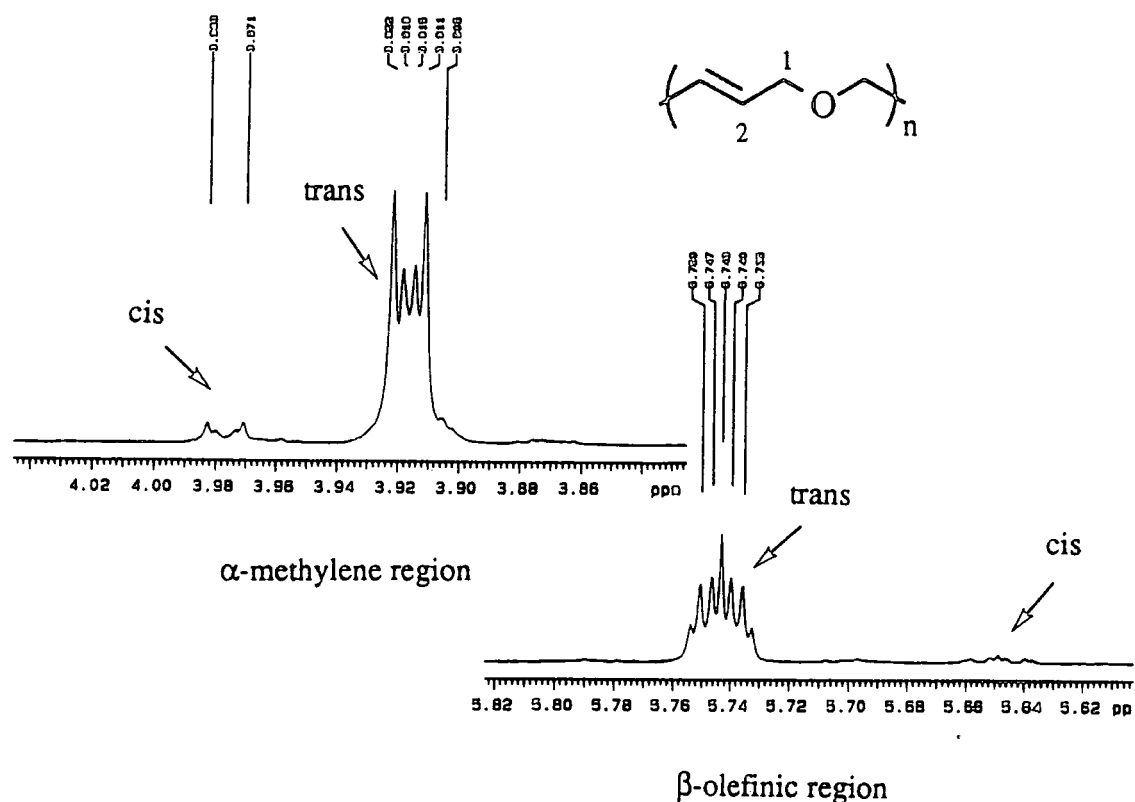
figure 4.3 *^{1}H NMR spectrum (400 MHz) of poly(oxy-1-butenylene) (1)*

The invariance of stereochemistry to the different initiators at first seemed somewhat suprising since many systems exist in which the cis / trans stereochemistry varies with the initiator used; most notably the polymerisation of 2,3- bis-(trifluoromethyl) norbornadiene with (I) generates a polymer with >98% trans content whereas (III) affords a polymer with >98% cis vinylene content[10-12]. A rationale for the observed invarient stereochemistry is given in section 4.2.7.

In ^{13}C NMR spectra, methylene carbons adjacent to a cis double bond in linear polyenes generally appear about 4 -5 ppm upfield of the respective trans resonance[21]. This indeed is found to be the case in the ^{13}C NMR spectrum of (1), with the cis resonance for C_1 being observed 4.2 ppm upfield of the trans, as shown in figure 4.4 (a). The ^{13}C resonances show fine structure due to dyad / triad splittings, which occur because the carbon environments are sensitive to the stereochemistry of the

151

neighbouring vinylene bonds. Dyads are observed for the α-methylene carbons (C_1), i.e they are sensitive to the two adjacent double bonds, as shown in figure 4.5:

$$\overset{t}{=} CHCH_2OCH_2CH \overset{t}{=} CHCH_2OCH_2CH \overset{c}{=} CHCH_2OCH_2CH \overset{t}{=}$$

$$\underset{tt}{\uparrow} \quad \underset{tt}{\uparrow} \qquad \underset{tc}{\uparrow} \quad \underset{ct}{\uparrow} \qquad \underset{ct}{\uparrow} \quad \underset{tc}{\uparrow}$$
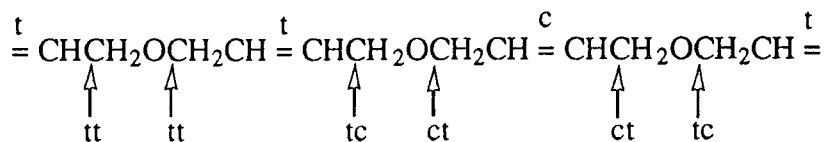
where t = trans, c = cis

figure 4.5 *The differing α-methylene carbon environments in poly(oxy-2-butenylene)*

The first letter in the above notation denotes the nearest double bond and the second the next nearest. From figure 4.5, it can clearly be seen that the number of ct resonances is equal to the number of tc resonances, hence the equal intensities of these signals observed in figure 4.4. The cc resonance can just about be discerned in the spectrum, present as a very low intensity resonance slightly downfield of the ct signal. The fraction of trans vinylenes is given by $\sigma_t = (tt + tc) / (cc + ct) = 0.93$, confirming the stereochemistry determined from the ^1H NMR spectrum. During the course of this work, the polymerisation of 2,5 DHF was reported with $Mo(NAr)(CHBu^t)(OR_f{}^6)_2$ by Wagener[13], and the polymer described as being 100% trans. However, close inspection of the ^{13}C NMR spectrum published shows the presence of the methylene ct resonance at δ 65.9, which escaped the notice of the authors.

The β-olefinic carbons (C_2) are sensitive to the nearest three double bonds (triad splitting), as shown in the ^{13}C NMR spectrum {figure 4.4 (b)}; the central letter in each triad refers to the nearest double bond, the first letter to the second nearest and the third letter to the third nearest, as depicted in figure 4.6:

$$\overset{t}{=} CHCH_2OCH_2CH \overset{t}{=} CHCH_2OCH_2CH \overset{c}{=} CHCH_2OCH_2CH \overset{t}{=}$$

$$\underset{ttc}{\uparrow} \quad \underset{ctt}{\uparrow} \qquad \underset{tct}{\uparrow} \quad \underset{tct}{\uparrow}$$
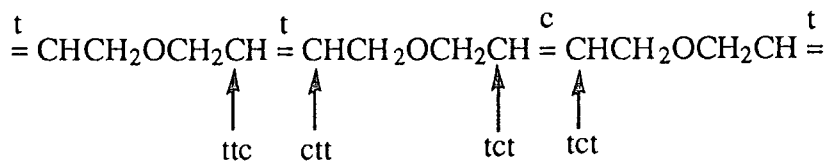
figure 4.6 *The β-olefinic carbons of poly(oxy-2-butenylene)*

figure 4.4 ^{13}C NMR spectrum (100 MHz) of poly(oxy-2-butenylene).
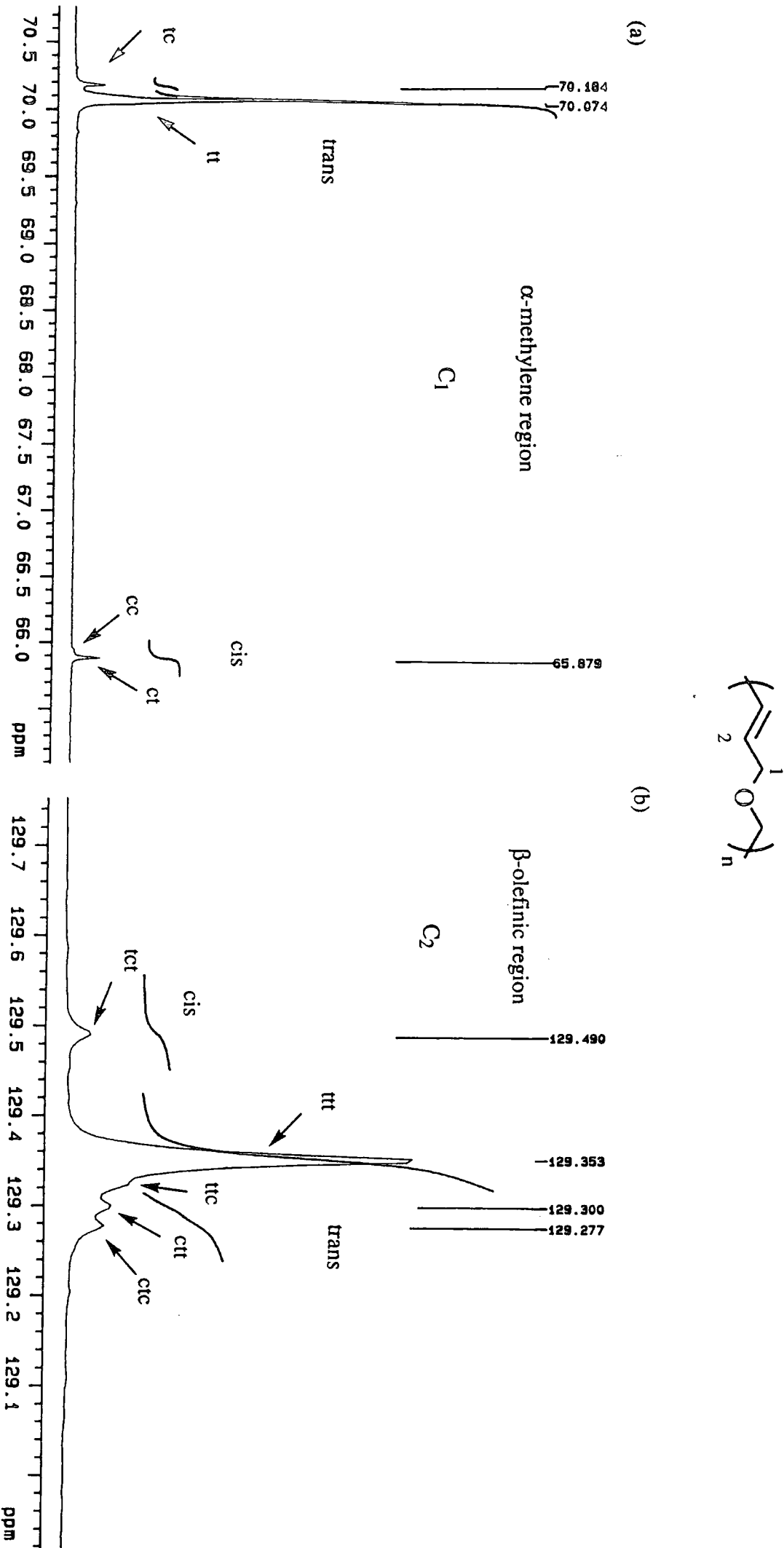
Only one signal is resolved for the cis olefinic carbons (tct) owing to the high trans content of (1). Interestingly, the dyad / triad splittings are reversed in the polymer produced from the structurally related silacyclopent-3-ene shown below, with dyads observed in the olefinic region and triads in the methylene region[6].
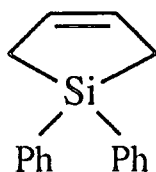
figure 4.7 *1,1-diphenylsilacyclopent-3-ene*

These splittings therefore appear to be dependent upon the hetero-functionality.

4.2.3   Reaction of 2,5 dihydrofuran with $Mo(NAr)(CHBu^t)(OR_f^3)_2$ in dilute solution

Two equivalents of 2,5 DHF was mixed with $Mo(NAr)(CHBu^t)(OR_f^3)_2$ in d_8-toluene at room temperature. The ^1H NMR (400 MHz) spectrum at this temperature showed very broadened signals for the monomer at δ 4.5 (υ = 350 Hz) and 5.45 (υ = 80 Hz), however no broadening or shift of the initiator resonances was observed. At -70°C, the singlet alkylidene resonance for the initiator was shifted significantly to δ 11.99 (free initiator at δ 11.62), and the resonances for the monomer were now sharp singlets at δ 4.48 and 5.17. It seems likely that adduct formation occurs at low temperature (shown in figure 4.8). At elevated temperatures 2,5 DHF is not as tightly bound to the metal centre and therefore an equilibrium is established between free and bound monomer; hence, an averaged environment is observed at room temperature. Similarly, tetrahydrofuran is known to bind to the Schrock initiators *via* the oxygen lone pair to the electrophilic metal centre, thereby reducing its reactivity[14].
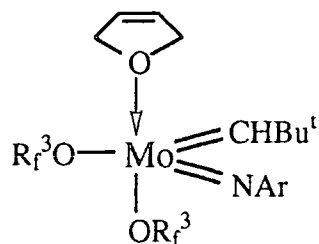
figure 4.8 *Proposed 2,5 DHF adduct of Mo(NAr)(CHBu^t)(OR$_f^3$)$_2$*

There was no evidence for any insertion products in the above experiment, even when the concentration of monomer was increased to 25 equivalents in d$_6$-benzene. Presumably, the concentration of monomer is below the critical level required for R.O.M.P to occur (see section 1.4.4).

4.2.4 Reaction of 2,3 dihydrofuran with Mo(NAr)(CHCMe$_2$Ph)(OR)$_2$

Preparation of poly(oxy-1-butenylene) (2).

Previously, the polymerisation of 2,3 DHF was reported by Höcker, utilising the Fischer type chromium carbene initiators (CO)$_5$Cr=CPh$_2$ and (CO)$_5$Cr=CPh(OMe)[7]. Poly(oxy-1-butenylene) was isolated in 30 - 50% yields and was found to contain equal proportions of cis and trans double bonds.

The reactivity of 2,3 DHF with well-defined molybdenum initiators was investigated so that the effect of moving the double bond (relative to 2,5 DHF) could be probed. Neat 2,3 DHF (1000 equivalents) was added to initiators I, II and III in three separate experiments at room temperature. For II and III, a red solution was formed instantly which became viscous over several minutes. After 30 minutes the reactions were judged to have gone to completion and benzaldehyde was added. No reaction occured for I, with the characteristic yellow solution of the free initiator remaining unchanged over several hours.

$$\text{(structure)} + \text{Mo} \rightleftharpoons \left(\begin{array}{c} 3 \quad 1 \\ 2 \end{array} O \begin{array}{c} 4 \end{array} \right)_n$$

(2)
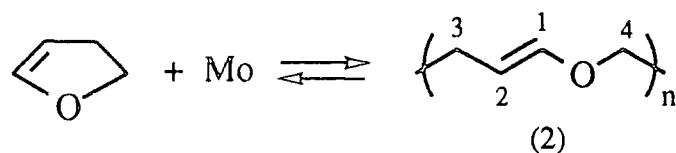
(4.2)

Poly(oxy-1-butenylene) (2) was isolated (in 45% yield) after precipitation by addition of a tetrahydrofuran solution to methanol (for II and III). The polymer was air sensitive, tending to cross-link over several hours, to give a markedly less soluble material. The number average molecular weights (M_n), polydispersities (PDI) and cis / trans content of (2) arising from initiators II and III are shown in table 4.2:

Initiator	Cis / Trans*	M_n	PDI
II	63% cis	6000	2.83
III	88% cis	4500	2.82

* as determined by ^{1}H and ^{13}C NMR

table 4.2 *Selected data for poly (oxy-1-butenylene)*

The polymers show a broad distribution of low molecular weight oligomers.

4.2.5 ^{1}H and ^{13}C NMR characterisation of poly(oxy-1-butenylene) - Assignment of polymer microstructure

In the ^{1}H NMR spectrum (400 MHz) of (2) synthesised from II (63% cis) in CDCl$_3$, the trans α- and β-olefinic protons are found characteristically downfield of the cis. The ^{13}C chemical shifts of the methylene carbons show dyad splitting, whereas higher order splittings are observed for the olefinic carbons (see figures 4.9 (a) and 4.9 (b) respectively). Notably, there is no evidence for head / tail isomerism in the ^{13}C NMR spectrum; 2,3 DHF is unsymmetric about the double bond and therefore could insert in two ways into the living polymer chain, producing a polymer of the type shown

figure 4.9 *13C NMR spectrum (100 MHz) of poly(oxy-1-butenylene)*.

(a) methylene region

(b) olefinic region
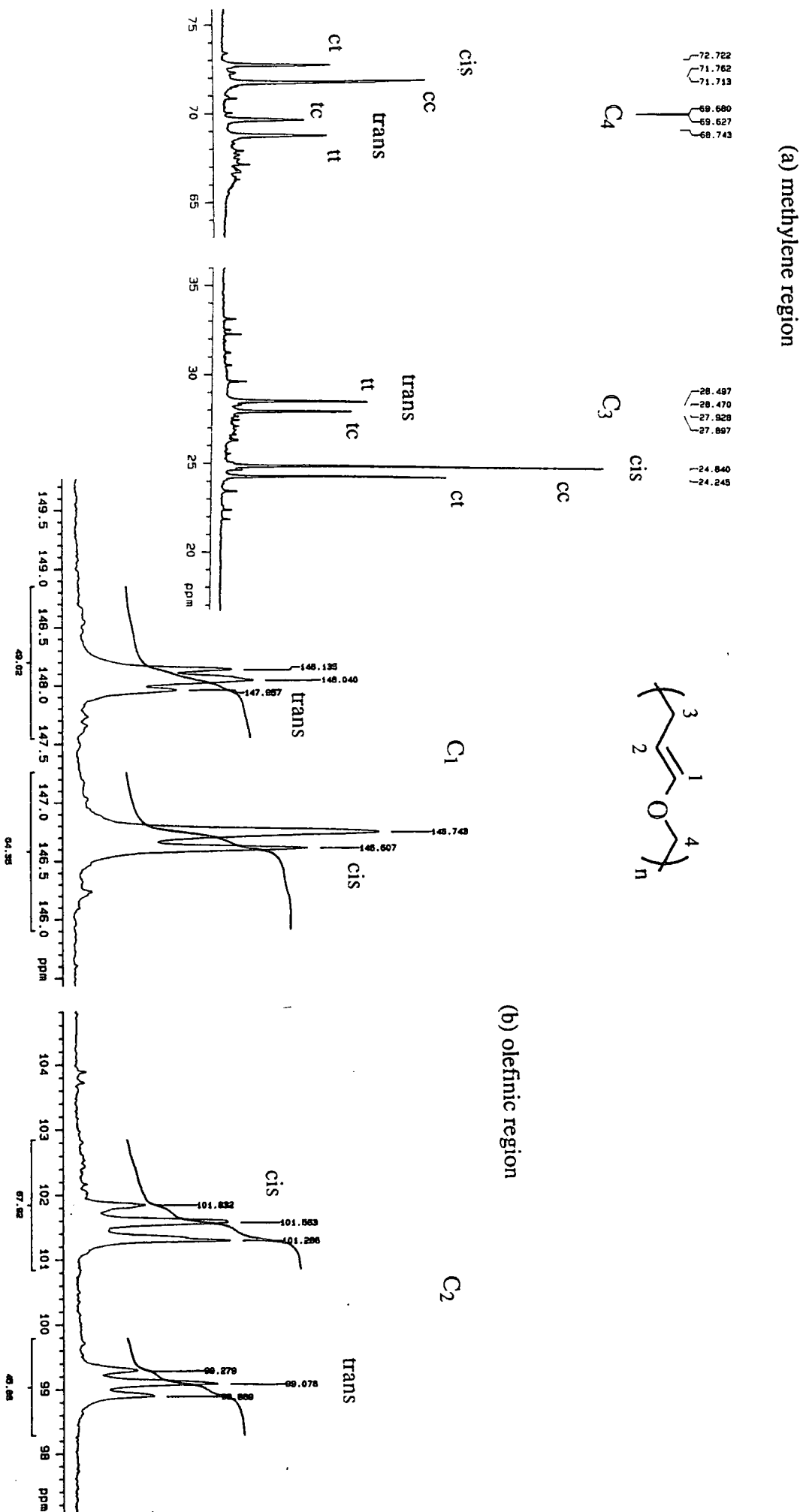
in figure 4.10(a) (where H is denoted as the oxygen end of the repeating monomer unit) . However, the monomer units insert to generate a polymer which is all HT, shown in figure 4.10(b).
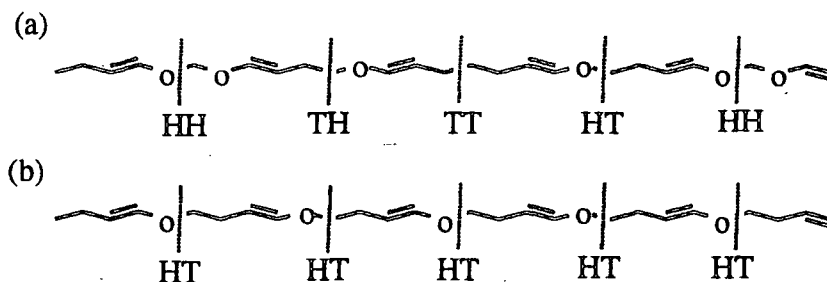
figure 4.10 *Head / tail isomerism for poly(oxy-1-butenylene)*

In order to form a HT regular polymer, the orientation of the incoming monomer with respect to the metal centre must always be the same, with the oxygen lining up as shown in figure 4.11. Initial coordination of the monomer oxygen to the metal centre could be responsible for this highly regioselective alignment followed by subsequent reorientation to bring the double bond over the plane of the metal alkylidene bond.
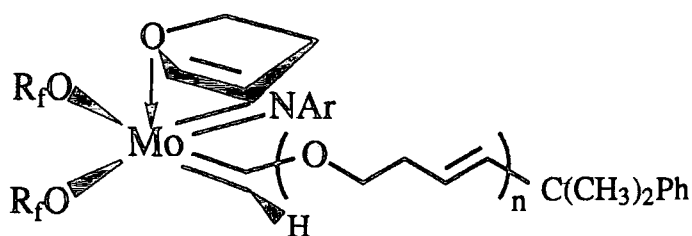
figure 4.11 *2,3 DHF orientation with respect to the initiator*

Ivin and Saegusa commented that the polymerisation of 2,3 DHF reported previously occured in an analogous manner, in this case with the oxygen lining up so as to stabilise the metallacarbene[15].

The polymers prepared from II and III show a tendency to be blocky, ie. the cis and trans vinylenes are not randomly distributed throughout the polymer backbone. The

$r_t r_c$ value (r_t = tt / tc and r_c = cc / ct) for the polymer prepared from III (63% cis) is approximately 2, calculated from the methylene carbon region. This value is indicative of blocks of adjacent cis vinylenes. For the polymer prepared from III (88% cis), $r_t r_c$ is approximately 10, showing the vinylenes to be very blocky in cis. In this polymer the tc and tt resonances are of similar intensity implying that the trans double bonds occur in pairs. This effect has been observed in polymers of cyclopentene[16] and norbornene[17,18].

4.2.6 Reaction of 2,3 dihydrofuran with $Mo(NAr)(CHBu^t)(OR_f^3)_2$ in dilute solution

When two equivalents of 2,3 DHF were mixed with $Mo(NAr)(CHBu^t)(OR_f^3)_2$ in d_8-toluene, there was no apparent change in chemical shift or peak width for either initiator or monomer. However at -78°C, the alkylidene resonance was slightly shifted at δ 11.67 from that of the free initiator (δ 11.62), but there were no corresponding changes for the monomer resonances, suggesting that appreciable adduct formation does not arise at this temperature. Furthermore, there was no evidence of any propagating alkylidene species in this experiment nor when 25 equivalents of 2,3 DHF was added to II. It would appear in both experiments that the concentration of monomer is insufficient for insertion products to be observed.

4.2.7 Comparison of the polymerisations of 2,3 and 2,5 dihydrofurans

The effects of changing the position of the double bond within the dihydrofuran ring are dramatic with diverse differences being observed in both the initial reactivity and the stereochemical outcome of the polymerisation processes.

2,5 DHF is found to polymerise slowly over several hours, which is attributed to it's strong coordination to the metal centre. In this mode the olefinic group is distant from the alkylidene moiety (see figure 4.8), and therefore decoordination would be necessary to enable the double bond to interact with the alkylidene. In contrast, initial coordination of 2,3 DHF would bring the vinylene into a favourable position for

interaction with the alkylidene, thereby rationalising the much increased rate of polymerisation observed for this species (over several minutes). This type of enhanced reactivity is similarly observed for 2,3 disubstituted 7-oxanorbornadienes[19], which are found to be much more reactive than their norbornadiene congeners. The unsubstituted C-C double bond would be expected to be electron deficient in such 7-oxanorbornadienes and hence less reactive. However, the rate enhancement is explained by initial coordination of an oxygen lone pair on the same side of the ring as the unsubstituted double bond (shown below in figure 4.12).
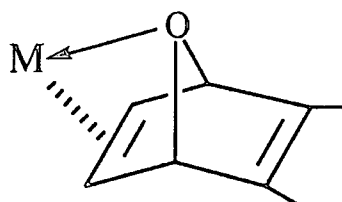
figure 4.12 *2,3 substituted 7-oxanorbornadienes*

The stereochemistry of the polymer generated from 2,5 DHF is invariant with the initiators used (I, II and III), having a high trans content (~ 93% trans), whereas for 2,3 DHF the stereochemistry of the resultant polymer is variable (63% and 88% cis, for II and III respectively) and in the opposite geometrical configuration. This difference in the stereochemical outcome for 2,3 and 2,5 DHF can be explained in terms of syn and anti rotamers of the initiator. Syn and anti rotamers have been observed in solution for Schrock initiators and are shown to interconvert, according to figure 4.13[14]:
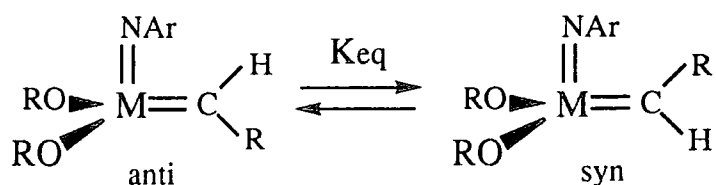
figure 4.13 *Interconversion of syn and anti rotamers*

The equilibrium constants for the interconversion of I, II and III are approximately K_{eq} ~ 10^3 (lying heavily in favour of the syn rotamer)[20]. However, the rates of

interconversion are found to vary drastically as the ancillary alkoxide ligands become more electron withdrawing, decreasing over 4 orders of magnitude in going from I to III. In studies with 2,3 bis-trifluoromethyl norbornadiene, the anti rotamer has been found to be at least two orders of magnitude more reactive than the syn, and to form (exclusively) trans vinylenes, whereas the syn rotamer forms cis double bonds. If syn / anti interconversion is fast relative to the rate of polymerisation, then the polymerisation would predominantly occur through the anti rotamer; conversely, if this rate is slow the polymerisation would occur through the syn rotamer. Figure 4.14 shows the stereochemical outcome for the ring opening polymerisation of 2,3 and 2,5 DHF through syn and anti rotamers respectively, where it can be seen that the former results in the formation of cis vinylene, whereas the latter affords a trans vinylene. The polymerisation of 2,3 DHF is relatively fast and therefore might be expected to go *via* the syn rotamer, especially in the case of the fluorinated alkoxide derivatives where the rate of syn / anti conversion is slow. This is consistent with the observed cis content on going from II (63% cis) to III (88% cis). For 2,5 DHF, the polymerisation is very slow and therefore would be predicted to go through the more active anti rotamer, to give a polymer with a high trans content (as observed, 93% trans). It is notable in this case that the polymerisation is sufficiently slow for the anti rotamer to be accessed for III (where the syn / anti interconversion rate is the slowest of the initiators employed).
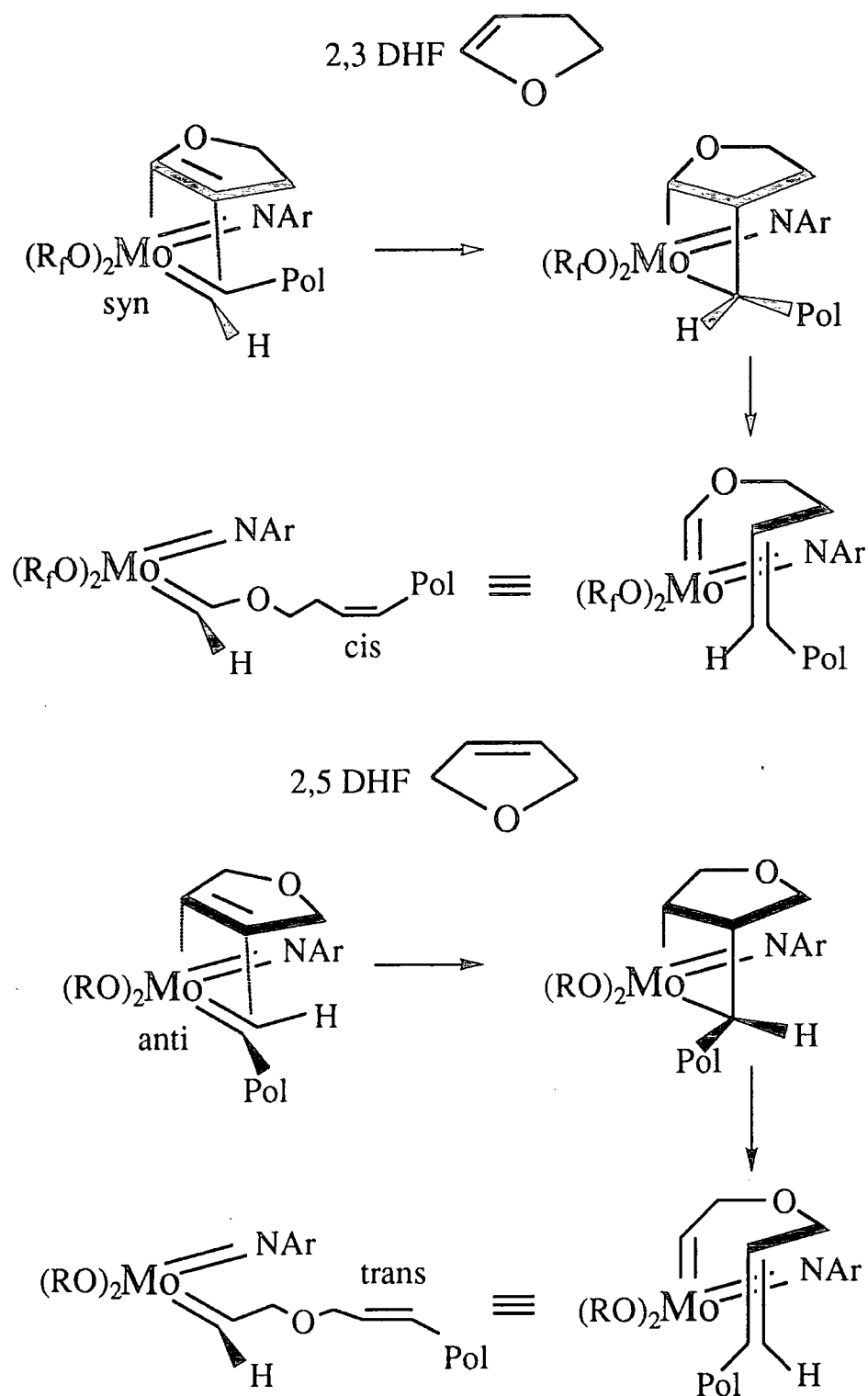
figure 4.14 *Cis / trans isomerism of 2,3 and 2,5 dihydrofurans via syn / anti rotamers*

160

4.2.8 Further reactivity studies of related oxygen heterocycles

a) Reaction of 2,5 dimethoxy dihydrofuran with $Mo(NAr)(CHCMe_2Ph)(OR)_2$

The commercially avaliable disubstituted analogue of 2,5 DHF - 2,5 dimethoxy dihydrofuran (shown in figure 4.15) was added neat (1000 equivalents) to initiators I, II and III at room temperature, where it was found that polymerisation did not occur.

figure 4.15 *2,5 dimethoxy dihydrofuran*

Polymerisation of this monomer could not be induced even at low temperature (-40°C) with these respective initiators. It can therefore be concluded that the methoxy groups are deactivating the ring to polymerisation either sterically or electronically (or both). In general, substituents have an unfavourable effect on the ΔG value of a reaction (in this case ΔG is likely to be positive under the conditions employed)[21].

b) Reaction of 3,4 dihydro-2H-pyran with $Mo(NAr)(CHCMe_2Ph)(OR)_2$

3,4 dihydro-2H-pyran (shown in figure 4.16) did not react with the initiators I, II and III at room temperature or at -65°C, with the characteristic yellow solutions of the free initiators maintained over several hours.
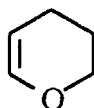
figure 4.16 *3,4 dihydro-2H-pyran*

Benzaldehyde was added to the mixtures at the latter temperature, and ^{1}H NMR spectra recorded for each sample, showing only unreacted monomer and initiator residues. The failure of 3,4 dihydro-2H-pyran to polymerise was attributed to the low strain energy associated with 6-membered rings. This is consistent with the observation that cyclopentene will polymerise whereas cyclohexene will not[21].

c) Reaction of vinylene carbonate with Mo(NAr)(CHCMe$_2$Ph)(OR)$_2$

Preparation of Mo(NAr)(CHCMe$_2$PhCH(O$_2$CO)CH)(OBu^t)$_2$ (3).

When one equivalent of vinylene carbonate (shown in figure 4.17) was added to I in d$_6$-benzene, a blood red solution was formed over 1 hour.
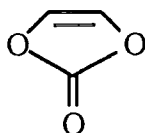
figure 4.17 *Vinylene carbonate*

The ^{1}H NMR spectrum after 15 minutes showed resonances due to a new species, as well as residual initiator and monomer signals (see figure 4.18). After 1 hour all the initiator and monomer had been consumed, and only signals due to this new species were present. Both COSY and ^{1}H - ^{13}C HETCOR NMR experiments allowed the assignment of proton and carbon resonances and were consistent with the metallacyclobutane species (3), shown with selected ^{1}H NMR data in figure 4.18.

In figure 4.18, (3) is depicted as the endo isomer (carbonate ring pointing down away from the imido ligand). However, a series of nOe experiments proved inconclusive in determining which isomer was formed (endo or exo). The stereochemistry of the metallacycle protons was deduced from the Karplus relationship of the variation in the observed J_{HH} coupling constants with the dihedral H-C-C-H angles[22]. Slow rotation around the nitrogen-aryl carbon bond was observed, signified by inequivalent diisopropyl methyl groups at δ 1.26 (d) and 1.28 (d). Related metallacycle

figure 4.18 *¹H NMR spectrum (400 MHz, C₆D₆) of the reaction of vinylene carbonate with I after 15 minutes.*

H₁ (d, 5.25 ppm, JH₁H₂ = 3.6 Hz)

H₂ (dd, 5.95 ppm, JH₂H₃ = 16 Hz, JH₂H₁ = 3.6 Hz)

H₃ (d, 6.09 ppm, JH₃H₂ = 16 Hz)
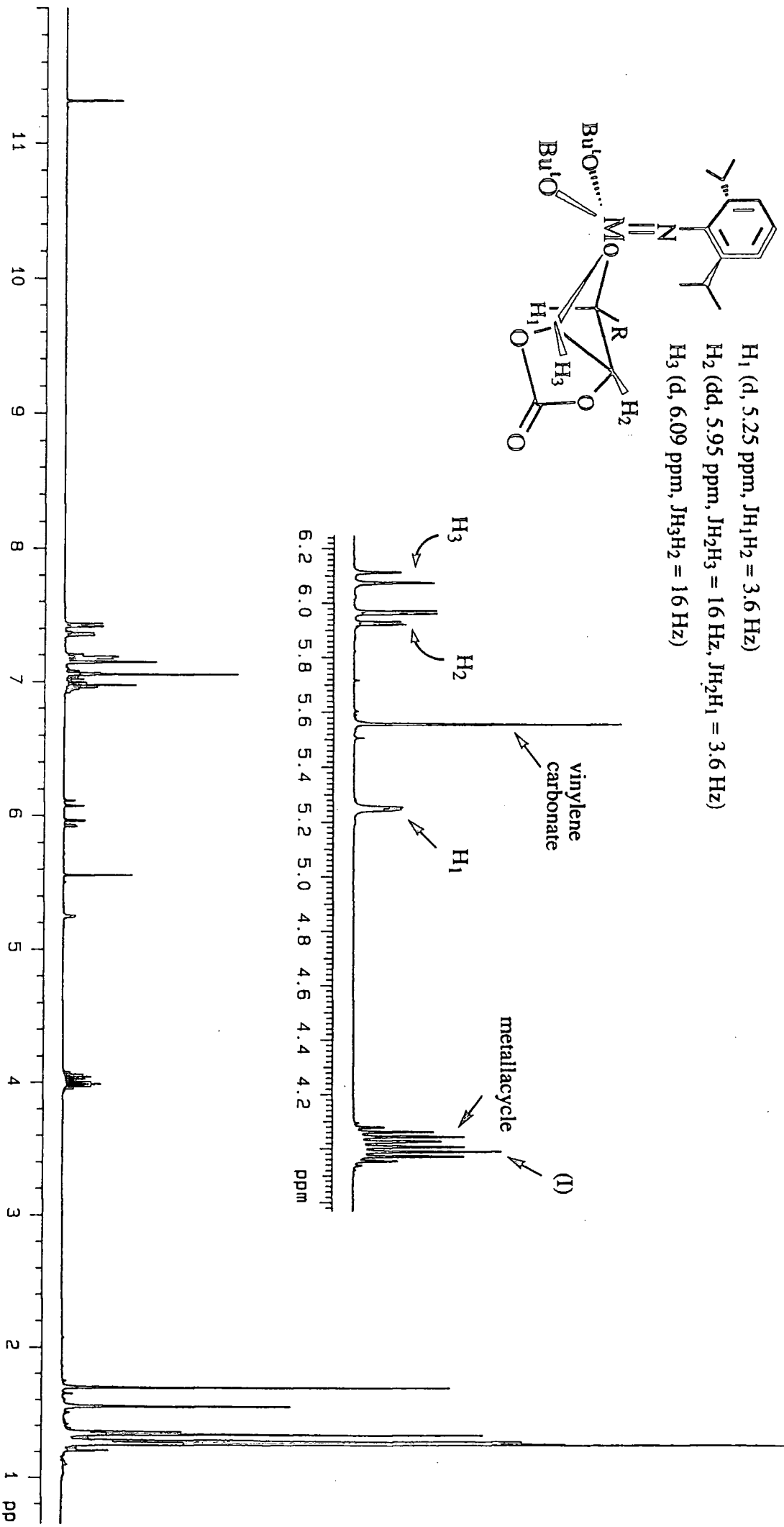
complexes which are stabilised by the coordination of oxygen to the metal centre have been observed for molybdenum[23] and tungsten[24], of which the closely related tunsten complex displays similar chemical shifts and coupling constants for the metallacycle protons. However, models of the complex suggest that the β-ether oxygen cannot approach sufficiently close to the electrophilic molybdenum centre for interaction to occur (Mo - oxygen distance ~ 3.0 Å).

The metallacycle once formed, persisted in solution; adding excess monomer (10 equivalents) to I in C_6D_6, did not result in the formation of any other products, nor did the addition of neat monomer (100 equivalents) to I. A similar metallacycle could be formed by mixing one equivalent of vinylene carbonate with II in d_6-benzene, although spectroscopic characterisation by NMR was difficult owing to the substantial fluxional behaviour of this complex at room temperature. Interestingly, no reaction was observed between vinylene carbonate and III.

Complex (3) could be isolated as a red crystalline solid when the reaction was performed on a preparative scale in n-pentane. Unfortunately, a structural determination did not prove possible since the crystals obtained were not of suitable quality for X-ray diffraction. The mass spectrum (EI, m/z, ^{98}Mo) of the complex showed an envelope centred at mass 594, attributable to the loss of CO_2 from the complex.

4.3   Reactivity of 1-amino-3-borolenes with $Mo(NAr)(CHCMe_2Ph)(OR)_2$

There have been no previous reports on the metathetical activity of heterocycles containing the boron functionality within a 5-membered ring, although the R.O.M.P of a substituted norbornene with a pendant boron functionality has been cited in the literature[25]. The synthesis of 5-membered borolenes are relatively straight forward and provide a convenient entry into this unexplored field[26,27].

4.3.1 Synthesis of 1-amino-3-borolenes

The synthesis of 1-(diisopropylamino)-3-borolene (shown in figure 4.20), has been reported by Herberich et. al[26]. This syntheric approach was used to prepare the diisopropyl species and its diphenylamino analogue (figure 4.20).

$$Ph_2NH + BCl_3 \xrightarrow{\text{(i) } CH_2Cl_2} Ph_2NH.BCl_3$$

(ii) Δ, toluene, 24 hours
-HCl

(iii) Et$_2$O

Mg .2 THF

- MgCl$_2$

Ph_2NBCl_2

B
|
NPh$_2$
(4)
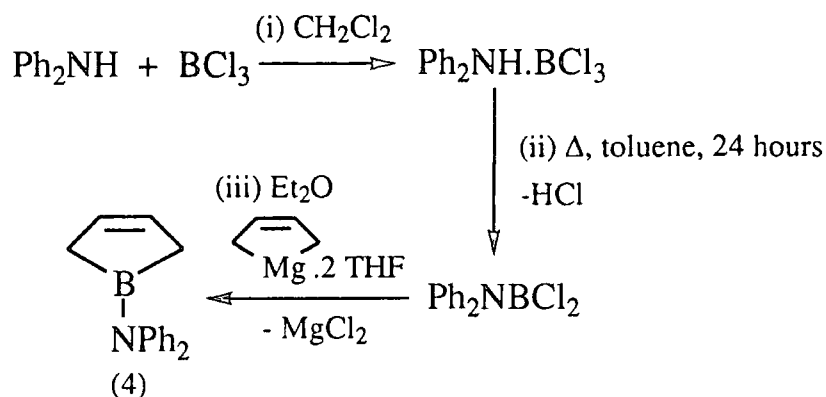
figure 4.20 *Reaction scheme for the preparation of 1-(diphenylamino)-3-borolene*

Steps (i) and (ii) afforded $Ph_2NH.BCl_3$ and Ph_2NBCl_2 respectively in high yield[28]. The reaction of Ph_2NBCl_2 with the magnesium-butadiene complex[29] in step (iii), afforded (4) after distillation (Bpt = 112-114°C at 10^{-2} mm Hg) in low yield (28%) as a colourless solid. A trace of an unidentified impurity was present (see section 4.4.3), which was removed by recrystallisation from n-pentane. Elemental analysis confirmed the stoichiometry of $BNC_{16}H_{16}$ and the parent molecular ion was observed in the mass spectrum (EI, m/z) at 233.

4.3.2 Reaction of 1-(diisopropylamino)-3-borolene with Mo(NAr)(CHCMe$_2$Ph)(OR)$_2$

1-(diisopropylamino)-3-borolene (100 equivalents) was added to the initiators I, II and III at room temperature with stirring. In each case decomposition of the free initiator occured over about 30 minutes, signified by considerable darkening of the

initial yellow solutions. Benzaldehyde was then added to cleave any active metal-alkylidene species. The ^{1}H NMR spectra of samples prepared from I and II showed resonances for unreacted monomer and initiator residues only, whereas the spectrum of the sample prepared from III revealed the presence of new low intensity signals. These resonances had an appearance reminiscent of those observed for previously synthesised 10-membered silicon rings, formed *via* intramolecular backbiting reactions of the living polymer chain (see section 1.4.4). When the initiator (III) : monomer ratio was increased to 1 : 50, the proportion of this new species was increased by a factor of 2 relative to that observed previously, indicating that the monomer is inherently destroying the initiator. Boron is very oxophilic and therefore one possible decomposition pathway would be the metathesis of the alkoxide units of the initiator with the boron-amide group.

Attempts to separate this new material from the monomer by distillation or by use of a silica column failed. Gas chromatography (G.C) showed that the monomer and the new species had close (but distinguishable) retention times. However, a G.C mass spectrum of the new species did not show any fragments of greater mass than that of the monomeric molecular ion (165).

When 10 equivalents of the monomer was added to III in C_6D_6, resonances due to the presence of this new species were found in the ^{1}H NMR, however there was no evidence for any living metal-alkylidene containing oligomers.

4.3.3 Reaction of 1-(diphenylamino)-3-borolene with Mo(NAr)(CHCMe$_2$Ph)(OR)$_2$

As a consequence of the instability of the initiator in the presence of 1-(diisopropylamino)-3-borolene, the diphenylamino derivative (4) was prepared in the hope that the decreased basicity of the amino nitrogen would prevent decomposition of the initiators. The low melting point of (3) *ca.* 60°C, enabled homogenous mixing with the initiators, as the initiators can tolerate this elevated temperature in solution for several hours. Typically, solid mixtures of the initiator (I, II or III) and monomer (70

equivalents) were warmed to 60°C, whereby on mixing, dark red solutions were formed almost immediately. After 1 hour benzaldehyde was added, and the mixtures allowed to cool to room temperature whereby solidification occured. The ^{1}H NMR spectra of samples from each of the mixtures showed that all the monomer had been consumed, and that new resonances similar to those observed in the previous section were now present exclusively. The resonances were identical to those of the impurity found in the monomer synthesis (see section 4.3.1). The mass spectrum (EI, m/z) of the solid showed the highest mass fragment to be the same as that of the monomer (233), again similar to the previous observations. Ultimately, the problem was solved by the structural determination of the product when suitable colourless crystals were isolated by sublimation (298K, < 10^{-3} mmHg). The molecular structure was solved by Professor W. Clegg of the University of Newcastle-upon-Tyne, where it was found to be the isomer - 1-(diphenylamino)-2-borolene. Figure 4.21 shows the molecular structure and table 4.3 gives selected bond lengths (Å) and angles (°); of note is the short C(3) - C(4) distance of 1.346(5)Å for the vinylene.
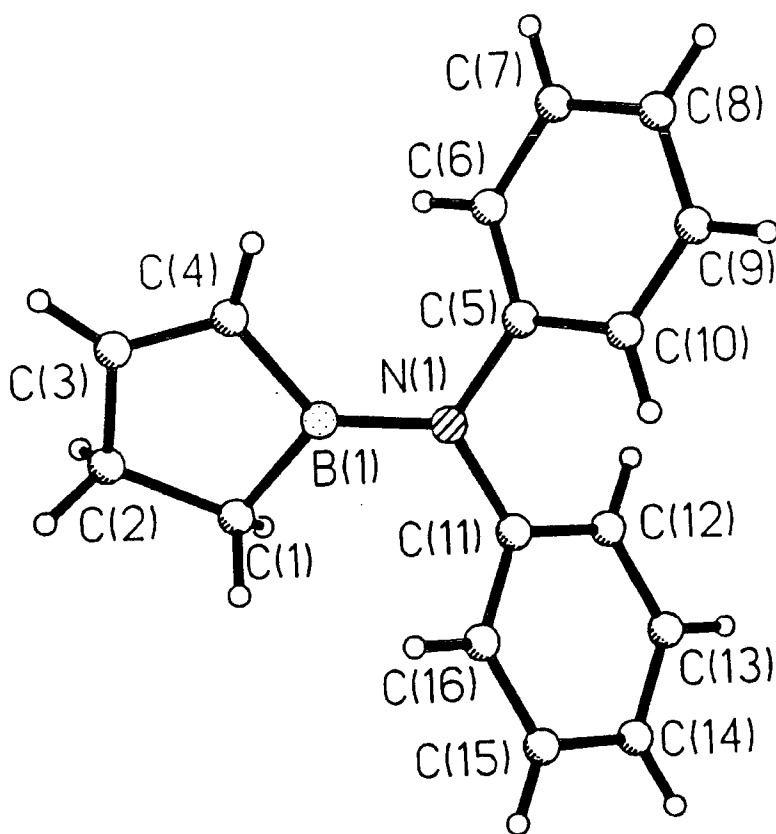
figure 4.21 *Molecular structure of 1-(diphenylamino)-2-borolene*

B (1) - N (1)	1.427 (5)	B (1) - C (4)	1.544 (6)
B (1) - C (1)	1.581 (6)	N (1) - C (11)	1.436 (5)
N (1) - C (5)	1.446 (4)	C (1) - C (2)	1.529 (5)
C(2) - C (3)	1.492 (6)	C (3) - C (4)	1.346 (5)
C (5) - C (6)	1.375 (5)	C (5) - C (10)	1.390 (5)
C (6) - C (7)	1.385 (5)	C (7) - C (8)	1.374 (6)
C (8) - C (9)	1.372 (6)	C (9) - C (10)	1.390 (5)
C (11) - C (12)	1.384 (5)	C (11) - C (16)	1.384 (5)
C (12) - C (13)	1.389 (6)	C (13) - C (14)	1.372 (6)
C (14) - C (15)	1.385 (6)	C (15) - C (16)	1.381 (5)

N (1) - C (1) - B (4)	128.3 (4)	N (1) - B (1) - C (1)	125.7 (4)
C (4) - B (1) - C (1)	106.1 (3)	B (1) - N (1) - C (11)	122.1 (3)
B (1) - N (1) - C (5)	121.6 (3)	C (11) - N (1) - C (5)	116.2 (3)
C (2) - C (1) - B (1)	104.7 (3)	C (3) - C (2) - C (1)	105.8 (3)
C (4) - C (3) - C (2)	115.2 (4)	C (3) - C (4) - B (1)	108.1 (4)
C (6) - C (5) - C (10)	119.7 (4)	C (6) - C (5) - N (1)	120.3 (4)
C (10) - C (5) - N (1)	120.0 (3)	C (5) - C (6) - C (7)	120.8 (4)
C (8) - C (7) - C (6)	119.4 (4)	C (9) - C (8) - C (7)	120.4 (4)
C (8) - C (9) - C (10)	120.6 (4)	C (5) - C (10) - C (9)	119.1 (4)
C (12) - C (11) - C (16)	119.0 (4)	C (12) - C (11) - N (1)	121.0 (3)
C (16) - C (11) - N (1)	120.0 (3)	C (11) - C (12) - C (13)	120.1 (4)
C (14) - C (13) - C (12)	120.5 (4)	C (13) - C (14) - C (15)	119.7 (4)
C (16) - C (15) - C (14)	119.8 (4)	C (15) - C (16) - C (11)	120.8 (4)

table 4.3 *Selected bond lengths (Å) and angles (°) for 1-(diphenylamino)-2-borolene*

The isomerisation of 3- to 2-borolenes has recently been reported using a classical rhodium olefin isomerisation initiator[30], as shown in equation 4.4:
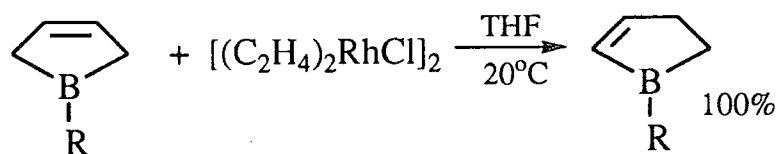
(4.4)

However, to our knowledge olefin isomerisation catalysed by metal-alkylidenes is unprecedented. The mechanism of the isomerisation process for the Schrock initiators is open to speculation, as it seems unlikely that the reaction could proceed *via* classical β-hydride elimination to generate π-allyl intermediates. The dark red colours observed for the reaction mixtures are characteristic of metallacycle species. Furthermore, the

presence of low intensity multiplets in the ^{1}H NMR (d$_6$-benzene) of samples of the crude reaction mixtures (prior to the addition of benzaldehyde) could possibly be consistent with such a species. It may therefore be possible that the isomerisation process is proceeding *via* such a species.

4.3.4 Reactivity of 1-(diphenylamino)-3-borolene with various reagents in dilute solution

The isomerisation presented in the previous section prompted a more detailed investigation of this transformation, in an attempt to identify how the process was being mediated. The initiators were found to catalyse the isomerisation of 1-(diphenylamino)-3-borolene (10 equivalents) to 1-(diphenylamino)-2-borolene in d$_6$-benzene at different rates. The percentage of 2-borolene present at a given time for each initiator is given in table 4.4, where the relative isomerisation rates are found to increase in the order, I < II < III, correlating with the increasing electrophilicity of the metal centre.

time (hours)	I	II	III
48	24	37	90
96	38	55	98
144	45	70	100
192	54	79	-
240	59	87	-

table 4.4 *% of 1-(diphenylamino)-2-borolene present with time*

In order to investigate if the isomerisation rate was entirely dependent upon the electrophilicity of the metal centre, a series of molybdenum (VI) complexes which did not possess the alkylidene moiety were employed under analogous conditions. Only one species of those tried was found to bring about the isomerisation, namely Mo(NAr)$_2$(OBu^t)$_2$, although only under forcing conditions (120 hours at 60°C for 51%

conversion). Notably, the classical isomerisation initiator - [(CO)₂RhCl]₂[31], was slower under these conditions only achieving 35% conversion over the same period. It can therefore be concluded that the presence of the alkylidene moiety is not necessarily required for the isomerisation to occur, although it is apparent that the activities displayed by the Schrock initiators are far greater than those of the other reagents tried. Of particular note was the evidence for ring-opened living oligomers in the ¹H NMR spectrum of III with ten equivalents of 1-(diphenylamino)-3-borolene, signified by a low intensity multiplet at δ 11.56. Whether these species are directly involved in the isomerisation process, or are just coincidentally formed remains uknown

4.4   Reactivity of 1-phenyl-3-pyrroline with Mo(NAr)(CHCMe₂Ph)(OR)₂

To our knowledge there are no previously reported examples of the R.O.M.P of five-membered rings containing a nitrogen functionality within the ring, although there are several examples for substituted norbornene derivatives, examples of which include lactam[32] and dicarboximide[33] functionalities.

4.4.1   Synthesis of 1-phenyl-3-pyrroline

The synthesis of 1-phenyl-3-pyrroline has been reported previously by several methods[34,35]. It is reported here starting from commercially avaliable cis 1,4 dichloro but-2-ene by reaction with dilithiated aniline, as shown in equation 4.5.

$$ \underset{Cl \qquad\quad Cl}{\diagdown\!\!=\!\!\diagup} \;+\; Li_2NPh \; \xrightarrow[50^{\circ}C]{THF} \; \underset{\substack{N \\ | \\ Ph}}{\diagdown\!\!=\!\!\diagup} \;+\; 2LiCl $$
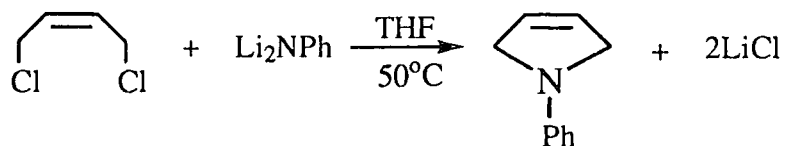
(4.5)

The above reaction proceeded slowly over 24 hours at 50°C. The product was isolated by recrystallisation from pentane in low yield (33%). Elemental analysis

confirmed the stoichiometry $NC_{10}H_{11}$, and the parent ion was observed in the mass spectrum (EI, m/z) at 145.

4.4.2 Attempted reaction of 1-phenyl-3-pyrroline with $Mo(NAr)(CHCMe_2Ph)(OR)_2$

Typically, THF (2-3 ml) was condensed onto a solid mixture of 1-phenyl-3-pyrroline (100 equivalents) and each initiator (I, II and III) at 77K. The mixtures were rapidly warmed to room temperature whereby yellow solutions (indicative of the free initiator) were formed. On cooling to -50°C for 1 hour, no apparent change in the viscosity of the mixtures was observed. After stirring overnight at ambient temperature, benzaldehyde (30 µl) was added and the solvent removed under reduced pressure shortly thereafter. The ^1H NMR (d_6-benzene) spectra of the resultant solids showed only unreacted monomer resonances.

4.5 Low temperature ^1H NMR study of heterocyclopentenes with $Mo(NAr)(CHCMe_2Ph)(OR_f{}^6)_2$

Owing to favourable polymerisation conditions at low temperature (outlined in section 1.4.4), it was decided to undertake a low temperature ^1H NMR study of 1-(diphenylamino)-3-borolene and 1-phenyl-3-pyrroline in order to possibly observe any living oligomers which may be formed. In each case 10 equivalents of monomer was mixed with III and dissolved in d_2-dichloromethane (800 µl). In addition, for comparitive purposes cyclopentene was also mixed separately with III under analogous conditions. Each sample was cooled to -70°C for 1 hour and then rapidly transferred to a NMR probe at the same temperature and the spectra acquired. For both 1-(diphenylamino)-3-borolene and 1-phenyl-3-pyrroline there was no evidence for ring-opening and formation of living oligomers. The ^1H NMR spectrum in each case revealed only unreacted monomer and free initiator resonances. However, in the experiment employing cyclopentene, the resonances for cyclopentene had almost

completely been replaced by numerous broadened signals at this temperature. Furthermore, this polymerisation was reversible; on warming to 60°C free cyclopentene and initiator were exclusively present, consistent with the observations observed reported for this monomer with W(NAr)(CHBu^t)(OBu^t)$_2$[36].

4.6   Factors affecting the ring-opening polymerisability of 5-membered hetero-cyclopentenes

An important consideration in determining whether ring-opening will occur for a given monomer is that of ring strain. In general, ring strain is small for 5-membered rings (see section 1.4.4). Cyclopentene can be successfully ring-opened utilising the Schrock initiators, although the polymerisation process is more favoured at low temperature. The relative strain of a 5-membered heterocycle (of the type shown in figure 4.22) compared to that of cyclopentene can be qualitatively assessed by a comparison of structural parameters.
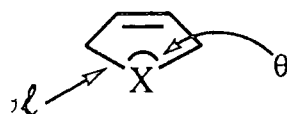
figure 4.22 *hetero cyclopent-3-ene*

For instance, ring strain will be increased by shortening X-C bond lengths (ℓ) (decreasing the covalent radius) and reducing C-X-C angles (θ). On this basis if we firstly consider 2,5 dihydrofuran (X = O), oxygen has a slightly smaller covalent radius (70 pm) than carbon (77 pm)[37]. Consequently, typical O-C bond lengths in five membered rings are shorter (1.44Å) than those of coresponding C-C bond lengths (1.54Å)[38]. Although both C-O-C and C-C-C angles in comparable systems are very similar (~ 109 - 110°), the relatively short O-C bond length would increase the ring strain in 2,5 DHF and hence provide a rationale for the increased reactivity of this monomer over cyclopentene at room temperature. The increased reactivity of 2,3 DHF over 2,5 DHF can also be explained from a strain energy viewpoint. For example,

171

calculations of the strain energy for the analogues 2,3 and 2,5 dihydrothiophene (X = S) show it to be greater in the case of the former (18 KJmol^{-1}) compared to 15.8 KJmol^{-1} for 2,5 dihydrothiophene[39].

In the case of the pyrroline ring, the covalent radius of nitrogen (74 pm)[37] is similar to that of oxygen and therefore so are the X-C bond lengths. However, a structurally related structurally characterised derivative (shown in figure 4.23) displays an almost planar ring and a large C-N-C bond angle (112.8°), presumably due to conjugation of the nitrogen lone pair with the phenyl ring[40].
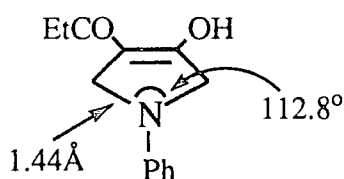
figure 4.23 *3-carboxylate-4-hydroxy-1-phenyl-3-pyrroline*

This large angle would significantly reduce the ring strain and therefore reduce the reactivity, as observed for 1-phenyl-3-pyrroline.

A closely related example of a structurally characterised 3-borolene is shown below in figure 4.24[41].
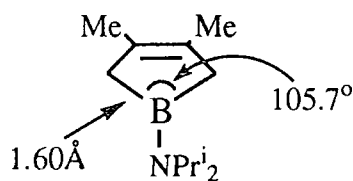
figure 4.24 *2,3 dimethyl-1-(diisopropylamino)-3-borolene*

The complex exhibits long B-C bond lengths (1.60Å) and a small C-B-C angle (105.7°). Clearly these parameters oppose one another in affecting the ring strain and therefore from a qualitative viewpoint it is difficult to assess the relative strain.

For a fuller, more quantitative analysis of evaluating the ring strain in these systems molecular modelling would be neccessary. Furthermore it should be noted that the above discussion neglects the effects of the electronic properties of the heteroatom

on the olefinic bond and also their coordinative abiltity to a metal centre, mainly because their effects are not readily assessed.

4.7   Acyclic Diene Metathesis (ADMET) studies

4.7.1   Reaction of diallyl ether with $Mo(NAr)(CHCMe_2Ph)(OR_f^6)_2$

Previously, unsaturated ethers have been metathesised using a classical initiator system - WCl_6 / $SnMe_4$, where it was observed that metathesis did not occur if there were less than two methylene spacer groups between the olefin and the ether oxygen[42]. Subsequently , diallyl ether (possessing only one methylene spacer group) was found to undergo an intramolecular cyclisation reaction, affording 2,5 dihydrofuran quantitatively, utilising a rhenium based classical initiator[43], shown in equation 4.6:

$$(4.6)$$
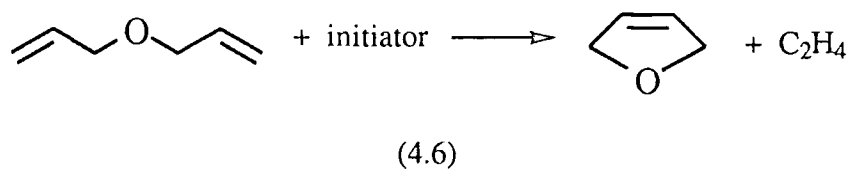
More recently, diallyl ether was shown to be mostly inactive with the well-defined tungsten Schrock initiator, $W(NAr)(CHBu^t)(OR_f^6)_2$, although the presence of several unidentified side products was noted in the ^1H and ^{13}C NMR spectra[44]. It was decided to probe the activity of diallyl ether with the molybdenum Schrock initiator $Mo(NAr)(CHMe_2Ph)(OR_f^6)_2$ (III), owing to the greater tolerance of functionality displayed by this initiator compared with its tunsten analogue[2,3].

The rapid evolution of a volatile species was observed when a mixture of diallyl ether (1000 equivalents) and III was warmed from 77K to room temperature under static vacuum. A sample of the volatile was collected and shown to be ethene by G.C mass spectrometry. Periodically, the mixture was cooled to 77K and the excess ethene removed *in vacuo* , whereby on warming to room temperature the reaction was found to

proceed with renewed vigour, until after 30 minutes ethylene visibly ceased to be evolved. The volatile components were removed by vacuum transfer, leaving a small quantity of oily dark residue behind. A ^{1}H NMR spectrum of the volatile fraction revealed the presence of an almost 1:1 mixture of 2,5 DHF and unreacted diallyl ether, whereas the ^{1}H NMR spectrum of the involatile residue showed resonances similar in lineshape to those of the previously synthesised poly(oxy-2-butenylene), see section 4.2.2. Analysis of this involatile fraction by G.P.C showed it to be a mixture of low molecular weight oligomers ($M_n \sim 300$), ranging from about 3 - 10 monomer units.

$$1000 \quad \diagup\!\!\diagup\!\!\diagdown\!\!\diagdown\!\!O\!\!\diagdown\!\!\diagdown\!\!\diagup \quad + \; III \quad \underset{\xleftarrow{}}{\overset{-\,C_2H_4}{\xrightarrow{}}} \quad \langle\!\!\_\!\!O\!\!\_\!\!\rangle \quad + \quad \left(\!\!\diagdown\!\!\diagup\!\!\diagdown\!\!\diagdown\!\!O\!\!\diagup\!\!\right)_n$$

Final %
composition   45%   48%   7%

(4.7)

Interestingly, the average cis/trans content of the oligomers was found to be in the range 90 - 95% trans, almost the same as that found for poly(oxy-2-butenylene) prepared *via* the R.O.M.P of 2,5 DHF (see section 4.2.2).

4.7.2   Reaction of diallyl ether with Mo(NAr)(CHCMe$_2$Ph)(OR$_f^6$)$_2$ in dilute solution

An attempt was made to find evidence for possible propagating alkylidene species by mixing diallyl ether (0.8 equivalents) with III in d$_6$-benzene at room temperature. The ^{1}H NMR spectrum after 5 minutes showed the alkylidene resonance for the free initiatior to have almost completely disappeared, however, no other new resonances were found in the low field region of the spectrum. 3-methyl-3-phenyl but-1-ene was observed, as were new resonances for the methine and methyl protons of the arylimido substituent of the initiator at δ 3.60 (sept) and 1.12 (d). Two further successive additions of 5 and 10 equivalents of diallyl ether resulted in the appearance of substantially broadened resonances for 2,5 DHF, and the evolution of ethene. The

presence of multiplet resonances throughout the additions at δ 2.70 and 2.23 were thought to possibly be consistent with α– and β-metallacycle protons[45]. When the reaction was repeated with 45 equivalents of diallyl ether with III in d_6-benzene, essentially 100% conversion to 2,5 DHF was observed. On a preparative scale (1300 equivalents of diallyl ether) in pentane, approximately 40% conversion to 2,5 DHF occured and a trace of oligomers was noted in the ^{1}H NMR spectrum. Figure 4.25 shows a postulated mechanism for the overall process.
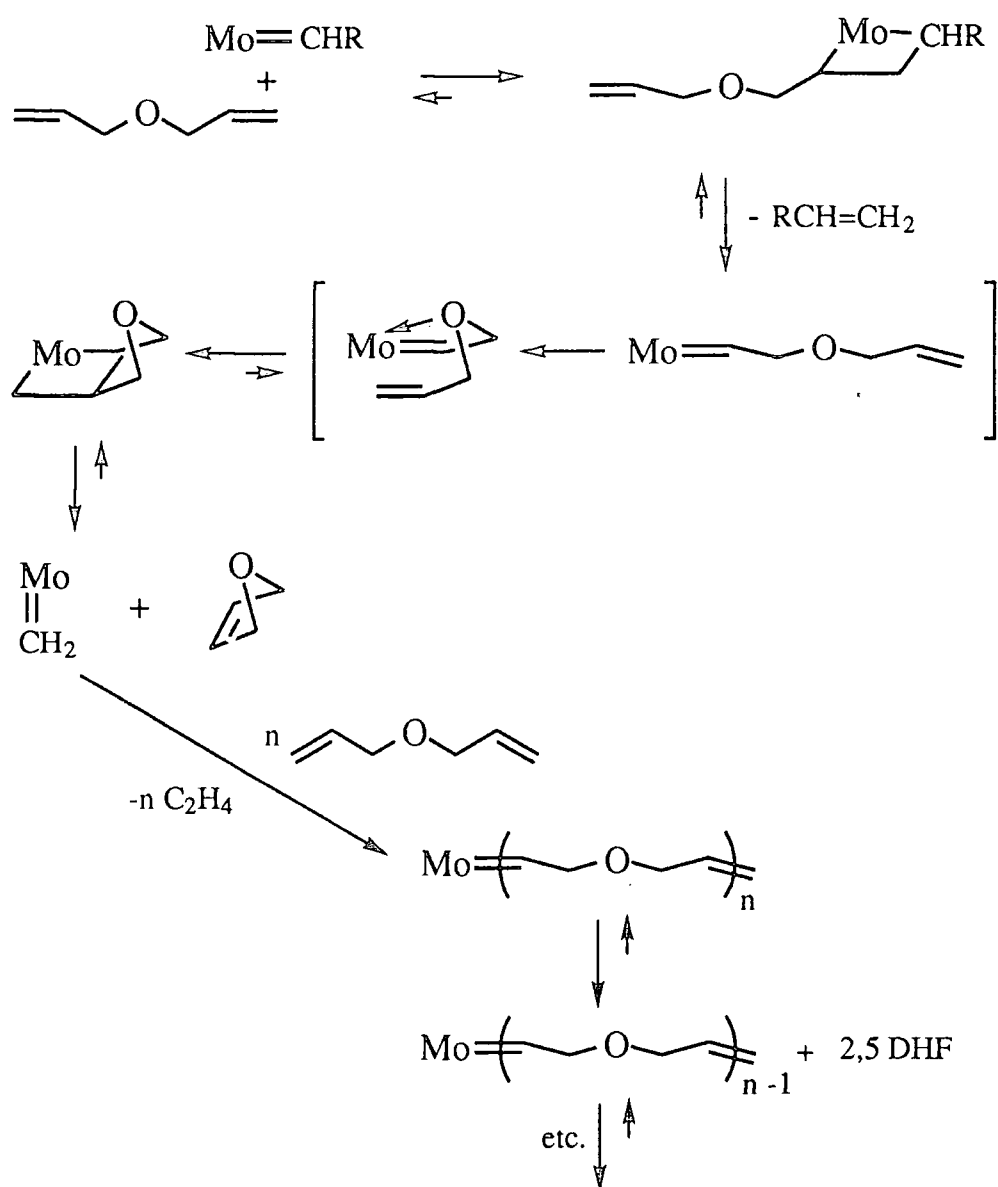
figure 4.25 *Mechanism for the reaction of diallyl ether with III*

It seems likely that coordination of the ether oxygen to the metal centre is occurring since similar types of interactions have been observed previously[23,24], and also that this coordination may assist in the favoured formation of the 5-membered ring, as shown in figure 4.25. This is further substantiated by the recent observation that α, ω-diene ether species readily undergo catalytic ring closure forming 5, 6 and 7-membered unsaturated oxygen heterocycles, when III is employed as the initiator[46]. Oligomer formation is slightly more favoured when diallyl ether is added neat to III, although overall the backbiting intramolecular cyclisation reaction appeares to be preferred in both situations. The fact that the polymeric product is more favoured when starting from 2,5 DHF could reflect the more efficient chain addition polymerisation of R.O.M.P, as opposed to the step condensation mechanism of ADMET.

4.7.3   Reaction of diallyl phenyl phosphine with Mo(NAr)(CHCMe₂Ph)(ORf⁶)₂

Diallyl phenyl phosphine (100 equivalents) was added neat to III, and a dynamic vacuum applied. Although an orange/red solution was formed initially which persisted for several hours, there was no visible evidence for evolution of ethene. A ^1H NMR spectrum after 24 hours showed only unreacted monomer to be present. However, when diallyl phenyl phosphine (10 equivalents) was added to III in d_6-benzene, the ^1H NMR spectrum showed both ethene and 3-methyl-3-phenyl but-1-ene to be evolved and new resonances which were consistent with those of 2,5 dihydro-1-phenyl-phospholene[47], shown in figure 4.26:
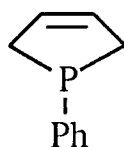
figure 4.26 *2,5 dihydrophenyl phospholene*

In the alkylidene region of the spectrum there were new resonances at δ 13.26 (t), 12.96 (m), 12.70 (d), 12.28 (q), however, no resonances for free initiator were present. No

further reaction of the significant amount of remaining monomer was observed over a period of several days. It seems likely that the phosphorous could bind strongly to the metal centre of III[48], thus preventing the high yield formation of oligomers/cyclic products.

4.7.4 Further attempted reactions of functionalised diallyl species with $Mo(NAr)(CHCMe_2Ph)OR_f^6)_2$

a) Reaction of diallyl amine with $Mo(NAr)(CHCMe_2Ph)(OR_f^6)_2$

When diallyl amine (1 equivalent) was mixed with III in d_6-benzene, new signals were observed in the alkylidene region of the ^{1}H NMR spectrum at δ 12.96 (d) and 12.11 (d), and both ethene and 3-methyl-3-phenyl but-1-ene evolved. However, there were many other low intensity signals present and therefore the identification of new species was not possible. Unfortunately, no new species were observed when the reaction was repeated on a larger scale (10 equivalents). Neat addition of diallylamine (100 equivalents) to III did not result in the observation of new products. Interestingly, the small scale intramolecular cyclisation of N-substituted diallyamine species to yield pyrroline derivatives has been reported recently[49].

b) Reaction of diallyl carbonate with $Mo(NAr)(CHCMe_2Ph)(OR_f^6)_2$

No reaction was observed when diallyl carbonate (1 and 10 equivalents) was added to III in d_6-benzene. Similarly, the neat monomer (100 equivalents) was found to be inactive towards III. This observation has also been reported by Wagener[50].

The number of methylene spacers between the functional group and the terminal olefin has been shown to be of significant importance in determining whether ADMET polymerisation will occur[3,10,14]. In most cases 3 methylene spacers are required in order for substantial polymerisation to occur. The nature of this effect is either due to coordination of the functional group to the metal centre, or an unfavourable polarisation of the double bond. The diallyl species in this study possess only one methylene spacer and therefore in the light of this relatively new evidence it is not

suprising that polymerisation is not observed. However, coordination of the functionality to the metal centre would account for the formation of the unsaturated heterocycles observed.

4.8   Summary

The activity of functionalised cyclopentenes has been explored with the well-defined molybdenum Schrock initiators. Of the various systems tried, 2,3 and 2,5 dihydrofurans proved to be successful to ring opening polymerisation, probably owing to favourable electronic and steric factors. However, substituted 3-borolenes and 3-pyrrolines were found to be inactive to ring opening; the former undergoing an unusual alkene isomerisation reaction. In the investigation of functionalised diallyl species in attempted ADMET reactions with the Schrock initiator $Mo(NAr)(CHCMe_2Ph)(ORf^6)_2$, diallyl ether was found to undergo a catalytic ring closure reaction. Diallyl phenyl phosphine was also found to undergo ring closure, although only on a limited scale.

4.9   References

1. R.R.Schrock, G.C.Bazan, M.Dimare, J.S.Murdzek, M.O'Regan, *J. Am. Chem. Soc.* 1990, **112**, 3875.

2. R.R.Schrock, J.S.Murdzek, *Macromolecules.* 1987, **20**, 2640.

3. R.R.Schrock, W.J.Feast, V.C.Gibson, G.Bazan, E.Khosravi, *Polymer. Commun.* 1990, **30**, 258.

4. R.R.Schrock, J.S.Murdzek, *Organometallics.* 1987, **6**, 1373.

5. H.Lammens, G.Sartori, J.Siffert, N.Sprechner, *J. Polymer. Sci., Polymer lett.* 1971, **9**, 341.

6. V.C.Gibson, S.P.Collingwood, J.T.Anhaus, W.Clegg, *Organometallics.* 1993, **12**, 1780.

7. H.Höcker, T.Bastelberger, C.T.Thu, *Makromol. Chem. Rapid.* 1991, **2**, 383.

8. K.B.Wagener, K.Brzezinska, *Macromolecules.* 1991, **24**, 5273.

9. N.Calderon, K.W.Scott, *Chem. Abstr.* 1981, **95**, 8034.

10. W.J.Feast, V.C.Gibson, G.C.Bazan, E.Khosravi, *Polymer. Commun.* 1989, **30**, 258.

11. R.R.Schrock, W.J.Feast, V.C.Gibson, G.C.Bazan, E.Khosravi, J.Thomas, M.O'Reagan, *J. Am. Chem. Soc.* 1990, **112**, 8378.

12. W.J.Feast, V.C.Gibson, E.L.Marshall, *J. Chem. Soc. Chem. Commun.* 1992, 1157.

13. K.B.Wagener, K.Brzezinska, *Macromol. Chem. Rapid. Commun.* 1992, **13**, 75.

14. R.R.Schrock, J.Oskam, *J. Am. Chem. Soc.* 1992, **114**, 7588.

15. K.J.Ivin, T.Saeguso, *"Ring Opening Polymerisation"*, VolumeI, Elsevier Applied Science, London and New York, 1984.

16. E.Ceausescu, A.Cornilescu, E.Nicolescu, M.Popescu, S.Coca, M.Cuzmici, C.Oprescu, M.Dimonie, G.Hubsca, M.Teodorescu, R.Orosescu, A.Vasilesu, V.Dragutan, *J. Mol. Catal.* 1986, **36**, 163.

17. K.J.Ivin, D.T.Leverty, J.H.O'Donnell, J.J.Rooney, C.D.Stewart, *Makromol. Chem.* 1979, **180**, 1989.

18. K.J.Ivin, J.G.Hamilton, R.M.E.Greene, J.J.Rooney, *Makromol. Chem.* 1986, 187, 619.

19. R.R.Schrock, G.C.Bazan, J.H.Oskam, H.N.Cho, L.Y.Park, *J. Am. Chem. Soc.* 1991, 113, 6899.

20. R.R.Schrock, G.C.Bazan, W.E.Crowe, M.Dimare, M.O'Regan, M.H.Schofield, *Organometallics,* 1991, 10, 1832.

21. K.J.Ivin, *"Olefin Metathesis"*, Academic press, London, 1983.

22. M.Karplus, *J. Chem. Phys.* 1959, 30, 11.

23. R.R.Schrock, H.H.Fox, J.K.Lee, L.Y.Park, *Organometallics.* 1993, 12, 759.

24. R.R.Schrock, W.M.Davis, J.Feldman, J.S.Murdzek, *Organometallics.* 1989, 8, 2260.

25. T.C.Chung, S.Ramakrishnan, M.W.Kim, *Macromolecules.* 1991, 24, 2675.

26. G.E.Herberich, B.Hessner, D.Söhnen, *J. Organomet. Chem.* 1976, 223, 201.

27. G.E.Herberich, B.Hessner, D.Söhnen, *J. Organomet. Chem.* 1983, 256, C23.

28. W.Gerrard, H.R.Hudson, E.F.Mooney, *J. Chem. Soc.* 1960, 5168.

29. K.Fujita, Y.Ohnuna, H.Yasuda, H.Tani, *J. Organomet. Chem.* 1983, 256, C23.

30. G.E.Herberich, W.Boveleth, B.Hessner, M.Hostalek, D.P.J.Köffer, H.Ohst, D.Söhnen, *Chem. Ber.* 1986, 119, 420.

31. R.Cramer, *Inorg. Synth.* 1974, 15, 14.

32. H-N.Cho, S-K.Choi, *J. Polymer. Sci.* 1985, 23, 1469.

33. R.R.Schrock, V.C.Gibson, G.C.Bazan, H.-N.Cho, *Macromolecules,* 1991, 24, 4495.

34. A.Arbuzov, L.Docklady, *Akad. Nauk. SSSR.* 1948, 63, 531.

35. Z.Ding, J.J.Tufariello, *Synth. Commun.* 1990, 20, 227.

36. R.R.Schrock, K.B.Yap, D.C.Yang, H.Sitzman, L.R.Sita, G.C.Bazan, *Macromolecules.* 1989, 22, 3191.

37. K.F.Purcell, J.C.Kotz, *"Inorganic Chemistry"*, W.B.Saunders and Co., London, Toronto and Philadelphia, 1977.

38. F.H.Allen, O.Kennard, D.G.Watson, L.Brammer, A.G-Orpen, R.Taylor, *J. Chem. Soc. Perkin Trans II,* 1987, S1.

39. A.R.Katrisky, C.W.Rees, *"Comprehensive Heterocyclic Chemistry"*, Vol. IV, Pergamon Press, 1987.

40. E.F.Paulus, E.Rivo, *Acta. Cryst.* 1988, **44**, 1242.

41. A.Mellor, D.Bromm, D.Stalke, A.Heine, G.M.Sheldrick, *J. Organomet. Chem.* 1990, **386**, 1.

42. W.Ast, G.Rheinwald, R.Kerber, *Rec. Trav. Chim. Pays-bas.* 1977, **96**, M127-130.

43. E.I.Bogolepova, R.A.Fridman, A.N.Bashrikov, *A.N.Izv. Akad. Nauk. SSSR, Ser kim.* 1978, **27**, 2429.

44. K.B.Wagener, K.Brzezinska, *Macromolecules.* 1991, **24**, 5273.

45. R.R.Schrock, W.M.Davis, J.Feldman, J.S.Murdzek, *Organometallics.* 1989, **8**, 2266.

46. R.H.Grubbs, G.C.Fu, *J. Am. Chem. Soc.* 1992, **114**, 5426.

47. G.Märkl, R.Potthast. *Tetrahedron. lett.* 1968, **24**, 1755.

48. G.C.Bazan, Ph.D Thesis, Massachussetts Institute of Technology. 1990.

49. R.H.Grubbs, G.C.Fu, *J. Am. Chem. Soc.* 1992, **114**, 7324.

50. K.B.Wagener, *Abs. Papers. Am. Chem. Soc.* 1992, **203**, 47.

Chapter Five

Experimental details.

5.1 General

5.1.1 Experimental Techniques

All manipulations of air and / or moisture sensitive mareials were performed on a conventional vacuum / inert atmosphere (nitrogen) line using standard Schlenk and canular techniques, or in an inert atmosphere (nitrogen) filled glove box.

Elemental analyses were performed by the microanalytical services of this department.

Infrared spectra were recorded on Perkin-Elmer 577 and 457 grating spectrophotometers using CsI windows. Absorbtions abbreviated as: vs (very strong), s (strong), m (medium), w (weak), br (broad), sh (sharp).

Mass spectra were recorded on a VG7070E Organic Mass Spectrometer,

NMR spectra were recorded on the following instruments, at the frequencies listed unless stated otherwise: Brucker AMX 500, ^1H (500.14 MHz), ^{13}C (125.77 MHz), ^{11}B (160.46 MHz); Varian VXR 400, ^1H (399.95 MHz), ^{19}F (376.29 MHz), ^{13}C (100.58 MHz); Brucker AC 250, ^1H (250.13 MHz); Varian Gemini 200, ^1H (199.98 MHz), ^{13}C (50.29 MHz); Varian XL 200, ^1H (199.98 MHz). The following abbreviations have been used for band multiplicities: s (singlet), d (doublet), t (triplet), q (quadruplet), sept (septet), m (multiplet). Chemical shifts are quoted as δ in ppm with respect to the following references, unless stated otherwise: ^1H (d_6-benzene, 7.15 ppm, d_8 - toluene, 6.98 ppm, d-chloroform, 7.26 ppm,), ^{13}C (d_6-benzene, 128.0 ppm, d_8-toluene, 125.2 ppm, d-chloroform 77.0 ppm).

GPC traces was recorded on a Viscotek differential refractometer fitted with a knauer HPLC pump 64 and two PLgel 10 μl mixed columns (THF, flow rate 1 ml / minute). Samples (0.1 - 0.3 % w/v ere filtered through a a Millex SR 0.5 mm filter before injection in order to remove particulates. The columns were calibrated using commercially avaliable polystyrene standards (Polymer laboratories Ltd.) ranging from 1206 to 1.03×10^6MW.

5.1.2 Solvents and Reagents

The following NMR solvents were dried by vacuum distillation from a suitable drying agent (in parentheses) and stored under nitrogen or vacuum prior to use: d_6-benzene (phosphorus (V) oxide), d_8-toluene (phosphorous (V) oxide), d-chloroform (phosphorus (V) oxide).

The following solvents were dried by prolonged heating over a suitable drying agent, being freshly distilled and deoxygenated prior to use (drying agent in parentheses): toluene (sodium metal), petroleum ether (40-60°C) (lithium aluminium hydride), n-pentane (lithium aluminium hydride) heptane (sodium metal), teterahydrofuran (sodium benzophenone ketyl), acetonitrile (calcium hydride), dichloromethane (calcium hydride), diethyl ether (lithium aluminium hydride) and dimethoxy ethane (mono-glyme) (potassium metal).

The following chemicals were prepared by previously published procedures or modifications thereof:

$LiOR^1$ (R = Bu^t, Pr^i, CMe_2CF_3, $CMe(CF_3)_2$), $LiNR^1R^2$ (R^1 = Bu^t, 2,6-$Pr^i_2C_6H_3$, R^2 = H; R^1 = R^2 = Et, Pr^i)[2], $CpNbCl_4$[3], $CpNb(NBu^t)Cl_2$[4], $CpNb(NAr)Cl_2$[4], $CpNb(NMe)Cl_2$[4], $CpNb(NBu^t)(NHBu^t)Cl$[5], $CpNb(NBu^t)(OBu^t)_2$[5], $Mo(NBu^t)_2Cl_2$[6], $Mo(NAr)_2(OBu^t)_2$[7,8], $CpMo(NBu^t)_2Cl$[9], $Mo(NR)_2Cl_2$.dme (R = Bu^t, 2,6-$Pr^i_2C_6H_3$)[10,11], $Mo(O)_2Cl_2$[2], $Mo(CHCMe_2Ph)(NAr)(OR)_2$[2] (R = CMe_3, CMe_2CF_3, $CMe(CF_3)_2$), $NHBu^t(SiMe_3)$[2], $Mg(-CH_2(CH)_2CH_2-).2THF$[12].

The following chemicals were obtained commercially and used as received unless stated otherwise: niobium pentachloride (Aldrich), molybdenum dioxide (Strem), sodium molybdate (anhydrous, Aldrich), chlorotrimethylsilane (Aldrich), tert-butanol (Aldrich, dried and stored over 4Å molecular seives), isopropanol (Aldrich, dried and stored over 4Å molecular seives), 2-trifluoromethyl-2-propanol (Fluorochem, distilled before use), 2,2 bis (trifluoromethyl)-2-propanol (Fluorochem, distilled before use), tert-butlyamine, diphenylamine, 2,6-diisopropylamine, aniline, triethylamine, diethylamine, diisopropylamine (all amines dried and distilled before use), pyrrole (Aldrich),

pentafluoroaniline (Fluorochem), 2,6-dichloroaniline (Aldrich, dried and distilled before use), n-butyl lithium (Aldrich, 1.6M in hexanes), boron trichloride (1.0M in heptane), azobenzene (Aldrich, sublimed before use), RNCO (Aldrich, distilled before use, R = Bu^t, Ph, 2,6-$Pr^i_2C_6H_3$), bis-(trimethylsilyl)lcarbodiimide (Aldrich), 2,5 and 2,3 dihydrofurans (dried and distilled before use), diallyl- (amine, carbonate, phenylphosphine, and ether) (dried and distilled before use), 1,4 dichloro-cis-but-2-ene (Aldrich, distilled before use).

5.1.3   Typical procedure for NMR reactions - Determination of rate constants

Typically, one equivalent of a reagent (38 μmols) is dissolved in d_6-benzene (400 μl) (unless otherwise stated) and mixed with a solution of the appropriate quantity of the other reagent in d_6-benzene (400 μl) at 298K. The resulting mixture is then transferred rapidly to an NMR tube, frozen immediately and sealed under nitrogen. The progress of the reactions at the various temperatures and times detailed in the text, are monitored exclusively by ^1H NMR spectroscopy. Spectra are aquired at appropriate time intervals (dependent upon the particular reaction examined), and a number of suitable signals chosen for integration . For the determination of rate constants each spectrum is normalised (for comparative purposes) by either integration of the solvent reference signal (d_6-benzene, 7.15 ppm), or integration of the total intensity of resonances present. The data is treated according to the appropriate rate law[13], and the errors in the rate constants calculated by standard linear regression[14]. Each experiment is repeated at least three times to check that the rate constants determined are consistent within calculated errors.

5.2 Experimental Details to Chapter 2

5.2.1 Reaction of Mo(NBu^t)$_2$Cl$_2$ with LiOBu^t

Preparation of Mo(NBu^t)$_2$(OBu^t)$_2$ (1).

To a mixture of Mo(NBu^t)$_2$Cl$_2$ (1.00g, 3.235 mmols) and LiOBu^t (0.521g, 6.51 mmols) was added chilled Et$_2$O (100 ml) at -78°C, and the resulting mixture allowed to reach room temperature and stirred for 2 hours, whereby a pale precipitate and a lime green solution had formed. Subsequent filtration and removal of the solvent under reduced pressure afforded a non-viscous oil, which could be induced to crystallise on cooling (Mpt = 25 - 27°C), affording a lime green crystalline solid in high yield (85% yield).

^{1}H NMR data (400 MHz, d$_6$-benzene, 298K): 1.38 (s, 18H, NC*Me$_3$* / OC*Me$_3$*), 1.36 (s, 18H, NC*Me$_3$* / OC*Me$_3$*).

^{13}C NMR data (100 MHz, d$_6$-benzene, 298K): 77.18 (s, OCMe$_3$), 67.94 (s, NCMe$_3$), 32.44 (q, NC*Me$_3$* / OC*Me$_3$*, J$_{CH}$ = 126.6 Hz), 32.16 (q, NC*Me$_3$* / OC*Me$_3$*, J$_{CH}$ = 125.5 Hz).

Infrared data (Neat, CsI, cm^{-1}): 2970 (s), 2925 (s, sh), 2900 (m, sh), 2880 (m, sh), 1545 (w, br), 1390 (m, sh), 1360 (s, sh), 1260 (s, sh), 1215 (s, br), 1180 (s, br), 1130 (m, sh), 1025 (w, sh), 960 (s, br), 910 (w), 805 (m, sh), 785 (m, sh), 585 (s, br), 470 (w), 380 (w, br), 270 (w).

Elemental Analysis for MoC$_{16}$N$_2$O$_2$H$_{36}$ (384.41) Found (Required): %C, 50.21 (50.00); %H, 9.52 (9.44); %N, 7.44 (7.29).

Mass spectral data (CI, m/z, ^{98}Mo): 387 [M + H]$^+$, 369 [M - Me]$^+$, 331 [M - C$_4$H$_8$], 74 [H$_3$NBu^t, H$_2$OBu^t]$^+$, 58 [Bu^{t}H]$^+$.

5.2.2 ^{1}H NMR investigation of imido exchange in Mo(NBu^t)$_2$(OBu^t)$_2$

The reactivity of the imido moiety in Mo(NBu^t)$_2$(OBu^t)$_2$ with various substrates was undertaken, and the characterising data for any new species observed presented herein.

NMR characterising data for:

(a) Mo(N-2,6-Pr$^i_2$C$_6$H$_3$)(NBu^t)(OBu^t)$_2$:

^{1}H NMR data (200 MHz, d$_6$-benzene, 298K): 7.11 (d, 2H, H$_m$ (Ar), J$_{HH}$ = 7.6 Hz), 6.98 (t, H$_p$ (Ar), J$_{HH}$ = 7.6 Hz), 3.73 (sept, 2H, C*H*Me$_2$, J$_{HH}$ = 7.6 Hz), 1.40 (s, 18H, OC*Me$_3$*), 1.33 (d, 12H, CH*Me$_2$*, J$_{HH}$ = 7.6 Hz), 1.20 (s, 9H, NC*Me$_3$*).

(b) Mo(N-2,6-Cl$_2$C$_6$H$_3$)(NBu^t)(OBu^t)$_2$:

^{1}H NMR data (200 MHz, d$_6$-benzene, 298K): 6.99 (d, 2H, H$_m$ (Ar), J$_{HH}$ = 8.0 Hz), 6.20 (t, H$_p$ (Ar), J$_{HH}$ = 8.0 Hz), 1.41 (s, 18H, OC*Me$_3$*), 1.25 (s, 9H, NC*Me$_3$*).

(c) Mo(N-C$_6$F$_5$)(NBu^t)(OBu^t)$_2$:

^{1}H NMR data (200 MHz, d$_6$-benzene, 298K): 1.34 (s, 18H, OCMe$_3$), 1.17 (s, 9H, NC*Me$_3$*).

(d) Mo(O)(NBu^t)(OBu^t)$_2$:

1H NMR data (200 MHz, d$_6$-benzene, 298K): 1.38 (s, 9H, NCMe$_3$), 1.25 (s, 18H, OCMe$_3$).

The reactivity to dry oxygen was undertaken by sealing the NMR tube under one atmosphere of cylinder dioxygen.

5.2.3 Reaction of Mo(NBu^t)$_2$(OBu^t)$_2$ with Mo(NAr)$_2$(OBu^t)$_2$

Preparation of Mo(NBu^t)(NAr)(OBu^t)$_2$

Heptane (100 ml, 298K) was added to a solid mixture of Mo(NBu^t)$_2$(OBu^t)$_2$ (1.01g, 2.63 mmol) and Mo(NAr)$_2$(OBu^t)$_2$ (1.56g, 2.63 mmol), and the mixture warmed to 60°C for 7 days. The attempted recrystallisation of the product at low temperature (-78°C) from the mother liquor failed, however, the pure product was isolated from n-pentane (20 ml) on cooling *ca.* -20°C, as a yellow-orange solid in low yield, 0.40g (15%).

1H NMR data (400 MHz, d$_6$-benzene, 298K): 7.11 (d, 2H, H$_m$ (Ar), J$_{HH}$ = 7.6 Hz), 6.98 (t, H$_p$ (Ar), J$_{HH}$ = 7.6 Hz), 3.73 (sept, 2H, CHMe$_2$, J$_{HH}$ = 7.6 Hz), 1.40 (s, 18H, OCMe$_3$), 1.33 (d, 12H, CHMe$_2$, J$_{HH}$ = 7.6 Hz), 1.20 (s, 9H, NCMe$_3$).

13C NMR data (100 MHz, d$_6$-benzene, 298K): 154.75 (s, C$_i$ (Ar)), 141.67 (s, C$_o$ (Ar)), 124.45 (d, C$_5$H$_5$, J$_{CH}$ = 159.4 Hz), 122.68 (d, C$_m$ (Ar), J$_{CH}$ = 156.1 Hz), 78.17 (s, OCMe$_3$), 71.61 (s, NCMe$_3$), 32.25 (q, OCMe$_3$, J$_{CH}$ = 125.5 Hz), 32.09 (q, NCMe$_3$, J$_{CH}$ = 127.0 Hz), 28.57 (d, CHCMe$_2$, J$_{CH}$ = 128.6 Hz), 23.70 (q, CHMe$_2$, J$_{CH}$ = 125.4 Hz).

Infrared data (Nujol, CsI, cm^{-1}): 2970 (s), 2925 (s, sh), 2900 (m, sh), 2880 (m, sh), 1545 (w, br), 1390 (m, sh), 1360 (s, sh), 1260 (s, sh), 1215 (s, br), 1180 (s, br), 1130 (m, sh), 1025 (w, sh), 960 (s, br), 910 (w), 805 (m, sh), 785 (m, sh), 585 (s, br), 470 (w), 380 (w, br), 270 (w).

Elemental Analysis for $MoC_{24}N_2O_2H_{43}$ (488.57) Found (Required): %C, 59.36 (59.00); %H, 8.97 (9.07); %N, 5.42 (5.73).

Mass spectral data (CI, m/z, ^{98}Mo): 491 $[M + H]^+$, 178 $[H_3NAr]^+$, 74 $[H_3NBu^t, H_2OBu^t]^+$, 58 $[Bu^tH]^+$.

5.2.4 ^1H NMR investigation of intermetal imido exchange in $Mo(NBu^t)_2XY$

The intermetal exchange reactivity of the imido moiety in $Mo(NBu^t)_2XY$ was investigated with various species, the ^1H NMR characterising data for the new complexes observed is given below.

NMR characterising data for:

(a) $CpNb(N-2,6-Pr^i_2C_6H_3)(OBu^t)_2$:

^1H NMR data (250 MHz, d_6-benzene, 298K): 7.1 - 6.9 (m, 3H, Ar), 6.16 (s, 5H, C_5H_5), 4.11 (sept, 2H, CHMe$_2$, J_{HH} = 7.0 Hz), 1.33 (d, 12H, CHMe_2, J_{HH} = 7.0 Hz), 1.29 (s, 18H, OCMe_3). Aryl proton resonances could not be accurately assigned due to overlap.

(b) $CpMo(NAr)(NBu^t)Cl$

^1H NMR data (200 MHz, d_6-benzene, 298K): 7.1 - 6.9 (m, 3H, Ar), 6.03 (s, 5H, C_5H_5), 3.63 (sept, 2H, CHMe$_2$, J_{HH} = 6.9 Hz), 1.29 (d, 6H, CHMe_2, J_{HH} = 6.9 Hz), 1.26 (d, 6H, CHMe_2, J_{HH} = 6.9 Hz), 1.19 (s, 9H, NCMe_3) Aryl proton resonances could not be accurately assigned due to overlap.

(c) $CpMo(NAr)_2Cl$

¹H NMR data (200 MHz, d₆-benzene, 298K): 7.1 - 6.9 (m, 6H, Ar), 6.08 (s, 5H, C₅H₅), 3.68 (sept, 4H, C*H*Me₂, J_{HH} = 6.8 Hz), 1.16 (d, 24H, CH*Me*₂, J_{HH} = 6.8 Hz) Aryl proton resonances could not be accurately assigned due to overlap.

5.2.5 Synthesis of Mo(NBu^t)$_2$X$_2$

(a) Reaction of Mo(NBu^t)$_2$Cl$_2$ with LiOCMe$_2$CF$_3$

Preparation of Mo(NBu^t)$_2$(OCMe$_2$CF$_3$)$_2$

Chilled Et$_2$O (100 ml, -78°C) was added to a powdered mixture of Mo(NBu^t)$_2$Cl$_2$ (0.537 g, 1.74 mmol) and LiOCMe$_2$CF$_3$ (0.467 g, 3.48 mmol), and the mixture allowed to warm to room temperature, during which time a pale green solution and a white flocculent precipitate were formed. Filtration of the supernatant solution from the solid, followed by concentration to quarter volume and cooling to *ca.* -78°C afforded a pale green solid. The low melting point solid (Mpt = 30 - 32 °C) was dried *in vacuo*. Yield, 0.66g (77%).

^{1}H NMR data (400 MHz, d$_6$-benzene, 298K): 1.27 (s, 18H, NC*Me$_3$*), 1.32 (q, 12H, OC*Me$_2$*CF$_3$, ^{4}J$_{HF}$ = 1.20 Hz).

^{19}F NMR data (376.3 MHz, d$_6$-benzene, 298K): -82.30 (s, OCMe$_2$C*F$_3$*).

^{13}C NMR data (100 MHz, d$_6$-benzene, 298K): 127.13 (q, OCMe$_2$*C*F$_3$, ^{1}J$_{CF}$ = 286.1 Hz), 78.80 (q, O*C*Me$_2$CF$_3$, ^{2}J$_{CF}$ = 28.6 Hz), 70.02 (s, N*C*Me$_3$), 31.84 (q, NC*Me$_3$*, J$_{CH}$ = 127.0 Hz), 24.70 (q, OC*Me$_2$*CF$_3$, J$_{CH}$ = 128.1 Hz).

Infrared data (Neat, CsI, cm^{-1}): 2970 (s), 1465 (w, br), 1390 (w, sh), 1365 (w, sh), 1325 (m, sh), 1260 (s), 1210 (s), 1160 (s, br), 1120 (s, br), 1015 (s, br), 900 (m, sh), 805 (s, br), 765 (m, sh), 645 (m), 600 (w), 540 (w, br), 475 (w, br), 385 (w, br), 270 (w).

Elemental Analysis for MoC$_{16}$N$_2$O$_2$F$_6$H$_{30}$ (492.35) Found (Required): %C, 39.01 (39.03); %H, 6.38 (6.14); %N, 5.57 (5.69).

Mass spectral data (CI, m/z, ^{98}Mo): 495 [M + H]$^+$, 476 [M + H - F], 74 [H$_3$NBu^t]$^+$, 58 [Bu^{t}H]$^+$.

(b) Reaction of Mo(NBu^t)$_2$Cl$_2$ with LiOCMe(CF$_3$)$_2$

Preparation of Mo(NBu^t)$_2$(OCMe(CF$_3$)$_2$)$_2$

A mixture of Mo(NBu^t)$_2$Cl$_2$ (0.729g, 2.36 mmol) and LiOCMe(CF$_3$)$_2$ (0.888 g, 4.72 mmol) in cold diethyl ether (-78°C, 100 mls) was allowed to reach ambient temperature with stirring, whereby a lime green solution and pale precipitate was formed. After 1.5 hours, the suspension was filtered to remove the precipitate (LiCl), and the solvent removed under reduced pressure to afford a dark green low melting point solid (Mpt = 32 - 34°C) in excellent yield, 1.17g (83%).

^{1}H NMR data (400 MHz, d$_6$-benzene, 298K): 1.39 (sept, 6H, OC*Me*(CF$_3$)$_2$, ^{4}J$_{HF}$ = 0.8 Hz), 1.18 (s, 18H, NC*Me$_3$*).

^{19}F NMR data (376.3 MHz, d$_6$-benzene, 298K): -78.15 (s, OCMe(*CF$_3$*)$_2$).

^{13}C NMR data (100 MHz, d$_6$-benzene, 298K): 123.89 (q, OCMe(*CF$_3$*)$_2$, ^{1}J$_{CF}$ = 288.8 Hz), 81.23 (sept, *O*CMe(CF$_3$)$_2$, ^{2}J$_{CF}$ = 29.8 Hz), 72.23 (s, *N*CMe$_3$), 31.32 (q, NC*Me$_3$*, J$_{CH}$ = 127.4 Hz), 18.86 (q, OC*Me*(CF$_3$)$_2$, J$_{CH}$ = 130.8 Hz).

Infrared data (Neat, CsI, cm^{-1}): 2970 (s), 2930 (s), 2900 (m), 2870 (m), 1455 (s), 1385 (m, sh), 1365 (m, sh), 1310 (s, br), 1220 - 1080 (s, v.br), 1025 (m), 980 (s), 865 (s, sh), 805 (s, sh), 770 (s, sh), 700 (s), 620 (m), 555 (m), 515 (m), 465 (w), 405 (w), 370 (w), 260 (m).

Elemental Analysis for MoC$_{16}$N$_2$O$_2$F$_{12}$H$_{24}$ (600.29) Found (Required): %C, 32.00 (32.01); %H, 4.08 (4.03); %N, 4.57 (4.66).

Mass spectral data (CI, m/z, ^{98}Mo): 603 [M + H]$^+$, 584 [M + H - F], 74 [H$_3$NBu^t]$^+$, 58 [Bu^{t}H]$^+$.

(c) Reaction of Mo(NBu^t)$_2$Cl$_2$.dme with LiOPr^i

Preparation of Mo(NBu^t)$_2$(OPr^i)$_2$

Chilled ether (100 ml, -78°C) was added to a powder mixture of Mo(NBu^t)$_2$Cl$_2$.dme (1.00g, 2.50 mmol) and LiOPr^i (0.34g, 5.07 mmol) with stirring. The resultant mixture was allowed to slowly attain room temperature, during which period a pale yellow solution and gelatinous precipitate had formed. Subsequent filtration, and removal of the solvent under reduced pressure afforded a pale yellow oil, which was found to crystallise on cooling below 15°C, ca. Mpt = 17 - 20°C.

^{1}H NMR data (500 MHz, d$_6$-benzene, 298K): 4.71 (sept, 2H, OC*H*Me$_2$, J$_{HH}$ = 5.8 Hz), 1.36 (s, 18H, NC*Me$_3$*), 1.27 (d, 12H, OCHM*e$_2$*, J$_{HH}$ = 5.8 Hz).

^{13}C NMR data (125 MHz, d$_6$-benzene, 298K): 78.30 (d, OCHMe$_2$, J$_{CH}$ = 145.7 Hz), 69.09 (s, NCMe$_3$), 33.16 (q, NC*Me$_3$*, J$_{CH}$ = 127.0 Hz), 27.35 (q, OCHM*e$_2$*, J$_{CH}$ = 125.0 Hz).

Infrared data (Neat, CsI, cm^{-1}): 2960 (s), 2915 (s), 2855 (m), 1450 (m), 1380 (m, sh), 1360 (s), 1330 (m), 1260 (s), 1210 (s, br), 1165 (m, sh), 1120 (s, br), 1025 (w, sh), 975 (s, br), 845 (s), 805 (m, sh), 795 (w), 755 (w), 620 (s, br), 580 (m), 470 (w), 370 (w), 275 (w).

Elemental Analysis for MoC$_{14}$N$_2$O$_2$H$_{32}$ (356.36) Found (Required): %C, 46.90 (47.19); %H, 9.05 (9.05); %N, 7.86 (8.03).

Mass spectral data (CI, m/z, ^{98}Mo): 359 [M + H]$^+$, 74 [H$_3$NBu^t]$^+$, 58 [Bu^{t}H]$^+$.

(d) Reaction of Mo(NBu^t)$_2$Cl$_2$.dme with LiNHBu^t

Preparation of Mo(NBu^t)$_2$(NHBu^t)$_2$

Chilled THF (100 ml, -30°C) was added to a solid mixture of Mo(NBu^t)$_2$Cl$_2$.dme (1.05g, 2.63 mmol) and LiNHBu^t (0.52g, 6.58 mmol) and the mixture was allowed to warm to room temperature with no apparent reaction occuring. However, at 60°C a slow reaction ensued, signified by the formation of a lemon yellow solution and a pale precipitate. The reaction was maintained at this elevated temperature for 48 hours whereby the solvent was removed under reduced pressure. The residue was extracted with pentane (2 x 50 ml, 298K) and the volatiles removed *in vacuo.* to afford a solid product ca. 95% purity. Sublimation (40°C, < 10^{-3} mmHg) afforded an analytically pure sample as a pale yellow powder, in 60% yield. This compound has also been prepared independantly by Wikinson and co-workers[15].

^{1}H NMR data (400 MHz, d$_6$-benzene, 298K): 5.69 (s, br, 2H, N*H*CMe3), 1.42 (s, 18H, NC*Me3*), 1.30 (s, 18H, NHC*Me3*).

^{13}C NMR data (100 MHz, d$_6$-benzene, 298K): 67.22 (s, N*C*Me3), 53.38 (s, NH*C*Me3), 33.64 (q, NHC*Me3*, J$_{CH}$ = 125.1 Hz), 32.84 (q, NC*Me3*, J$_{CH}$ = 126.2 Hz).

Infrared data (Nujol, CsI, cm^{-1}): 3350 (w,br), 1355 (m,sh), 1255 (w), 1210 (s, br), 1120 (w), 960 (m), 800 (w, sh), 770 (m, sh), 635 (w, br).

Elemental Analysis for MoC$_{16}$N$_4$H$_{38}$ (382.44) Found (Required): %C, 50.10 (50.25); %H, 10.18 (10.01); %N, 14.41 (14.65).

Mass spectral data (CI, m/z, ^{98}Mo): 384 [M + H]$^+$, 74 [H$_3$NBu^t]$^+$, 58 [Bu^{t}H]$^+$.

5.2.7 Synthesis of Mo(O)₂(OR)₂

$$5.2.7 \quad \text{Synthesis of } Mo(O)_2(OR)_2$$

(a) Reaction of Mo(O)₂Cl₂ with LiOCMe₂CF₃

Preparation of Mo(O)₂(OCMe₂CF₃)₂

Chilled Et₂O (100 ml, -78°C) was added to a solid mixture of Mo(O)₂Cl₂ (1.33g, 6.70 mmol) and LiOCMe₂CF₃ (1.80g, 13.40 mmol) and the resultant green suspension allowed to slowly reach room temperature. During which time a straw yellow solution and pale precipitate formed. After a further 1.5 hours, the suspension was filtered and the solvent removed under reduced pressure to afford a semi-solid pale yellow product. Yield, 2.01g (79%).

¹H NMR data (400 MHz, d₆-benzene, 298K): 1.08 (s, br, 12H, OC*Me*₂CF₃).

¹⁹F NMR data (376.3 MHz, d₆-benzene, 298K): -82.73 (s, OCMe₂*CF₃*).

¹³C NMR data (100 MHz, d₆-benzene, 298K): 125.26 (q, OCMe₂*C*F₃, $^1J_{CF} = 280.4$ Hz), 84.36 (q, O*C*Me₂CF₃, $^2J_{CF} = 30.6$ Hz), 22.27 (q, OC*Me*₂CF₃, $J_{CH} = 129.7$ Hz).

Infrared data (Neat, CsI, cm⁻¹): 3000 (m, sh), 2975 (w), 1475 (m), 1445 (w), 1400 (m, sh), 1380 (m, sh), 1330 (s, sh), 1215 (w), 1190 - 1110 (s, v.br), 1000 (s, br), 960 (s, br), 900 (s), 850 (s, sh), 800 (w), 775 (s, sh), 660 (m), 600 (m, sh), 535 (m), 475 (m), 390 (m, br), 340 (m), 265 (w, sh).

Elemental Analysis for MoC₈O₄F₆H₁₂ (382.10) Found (Required): %C, 25.44 (25.15); %H, 2.98 (3.17).

(b) Reaction of Mo(O)$_2$Cl$_2$ with LiOCMe(CF$_3$)$_2$

Preparation of Mo(O)$_2$(OCMe(CF$_3$)$_2$)$_2$

A solid mixture of Mo(O)$_2$Cl$_2$ (1.02g, 5.11 mmol) and LiOCMe(CF$_3$)$_2$ (1.91g, 10.20 mmol) in cold diethyl ether (100 ml) *ca.*-78°C, was allowed to slowly attain ambient temperature. On reaching this temperature a colourless solution and milky white precipitate was formed. The mixture was stirred for a further 2 hours and subsequently filtered, the solution from which reduced to half volume and cooled to -78°C overnight to afford fine colourless needles, which were dried *in vacuo* Yield, 1.81g (72%).

^{1}H NMR data (400 MHz, d$_6$-benzene, 298K): 1.11 (s, br, 6H, OC*Me*(CF$_3$)$_2$).

^{19}F NMR data (376.3 MHz, d$_6$-benzene, 298K): -78.12 (s, OCMe(*CF$_3$*)$_2$).

^{13}C NMR data (100 MHz, d$_6$-benzene, 298K): 122.52 (q, OCMe(*CF$_3$*)$_2$, $^1J_{CF}$ = 287.2 Hz), 84.92 (sept, OCMe(CF$_3$)$_2$, $^2J_{CF}$ = 31.3 Hz), 16.35 (q, OC*Me*(CF$_3$)$_2$, J_{CH} = 135.8 Hz).

Infrared data (Nujol, CsI, cm^{-1}): 1310 (s), 1225 (s, br), 1150 (s, br), 1120 (s), 1085 (s), 970 (s), 920 (s, br), 870 (m, sh), 785 (m, sh), 725 (m), 700 (s, sh), 615 (m), 540 (w), 515 (m), 420 (w, br), 380 (m), 280 (w).

Elemental Analysis for MoC$_8$O$_4$F$_{12}$H$_6$ (490.05) Found (Required): %C, 19.59 (19.60); %H, 1.17 (1.23).

5.2.8 Synthesis of four coordinate oxo-imido molybdenum (VI) complexes *via* intermetal oxo-imido exchange

(a) Reaction of Mo(NBu^t)$_2$(OBu^t)$_2$ with Mo(O)$_2$(OBu^t)$_2$

Preparation of Mo(O)(NBu^t)(OBu^t)$_2$

A yellow toluene solution (25 ml) of Mo(O)$_2$(OBu^t)$_2$ (0.21g, 0.78 mmol) was added rapidly with stirring to a pale green solution of Mo(NBu^t)$_2$(OBu^t)$_2$ (0.30g, 0.79 mmol) in toluene (25ml, 298K), and the resultant mixture stirred for 1.5 hours. The solvent was removed under reduced pressure and the residue recrystallised from a small quantity of pentane *ca.* 10 ml. at -78°C, whereby a pale brown amorphous powder was isolated. Sublimation (298K, < 10^{-3} mmHg) afforded a colourless crystalline material. Yield, 0.33g (68%).

^{1}H NMR data (400 MHz, d$_6$-benzene, 298K): 1.38 (s, 9H, NC*Me$_3$*), 1.25 (s, 18H, OC*Me$_3$*).

^{13}C NMR data (100 MHz, d$_6$-benzene, 298K): 79.83 (s, OC*Me$_3$*), 70.74 (s, NC*Me$_3$*), 31.47 (q, OC*Me$_3$*, J$_{CH}$ = 126.4 Hz), 30.75 (q, NC*Me$_3$*, J$_{CH}$ = 127.3 Hz).

Infrared data (Nujol, CsI, cm^{-1}): 1370 (m), 1265 (m), 1235 (w, br), 1170 (m, br), 1090 (m, br), 1020 (m, br), 950 (s), 930 (s, sh), 795 (s, br), 720 (w), 590 (w).

Elemental Analysis for MoC$_{12}$NO$_3$H$_{27}$ (329.29) Found (Required): %C, 43.48 (43.77); %H, 3.99 (4.25); %N, 5.62 (5.47).

Mass spectral data (CI, m/z, ^{98}Mo): 332 [M + H]$^+$, 74 [H$_3$NBu^t]$^+$, 58 [Bu^{t}H]$^+$.

(b) Reaction of Mo(NBu^t)$_2$(OCMe(CF$_3$)$_2$)$_2$ with Mo(O)$_2$(OCMe(CF$_3$)$_2$)$_2$

Preparation of Mo(O)(NBu^t)(OCMe(CF$_3$)$_2$)$_2$

Diethyl ether (100 ml) was added to a solid mixture of Mo(O)$_2$(OCMe(CF$_3$)$_2$)$_2$ (0.19g, 39 mmol) and Mo(NBu^t)$_2$(OCMe(CF$_3$)$_2$)$_2$ (0.24g, 40 mmol) and the mixture stirred at ambient temperature for 4 days, whereby a yellow-green solution was formed. Concentration of this solution to half volume and cooling to -78°C afforded a yellow crystalline material in moderate yield, 2.10g (49%).

^{1}H NMR data (400 MHz, d$_6$-benzene, 298K): 1.27 (sept, 6H, OCMe(CF$_3$)$_2$, ^{4}J$_{HF}$ = 1.1 Hz), 1.14 (s, 9H, NCMe_3).

^{19}F NMR data (376.3 MHz, d$_6$-benzene, 298K): -78.03 (q, OCMe(C^1F$_3$)(C^{2}F$_3$), ^{4}J$_{FF}$ = 8.7 Hz), -78.15 (q, OCMe(C^{1}F$_3$)(C^2F$_3$), ^{4}J$_{FF}$ = 8.7 Hz).

^{13}C NMR data (100 MHz, d$_6$-benzene, 298K): 123.27 (q, OCMe(CF_3)$_2$, ^{1}J$_{CF}$ = 288.0 Hz), 82.24 (m, OCMe(CF$_3$)$_2$), 76.45 (s, NCMe$_3$), 29.22 (q, NCMe_3), J$_{CH}$ = 128.1 Hz), 17.86 (q, OCMe(CF$_3$)$_2$, J$_{CH}$ = 131.7 Hz).

Infrared data (Nujol, CsI, cm^{-1}): 1300 (s), 1240 (m), 1210 (m), 1130 (s), 985 (m,br), 890 (m, sh), 770 (m), 700 (w), 655 (m), 540 (w), 540 (m), 435 (w), 390 (w), 270 (w).

Elemental Analysis for MoC$_{12}$NO$_3$F$_{12}$H$_{15}$ (545.17) Found (Required): %C, 25.59 (26.44); %H, 3.01 (2.77); %N, 2.40 (2.57).

Mass spectral data (EI, m/z, ^{98}Mo): 531 [M - CH$_4$]$^+$, 69 [CF$_3$]$^+$, 57 [Bu^t]$^+$.

(c) Reaction of Mo(NBu^t)$_2$Cl$_2$.dme with Mo(O)$_2$Cl$_2$.dme

Preparation of Mo(O)(NBu^t)Cl$_2$.dme

Diethyl ether (100 ml) was added to a solid mixture of Mo(O)$_2$Cl$_2$.dme (0.21g, 0.73 mmol) and Mo(NBu^t)$_2$Cl$_2$.dme (0.29g, 0.73 mmol), and the resultant mixture stirred for 5 days at room temperature, whereby a pale yellow solution was formed. Recrystallisation of the supernatant solution at *ca.* -78°C, afforded a pale green powder which was dried *in vacuo*. Yield, 0.13g (26%).

^{1}H NMR data (500 MHz, d$_6$-benzene, 298K): 3.41 (s, 6H, Me (dme)), 3.00 (s, 4H, CH$_2$ (dme)), 1.41 (s, 9H, NC*Me$_3$*).

^{13}C NMR data (125 MHz, d$_6$-benzene, 298K): 74.86 (s, NCMe3), 70.60 (t, CH$_2$ (dme), J$_{CH}$ = 148.4 Hz), 63.27 (q, br, Me (dme)), 27.80 (q, NC*Me$_3$*, J$_{CH}$ = 102.5 Hz).

Infrared data (Nujol, CsI, cm^{-1}): 1260 (w), 1230 (w), 1080 (m, br), 1040 (s, br), 1015 (m, br), 910 (s, sh), 860 (s, sh), 800 (m, br), 335 (m, br).

Elemental Analysis for MoC$_8$NO$_3$Cl$_2$H$_{19}$ (344.09) Found (Required): %C, 27.79 (27.93); %H, 5.57 (5.57); %N, 3.54 (4.07).

Mass spectral data (EI, m/z, ^{98}Mo, ^{35}Cl): 240 [Mo(O)Cl$_2$.C$_4$H$_8$]$^+$, 225 [Mo(O)Cl$_2$.C$_3$H$_5$]$^+$, 184 [Mo(O)Cl$_2$]$^+$, 149 [Mo(O)Cl]$^+$, 57 [Bu^t]$^+$.

5.2.9 ^{1}H NMR investigation of alkoxide exchange in Mo(NAr)(CHCMe$_2$Ph)(OR)$_2$

The intermetal exchange reactivity of the alkoxide ligands in Mo(CHCMe$_2$Ph)(NAr)(OR)$_2$ was investigated, the ^{1}H NMR characterising data for the new complexes observed is given below.

NMR characterising data for:

(a) Mo(NAr)(CHCMe$_2$Ph)(OBu^t)(OCMe$_2$CF$_3$):

^{1}H NMR data (400 MHz, d$_6$-benzene, 298K): 11.50 (s, CHCMe$_2$Ph), 7.34 (d, 2H, Ar), 7.12 - 6.97 (m, 6H Ar), 3.86 (sept, 2H, CHMe$_2$), 1.64 (s, 3H, CHCMe^1Me^{2}Ph), 1.63 (s, 3H, CHCMe^1Me^2), 1.26 (s, 6H, OCMe_2CF$_3$), 1.23 (d, 12H, CHMe_2), 1.22 (s, 9H, OCMe_3). Aryl proton resonances could not be accurately assigned due to overlap.

(b) Mo(CHCMe$_2$Ph)(NAr)(OCMe$_2$CF$_3$)(OCMe(CF$_3$)$_2$):
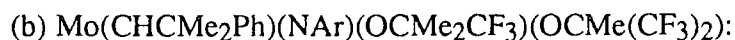
^{1}H NMR data (400 MHz, d$_6$-benzene, 298K): 11.89 (s, CHCMe$_2$Ph), 7.22 (d, 2H, Ar), 7.12 - 6.92 (m, 6H, Ar), 3.66 (sept, 2H, CHMe$_2$, J$_{HH}$ = 6.8 Hz), 1.57 (s, 3H, CHCMe^1Me^{2}Ph), 1.54 (s, 3H, CHCMe^1Me^2Ph), 1.22 (s, 6H, OCMe_2CF$_3$), 1.19 (d, 12H, CHMe_2, J$_{HH}$ = 6.8 Hz), 1.19 (s, 9H, OCMe_3). Aryl proton resonances could not be accurately assigned due to overlap.

5.2.10 ^{1}H NMR investigation of alkoxide exchange in Mo(O)$_2$(OR)$_2$

The intermetal exchange reactivity of the alkoxide ligands in Mo(O)$_2$(OR)$_2$ was investigated, the ^{1}H NMR characterising data for the new complexes observed is given overleaf.

(a) $Mo(O)_2(OBu^t)(OCMe_2CF_3)$:
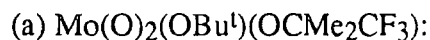
^{1}H NMR data (200 MHz, d$_6$-benzene, 298K): 1.11 (s, br, 15H, coincident OC*Me$_3$* and OC*Me$_2$*CF$_3$ resonances).

(b) $Mo(O)_2(OBu^t)(OCMe(CF_3)_2)$:
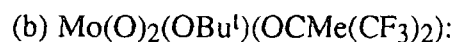
^{1}H NMR data (200 MHz, d$_6$-benzene, 298K): 1.24 (sept, 3H, OC*Me*(CF$_3$)$_2$, $^4J_{HF}$ = 1.1Hz), 1.03 (s, 9H, OC*Me$_3$*).

(c) $Mo(O)_2(OCMe_2CF_3)(OCMe(CF_3)_2)$

^{1}H NMR data (200 MHz, d$_6$-benzene, 298K): 1.14 (sept, br, 3H, OC*Me*(CF$_3$)$_2$), 1.02 (m, br, 6H, OC*Me$_2$*CF$_3$).

5.2.11 Reaction of $Mo(NBu^t)_2(OBu^t)_2$ with $(CF_3)_2MeCOH$

Observation of $Mo(NBu^t)_2(OCMe(CF_3)_2)_2.Bu^tOH$

^{1}H NMR data (200 MHz, d$_6$-benzene, 298K): 1.35 (s, 9H, HOC*Me$_3$*), 1.23 (s, 18H, NC*Me$_3$*), 1.19 (sept, 6H, OC*Me*(CF$_3$)$_2$, $^4J_{HF}$ = 1.2 Hz).

5.3 Experimental Details to Chapter 3

5.3.1 Reaction of CpNb(NBu^t)Cl$_2$ with LiNEt$_2$

Preparation of CpNb(NBu^t)(NEt$_2$)Cl

To a mixture of (C$_5$H$_5$)Nb(NBu^t)Cl$_2$ (1.5g, 5.17 mmol) and LiNEt$_2$ (0.41g, 5.18 mmol), Et$_2$O (100 mls) was added at -78°C and the solution allowed to reach room temperature and stirred overnight, whereby a pale precipitate and a red solution was formed. Subsequent filtration and removal of the solvent under reduced pressure afforded a dark red oil in a quantitative yield, 1.57g (90%).

^{1}H NMR data (400 MHz, d$_6$-benzene, 298K): 5.94 (s, 5H, C$_5$H$_5$), 4.15 (m, NC^{1}HHMe, J$_{HH}$ = 6.8 Hz), 3.70 (m, NC^{1}HHMe, J$_{HH}$ = 6.8 Hz), 3.26 (m, NC^{2}HHMe, J$_{HH}$ = 6.8 Hz), 3.01 (m, NC^{2}HHMe, J$_{HH}$ = 6.8 Hz), 1.13 (s, 9H, NCMe$_3$), 1.04 (m, 3H, NC^{1}H$_2$Me, J$_{HH}$ = 6.8 Hz), 0.91 (m, 3H, NC^{2}H$_2$Me, J$_{HH}$ = 6.8 Hz).

^{13}C NMR data (100 MHz, d$_6$-benzene, 298K): 107.77 (d, C$_5$H$_5$, J$_{CH}$ = 173.2 Hz), 67.80 (s, NCMe$_3$), 59.95 (t, NC^{1}H$_2$Me, J$_{CH}$ = 130.2 Hz), 51.62 (t, NC^{2}H$_2$Me, J$_{CH}$ = 126.4 Hz), 31.54 (q, NCMe$_3$, J$_{CH}$ = 126.4 Hz), 17.67 (q, NC^{1}H$_2$Me, J$_{CH}$ = 126.3 Hz), 13.34 (q, NC^{2}H$_2$Me, J$_{CH}$ = 126.6 Hz).

Infrared data (Neat, CsI, cm^{-1}): 3100 (w, br), 2975 (s, sh), 2930 (m, sh), 2865 (m), 1448 (m, br), 1358 (m, sh), 1242 (s), 1216 (m, sh), 1188 (w), 1146 (w), 1130 (w), 1090 (w), 1065 (w), 1045 (w), 1010 (m), 890 (m, sh), 800 (s, br), 580 (w, br), 538 (w, br).

Elemental Analysis for NbC$_{13}$N$_2$H$_{24}$Cl (336.71) Found (Required): %C, 45.95 (46.37); %H, 6.88 (7.18); %N, 8.07 (8.32).

Mass spectral data (EI, m/z, ^{35}Cl): 336 [M]$^+$, 321 [M - Me]$^+$, 299 [M - Cl, 2H]$^+$, 286 [M - Cl, Me, 2H]$^+$, 228 [M - Cl, HNEt$_2$ / H$_2$NBu^t]$^+$, 74 [H$_2$NEt$_2$, H$_3$NBu^t]$^+$, 65 [C$_5$H$_5$]$^+$, 58 [Bu^{t}H]$^+$.

5.3.2   (a) Reaction of CpNb(NBu^t)Cl$_2$ with LiNHAr

(b) Reaction of CpNb(NAr)Cl$_2$ with LiNHBu^t

Preparation of CpNb(NAr)(NHBu^t)Cl (Ar = 2,6-Pr$^i_2$C$_6$H$_3$)

(a) Chilled Et$_2$O (100 ml, -78°C) was added to a solid mixture of (C$_5$H$_5$)Nb(NBu^t)Cl$_2$ (0.99g, 3.30 mmol) and LiNHAr (0.61g, 3.33 mmol), and the mixture allowed to reach room temperature. On stirring for 12 hours, a pale flocculent precipitate and an orange-red solution was formed. Subsequent filtration and removal of the solvent under reduced pressure afforded an orange-red oil. This oil was washed with 3 portions (15 ml) of cold P.E (40-60°C, -30°C) and the yellow powder residue recrystallised from toluene at *ca.* -78°C to afford yell ow crystals, which were collected and dried *in vacuo*. Yield, 0.45g (31%).

(b) CpNb(NAr)Cl$_2$ (0.56g, 1.39 mmol) was added to LiNHBu^t (0.11g, 1.39 mmol) and cold diethyl ether (100 ml) added *ca.* -78° C. The mixture was allowed to slowly attain ambient temperature and stirred for 16 hours, whereby a pale precipitate and orange solution was formed. The suspension was filtered from the supernatant solution, which was concentrated to half volume and cooled to ca. -20°C to afford yellow cubic crystals. The crystals were collected, washed with cold pentane (10 ml) and dried *in vacuo*. Yield, 0.21g (34%).

^{1}H NMR data (400 MHz, d$_6$-benzene, 298K): 8.0 (s, br, $\Delta^1/_2$ *ca.* 144 Hz, H, N*H*CMe$_3$), 7.06 (d, 2H, H$_m$(Ar), J$_{HH}$ = 7.3 Hz), 6.97 (t, H, H$_p$(Ar), J$_{HH}$ = 6.7 Hz), 5.89 (s, 5H, C$_5$H$_5$), 4.03 (sept, 2H, C*H*(CH$_3$)$_2$(Ar), J$_{HH}$ = 6.7.Hz), 1.32 (d, 12H, CH*Me$_2$*, J$_{HH}$ = 6.7 Hz), 1.15 (s, 9H, NC*Me$_3$*).

13C NMR data (100 MHz, d$_6$-benzene, 298K): 152.14 (s, C$_i$ (Ar)), 144.78 (s, C$_o$(Ar)), 124.29 (d, C$_p$(Ar), J$_{CH}$ = 157.6 Hz), 122.97 (d, C$_m$ (Ar), J$_{CH}$ = 157.6 Hz), 110.00 (d, C$_5$H$_5$, J$_{CH}$ = 174.4 Hz), 59.54 (s, NCMe$_3$), 32.64 (q, CH*Me$_2$*, J$_{CH}$ = 125.5 Hz), 28.08 (d, C*H*Me$_2$, J$_{CH}$ = 129.2 Hz), 24.57 (q, NC*Me$_3$*, J$_{CH}$ = 126.7 Hz).

Infrared data (Nujol, CsI, cm^{-1}): 3274 (w), 1332 (s), 1200 (m, br), 1100 (w, br), 1020 (w, br), 980 (w, sh), 965 (m, sh), 812 (s, sh), 800 (m, sh), 788 (m, sh), 760 (s, sh), 720 (w, br), 570 (w, br), 455 (m, br), 378 (m, sh), 368 (m, sh).

Elemental Analysis for NbC$_{21}$N$_2$H$_{32}$Cl (440.86) Found (Required): % C, 54.73 (54.50); % H, 6.94 (7.32); % N, 6.03 (6.35).

Mass spectral data (EI, m/z, ^{35}Cl): 440 [M]$^+$, 425 [M - Me]$^+$, 405 [M - Cl]$^+$, 403 [M - Cl, 2H]$^+$, 367 [M - H$_2$NBu^t]$^+$, 284 [M - C$_5$H$_5$, Bu^t, Cl]$^+$, 228 [M - H$_2$NAr, Cl]$^+$.

5.3.3 **a) Reaction of CpNb(NBu^t)(NEt$_2$)Cl with LiNHBu^t**

b) Reaction of CpNb(NBu^t)(NHBu^t)Cl with LiNEt$_2$

Preparation of CpNb(NBu^t)(NHBu^t)(NEt$_2$)

(a) An ethereal solution (30 ml) of (C$_5$H$_5$)Nb(NBu^t)(NEt$_2$)Cl (1.16g, 3.44 mmol) was added at -78°C to a stirring suspension of LiNHBu^t (0.272g, 3.44 mmol) in Et$_2$O (50 mls) at room temperature. The mixture was stirred overnight allowing a pale precipitate and an orange-red solution to form. Filtration, followed by subsequent removal of the solvent under reduced pressure afforded an orange-brown viscous oil in a near quantitative yield, 1.11g (86%).

(b) Chilled Et$_2$O (100 ml, -78°C) was added to a solid mixture of CpNb(NBu^t)(NHBu^t)Cl (0.50g, 1.48 mmol) and LiNEt$_2$ (0.12g, 1.50 mmol) and the mixture allowed reach ambient temperature. A pale precipitate was slowly formed over a period of 24 hours and the suspension filtered to give an orange-brown solution. The volatiles were removed under reduced pressure affording an orange-brown viscous oil.

¹H NMR data (400 MHz, d₆-benzene, 298K): 5.87 (s, 5H, C₅H₅), 4.55 (s, br, NHCMe₃), 3.50 (m, 2H, N(C*H*HMe)₂, J_{HH} = 6.8 Hz), 3.27 (m, 2H, N(CH*H*Me)₂, J_{HH} = 6.8 Hz), 1.37 (s, 9H, NHC*Me₃*), 1.26 (s, NC*Me₃*), 1.08 (t, 6H, N(CH₂*Me*)₂, J_{HH} = 6.8 Hz).

¹³C NMR data (100 MHz, d₆-benzene, 298K): 106.18 (d, C₅H₅, J_{CH} = 171.3 Hz), 65.66 (s, NCMe₃), 53.99 (t, N(CH₂Me)₂, J_{CH} = 132.8 Hz), 34.68 (q, NHC*Me₃*, J_{CH} = 125.5 Hz), 32.78 (q, NC*Me₃*, J_{CH} = 125.5 Hz), 15.33 (q, N(CH₂*Me*)₂, J_{CH} = 125.2 Hz).

Infrared data (Neat, CsI, cm⁻¹): 3345 (w, br), 3100 (w), 2970 (s, br), 2925 (s), 2900 (s), 2860 (s), 1785 (w), 1685 (w), 1470 (m, sh), 1460 (m), 1445 (m), 1385 (m), 1355 (s, sh), 1240 (s, br), 1210 (s, br), 1185 (m, sh), 1150 (w, sh), 1065 (w, sh), 1010 (m, sh), 970 (m), 880 (m, sh), 795 (s, br), 745 (m), 570 (m, br), 530 (w).

Elemental Analysis for NbC₁₇N₃H₃₄ (373.38) Found (Required): % C, 54.05 (54.69); % H, 8.87 (9.18); % N, 11.02 (11.25).

Mass spectral data (EI, m/z): 373 [M]⁺, 358 [M - Me]⁺, 299 [M - H₃NBuᵗ / H₂NEt₂]⁺, 74 [H₃NBuᵗ / H₂NEt₂]⁺, 58 [BuᵗH]⁺.

5.3.4   Reaction of CpNb(NBuᵗ)(NHBuᵗ)Cl with LiNHBuᵗ

Preparation of CpNb(NBuᵗ)(NHBuᵗ)₂

To a solid mixture of (C₅H₅)Nb(NBuᵗ)(NHBuᵗ)Cl (0.399g, 1.19 mmol) and LiNHBuᵗ (93.6 mg, 1.18 mmol), Et₂O (100 mls) was added at -78°C and the mixture allowed to reach room temperature and stirred overnight., whereby a pale precipitate and a yellow-orange solution had formed. Subsequent filtration and removal of the solvent under reduced pressure yielded a light brown viscous oil . Yield, 0.31g (70%).

¹H NMR data (400 MHz, d$_6$-benzene, 298K): 5.87 (s, 5H, C$_5$H$_5$), 4.80 (s, br, 2H, NHCMe$_3$), 1.30 (s, 18H, NHCMe_3), 1.26 (s, 9H, NCMe_3).

¹³C NMR data (100 MHz, d$_6$-benzene, 298K): 106.73 (d, C$_5$H$_5$, J$_{CH}$ = 171.6 Hz), 65.65 (s, NCMe$_3$), 53.78 (s, NHCMe$_3$), 34.24 (q, NHCMe_3, J$_{CH}$ = 124.4 Hz), 32.45 (q, NCMe_3, J$_{CH}$ = 125.9 Hz).

Infrared data (Neat, CsI, cm^{-1}): 3355 (w, br), 3100 (w), 2970 (s, br), 2925 (s), 2900 (s), 2860 (s), 1790 (w), 1690 (w), 1595 (w), 1470 (m, sh), 1455 (m), 1385 (m), 1355 (s, sh), 1240 (s, br), 1210 (s, br), 1125 (m), 1100 (s), 1060 (w), 1015 (m), 970 (s, br), 910 (w), 795 (s, br), 775 (m), 750 (m), 590 (m), 570 (m), 535 (m).

Elemental Analysis for NbC$_{17}$N$_3$H$_{34}$ (373.38) Found (Required): % C, 54.11 (54.69); % H, 8.98 (9.18); % N, 10.98 (11.25).

Mass spectral data (EI, m/z): 373 [M]$^+$, 358 [M - Me]$^+$, 74 [H$_3$NBu^t / H$_2$NEt$_2$]$^+$, 58 [Bu^{t}H]$^+$.

5.3.5 Reaction of CpNb(NBu^t)(NHBu^t)Cl with LiNHAr

Preparation of CpNb(NBu^t)(NHBu^t)(NHAr)

Chilled diethylether (100 mls) at *ca.* -78°C was added to a solid mixture of (C$_5$H$_5$)Nb(NBu^t)(NHBu^t)Cl (0.506g, 1.50 mmol) and LiNHAr (0.276g, 1.51 mmol) and the solution allowed to reach room temperature. After 12 hours a white precipitate and a pale orange solution was formed. The solution was filtered followed by removal of the solvent under reduced pressure to afford a viscous brown oil.

¹H NMR data (400 MHz, d$_6$-benzene, 298K): 7.20 (d, 2H, H$_m$ (Ar), J$_{HH}$ = 7.5 Hz), 7.07 (t, H$_p$ (Ar), J$_{HH}$ = 7.5 Hz), 6.94 (s, br, NH), 5.69 (s, 5H, C$_5$H$_5$), 5.47 (s, br, NH),

3.53 (sept, 2H, C*H*Me₂, J$_{HH}$ = 6.9 Hz), 1.43 (s, 9H, NHC*Me₃*), 1.28 (d, 12H, CH*Me₂*, J$_{HH}$ = 7.2 Hz), 1.24 (s, 9H, NC*Me₃*).

5.3.6 ¹H NMR investigation of imido exchange in CpNb(NBuᵗ)X₂

The reactivity of the imido moiety in CpNb(NBuᵗ)X₂ (X = Cl, OBuᵗ) with various substrates was undertaken, and the characterising data for any new species observed presented herein.

NMR chatacterising data for:

(a) CpNb(N-2,6-Cl₂C₆H₃)(OBuᵗ)₂

¹H NMR data (200 MHz, d₆-benzene, 298K): 7.04 (d, H$_m$ (Ar), J$_{HH}$ = 8.0 Hz), 6.22 (s, 5H, C₅H₅), 6.09 (t, H$_p$ (Ar), J$_{HH}$ = 8.0 Hz), 1.32 (s, 18H, OCMe₃).

(b) CpNb(N-C₆F₅)(OBuᵗ)₂
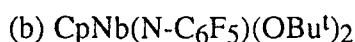
¹H NMR data (200 MHz, d₆-benzene, 298K): 6.10 (s, 5H, C₅H₅), 1.27 (s, 18H, OC*Me₃*).

(c) CpNb(OBuᵗ)₂Cl₂
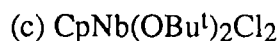
¹H NMR data (200 MHz, d₆-benzene, 298K): 6.23 (s, 5H, C₅H₅), 1.35 (s, 18H, OC*Me₃*).

5.3.7 Synthesis of CpNb(NBu^t)X$_2$

(a) Reaction of CpNbBr$_4$ with (SiMe$_3$)NHBu^t

Preparation of CpNb(NBu^t)Br$_2$

(SiMe$_3$)NHBu^t (3.02g, 20.92 mmol) in methylene chloride (50 ml) was added dropwise *via* canula to a stirring methylene chloride solution of CpNbBr$_4$ (4.99g, 10.45 mmol), over a period of one hour with no apparent reaction. After 24 hours a dark orange-brown solution had formed, from which the volatiles were removed under reduced pressure to yield an orange-brown solid. Extraction of the solid with methylene chloride *ca.* 100 ml followed by concentration and cooling to -78°C afforded orange crystals in low yield, 0.95g (23%).

^{1}H NMR data (400 MHz, d$_6$-benzene, 298K): 5.89 (s, 5H, C$_5$H$_5$), 1.06 (s, 9H, NC*Me$_3$*).

^{13}C NMR data (100 MHz, d$_6$-benzene, 298K): 111.77 (d, C$_5$H$_5$, J$_{CH}$ = 177.4 Hz), 69.92 (s, NC*Me$_3$*), 30.18 (q, NC*Me$_3$*, J$_{CH}$ = 127.4 Hz).

Infrared data (Nujol, CsI, cm^{-1}): 3080 (w), 1600 (w), 1405 (w), 1360 (m, sh), 1300 (w), 1245 (m), 1220 (m), 1140 (w), 1015 (m, br), 840 (m), 800 (s, sh), 720 (m, br), 550 (w), 530 (w), 445 (w), 385 (w), 270 (w), 255 (m, sh), 240 (m, sh).

Elemental Analysis for NbC$_9$NH$_{14}$Br$_2$ (388.93) Found (Required): %C, 27.76 (27.79); %H, 3.78 (3.63); %N, 3.47 (3.68).

Mass spectral data (CI, m/z, ^{79}Br): 389 [M + H]$^+$, 374 [M - Me]$^+$, 317 [M - NBu^t]$^+$, 310 [M + H - Br], 74 [H$_3$NBu^t]$^+$, 58 [Bu^{t}H]$^+$.

(b) Reaction of CpNb(NBu^t)Cl$_2$ with LiOPr^i

Preparation of CpNb(NBu^t)(OPr^i)$_2$

Chilled diethylether (100 ml, -78°C) was added to a solid mixture of CpNb(NBu^t)Cl$_2$ (1.00g, 3.33 mmol) and LiOPr^i (0.45g, 6.65 mmol) and the mixture allowed to reach room temperature and stirred for two hours. During which time, a white flocculent precipitate and a pale yellow-orange solution was formed. Subsequent filtration and removal of the solvent under reduced pressure afforded a pale orange non-viscous oil in high yield, 0.97g (83%).

^{1}H NMR data (400 MHz, d$_6$-benzene, 298K): 6.17 (s, 5H, C$_5$H$_5$), 4.74 (sept, 2H, OCHMe$_2$, J$_{HH}$ = 6.0 Hz), 1.29 (d, 6H, OCHMe^1Me^2, J$_{HH}$ = 6.0 Hz), 1.25 (d, 6H, OCHMe^1Me^2, J$_{HH}$ = 6.0 Hz), 1.17 (s, 9H, NCMe_3).

^{13}C NMR data (100 MHz, d$_6$-benzene, 298K): 109.14 (d, C$_5$H$_5$, J$_{CH}$ = 172.5 Hz), 78.34 (d, OCHMe$_2$, J$_{CH}$ = 141.9 Hz), 65.47 (s, NCMe$_3$), 32.90 (q, NCMe_3, J$_{CH}$ = 125.9 Hz), 26.67 (q, OCHMe^1Me^2, J$_{CH}$ = 125.1 Hz), 26.55 (q, OCHMe^1Me^2, J$_{CH}$ = 125.1 Hz).

Infrared data (Neat, CsI, cm^{-1}): 3090 (w, br), 2965 (s, sh), 2920 (m, sh), 2860 (m, sh), 1595 (w, br), 1450 (m, br), 1380 (m, sh), 1365 (m, sh), 1330 (m, sh), 1250 (s), 1220 (m, sh), 1170 (m), 1125 (s, br), 1015 (m), 980 (s, br), 845 (m), 800 (s), 790 (m), 600 (m, br), 555 (w), 545 (w), 460 (w, br), 380 (w), 295 (w).

Elemental Analysis for NbC$_{15}$NO$_2$H$_{28}$ (347.30) Found (Required): %C, 51.05 (51.90); %H, 8.25 (8.13); %N, 4.11 (4.03).

Mass spectral data (CI, m/z): 348 [M + H]$^+$, 332 [M - Me]$^+$, 305 [M + H - C$_3$H$_7$]$^+$.

(c) Reaction of CpNb(NBu^t)Cl$_2$ with LiOCMe$_2$CF$_3$

Preparation of CpNb(NBu^t)(OCMe$_2$CF$_3$)$_2$

Cold diethyl ether (100 ml, -78°C) was added to a solid mixture of CpNb(NBu^t)Cl$_2$ (0.35g, 1.18 mmol) and LiOCMeCF$_3$ (0.32g, 2.39 mmol) and the mixture allowed to slowly attain ambient temperature and stirred for 16 hours. During which period a white flocculent precipitate and a pale yellow solution was formed. The suspension was filtered, the solution from which reduced to a small volume *ca.* 10 ml and cooled to -78°C, affording colourless crystals which were dried *in vacuo*. A second crop of crystals was isolated when the mother liquer was concentrated further and cooled to -78°C. Yield, 0.48g (84%).

^{1}H NMR data (400 MHz, d$_6$-benzene, 298K): 6.10 (s, 5H, C$_5$H$_5$), 1.32 (m, 6H, OC*Me^1*Me^{2}CF$_3$), 1.30 (m, 6H, OCMe^1*Me^2*CF$_3$), 1.02 (s, 9H, NC*Me$_3$*).

^{19}F NMR data (376.3 MHz, d$_6$-benzene, 298K): -82.53 (s, OCMe$_2$*CF$_3$*).

^{13}C NMR data (100 MHz, d$_6$-benzene, 298K): 127.38 (q, OCMe$_2$CF$_3$, $^1J_{CF}$ = 285.7 Hz), 110.43 (d, C$_5$H$_5$, J$_{CH}$ = 173.6 Hz), 78.17 (q, OCMe$_2$CF$_3$, $^2J_{CF}$ = 28.3 Hz), 66.55 (s, NCMe$_3$), 32.03 (q, NC*Me$_3$*, J$_{CH}$ = 126.3 Hz), 24.74 (q, OC*Me^1*Me^{2}CF$_3$, J$_{CH}$ = 128.2 Hz), 24.43 (q, OCMe^1*Me^2*CF$_3$, J$_{CH}$ = 127.8 Hz).

Infrared data (Nujol, CsI, cm^{-1}): 1355 (w), 1320 (w, sh), 1260 (w, sh), 1240 (m), 1210 (w), 1190 (m), 1155 (s, br), 1120 (s, br), 1015 (s, br), 895 (m, sh), 795 (s, sh), 760 (w, sh), 640 (w, sh), 610 (w, sh), 535 (w), 525 (w), 475 (w, br), 380 (w, br).

Elemental Analysis for NbC$_{17}$NO$_2$F$_6$H$_{26}$ (483.29) Found (Required): %C, 42.28 (42.25); %H, 5.54 (5.42); %N, 2.77 (2.90).

(d) Reaction of CpNb(NBuᵗ)Cl₂ with LiOCMe₂(CF₃)₂

Preparation of CpNb(NBuᵗ)(OCMe(CF₃)₂)₂

A solid mixture of CpNb(NBuᵗ)Cl₂ (0.40g, 1.33 mmol) and LiOCMe(CF₃)₂ (0.50g, 2.66 mmol) had cold Et₂O added (100 ml, -78°C), and the resultant mixture allowed to reach room temperature and stirred for 16 hours, whereby a white precipitate and a pale brown solution had formed. The suspension was filtered and the solvent removed under reduced pressure to yield a residue which was extracted with pentane (50 ml). Concentration and cooling to *ca.* -40°C afforded impure pale brown flakes, which sublimed (< 10⁻³mm Hg) to afford colourless crystals. Yield, 0.61g (77%).

¹H NMR data (400 MHz, d₆-benzene, 298K): 6.05 (s, 5H, C₅H₅), 1.44 (sept, OC*Me*(CF₃)₂, $^4J_{HF}$ = 1.12 Hz), 0.92 (s, 9H, NC*Me₃*).

¹⁹F NMR data (376.3 MHz, d₆-benzene, 298K): -77.93 (q, OCMe(C*F₃*)¹(CF₃)², $^4J_{FF}$ = 9.4 Hz), -78.57 (q, OCMe(CF₃)¹(C*F₃*)², $^4J_{FF}$ = 9.4 Hz).

¹³C NMR data (100 MHz, d₆-benzene, 298K): 124.10 (q, OCMe(C*F₃*)¹(CF₃)², $^1J_{CF}$ = 287.2 Hz), 123.94 (q, OCMe(CF₃)¹(C*F₃*)², $^1J_{CF}$ = 287.2 Hz), 80.93 (m, OCMe(CF₃)₂), 68.04 (s, NCMe₃), 31.43 (q, NC*Me₃*, J_{CH} = 126.6 Hz), 18.34 (q, OC*Me*(CF₃)₂, J_{CH} = 130.9 Hz).

Infrared data (Nujol, CsI, cm⁻¹): 1360 (w), 1300 (m), 1210 (s, br), 1170 (s, br), 1110 (m, sh), 1080 (s, sh), 980 (m, sh), 865 (w, sh), 825 (w), 805 (m), 770 (m, sh), 700 (s, sh), 620 (w), 545 (w), 530 (w).

Elemental Analysis for NbC₁₇NO₂F₁₂H₂₀ (591.23) Found (Required): %C, 34.30 (34.54); %H, 3.41 (3.57); %N, 2.22 (2.37).

(e) Reaction of CpNb(NBu^t)Cl$_2$ with LiNC$_4$H$_4$

Preparation of CpNb(NBu^t)(NC$_4$H$_4$)$_2$

Chilled Et$_2$O (100 ml, -78°C) was added to a solid mixture of CpNb(NBu^t)Cl$_2$ (0.77g, 2.58 mmol) and LiNC$_4$H$_4$ (0.38g, 5.18 mmol) and the mixture allowed to reach room temperature with stirring. During which period a pale flocculent precipitate and a pale yellow solution was formed. The mixture was stirred for 16 hours, filtered, and the solution concentrated to half volume and cooled to -40°C, whereby a pale yellow solid was afforded in low yield, 0.30g (32%).

^{1}H NMR data (500 MHz, d$_6$-benzene, 298K): 7.14 (t, 4H, H$_\alpha$ (NC$_4$H$_4$)), 6.38 (t, 4H, H$_\beta$ (NC$_4$H$_4$)), 5.83 (s, 5H, C$_5$H$_5$), 1.09 (s, 9H, NCMe_3).

^{13}C NMR data (125 MHz, d$_6$-benzene, 298K): 133.12 (dq, C$_\alpha$ (NC$_4$H$_4$), J$_{CH}$ = 181.0 Hz), 109.86 (dm, C$_\beta$ (NC$_4$H$_4$), J$_{CH}$ = 174.0 Hz), 109.73 (d, C$_5$H$_5$, J$_{CH}$ = 172.0 Hz), 68.96 (s, NCMe_3), 31.75 (q, NCMe_3, J$_{CH}$ = 126.9 Hz).

Infrared data (Nujol, CsI, cm^{-1}): 3040 (w), 1265 (m), 1230 (m), 1155 (m), 1080 (m), 1070 (m), 1050 (m), 1025 (s, sh), 835 (w), 820 (m), 800 (m), 740 (m), 730 (s), 630 (m), 550 (w), 450 (w), 385 (w), 340 (w).

Elemental Analysis for NbC$_{17}$N$_3$H$_{22}$ (361.29) Found (Required): %C, 56.01 (56.52); %H, 5.89 (6.14); %N, 11.24 (11.63).

Mass spectral data (CI, m/z): 362 [M + H]$^+$, 304 [M - Bu^t]$^+$, 74 [H$_3$NBu^t], 68 [H$_2$NC$_4$H$_4$]$^+$.

5.4.1 Reaction between 2,5 dihydrofuran and Mo(NAr)((CHCMe$_2$Ph)(OR)$_2$

Preparation of Poly (oxy-2-butenylene)

Typically, 2,5 dihydrofuran (1000 equivalents) was added neat with stirring to the appropriate initiator (I, II and III, approximately 20 mg) at room temperature. In each case an orange/red solution was formed and the mixture gradually became more viscous until after 16 hours, where no further change in viscosity was observed. An excess of benzaldehyde (30 µl) was added to terminate the living metal centre. Precipitation of the polymer was achieved by adding a toluene solution (10 ml) dropwise to methanol, followed by filtration and removal of the volatiles *in vacuo* , to afford a pale yellow oil in low yield (10%).
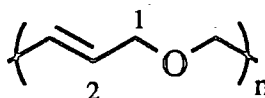
^{1}H NMR data (400 MHz, d-chloroform, 298K): 5.74 (m, C^{2}H, trans), 5.65 (m, C^{2}H (cis), 3.92 (m, C^{1}H$_2$, cis), 3.98 (m, C^{1}H$_2$, trans).

^{13}C NMR data (100 MHz, d-chloroform, 298K): 129.49* (C^{2}H, cis (tct)), 129.35, 129.32 129.30, 129.28, (d, C^{2}H, trans (ttt, ttc, ctt and ctc respectively), J$_{CH}$ = 153.7 Hz), 70.18, 70.07, (t, C^{1}H$_2$, trans (tc and tt respectively), J$_{CH}$ = 141.2 Hz), 65.93, 65.88 (t, C^{1}H$_2$, cis (cc and ct respectively), J$_{CH}$ ~ 140 Hz).* one of the doublet signals is obscured in the coupled ^{13}C NMR spectrum.

GPC	Poly (oxy-2-butenylene) prepared from I, II and III		
data	I	II	III
M_n	6800	14200	4300
M_w	9300	21900	10100
PDI (M_w / M_n)	1.36	1.63	2.34

5.4.2 Reaction of 2,5 dihydrofuran with $Mo(NAr)(CHBu^t)(OCMe_2CF_3)_2$ in d_6-benzene

2,5 dihydrofuran (3.3 mg, 48 μmol, 1.9 equivalents) was added to a solution of $Mo(CHBu^t)(NAr)(OCMe_2CF_3)_2$ (16.2mg, 25 μmol) in d_8-toluene (800 μl), and the mixture cooled to -70°C. New resonances were observed in the ^1H NMR spectrum as described in chapter 4.

5.4.3 Reaction of 2,3 dihydrofuran with $Mo(NAr)(CHCMe_2Ph)(OR)_2$

Preparation of Poly (oxy-1-butenylene)

Typically, 2,3 dihydrofuran (1000 equivalents) was added neat with stirring to the appropriate initiator (I, II and III, approximately 20 mg) at room temperature. For II and III, a red solution was immediately formed and the mixture became rapidly viscous, whereas for I there was no apparent reaction with the characteristic yellow colour of the free initiator in solution persisting. An excess of benzaldehyde (30 μl) was added to cleave the polymer from the living metal centre. Precipitation of the polymer was achieved by adding a tetrahydrofuran solution (10 ml) dropwise to methanol, followed by filtration and removal of the volatiles *in vacuo* , to afford a pale solid in 45% yield.
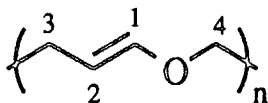
¹H NMR data (400 MHz, d-chloroform, 298K): 6.30 (m, C^1H, trans), 6.01 (m, C^1H, cis), 4.72 (m, C^2H, trans), 4.34 (m, C^4H, cis), 3.67 (m, C^4H_2, cis and trans), 2.39 (m, C^3H_2, cis), 2.23 (m, C^3H_2, trans).

¹³C NMR data (100 MHz, d-chloroform, 298K): 148.13, 148.04, 147.96 (C^1H, trans), 146.74, 146.61 (C^1H, cis), 101.83, 101.56, 101.29 (C^2H, cis), 99.28, 99.08, 98.89 (C^2H, trans), 72.72, 71.76 (C^4H_2, cis (ct and cc respectively), 69.65, 68.74 (C^4H_2, trans (tc and tt respectively)), 28.48, 27.91 (C^3H, trans (tt and tc respectively)), 24.84, 24.25 (C^3H, cis (cc and ct respectively)).

Gel Permeation Chromatography:

GPC data	Poly (oxy-1-butenylene) prepared from II and III	
	II	III
M_n	6000	4500
M_w	12300	12800
PDI (M_w / M_n)	2.83	2.82

5.4.4   Reaction of 2,3 dihydrofuran with $Mo(NAr)(CHCMe_2Ph)(OCMe_2CF_3)_2$ in d_6-benzene

2,5 dihydrofuran (3.2mg, 45 μmol, 2.0 equivalents) was added to a solution of $Mo(CHBu^t)(NAr)(OCMe_2CF_3)_2$ (15.0mg, 23 μmol) in d_8-toluene (800 μl), and the mixture cooled to -70°C. New resonances were observed in the ¹H NMR spectrum as described in chapter 4.

5.4.5   Reaction of vinylene carbonate with Mo(NAr)(CHCMe₂Ph)(OBuᵗ)₂

Preparation of Mo(NAr)(CHCMe₂PhCH(O₂CO)CH)(OBuᵗ)₂ (3).

Vinylene carbonate (17.0mg, 2.0 mmol) was added to a solution of Mo(NAr)(CHCMe2Ph)(OBuᵗ)₂ (109mg, 2.0 mmol) in n-pentane (5 ml) at room temperature, whereby a dark red solution was formed over 1 hour. On cooling the solution to *ca.* -78°C, red crystals were afforded which were collected and dried *in vacuo.* Yield, 71mg (52%).

^{1}H NMR data (400 MHz, d₆-benzene, 298K): 7.36 (d, 2H, Ar), 7.05 - 6.92 (m, 6H, Ar), 6.09 (d, H₃, J_{HH} = 16.0 Hz), 5.95 (dd, H₂, J_{HH} = 16 Hz, J_{HH} = 4.0 Hz), 5.25 (d, H₁, J_{HH} = 3.6 Hz), 4.04 (sept, C*H*Me₂, J_{HH} = 6.8 Hz), 1.55 (s, 9H, OC^1*Me₃*), 1.36 (s, 3H, CH*Me^1*Me²Ph), 1.35 (s, 3H, CHMe^1*Me²*Ph), 1.33 (s, 9H, OC²*Me₃*), 1.28 (d, 6H, C^{1}H*Me₂*, J_{HH} = 6.8 Hz), 1.26 (d, 6H, C²H*Me₂*, J_{HH} = 6.8 Hz). H₁, H₂ and H₃ are the metallacycle protons as labelled in chapter 4. Aryl proton resonances could not be accurately assigned due to overlap.

^{13}C NMR data (100 MHz, d₆-benzene, 298K): 152.90, 149.58, 144.97, 128.32, 126.88, 126.59, 126.06, 122.98 (CH (Ar)), 137.37 (d, C³H, J_{CH} = 154.9 Hz), 130.79 (d, C²H, J_{CH} = 150.1 Hz), 87.60 (d, C^{1}H, J_{CH} = 172.01 Hz), 83.22 (s, OCMe₃), 81.39 (s, OCMe₃), 40.28 (s, CMe₂Ph), 31.98 (q, OC*Me₃*, J_{CH} = 125.9 Hz), 29.31 (q, C*Me₂*Ph, J_{CH} = 126.3 Hz), 28.55 (d, C*H*Me₂, J_{CH} = 128.9 Hz), 24.03 (q, C^{1}H*Me₂*, J_{CH} = 126.3 Hz), 23.83 (q, C²H*Me₂*, J_{CH} = 126.2 Hz). C^1, C² and C³ are the metallacycle carbons attached to H₁, H₂ and H₃ respectively.

Infrared data (Nujol, CsI, cm^{-1}): 3110 (w), 2960 (s), 2940 (s), 1650 (w), 1525 (w), 1315 (m), 1285 (m), 1140 (s, br), 1020 (m), 975 (m), 950 (m), 840 (m,br), 700 (m), 650 (w), 555 (w), 460 (w), 385 (w, br).

Elemental Analysis for MoC$_{33}$NO$_5$H$_{49}$ (635.69) Found (Required): %C, 62.01 (62.35); %H, 7.52 (7.77) %N, 2.54 (2.20).

Mass spectral data (EI, m/z, ^{98}Mo): 594 [M - CO$_2$]$^+$, 176 [HNAr]$^+$, 77 [Ph]$^+$, 57 [Bu^t]$^+$.

5.4.6 Synthesis of 1-(diphenylamino)-3-borolene

(a) Reaction of diphenylamine with boron trichloride

Preparation of Ph$_2$NBCl$_2$

Ph$_2$NH (50 g, 0.30 mol) in dichloromethane (100 ml) was added at low temperature *ca.* -50° C to a solution of BCl$_3$ in heptane (1.0M solution, 300 ml) over a period of 30 minutes. A white precipitate was formed during the course of the addition. The solvent was removed under reduced pressure to afford a solid mixture of [Ph$_2$NH]$^+$[BCl$_4$]$^-$, Ph$_2$NH.BCl$_3$ and Ph$_2$NBCl$_2$. These residues were dissolved in toluene (250 ml) and refluxed for 24 hours, venting periodically with nitrogen until the evolution of HCl ceased, and the toluene removed under reduced pressure. Distillation under reduced pressure (172 - 178°C, 16-18 mm Hg) afforded pure Ph$_2$NBCl$_2$ (25g, 33% yield), as a colourless solid (Mpt = 65-68° C).

(b) Reaction of Ph$_2$NBCl$_2$ with MgC$_4$H$_6$. 2THF

Preparation of 1-(diphenylamino)-3-borolene

A chilled ethereal solution of Ph$_2$NBCl$_2$ (10.03g, 40.1 mmol) was added to a suspension of MgC$_4$H$_6$. 2THF (10.69g, 48 mmol, 1.2 equivalents) in diethyl ether (300 ml, -78°C). The mixture was stirred for 2 hours at -78°C and allowed to warm to room temperature and stirred for 16 hours, whereby a grey precipitate and a clear solution was formed. The suspension was filtered and the precipitate washed with Et$_2$O (2x50 ml), and the washings combined with the solution. Removal of the Et$_2$O from the solution

under reduced pressure, followed by distillation of the oily residue (112-114°C, 2×10^{-2} mm Hg) afforded a white solid (Mpt = 59.5 - 60.5 °C) in low yield, 2.53g (28%).

^{1}H NMR data (400 MHz, d_6-benzene, 298K): 7.05 - 6.88 (m, 10H, NPh_2), 6.06 (s, 2H, CH), 1.79 (s, 4H, CH_2).

^{11}B NMR data (160 MHz, d_6-benzene, 298K): 55.05 (s, br).

^{13}C NMR data (100 MHz, d_6-benzene, 298K): 149.33 (s, C_i (Ph)), 133.07 (d, CH, J_{CH} = 158.3 Hz), 129.13 (d, C_o (Ph), J_{CH} = 162.4 Hz), 126.54 (d, C_m (Ph), J_{CH} = 160.2 Hz), 125.21 (d, C_p (Ph), J_{CH} = 161.0 Hz), 25.70 (t, br, CH_2, J_{CH} = 123.0 Hz).

Infrared data (Nujol, CsI, cm^{-1}): 3020 (w), 1585 (m), 1485 (m), 1400 (m, br), 1255 (m, sh), 760 (m), 700 (s, sh), 670 (s, sh).

Elemental Analysis for $BC_{16}NH_{16}$ (233.12) Found (Required): %C, 82.73 (82.43); %H, 7.14 (6.92); %N, 5.87 (6.01).

Mass spectral data (EI, m/z): 233 $[M]^+$, 218 $[M - Me]^+$, 169 $[HNPh_2]^+$, 77 $[Ph]^+$.

5.4.7 Reaction of 1-(diisopropylamino)-3-borolene with $Mo(CHCMe_2Ph)(NAr)(OCMe(CF_3))_2$
Observation of 1-(diisopropylamino)-2-borolene

1-(diisopropylamino)-3-borolene (0.41g, 2.48 mmol, 109 equivalents) was added neat to $Mo(CHCMe_2Ph)(NAr)(OCMe(CF_3)_2)_2$ (17.4mg, 22.7 μmol) with stirring. A yellow solution was formed which darkened rapidly over 30 minutes. After 24 hours an excess of benzaldehyde (30 ml) was added and a sample of the solution dissolved in d_6-benzene. The ^{1}H NMR spectrum showed the presence of 1-(diisopropylamino)-2-borolene[16].

^1H NMR data (400 MHz, d_6-benzene, 298K): 7.19 (d, br, 3-CH, J_{HH} = 7.6 Hz), 6.36 (dt, 2-CH, J_{HH} = 8.0 Hz, 2.0 Hz), 3.49 (sept, C^1HMe$_2$, J_{HH} = 6.9 Hz), 3.30 (sept, C^2HMe$_2$, J_{HH} = 6.9 Hz), 2.34 (m, 2H, 4-CH$_2$), 1.14 (d, 6H, C^2HMe_2, J_{HH} = 6.9 Hz), 1.09 (m, 2H, 5-CH$_2$), 0.96 (d, C^1HMe_2, J_{HH} = 6.9 Hz).

G.C Mass spectral data (EI, m/z): 165 [M]$^+$, 150 [M - Me]$^+$, 54 [C$_4$H$_6$]$^+$.

5.4.8 Reaction of 1-(diphenylamino)-3-borolene with Mo(NAr)(CHMe$_2$Ph)(OR)$_2$

Preparation of 1-(diphenylamino)-2-borolene

Typically, a solid mixture of 1-(diphenylamino)-3-borolene (70 equivalents) and the appropriate initiator (I, II and III, approximately 20 mg) was warmed to 60°C, whereby a dark red solution was formed almost immediately. After a period of 1 hour, benzaldehyde (30 ml) was added and the mixture allowed to cool to room temperature, whereby solidification occured. Sublimation (< 10^{-3} mmHg, 298K) afforded colourless crystals in excellent yield, 90%.

^1H NMR data (400 MHz, d_6-benzene, 298K): 7.28 (dt, br, 3-CH, J_{HH} = 8.0 Hz, 2.2 Hz), 7.12 - 6.80 (m, NPh$_2$), 6.25 (dt, 2-CH, J_{HH} = 8.0 Hz, 2.0 Hz), 2.37 (m, 2H, 4-CH$_2$, J_{HH} = 2.4 Hz), 1.18 (m, 2H, 5-CH$_2$, J_{HH} = 2.5 Hz).

^{11}B NMR data (160 MHz, d_6-benzene, 298K): 50.26 (s, br).

^{13}C NMR data (100 MHz, d_6-benzene, 298K): 166.25 (d, 3-CH, J_{CH} = 154.1 Hz), 149.58 (s, C$_i$ (Ph)), 135.61 (d, br, 2-CH, J_{CH} = 154.9 Hz), 129.04 (d, C$_o$ (Ph), J_{CH} = 152.4 Hz), 126.68 (d, C$_m$ (Ph), J_{CH} = 162.1 Hz), 124.80 (d, C$_p$(Ph), J_{CH} = 162.5 Hz), 33.59 (t, 4-CH$_2$, J_{CH} = 132.0 Hz), 17.07 (t, br, 5-CH$_2$, J_{CH} = 117.4 Hz).

Infrared data (Nujol, CsI, cm^{-1}): 3020 (w), 1590 (m), 1485 (m), 1400 (m, br), 1255 (m, sh), 775 (m), 700 (s, sh), 660 (s, sh).

Elemental Analysis for BC$_{16}$NH$_{16}$ (233.12) Found (Required): %C, 81.89 (82.43); %H, 6.91 (6.92); %N, 5.76 (6.01).

Mass spectral data (EI, m/z): 233 [M]$^+$, 218 [M - Me]$^+$, 169 [HNPh$_2$]$^+$, 77 [Ph]$^+$.

5.4.9 Synthesis of 1-phenyl-3-pyrroline

Chilled THF (100 ml, -78°C) was added slowly to Li$_2$NPh (6.88g, 65.5 mmol) with stirring. 1,4 dichloro cis but-2-ene was then added dropwise to the suspension whereby a dark red-purple solution was formed. The resultant mixture was stirred at -78°C for 1 hour and then allowed to attain room temperature, before finally being maintained at 50°C for 24 hours. After which period a pale flocculent precipitate and a yellow solution was formed. The mixture was filtered and the volatiles removed *in vacuo* to give an oily residue which was extracted with n-pentane (2x50 ml), which when concentrated and cooled to -40°C afforded a pale yellow flackey solid. Yield, 2.85g (33%).

^{1}H NMR data (400 MHz, d$_6$-benzene, 298K): 7.28 (m, 2H, H$_m$ (Ph)), 6.80 (m, H$_p$ (Ph)), 6.43 (m, 2H, H$_o$ (Ph)), 5.43 (s, 2H, CH), 3.72 (s, 4H, CH$_2$).

^{13}C NMR data (100 MHz, d$_6$-benzene, 298K): 147.39 (s, C$_i$ (Ph)), 129.57 (dd, C$_m$ (Ph), J$_{CH}$ = 156.0 Hz), 126.40 (d, CH, J$_{CH}$ = 171.3 Hz), 116.14 (dt, C$_p$ (Ph), J$_{CH}$ = 160.2 Hz), 111.62 (dm, C$_o$ (Ph), J$_{CH}$ = 156.4 Hz), 54.35 (tt, CH$_2$, J$_{CH}$ = 140.4 Hz).

Infrared data (Nujol, CsI, cm^{-1}): 3020 (w, br), 1625 (w), 1590 (s, br), 1560 (w), 1500 (m), 1380 (s), 1255 (m, sh), 1185 (s, sh), 1150 (w, sh), 1080 (m, br), 1015 (m, br), 940 (w, sh), 855 (w), 800 (s, br), 755 (s, sh), 670 (s, sh), 510 (w), 450 (w, sh).

Elemental Analysis for $NC_{10}H_{11}$ (145.20) Found (Required): %C, 82.58 (82.72); %H, 7.72 (7.63); %N, 9.41 (9.65).

Mass spectral data (EI, m/z): 145 [M]$^+$, 77 [Ph]$^+$.

5.4.10 Reaction of diallyl ether with $Mo(CHCMe_2Ph)(NAr)(OCMe(CF_3)_2)_2$

(a) Neat addition

Diallyl ether (3.10g, 31.6 mmol, 1000 equivalents) was transferred under reduced pressure onto $Mo(CHCMe_2Ph)(NAr)(OCMe(CF_3)_2)$ (24.1mg, 31.5 μmol) at 77K. On warming rapidly to room temperature the evolution of a volatile species was observed and an a orange-red solution formed. A sample of the volatile species was collected and shown to be ethylene by G.C Mass spectrometry. Periodically, as the rate of evolution of ethylene slowed, the mixture was cooled to -78°C and the excess ethylene removed under reduced pressure. On re-warming to room temperature, further evolution of ethylene was stimulated until finally after 30 minutes ethylene ceased to be evolved even on warming to 40°C. The reaction was quenched to air, and the volatile components removed and collected under reduced pressure. The ^1H NMR spectrum (d$_6$-benzene) of a sample of the volatiles showed it to comprise of *ca.* 48% 2,5 dihydrofuran and 45% unreacted diallyl ether, whereas the involatile fraction consisting of oligomers ($M_n \sim 300$) accounted for 7% of the total mass.

(b) In dilute solution

(i) NMR scale

Diallyl ether (3.6 μl, 29.4 μmol, 0.8 equivalents) was added to a solution of $Mo(CHCMe_2Ph)(NAr)(OCMe(CF_3)_2)_2$ (27 mg, 35.5 μmol) in d$_6$-benzene (800 μl) at room temperature. After 24 hours the NMR tube was cracked under nitrogen and a

further 18 µl (4.1 equivalents) added to the mixture and the NMR tube stoppered and resealed. A further addition of 10 equivalents of diallyl ether was added after 3 days in an analogous manner. Neophylidene was observed in the ^{1}H NMR spectrum at δ 5.95 (dd, CH(CMe$_2$Ph)), 4.97 (m, 2H, CH$_2$), 1.27 (s, 6H, CH(CMe_2Ph)) and ethene at δ 5.24 (s, 4H, CH$_2$).

(ii) Preparative scale

Diallyl ether (2.01g, 20.5 mmol, 1300 equivalents) was added to a solution of Mo(CHCMe$_2$Ph)(NAr)(OCMe(CF$_3$)$_2$)$_2$ (12.4mg, 16.1 µmol) in n-pentane (5 ml) with stirring whereby the evolution of ethylene was noted. Ethylene ceased to be evolved after 30 minutes and the reaction was exposed to air. The mixture was cooled to -78°C and the pentane removed under reduced pressure. The ^{1}H NMR spectrum (d$_6$-benzene) of the residue showed it to comprise of 2,5 dihydrofuran and unreacted diallyl ether in a 2:3 ratio respectively, with a trace of oligomers also present.

5.4.11 Reaction of diallyl phenyl phosphine with

Mo(NAr)(CHCMe$_2$Ph)(OCMe(CF$_3$)$_2$)$_2$ in d$_6$-benzene.

Observation of 2,5 dihydro-1-phenyl-phospholene

Diallyl phenyl phosphine (49.7 mg, 0.26 mmol) was mixed with Mo(NAr)(CHCMe$_2$Ph)(OCMe(CF$_3$)$_2$)$_2$ (20.0 mg, 26 µmol) in d$_6$-benzene (800 µl) at room temperature. A red solution was formed over a period of 1 hour. Resonances attributed to 2,5 dihydro-1-phenyl-phospholene were present in the ^{1}H NMR (400 MHz) at δ 7.46 - 7.06 (m, 5H, Ph), 5.64 (d, 2H, CH, ^{3}J$_{HP}$ = 8.0 Hz), 2.62 - 2.48 (m, 4H, CH$_2$).

5.5 References

1. T.V.Lubben, P.T.Wolczanski, G.D.Van Duyne, *Organometallics*. 1984, 3, 982.

2. R.R.Schrock, J.S.Murdzek, G.C.Bazan, M.Dimare, J.Robbins, M.O'Regan, *J. Am. Chem. Soc*. 1990, 112, 3875.

3. M.J.Bunker, A.De Cian, M.L.H.Green, J.J.E.Moreau, N.Siganporia, *J. Chem. Soc. Dalton Trans*, 1980, 2155.

4. V.C.Gibson, D.N.Williams, A.D.Poole, U.Siemeling, J.P.Mitchell, D.C.R.Hockless, P.A.O'Neil, W.Clegg, *J. Chem. Soc. Dalton Trans*. 1992, 739.

5. D.N.Williams, Ph.D Thesis, University of Durham, 1990.

6. J.A.Osborn, J.Kress, G.Schoettel, *J. Chem. Soc. Chem. Commun*. 1989, 1062.

7. V.C.Gibson, J.P.Mitchell, M.Jolly, *J. Chem. Soc. Chem. Commun*. 1992, 1331.

8. G.C.Bazan, Ph.D Thesis, Massachussetts Institute of Technology, 1990.

9. J.Sundermayer, *Chem. Ber*. 1991, 1977.

10. V.C.Gibson, J.A.K.Howard, P.W.Dyer, B.Whittle, C.Wilson, *J. Chem. Soc. Chem. Commun*. 1992, 1666.

11. R.R.Schrock, H.H.Fox, K.B.Yap, J.Robbins, S.Cai, *Inorg. Chem*. 1992, 31, 2287.

12. K.Fujita, Y.Ohnuna, H.Yasuda, H.Tani, *J. Organomet. Chem*. 1983, 256, C23.

13. A.A.Frost, R.G.Pearson, *"Kinetics and Mechanism"*, Wiley, New York, 1961.

14. D.M.Hirst, *"Mathematics for Chemists"*, Macmillan education, pg 266-273, 1976.

15. G.Wilkinson, A.A.Danopoulos, B.H-Bates, M.B.Hursthouse, *J. Chem. Soc. Dalton Trans*. 1990, 2753.

16. G.E.Herberich, W.Boveloth, B.Hessner, M.Hostalek, D.P.J.Köffer, H.Ohst, D.Söhnen, *Chem. Ber*. 1986, 119, 420.

Appendices

Appendix 1A: Crystal data for Mo(NBu^t)$_2$(OBu^t)$_2$

MoN$_2$O$_2$C$_{16}$H$_{36}$	384.4
Crystal system	Monoclinic
Space Group	P2$_1$/c
Cell Dimensions	a = 17.969(4) Å
	b = 7.885(2) Å
	c = 17.881(4) Å
	β = 119.64(3)^o
	V = 2201.9(9) Å^3
	Z = 4
	D$_c$ = 1.16 g cm^{-3}
Final R-value	0.0435 (R$_w$ = 0.0505)

Appendix 1B Crystal data for CpNb(NAr)(NHBu^t)Cl

NbN$_2$ClC$_{21}$H$_{32}$	483.3
Crystal system	Monoclinic
Space Group	P2$_1$/n
Cell Dimensions	a = 9.165(2) Å
	b = 14.166(4) Å
	c = 16.807(3) Å
	β = 96.78(3)^o
	V = 2166.8(9) Å^3
	Z = 4
	D$_c$ = 1.351 g cm^{-3}
Final R-value	0.0394 (R$_w$ = 0.0612)

223

Appendix 1C Crystal data for CpNb(NBu^t)(OCMe$_2$CF$_3$)$_2$

NbNO$_2$F$_6$C$_{14}$H$_{26}$	483.3
Crystal system	Monoclinic
Space Group	C2/c
Cell Dimensions	a = 25.9001(114) Å
	b = 10.2142(45) Å
	c = 16.3773(45) Å
	β = 96.0376(292)^o
	V = 2166.8(9) Å^3
	Z = 8
	D$_c$ = 1.49 g cm^{-3}
Final R-value	0.0754 (R$_w$ = 0.1014)

Appendix 1D Crystal data for 1-(diphenylamino)-2-borolene

BNC$_{16}$H$_{16}$	233.11
Crystal system	Monoclinic
Space Group	P2$_1$/c
Cell Dimensions	a = 8.447(3) Å
	b = 9.637(4) Å
	c = 32.41(2) Å
	β = 92.00(3)^o
	V = 2637(2) Å^3
	Z = 8
	D$_c$ = 1.174 g cm^{-3}
Final R-value	0.0514

Appendix 2

First Year Induction Courses: October 1990

The course consists of a series of one hour lectures on the services available in the department.

1.　Departmental Safety

2.　Safety Matters

3.　Electrical Appliances and Infrared Spectroscopy

4.　Chromatography and Microanalysis

5.　Atomic Absorbtion and Inorganic Analysis

6.　Library Facilities

7.　Mass Spectroscopy

8.　Nuclear Magnetic Resonance

9.　Glass Blowing Techniques

Examined Lecture Courses: October 1990-April 1991

Three courses were attended consisting of 6 one hour lectures followed by a written examination in each.

"Assymetric Synthesis", Dr. P.Steele

"NQR and Mössbauer spectroscopy", Dr. M.Kilner and Dr. K.B.Dillon.

"Heterogenous catalysis", Dr. M.Kilner.

Research Colloquia, Seminars and Lectures Organised By the Department of Chemistry.

* - Indicates Colloquia attended by the author.

During the Period 1990-1991

4th October | * Dr. M. Bochmann, University of East Anglia, *"Synthesis, Reactions and Catalytic Activity of Cationic Titanium Alkyls."*

11th October | Dr. W.A. MacDonald, ICI Wilton, *"Materials for the Space Age."*

26th October | * Prof. R. Soulen, South Western University, Texas, *"Preparation and Reactions of Bicycloalkenes."*

31st October | Dr. R. Jackson, Newcastle University, *"New Synthetic Methods: a-Amino Acids and Small Rings.*

1st November | Dr. N. Logan, Nottingham University, *"Rocket Propellants."*

6th November | * Dr. P. Kocovsky, Uppsala University, *"Stereo-Controlled Reactions Mediated by Transition and Non-Transition Metals."*

8th November | Dr. S.K. Scott, Leeds University, *"Clocks, Oscillations and Chaos."*

14th November | Prof. T. Bell, SUNY, Stoney Brook, U.S.A., *"Functional Molecular Architecture and Molecular Recognition."*

21st November	* Prof. J. Prichard, Queen Mary & Westfield College, London University, *"Copper Surfaces and Catalysts."*
28th November	Dr. B.J. Whitaker, Leeds University, *"Two-Dimensional Velocity Imaging of State-Selected Reaction Products."*
29th November	Prof. D. Crout, Warick University, *"Enzymes in Organic Synthesis."*
5th December	* Dr. P.G. Pringle, Bristol University, *"Metal Complexes with Functionalised Phosphines."*
13th December	* Prof. A.H. Cowley, University of Texas, *"New Organometallic Routes to Electronic Materials."*
15th January	Dr. B.J. Alder, Lawerence Livermore Labs., California *"Hydrogen in all its Glory."*
17th January	Dr. P. Sadler, Nottingham University, *"Comet Chemistry."*
30th January	Prof. E. Sinn, Hull University, *"Coupling of Little Electrons in Big Molecules. Implications for the Active Sites of (Metalloproteins and other) Macromolecules."*
31st January	Dr. D. Lacey, Hull University, *"Liquid Crystals."*
6th February	Dr. R. Bushby, Leeds University, *"Biradicals and Organic Magnets."*
14th February	Dr. M.C. Petty, Durham University, *"Molecular Electronics."*

20th February	* Prof. B.L. Shaw, Leeds University), *"Synthesis with Coordinated, Unsaturated Phosphine Ligands."*
28th February	* Dr. J. Brown, Oxford University, *"Can Chemistry Provide Catalyts Superior to Enzymes?"*
6th March	Dr. C.M. Dobson, Oxford University, *"NMR Studies of Dynamics in Molecular Crystals."*
6th March	Dr. D. Gerrard, British Petroleum, *"Raman Spectroscopy for Industrial Analysis."*
7th March	Dr. J. Markam, ICI Pharmaceuticals, *"DNA Fingerprinting."*
24th April	* Prof. R.R. Schrock, M.I.T, *"Metal-Ligand Multiple Bonds and Metathesis Initiators."*
25th April	Prof. T. Hudlicky, Virginia Polytechnic Institute, *"Biocatalysis and Symmetry Based Approaches to the Efficient Synthesis of Complex Natural Products."*
30th June	* Prof. M.S. Brookhart, University of N. Carolina, *"Olefin Polymerisation, Oligomerisation and Dimerization Using Electrophilic Late Transition Metal Catalysts."*
29th July	Dr. M.A. Brimble, Massey University, New Zealand, *"Synthetic Studies Towards the Antibiotic Griseusin-A."*

17th September   * Prof. R.D. Fischer, University of Hamburg, *"From Organo-f-Element Systems to Organo-Main-Group Polymers."*

17th October   Dr. J.A. Salthouse, University of Manchester, *"Son et Luminere - a Demonstration Lecture."*

31st October   Dr. R. Keeley, Metropolitan Police Forensic Science, *"Modern Forensic Science."*

6th November   * Prof. B.F.G. Johnson, Edinburgh University, *"Cluster-Surface Analogies."*

7th November   Dr. A.R. Butler, St. Andrews University, *"Traditional Chinese Herbal Drugs: a Different Way of Treating Disease."*

13th November   Prof. D. Gani, St Andrews University, *"The Chemistry of PLP Dependant Enzymes."*

20th November   * Dr. R. More O'Ferrall, University College, Dublin, *"Some Acid-Catalysed Rearrangements in Organic Chemistry."*

28th November   Prof. I.M. Ward, IRC in Polymer Science, University of Leeds, *The SCI Lecture, "The Science and Technology of Orientated Polymers."*

5th December   Dr. W.D. Cooper, Shell Research, *"Colliod Science, Theory and Practice."*

4th December	* Prof. R. Grigg, Leeds University, *"Palladium Catalysed Cyclisation and Ion Capture Processes."*
5th December	Prof. A.L. Smith, ex Unilever, *"Soap, Detergents and Black Puddings."*
22nd January	Dr. K.D.M. Harris, St. Andrews University, *"Understanding the Properties of Solid Inclusion Compounds."*
29th January	Dr. A. Holmes, Cambridge University, *"Cycloaddition Reactions in the Service of the Synthesis of Piperdine and Indolizidine Natural Products."*
30th January	Dr. M. Anderson, Shell Research, *"Recent Advances in the Safe and Selective Chemical Control of Insect Pests."*
12th February	* Prof. D.E. Fenton, Sheffield University, *"Polynuclear Complexes of Molecular Clefts as Models for Copper Biosites."*
13th February	Dr. J. Saunders, Glaxo Group Research Ltd., *"Molecular Modelling in Drug Discovery."*
19th February	* Prof. E.J. Thomas, Manchester University, *"Applications of Organostannanes to Organic Synthesis."*
20th February	* Prof. E. Vogel, University of Cologne, *The Musgrave Lecture*, *"Porphyrins, Molecules of Interdisciplinary Interest."*

25th February	Prof. J.F. Nixon, University of Sussex, *The Tilden Lecture*, *"Phosphaalkynes, New Building Blocks in Inorganic and Organometallic Chemistry."*
26th February	Prof. M.L. Hitchman, Strathclyde University, *"Chemical Vapour Deposition."*
11th March	* Dr. S.E. Thomas, Imperial College, *"Recent Advances in Organoiron Chemistry."*
5th March	* Dr. N.C. Billingham, University of Sussex, *"Degradable Plastic - Myth or Magic?"*
12th March	Dr. R.A. Hann, ICI Imagedata, *"Electronic Photography - An Image of the Future."*
18th March	Dr. H. Maskill, Newcastle University, *"Concerted or Stepwise Fragmentation in a Deamination-Type Reaction."*
7th April	Prof. D.M. Knight, Philosophy Department, University of Durham, *"Interpreting Experiments: the Beginning of Electrochemistry."*
6th May	* Prof. T. Marder, University of Waterloo, *"Metal Catalysed Alkene Hydroboration."*
13th May	Dr. J.C. Gehret, Ciba Geigy, Basel, *"Some Apects of Industrial Agrochemical Research."*

15th October   Dr. M. Glazer and Dr. S. Tarling, Oxford University and Birbeck College, London, *"It pays to be British!- The Chemists Rôle as an Expert Witness in Patent Litigation."*

20th October   * Dr. H.E. Bryndza, Du Pont Central Research, *"Synthesis, Reactions and Thermochemistry of Metal (Alkyl) Cyanide Complexes and Their Impact on Olefin Hydrocyanation Catalysis."*

22nd October   Prof. A. Davies, University College London, The *Ingold-Albert Lecture "The Behaviour of Hydrogen as a Pseudometal."*

28th October   * Dr. J.K. Cockcroft, University of Durham, *"Recent Developments in Powder Diffraction."*

29th October   * Dr. J. Emsley, Imperial College, London, *"The Shocking History of Phosphorus."*

4th November   * Dr. T.P. Kee, University of Leeds, *"Synthesis and Co-ordination Chemistry of Silylated Phosphites."*

5th November   Dr. C.J. Ludman, University of Durham, *"Explosions, A Demonstration Lecture."*

11th November   Prof. D. Robins, Glasgow University, *"Pyrrolizidine Alkaloids: Biological Activity, Biosynthesis and Benefits."*

12th November	Prof. M.R. Truter, University College, London, *"Luck and Logic in Host-Guest Chemistry."*
18th November	* Dr. R. Nix, Queen Mary College, London, *"Characterisation of Heterogeneous Catalysts."*
25th November	Prof. Y. Vallee, University of Caen, *"Reactive Thiocarbonyl Compounds."*
25th November	Prof. L.D. Quin, University of Massachusetts, Amerherst, *"Fragmentation of Phosphorus Heterocycles as a Route to Phosphoryl Species with Uncommon Bonding."*
26th November	* Dr. D. Humber, Glaxo, Greenford, *"AIDS- The Development of a Novel Series of Inhibitors of HIV."*
2nd December	* Prof. A.F. Hegarty, University College, Dublin, *"Highly Reactive Enols Stabilised by Steric Protection."*
2nd December	Dr. R.A. Aitken, University of St. Andrews, *"The Versatile Cycloaddition Chemistry of Bu3P.CS2."*
3rd December	Prof. P. Edwards, Birmingham University, *The SCI Lecture*, *"What is Metal?"*
9th December	Dr. A.N. Burgess, ICI Runcorn, *"The Structure of Perfluorinated Ionomer Membranes."*
20th January	Dr. D.C. Clary, University of Cambridge, *"Energy Flow in Chemical Reactions."*

21st January	Prof. L. Hall, Cambridge, *"NMR- Window to the Body."*
27th January	* Dr. W. Kerr, University of Strathclyde, *"Development of the Pauson-Khand Annulation Reaction: Organocobalt Mediated Synthesis of Natural and Unnatural Products."*
28th January	Prof. J. Mann, University of Reading, *"Murder, Magic and Medicine."*
3rd February	Prof. S.M. Roberts, University of Exeter, *"Enzymes in Organic Synthesis."*
10th February	Dr. D. Gillies, University of Surrey, *"NMR and Molecular Motion in Solution."*
11th February	* Prof. S. Knox, Bristol University, The Tilden Lecture, *"Organic Chemistry at Polynuclear Metal Centres."*
17th February	Dr. R.W. Kemmitt, University of Leicester, *"Oxatrimethylenemethane Metal Complexes."*
18th February	Dr. I. Fraser, ICI Wilton, *"Reactive Processing of Composite Materials."*
22nd February	Prof. D.M. Grant, University of Utah, *"Single Crystals, Molecular Structure, and Chemical Shift Anisotropy."*
24th February	Prof. C.J.M. Stirling, University of Sheffield, *"Chemistry of Flat-Reactivity of Ordered Systems."*

10th March	* Dr. P.K. Baker, University College of North Wales, Bangor, *"Chemistry of Highly Versatile 7-Coordinate Complexes."*
11th March	Dr. R.A.Y. Jones, University of East Anglia, *"The Chemistry of Wine Making."*
17th March	Dr. R.J.K. Taylor, University of East Anglia, *"Adventures in Natural Product Synthesis."*
24th March	Prof I.O. Sutherland, University of Liverpool, *"Chromogenic Reagents for Cations."*
13th May	* Prof. J.A. Pople, Carnegie-Mellon University, Pittsburgh, USA, *The Boys-Rahman Lecture*, *"Applications of Molecular Orbital Theory."*
21st May	* Prof. L. Weber, University of Bielefeld, *"Metallo-phospha Alkenes as Synthons in Organometallic Chemistry."*
1st June	Prof. J.P. Konopelski, University of California, Santa Cruz, *"Synthetic Adventures with Enantiomerically Pure Acetals."*
2nd June	* Prof. P. Ciardelli, University of Pisa, *"Chiral Discrimination in the Stereospecific Polymerisation of Alpha Olefins."*
7th June	Prof. R.S. Stein, University of Massachusetts, *"Scattering Studies of Crystalline and Liquid Crystalline Polymers."*

16th June   Prof. A.K. Covington, University of Newcastle, *"Use of Ion Selective Electrodes as Detectors in Ion Chromatography."*

17th June   Prof. O.F. Nielson, H.C. Ørsted Institute, University of Copenhagen, *"Low-Frequency IR and Raman Studies of Hydrogen Bonded Liquids."*

Conferences and Symposia Attended.

1. *"Symposium in Honour of Professor Peter L. Pauson:-Organometallic Chemistry of the Transition Metals,"*
   University of Strathclyde, Glasgow, 19th October 1990.

2. *"Waddington Graduate Symposium on Inorganic Chemistry,* University of Durham, 17th December 1990.

3. *"Autumn Meeting of the Royal Society of Chemistry"*, University of York, 29th September 1991.

4. *"North East Graduate Symposium,"*
   University of Durham, 3rd April 1992.

Publications

Imido ligand reactivity in four coordinate bis imido complexes of molybdenum (VI).

V.C.Gibson, M.Jolly, J.P.Mitchell, *J. Chem. Soc. Dalton Trans.* 1992, 1329.

Inter-metal exchange of oxo, imido and alkylidene ligands.

V.C.Gibson, M.Jolly, J.P.Mitchell, *J. Chem. Soc. Dalton Trans.* 1992, 1331.

Mechanistic studies on the inter-metal exchange of mono- and dianionic ligands
in early transition metal systems and synthetic applications, V.C.Gibson, M.Jolly,
to be published.

The R.O.M.P of 2,3 and 2,5 dihydrofurans using well-defined molybdenum Schrock
initiators and related studies, V.C.Gibson, M.Jolly, to be published.